

Isolation and Characterization of Antiinfective Metabolites from Cyanobacteria

Dissertation

der Mathematisch-Naturwissenschaftlichen Fakultät
der Eberhard Karls Universität Tübingen
zur Erlangung des Grades eines
Doktors der Naturwissenschaften
(Dr. rer. nat.)

vorgelegt von
Ronja Kossack
aus Herdecke

Tübingen
2020

Gedruckt mit Genehmigung der Mathematisch-Naturwissenschaftlichen Fakultät der
Eberhard Karls Universität Tübingen.

Tag der mündlichen Qualifikation:

04.03.2021

Stellvertretender Dekan:

Prof. Dr. József Fortágh

1. Berichterstatter:

Prof. Dr. Timo Niedermeyer

2. Berichterstatter:

Prof. Dr. Karl Forchhammer

Table of Contents

I. Zusammenfassung.....	1
II. Summary.....	3
III. Publication.....	5
1. Introduction.....	6
1.1. Microbial Diversity as Source for Natural Products.....	6
1.2. Morphological Diversity of Cyanobacteria.....	7
1.3. Natural Product Diversity of Cyanobacteria.....	11
1.3.1. Natural Products from Cyanobacteria as Protease Inhibitors.....	11
1.4. Human African Trypanosomiasis (HAT).....	14
1.4.1. Lifecycle of <i>T. brucei rhodesiense</i> and <i>gambiense</i>	15
1.4.2. Diagnosis.....	16
1.4.3. Treatment.....	17
1.4.4. Rhodesain as Target for New Treatments.....	18
1.5. Research Objective.....	22
2. Material & Methods.....	23
2.1. Instruments.....	23
2.2. Establishing a Cyanobacteria Strain Collection.....	24
2.2.1. Media.....	24
2.2.2. Sampling Procedure.....	25
2.2.2.1. Blooms and Biofilms.....	25
2.2.2.2. Waterbodies.....	25
2.2.3. Strain Isolation and Purification Techniques.....	26
2.2.3.1. Single-Cell Isolation.....	26
2.2.3.2. Separation by Filtration.....	26
2.2.3.3. Phototaxis.....	26
2.2.3.4. Streak Plate Method.....	27
2.2.4. Taxonomy.....	27
2.2.5. Strain Maintenance.....	27

2.3.	Establishing a Cyanobacteria Extract Collection	27
2.3.1.	Biomass Production	27
2.3.1.1.	Cultivation in Aerated 50 mL Centrifuge Tubes	28
2.3.1.2.	Cultivation in Aerated Laboratory Bottles	28
2.3.1.3.	Cultivation in Shake Flasks	28
2.3.1.4.	Cultivation in High-Density Cultivators.....	28
2.3.1.5.	Growth Monitoring.....	29
2.3.1.6.	Recovery of Biomass and Medium	29
2.3.2.	Preparation of Biomass Extracts.....	29
2.4.	Bioactivity Screening	31
2.4.1.	Rhodesain Inhibition Assay	31
2.4.1.1.	Determination of the Inner Filter Effect.....	32
2.4.1.2.	Determination of IC ₅₀ and K _i	33
2.4.2.	Antimicrobial Activity	34
2.4.2.1.	Cyanobacterial Extracts.....	34
2.4.2.2.	Pure Compounds	34
2.4.3.	Quorum Sensing Inhibition.....	35
2.4.3.1.	Violacein Production Assay	35
2.4.3.2.	B-Galactosidase Assay.....	36
2.4.3.3.	Prodigiosin Production Assay	36
2.4.3.4.	Bioluminescence Assay	37
2.5.	Chemical Screening.....	38
2.5.1.	Mass Spectrometry, Tandem Mass Spectrometry and High-Resolution Electrospray Ionisation Mass Spectrometry	38
2.6.	Dereplication of Isolated Compounds	38
2.7.	Bioactivity-Guided Isolation.....	38
2.7.1.	Fractionation with Flash-Chromatography	39
2.7.2.	Time-based Fractionation with HPLC.....	39
2.7.3.	Isolation of Bioactive Compounds.....	39
2.7.3.1.	Semi-Preparative HPLC.....	40

2.7.3.2.	Preparative HPLC	40
2.8.	NMR Analysis and Structure Elucidation of Isolated Compounds	40
2.9.	Quantification by Evaporative Light Scattering Detection (ELSD).....	41
3.	Results and Discussion.....	42
3.1.	Establishing a Cyanobacteria Strain Collection	42
3.1.1.	Sampling in Germany.....	42
3.1.2.	Sampling in Indonesia	44
3.1.3.	Exemplary Isolation Procedure	44
3.2.	Screening of the Cyanobacteria Extract Collection	50
3.2.1.	Screening for Rhodesain Inhibitory Activity	50
3.2.2.	Screening for Antimicrobial Activity.....	51
3.2.3.	Screening for Quorum Sensing Activity	51
3.2.4.	Best-Hit Extracts: Taxonomic Description and Chemical Profiling.....	53
3.2.4.1.	AnoTü10: Origin and Morphological Characterization.....	54
3.2.4.2.	AnoTü10: Chemical Profile	56
3.2.4.3.	AnoTü20: Origin and Morphological Characterization.....	57
3.2.4.4.	AnoTü 20: Chemical Profile	58
3.2.4.5.	An-Al000: Origin and Morphological Characterization	61
3.2.4.6.	An-Al000: Chemical Profile	63
3.2.4.7.	An-Al115: Origin and Morphological Characterization	65
3.2.4.8.	An-Al115: Chemical Profile	66
3.2.4.9.	An-Al061.1: Origin and Morphological Characterization.....	69
3.2.4.10.	An-Al061.1: Chemical Profile.....	70
3.2.4.11.	An-Al006.1: Origin and Morphological Characterization.....	73
3.2.4.12.	An-Al006.1: Chemical Profile.....	74
3.3.	Screening of the Cyano Biotech GmbH Extract Collection for Rhodesain Inhibitory Activity.....	76
3.3.1.	Isolation of Inhibitory Compounds from the Biomass Extract <i>Nostoc</i> 3.....	78
3.3.1.1.	Compound Isolation and Characterization	84
3.3.1.2.	<i>Nostoc</i> 3 Biomass Extract - Summary and Future Perspectives	86

3.3.2.	Isolation of Inhibitory Compounds from the Medium Extract <i>Nostoc</i> 6	87
3.3.2.1.	Nostotrebin 6 Related Cyclopentenediones and δ -lactones with Broad Activity Spectrum Isolated from the Cultivation Medium of the Cyanobacterium <i>Nostoc</i> sp. CBT115387	
3.3.2.2.	Studies on Rhodesain Inhibition Mechanism.....	97
4.	Conclusions and Future Perspectives.....	100
5.	References.....	103
6.	Appendix: Supplementary Data.....	117
6.1.	List of Abbreviations.....	117
6.2.	Supporting Data.....	119
6.3.	Supporting Information “Nostotrebin 6 Related Cyclopentenediones and δ -Lactones with Broad Activity Spectrum Isolated from the Cultivation Medium of the Cyanobacterium <i>Nostoc</i> sp. CBT1153”	136
6.4.	Acknowledgements	179
6.5.	Rights of Use for Third Party Property	180

I. Zusammenfassung

Cyanobakterien sind als wertvolle Quelle strukturell vielfältiger und pharmakologisch aktiver Metaboliten, wie z.B. Proteaseinhibitoren, bekannt. Im Rahmen des Kooperations-Projektes "Accessing Novel Bacterial Producers from Biodiversity-rich Habitats in Indonesia" (ANoBIn) ist es das Ziel der vorliegenden Arbeit antiinfektive Metabolite, insbesondere Proteaseinhibitoren, aus Cyanobakterien zu isolieren. Hierzu wurden neben einer eigens etablierten Cyanobakterien-Stamm- und -Extraktssammlung auch Biomasse- und Medienextrakte aus der Extraktbibliothek der Cyano Biotech GmbH, Berlin, gegen die Cysteinprotease Rhodesain getestet. Das Screening wurde in Kooperation mit Prof. Dr. Tanja Schirmeister (Johannes-Gutenberg-Universität Mainz) durchgeführt.

Aus Proben verschiedener Ökosysteme in Deutschland und Indonesien wurden Cyanobakterien isoliert und eine Stammsammlung mit 147 terrestrischen und aquatischen Cyanobakterien aufgebaut. Aus deutschen Umweltproben konnten insgesamt 55 Cyanobakterien isoliert werden. Anhand morphologischer Merkmale wurden 30.9% den Chroococcales, 65.5% den Oscillatoriales und 3.6% den Nostocales zugeordnet. Die Beprobung von Habitaten in Indonesien führte zur Isolierung von 92 Cyanobakterien-Stämmen. Hier ergab die morphologische Charakterisierung 17.4% Chroococcales, 38.0% Oscillatoriales, 34.8% Nostocales und 9.8% Stigonematales. Mehr als 60 Biomasseextrakte wurden auf ihren Einfluss auf drei unterschiedliche Quorum Sensing (QS)-Systeme und die antimikrobielle Aktivität gegen *Bacillus subtilis* und *Staphylococcus aureus* untersucht. Der Fokus dieser Arbeit liegt jedoch auf neuen Inhibitoren gegen die Cathepsin L-ähnliche Cysteinprotease Rhodesain, welche eine essentielle Rolle im Metabolismus von *Trypanosoma brucei* spielt, dem Parasiten, der die menschliche afrikanische Trypanosomiasis auslöst. Einige Extrakte zeigten QS-verstärkende und -inhibierende, aber auch antimikrobielle Eigenschaften. Bei sechs von 52 Biomasseextrakten (11.5%) wurden mehr als 50% Inhibierung von Rhodesain bei einer Konzentration von 0.1 mg/mL, festgestellt. Ein *Oscillatoria* sp. Biomasseextrakt zeigte mehr als 70% Inhibierung von Rhodesain. Obwohl 51.9% der untersuchten Stämme zu Oscillatoriales gehörten, zeigten nur 7.4% der Oscillatoriales Rhodesain-inhibierende Aktivität, während 15.4% der getesteten Chroococcales, 12.5% der Nostocales und 25% der Stigonematales mehr als 50% Inhibierung zeigten. Auf Basis der Bioaktivitäten und des chemischen Profils wurden fünf Extrakte intensiver untersucht.

Zusätzlich zu der im Rahmen von ANoBIn etablierten Stammsammlung wurde eine kommerzielle Bibliothek von 572 Cyanobakterien-Extrakten (Cyano Biotech GmbH, Berlin)

getestet. Im Screening zeigten 2.7% der Biomasseextrakte eine inhibitorische Aktivität von mehr als 70% bei 0.1 mg/mL und 14.8% der Medienextrakte eine Inhibierung von mehr als 70% bei 0.2 mg/mL.

Der Biomasseextrakt von einem *Nostoc* sp. Stamm zeigte 98% Inhibierung bei einer Konzentration von 0.1 mg/mL. In diesem Extrakt konnten neun Verbindungen identifiziert werden, von denen fünf eine ausgeprägte Aktivität zeigten. Da die Rhodesain inhibierenden Verbindungen nur in kleinen Mengen im Extrakt enthalten waren, konnten nur mit einer nicht-inhibierenden Verbindung NMR-Experimente durchgeführt werden. Die Auswertung der NMR Spektren identifizierte Teile der Struktur: ein Zuckerrückgrat (Triose) und eine stickstoffreiche Seitenkette. Mit mehr als 90% Inhibierung zog zudem ein *Nostoc* sp. Mediumextrakt Aufmerksamkeit auf sich. Aus diesem Mediumextrakt wurden das bereits bekannte Cyclopentandion (CPD) Nostotrebins 6 und weitere unbekannte, biosynthetisch verwandte Oligomere isoliert: einem dreisubstituiertem CPD oder einem dreisubstituiertem, ungesättigtem δ -Lacton. Nostotrebins 6 ist das bislang einzige bekannte CPD cyanobakteriellen Ursprungs, das bereits aus einem *Nostoc* sp. Biomasseextrakt isoliert wurde. In der Literatur wird von verschiedenen Bioaktivitäten berichtet, was auf eine unspezifische Aktivität hindeutet. Als Substanz mit unspezifischer Aktivität ist Nostotrebins 6 den pan-assay interference compounds (PAINs) zuzuordnen. Die Ergebnisse eines vergleichenden Bioaktivitätsscreenings deuten darauf hin, dass auch die neu isolierten Oligomere unspezifisch reagieren. Hierbei scheint die Intensität der Inhibierung von der Anzahl der freien phenolischen Hydroxylgruppen pro Molekül abzuhängen.

Nach aktuellem Stand handelt es sich bei der vorliegenden Studie um die erste, welche Cyanobakterien als mögliche Quelle für Rhodesain-Inhibitoren untersucht. In dem Screening der hier etablierten Stammsammlung zeigten 2% der Biomasse-Extrakte mehr als 70% Inhibierung bei einer Konzentration von 0.1 mg/mL. Diese Werte sind vergleichbar mit dem Screening der Extraktbibliothek der Cyano Biotech GmbH, wo 2.7% der 450 Biomasseextrakte mehr als 70% Inhibierung von Rhodesain zeigten und das Screening von 122 Medienextrakten 14.7% mit mehr als 70% Inhibierung bei 0.2 mg/mL ergab. 55.6% der aktiven Extrakte wurden von Cyanobakterien der Sektion Nostocales (IV) gewonnen. Das lässt die Schlussfolgerung zu, dass Cyanobakterien, insbesondere deren Medienextrakte, eine bislang wenig untersuchte, aber vielversprechende Ressource für Protease-Inhibitoren, und somit für die Entwicklung neuer Therapien für die menschliche afrikanische Trypanosomiasis darstellen.

II. Summary

Cyanobacteria, whilst initially having been neglected by natural product research for a long time, nowadays are recognized as a prolific source of structurally diverse and pharmacologically active natural products, like protease inhibitors. The present study is embedded in the bilateral project "Accessing Novel Bacterial Producers from Biodiversity-rich Habitats in Indonesia" (AnoBIn) and aims to identify and isolate anti-infective metabolites from cyanobacteria, particularly inhibitors of the trypanosomal cysteine protease rhodesain. Therefore, we screened a cyanobacteria extract collection generated as part of the ANoBIn project, as well as a library of 572 cyanobacteria extracts, kindly provided by Cyano Biotech GmbH, Berlin, against the trypanosomal cysteine protease rhodesain in cooperation with Prof. Dr. Tanja Schirmeister (Johannes Gutenberg University Mainz).

In order to constitute a cyanobacteria strain collection, various aquatic and terrestrial ecosystems in Germany and Indonesia were sampled, followed by the isolation, characterization and biobanking of 147 cyanobacterial strains. The sampling in Germany led to the isolation of 55 strains from which 30.9% were belonging to the Chroococcales, 65.5% to the Oscillatoriales and 3.6% to the Nostocales. From 92 cyanobacterial strains isolated from Indonesian samples, 17.4% were allocated to the Chroococcales, 38.0% to the Oscillatoriales, 34.8% to the Nostocales and 9.8% to the Stigonematales.

About 60 biomass extracts of the newly established strain collection were tested against three different reporter strains for activity on Quorum Sensing (QS) systems, antimicrobial activity against *Bacillus subtilis* and *Staphylococcus aureus*, and against the cysteine protease rhodesain. The Cathepsin L like cysteine protease rhodesain plays an essential physiological role in the metabolism of the parasite *Trypanosoma brucei*. A human infection with *Trypanosoma brucei* is known as human African trypanosomiasis (HAT). Because of its important role, rhodesain is regarded as a promising target for the development of new medications. Of 52 tested extracts, 11.5% showed more than 50% inhibition of rhodesain at 0.1 mg/mL. Although 27 of the tested strains belonged to Oscillatoriales (III), only 7.4% of all tested Oscillatoriales strains showed pronounced inhibitory activity, while 15.4% of the Chroococcales (I), 12.5% of the Nostocales (IV) and 25% of the Stigonematales (V) strains showed more than 50% inhibition. Five of the screened extracts, revealing interesting bioactivity combined with a promising chemical profile, were selected for more intensive evaluation. The obtained HPLC-DAD and HPLC-MS data were assessed, and several known and new intriguing, possibly bioactive compounds could be identified.

Additionally, a library of 572 cyanobacteria extracts (kindly provided by Cyano Biotech GmbH, Berlin, Germany), was screened against the trypanosomal cysteine protease rhodesain. The screening revealed 2.7% of the biomass extracts showing an inhibitory activity of more than 70% at 0.1 mg/mL, whilst 14.8% of the medium extracts featured an inhibition higher than 70% at 0.2 mg/mL. The biomass extract of a *Nostoc* sp. strain showed 98% inhibition at 0.1 mg/mL. Processing of this promising extract resulted in the isolation of 9 compounds, from which 5 showed pronounced inhibitory activity. Due to low yields, solely one compound was subjected to nuclear magnetic resonance (NMR) experiments, which successfully led to partial elucidation of this compound with a mass of $[M+H]^+$ m/z 604.24 and a suggested molecular formula $C_{24}H_{38}N_5O_{13}$, comprising a sugar backbone (triose) and a nitrogen-rich side chain.

With an inhibition of more than 90%, a distinct *Nostoc* sp. medium extract revealed conspicuous activity. We identified the known compound nostotrebin 6 and several novel biosynthetically related structures as active substances. Nostotrebin 6 is the only cyanobacterial cyclopentenedione (CDP) known to date and was already isolated from a *Nostoc* sp. biomass extract. It has been found to be active in a broad variety of assays, possibly convicting it as pan-assay interference compound (PAIN). The additionally isolated derivatives of nostotrebin 6 were found to be oligomeric molecules, composed of two core monomeric structures, a trisubstituted CPD or a trisubstituted unsaturated δ -lactone. A comparative bioactivity testing revealed possibly unspecific rhodesain inhibition, antimicrobial activity and cytotoxicity, depending on the amount of free phenolic hydroxyl groups per molecule.

To our knowledge, this work is the first to consider cyanobacteria as a source for rhodesain inhibitors. Within this study, we found 2% of a self-established biomass extract collection to show rhodesain inhibiting activity higher than 70% at 0.1 mg/mL. These results were in line with the screening of the commercial extract collection provided by the Cyano Biotech GmbH, where 2.7% of the biomass extracts showed an inhibition equal or higher than 70% at 0.1 mg/mL. Here, the section Nostocales displayed the major amount of inhibitory active strains with 55.6%. Until today, only few compounds from cyanobacteria cultivation media are known, but the present findings suggest that cyanobacteria, especially cyanobacterial medium extracts, provide a valuable source for protease inhibitors.

III. Publication

This thesis includes the following publication:

Nostotrebin 6 Related Cyclopentenediones and δ -Lactones with Broad Activity Spectrum Isolated from the Cultivation Medium of the Cyanobacterium *Nostoc* sp. CBT1153

Kossack, Ronja; Breinlinger, Steffen; Nguyen, Trang; Straetener, Jan; Berscheid, Anne; Moschny, Julia; Brötz-Oesterhelt, Heike; Enke, Heike; Schirmeister, Tanja; Niedermeyer, Timo Horst Johannes

Journal of Natural Products (2020); doi: 10.1021/acs.jnatprod.9b00885

Status in publication process: Published; 24.01.2020

Author	Author position	Scientific ideas [%]	Data generation [%]	Analysis, Interpretation [%]	Paper Writing [%]
Ronja Kossack	1	50	40	40	50
Steffen Breinlinger	2	30	30	30	22.5
Trang Nguyen	3	5	7.5	5	
Jan Straetener	4		2.5	2.5	
Anne Berscheid	5		2.5	2.5	2.5
Julia Moschny	6		2.5	2.5	
Heike Brötz-Oesterhelt	7		2.5	2.5	2.5
Heike Enke	8		2.5		
Tanja Schirmeister	9				2.5
Timo Horst Johannes Niedermeyer	10	15	10	15	20

1. Introduction

1.1. Microbial Diversity as Source for Natural Products

Microorganisms represent the world's largest genetic reservoir, with bacteria showing an extremely high biodiversity.¹ Due to close associations with each other, and also with plants and animals, microorganisms developed various interaction mechanisms. Within this interaction network, chemical compounds play a major role as regulatory factors, and represent a valuable source for urgently needed new antiinfectives.² Hence, natural product researchers are keen to find unexplored microbial resources. For many years, it was common belief that biodiversity hotspots like Brazil or Indonesia would serve as rampant sources for genetic material.³ Since most biodiversity hotspots, defined by the diversity of vascular plants, are located in the Global South, collaborations between countries of the southern and northern hemisphere were regarded as promising partnerships, with the first serving as providers of genetic resources and the latter ones as providers of financial capital, equipment, and know-how.^{3,4}

As many biologically active natural compounds isolated from plants or sponges were later found to be derived from associated bacteria, one might conclude that an extraordinary biodiversity of such higher organisms is reflected in the microbial diversity.⁵⁻⁹ However, microorganisms can cross the Pacific Ocean within 7 to 9 days and the Atlantic Ocean within 3 days as stowaways in dust storms, making them multinational inhabitants of our earth.¹⁰ Thus, it is not surprising, that latest publications found more than 99% sequence identity, up to 93% shared genes, and identical secondary metabolites of microorganisms isolated from locations with up to 18.000 km distance from each other.^{11,12} Differences in the genetic makeup based on geographic barriers were only identified in case of insulated habitats like geothermal hot springs or phototrophic consortia, and are restricted to about 1% of all positions in the genome.^{13,14} Thus, the hypothesis that biodiversity hotspots of vascular plants exhibit an equally valuable microbial diversity is not scientifically confirmed. Actually, 1 g soil contains about five times more bacterial species than known to date, regardless whether its origin is located in the Global North or South.³ Only a small fraction (10^4 species) of the bacterial diversity (up to 10^9 species) has been described,¹⁵ and even a smaller number has been isolated, characterized, and cultivated.¹⁶ Hence, only a small part of their potential has been exploited, and most species investigated in research and industry belong to only four of 90 bacterial phyla known so far: Actinobacteria, Firmicutes, Proteobacteria and Bacteroidetes, with the remaining ones being poorly studied.¹⁶

1.2. Morphological Diversity of Cyanobacteria

One scientifically neglected group of microorganisms is the phylum cyanobacteria (cyanoprokaryotes). Even though cyanobacteria have long been known for their broad spectrum of specialized metabolites, the interest of natural product chemists has risen only slowly.¹⁷ Cyanobacteria have been inhabiting the earth since more than three billion years, and thus belong to the oldest organisms known.¹⁸ Some fossil cyanobacteria even show a morphology similar to present species.¹⁹ During this time, they developed a highly diverse physiology allowing them to even populate extreme habitats.²⁰ Thus, cyanobacteria are particularly challenging to classify.²¹ The first classification systems were published by Gomont in 1892 and Bornet & Flauhault from 1886-1888,^{22,23} and several more have been proposed and reviewed ever since.²¹ In 1979, Rippka *et al.* proposed five sections: I (Chroococcales), II (Pleurocapsales), III (Oscillatoriales), IV (Nostocales) and V (Stigonematales),²⁴ which were adopted as fundamental base for the nomenclatural classification in Bergey's Manual of Systematic Bacteriology.²⁵ But the development of electron microscopy and molecular and genetic methods led to profound changes in the classifications systems of cyanobacteria.²¹ In 2014 Komárek *et al.* proposed a polyphasic approach, which mirrors evolutionary history and includes monophyletic taxa, though the authors admit, that such a taxonomic system is not available yet.²¹ The afore mentioned classification in five sections is shown in Table 1. These sections are not regarded as being conform with major taxa, but serve as rough classification by morphological characteristics.²⁴

Table 1. Major sub-groups of cyanobacteria by Rippka *et al.*²⁴

Section	Order	Thallus organization	Characteristics
I	Chroococcales	unicellular	Reproduction by binary fission or by budding
II	Pleurocapsales	unicellular	Reproduction by multiple fission giving rise to small daughter cells (baeocytes), or by both multiple fission and binary fission
III	Oscillatoriales	filamentous	Division in only one plane, no formation of heterocysts nor akinetes
IV	Nostocales	filamentous	Division in only one plane, formation of heterocysts and akinetes
V	Stigonematales	filamentous	Division in only one or more planes (true branching), formation of heterocysts and akinetes

Section I (Chroococales) comprises unicellular cyanobacteria, which are, regarding their morphology, the simplest cyanobacteria. They reproduce by binary fission or budding and

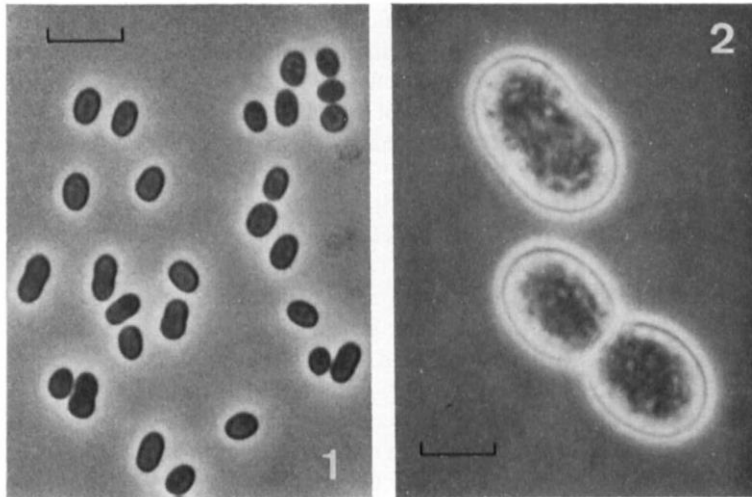


Figure 2. *Synechococcus* PCC 7335 (1) and PCC 7424 (2), respectively, as representatives for Section I. All phase contrast; bar markers represent 5 μ m. Pictures taken from Rippka *et al.*, 1979.²⁴

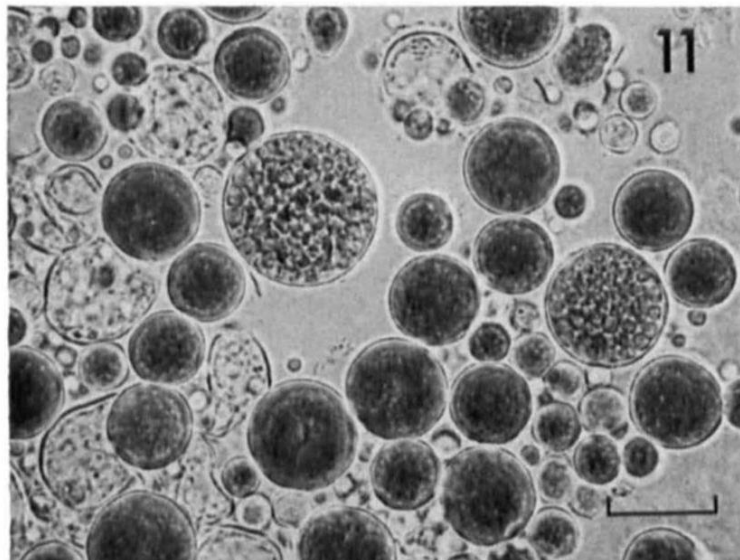


Figure 1. Representative of the pleurocapsalean genera. *Dermocarpa* PCC 7437 (11). All phase contrast; bar markers represent 20 μ m. Picture taken from Rippka *et al.*, 1979.²⁴

their cells are spherical, cylindrical or oval (Figure 2). Cyanobacteria of Section II (Pleurocapsales) are as well unicellular, but in contrast to Section I, Pleurocapsales share a special form of reproduction called multiple fission (Figure 1). Vegetative cells are always surrounded by a fibrous layer additionally to the outer membrane and reproduce by binary fission within this fibrous layer and without parallel growth. This way, the parental cell produces between 4 and 1000 so-called baeocytes (Greek: 'small cell'). The baeocytes are released when the fibrous layer breaks up.^{24,26}

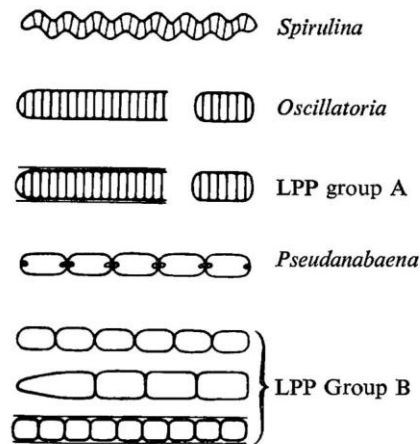


Figure 3. **Schematic presentation of genera assigned to Section III.** Thin lines surrounding trichomes designate sheath material. Polar bodies (Pseudanabaena) represent gas vacuoles. The LPP group, derives its name from many of the strains included falling within the broad confines of the genera Lyngbya, Phormidium and Plectonema.²⁴

Cyanobacteria of Sections III to V share a filamentous thallus organization. This so called trichome elongates by intercalary division. Breakage of the trichome results in short filaments (hormogonia), which can differ from the mature trichome in various properties. Some are motile, show different cell size and shape or posses gas vacuoles. In case of heterocystous cyanobacteria, hormogonia might lack heterocysts, even in a sourrounding without a source

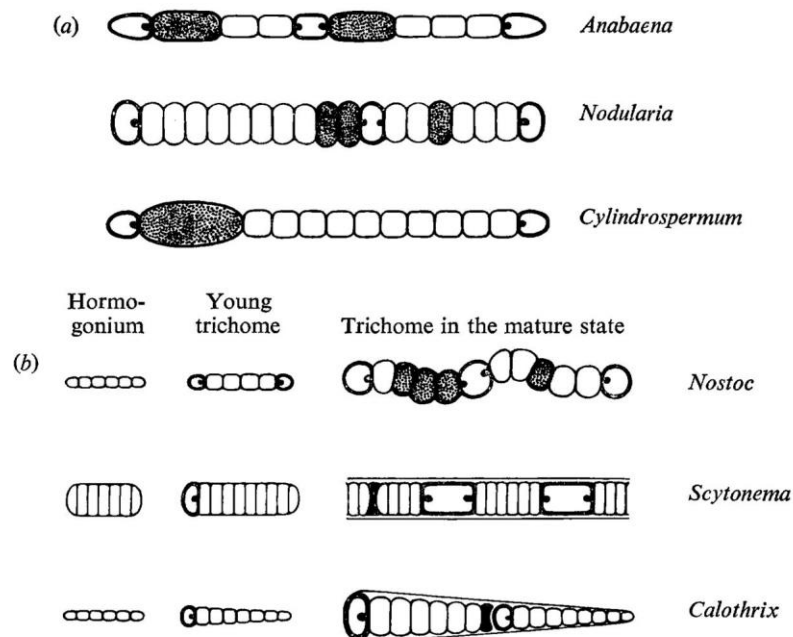


Figure 4. **Schematic presentation of genera assigned to Section IV.** (a) without developmental cycle; (b) with developmental cycle. Heavy-walled cells with polar granules represent heterocysts; heavy-walled cells that are dotted represent akinetes; thin lines surrounding trichomes designate sheath material.²⁴

of nitrogen. The always uniserate (one cell thick) trichome of cyanobacteria in Section III (Oscillatoriales, Figure 3) solely consists of vegetative cells, which may be enclosed by tubular sheaths. In contrast to Sections IV and V, Oscillatoriales are not capable of cell differentiation.

The cells of sections IV (Nostocales; Figure 4) and V (Stigonematales; Figure 5) are able to differentiate to heterocysts when no combined nitrogen source is available. These cells, which can be recognized by a thick cell wall, low pigmentation and granules, provide special anaerobic conditions and offer the perfect environment for the enzyme catalysing atmospheric N₂ fixation, called nitrogenase.²⁷ In stationary phase, some cyanobacteria of Sections IV and V produce akinetes, a form of resting cells with apparent, thick walls.²⁸

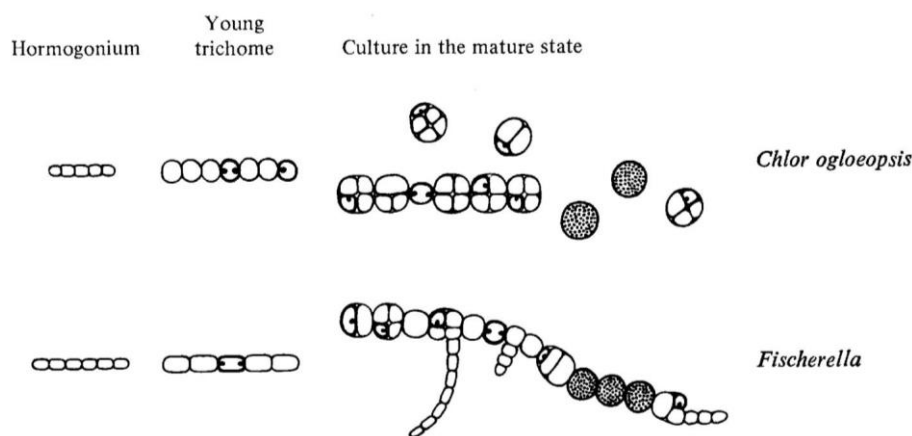


Figure 5. **Schematic presentation of the genera assigned to Section V.** Heavy walled cells with polar granules represent heterocysts; heavy-walled cells that are dotted represent akinetes; thin lines surrounding groups of cells designate sheath material.²⁴

While Section V shows division in only one plane, cyanobacteria of Section V are able to divide in more planes. Hormogonia are usually uniserate and unbranched, but cells start to divide in various planes during growth of the trichome. This so-called 'true branching', needs to be distinguished from 'false branching', which can occur in Section III and IV. Here, the trichome breaks within its sheath followed by the elongation of the two emerging daughter filaments. If one or both filaments protrude through the sheath in an angular position, it is called 'false branching'.^{24,29}

1.3. Natural Product Diversity of Cyanobacteria

In their natural surroundings, cyanobacteria compete with other phototrophs for resources, and are grazed by eukaryotic predators.³⁰ The need of defence against these environmental stressors might explain why most cyanobacterial natural products show some kind of bioactivity.³¹ Accordingly, cyanobacteria present a promising source for compounds that inhibit eukaryotes, such as fungi or protozoa. Even though this cytotoxicity restricts the potential use as anti-infectives, cyanobacterial natural products may serve as lead compounds for the development of less toxic, but still anti-infective, derivatives.³¹

Neglected by natural product researchers for a long time, cyanobacteria are nowadays recognized as a prolific source of structurally diverse and pharmacologically active natural products.³²⁻³⁵ Many cyanobacterial metabolites are composed of molecules originating from a mixture of nonribosomal peptide synthetase (NRPS), polyketide synthase (PKS), terpene, and sugar biosynthetic pathways. More than a few of those metabolites show halogenations, methyl groups or oxidations.³⁶

Several cyanobacterial metabolites have served as potent lead structures inspiring drug development programs, e.g. the dolastatins,³⁷⁻³⁹ the cryptophycins,⁴⁰⁻⁴² the saxitoxins,^{43,44} and the anabaenopeptins.^{45,46} One of the better-studied cyanobacteria genera is *Nostoc*, from which numerous compounds have been isolated.^{35,47} These are mainly non-ribosomal peptides and depsipeptides, but a variety of other chemically diverse structures, such as polyketides, alkaloids, or terpenoids, were also found. Often, cyanobacterial metabolites show pronounced cytotoxicity, but another activity that is frequently observed for cyanobacterial non-ribosomal peptides is the inhibition of proteases.^{36,48-52} A

1.3.1. Natural Products from Cyanobacteria as Protease Inhibitors

Proteases are involved in the pathogenesis of many infectious diseases,^{53,54} and promising targets for new therapeutic approaches. That is why natural product researchers are on the quest for novel protease inhibitors, and cyanobacteria are a rich source for such molecules.^{48,55,56} Freshwater, as well as marine cyanobacteria are promising resources for protease inhibitors.^{36,57} Table 2 summarizes selected cyanobacterial protease inhibitors and their activities.

^A Paragraph adapted from Kossack, R.; Breinlinger, S.; Nguyen, T.; Moschny, J.; Straetener, J.; Berscheid, A. et al. (2020) Nostotrebin 6 Related Cyclopentenediones and δ -Lactones with Broad Activity Spectrum Isolated from the Cultivation Medium of the Cyanobacterium *Nostoc* sp. CBT1153. *J. Nat. Prod.* DOI: 10.1021/acs.jnatprod.9b00885

Table 2. Activities of selected cyanobacterial protease inhibitors.

Compound	Protease Inhibition (IC ₅₀ [nM])										ref.
	Serine Proteases				Cystein Proteases						
	tr	ch	th	pl	hCatL	cr	fp2	fp3	pa		
Linear cyanopeptides											
Aeruginosin 298-A	1654	----	496	----	----	58	
Aeruginosin 102-A	273	.	55	41	59	
Gallinamide A	5	0.3	.	.	.	60	
Gallinamide A (analog 2)	12	67	.	61	
Gallinamide A (analog 3)	5	81	.	61	
Circinamide	1035	62	
Cyclic cyanopeptides											
Symplocamide A	80	0.4	55	
A90720A	10	.	259	29	63	
Cyanopeptolin S	216	64	
Cyanopeptolin A	209	65	

. no information; ---- no inhibition (no concentration); tr = trypsin; ch = chymotrypsin; th = thrombin; pl = plasmin; hCatL = Human cathepsin L; cr = cruzain; fp2 = falcipain 2; fp3 = falcipain 3; pa = papain

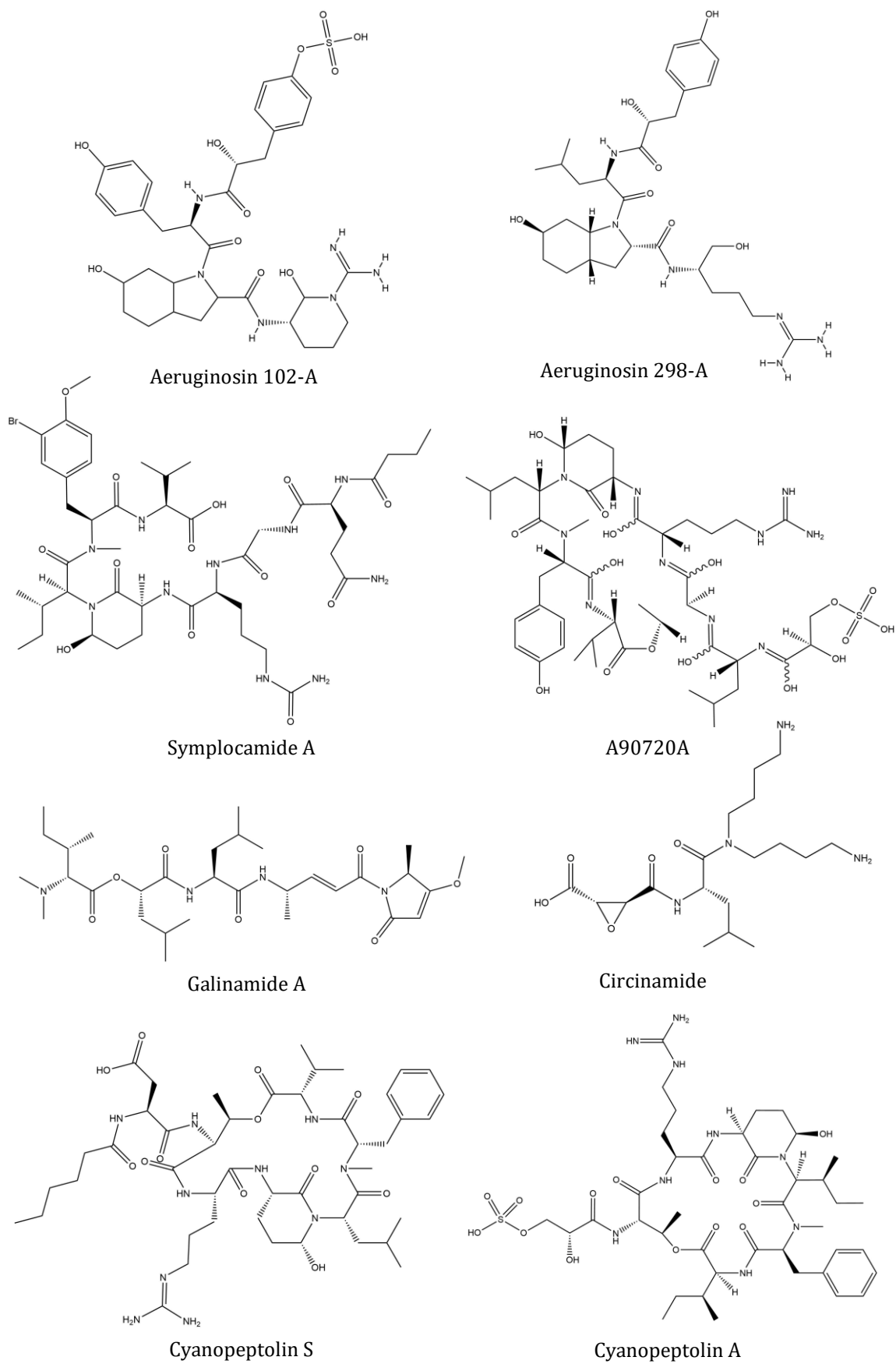


Figure 6. Selected cyanobacterial protease inhibitors; activities summarized in Table 2.

Many cyanopeptides inhibit serine proteases, which contain serine as central amino acid in their active site. Besides the amino acid sequence, the conformation and configuration of the cyanopeptides is essential for the inhibitors selectivity.⁴⁸ A potent serine protease inhibitor is the depsipeptide symplamide A, produced by *Symploca* sp., with pronounced cytotoxicity against H-460 lung cancer cells (IC₅₀ 40 nM) and neuro-2a neuroblastoma cells (IC₅₀ 29 nM).⁵⁵

As cysteine and serine comprise similar structures and properties (polar, uncharged), serine protease inhibitors might equally function as inhibitors against cysteine proteases like rhodesain. The first described cyanobacterial cysteine protease inhibitor was circinamide, a papain inhibitor isolated from *Anabaena circinalis* NIES-41.⁶² Circinamide contains 2,3-epoxy succinic acid and homospermidine, and is related to the potent cysteine-protease inhibitor E-64 from *Aspergillus japonicus*.⁶⁶ A screening of various fractionated extracts derived from marine cyanobacteria against Human cathepsin L (hCatL) revealed numerous hits and resulted in the identification of gallinamide A as a selective inhibitor.^{36,67} The cysteine protease hCatL has been identified as potential target enzyme for anticancer therapy, and related cysteine proteases are potential targets for novel treatments of various infectious diseases, like malaria, leishmaniasis and trypanosomiasis.^{68,69} Gallinamide A showed pronounced inhibitory activity against cruzain (IC₅₀ = 0.3 nM) an essential *Trypanosoma cruzi* cysteine protease.⁶⁰ And analogues of gallinamide A exhibited inhibitory activity on the cysteine proteases falcipain 2 and falcipain 3 of *Plasmodium falciparum* in a low nanomolecular range.⁶¹ In case of trypanosomiasis, the cysteine protease rhodesain is considered as valuable target, but except for gallinamide A, no cyanobacterial derived compound was identified as inhibitor for hCatL or hCatL-like cysteine proteases so far.

1.4. Human African Trypanosomiasis (HAT)

Trypanosoma brucei is a protozoon belonging to the genus *Trypanosoma*, causing the parasitose Human African Trypanosomiasis (HAT or sleeping sickness). The sub-species *T. brucei rhodesiense* causes an acute form of HAT, which is endemic in eastern and southern Africa. The more common, chronic form of HAT is caused by *T. brucei gambiense* and is prevalent in western and central Africa.^{70,71} The latter one is responsible for about 95–97% of total HAT infections, while *T. brucei rhodesiense* is primarily a zoonosis, rarely infecting humans, thus causing only 3-5% of total HAT infections.^{72,73} Interestingly, around two-thirds of cases occurring outside of Africa in the US and Europe are visitors of safari parks in eastern Africa, infected by *T. b. rhodesiense*.⁷⁴ Even though HAT caused by *T. b. rhodesiense* represents only a small part of infections, its elimination is rather complicated, as cattle serve as reservoirs for the human parasite (Figure 7).⁷⁵

In 1998, the World Health Organisation (WHO) reported about 300,000 new cases of HAT every year.⁷⁶ Since then, the cooperation of the WHO, African governments, non-governmental organisations (NGOs), charities, and others led to a fast and sustainable decrease in the annual number of new infections, with only 1446 reported cases in 2017.^{73,77}

1.4.1. Lifecycle of *T. brucei rhodesiense* and *gambiense*

The lifecycle of Life cycle of *T. b. gambiense* and *T. b. rhodesiense* is pictured in Figure 7. The infectious metacyclic trypomastigotes are transmitted by the bites of tsetse flies (genus *Glossina*), causing a skin reaction known as trypanosomal chancre within 5-15 days ①. After proliferation into bloodstream trypomastigotes, the parasites diffuse in the bloodstream, initializing the early “hemolymphatic stage” ②. The parasite starts to migrate into the lymph nodes, spleen and spinal fluid, leading to nonspecific symptoms like fever, malaise, muscle aches and headache, and replicates by binary fission ③. During this early stage, or stage one, symptoms are unspecific and easily confounded with other infectious diseases like malaria.⁷⁸ Untreated, the late stage, acute phase or “meningo-encephalitic stage” is induced by the penetration of the parasite into the central nervous system, revealing characteristic symptoms like psychiatric, motor and sensory disturbances, and abnormal reflexes ④.

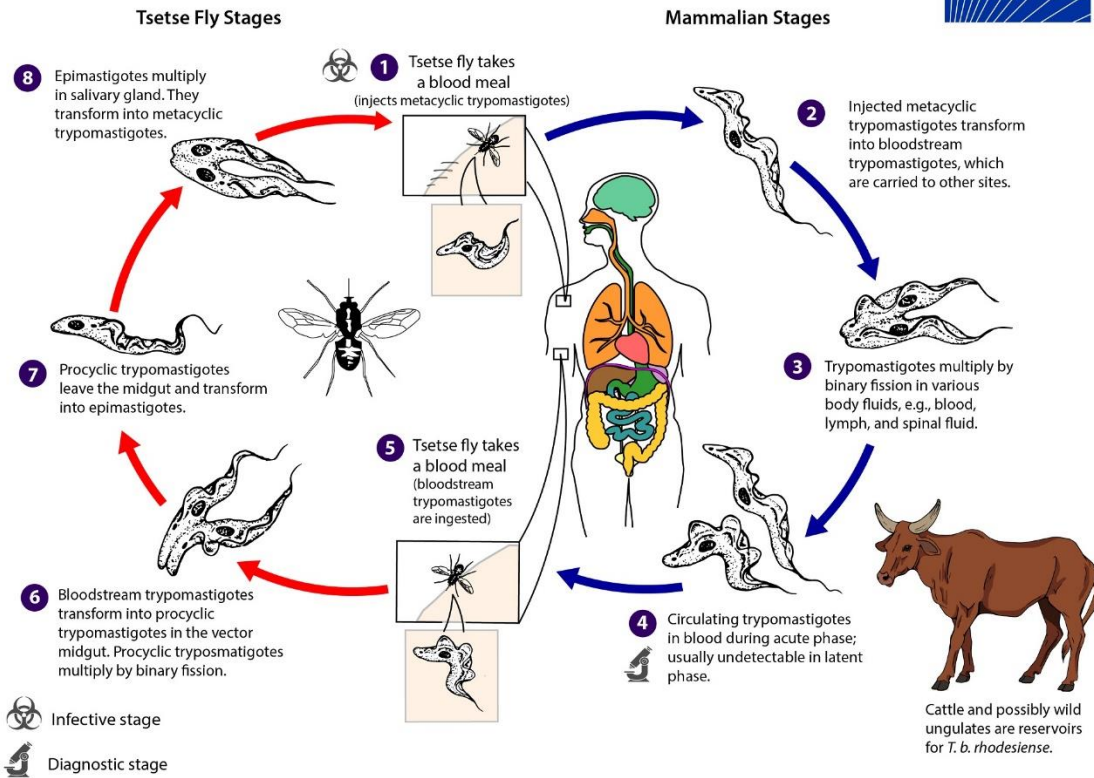


Figure 7. Life cycle of *T. b. gambiense* and *T. b. rhodesiense*.⁷⁴

The disease's trivial name, sleeping sickness, originates from the severe sleep disturbance shown by about three-quarters of patients.⁷⁹ Untreated, the infection leads to coma and death. The circulating trypomastigotes are usually solely detectable during the acute and not in the latent phase. When a tsetse fly bites an infected mammalian host, which can be cattle or wild ungulates in case of *T. b. rhodesiense*, it ingests bloodstream trypomastigotes (5). Here, the parasites first transform into procyclic trypomastigotes (6), and after leaving the midgut, proliferate into epimastigotes (7). The epimastigotes immigrate into the fly's salivary glands and reproduce by binary fission (8). The lifecycle in the tsetse fly spans about 3 weeks.⁸⁰

1.4.2. Diagnosis

Most contemporary staging methods rely on the counting of white blood cells (WBC) and the microscopic detection of trypanosomes in the bloodstream, within the lymph nodes, or in the cerebrospinal fluid (CSF).⁷⁵ According to the WHO, patients showing ≤ 5 WBC/ μ L and no trypanosomes are in the first stage of the disease, while patients having more than 5 WBC/ μ L and/or if trypanosomes are detected in the CSF are considered as stage 2 or acute stage.⁷³ As these diagnosis methods show weak accuracy and are only applicable in late stages, new

assessments like rapid diagnostic tests (RDTs) have been developed. The SD BIOLINE HAT, used for the detection of *T. brucei gambiense*, is highly specific and sensitive, and identifies distinctive variable surface glycoproteins (VSG).⁷⁸ Still, more reliable tests for the detection of *T. brucei rhodesiense* are lacking. One possibility is to apply immune mediators used for the staging of *T. b. gambiense* HAT to stratify *T. b. rhodesiense* patients. Here the measurement of Immunoglobulin M (IgM), matrix metalloproteinase 9 (MMP-9) and chemokine (C-X-C motif) ligand 13 (CXCL13), alone or combined with chemokine (C-X-C motif) ligand 10 (CXCL10) were positively evaluated as markers for the detection of the meningo-encephalitic stage of *T. b. rhodesiense* HAT, enabling to adjust the treatment.⁸¹

1.4.3. Treatment

As trypanosomes are able to elude the host immune system by antigenic variation of their VSGs, development of a preventive vaccine is not possible.⁸² Furthermore, a drug for the safe treatment of both early-stage and late-stage of rhodesiense HAT is still not available. Currently recommended drugs for the treatment of rhodesiense HAT are Suramin and Melarsoprol (Figure 8).

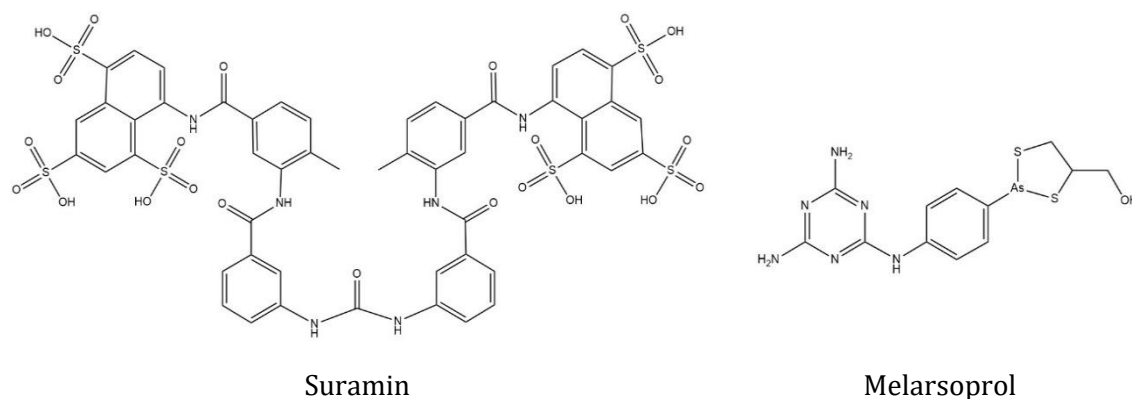


Figure 8. **Suramin and Melarsoprol: Currently recommended drugs for the treatment of rhodesiense HAT.**

Suramin was introduced in 1922 and has been used for the therapy of early stage HAT ever since. Its mode of action is still not fully understood, though it is known not to cross the blood-brain barrier. Common secondary effects include urticarial rash, pyrexia, nausea, and reversible nephrotoxicity.⁸² While treatment for early-stage rhodesiense HAT is effective and shows only mild side-effects, the only known therapy for the late-stage is Melarsoprol.⁷⁷ Melarsoprol causes post-treatment reactive encephalopathy (PTRE) in ~8% of patients and fatalities in ~57% of these cases, and is therefore one of the most apprehensive drugs used for therapy of infectious diseases.⁸³ The treatment with Melarsoprol can further cause side-effects like agranulocytosis, skin rashes, peripheral neuropathy, cardiac arrhythmias, and

multifocal inflammatory disorder.⁷⁷ In case of central nervous system (CNS) *T. b. gambiense*, the first-line therapy is NECT (nifurtimox–eflornithine combination therapy), but this mixture is not effective against CNS *T. b. rhodesiense*.⁷⁷ In-vitro and in-vivo studies proved fexinidazole as possible agent against *T. b. rhodesiense*, but clinical trials are still on-going.⁷³

The Drugs for Neglected Diseases Initiative, founded in 2003 by seven partners, all of which are centres of excellence in neglected disease research and/or patient care, published a target product profile (TPP) for an ideal drug which would be effective against both early- and late-stage disease.⁸⁴ The profile includes oral administration over a relatively short course (i.e., 7 days), safety for all persons including children and pregnant women, and less than 30€ costs per course. It is obvious that the present therapies against HAT do not satisfy those criteria, and more effective and less harmful drugs are needed. Hence, research projects are running, and latest achievements indicate improvements in the next decade.⁸⁵ Parasitic enzymes with human homologues are considered as interesting drug targets, as already available technologies developed for targeting human enzymes could be exploited. Issues regarding parasite compared to host specificity could be addressed by adding parasite-specific structural features.⁸⁶ Cysteine proteases of the papain superfamily represent such a group of enzymes, which is omnipresent in humans and protozoans. Due to their important function in parasitic infection, they are expedient targets for the therapy of various parasitic diseases.⁸⁷

1.4.4. Rhodesain as Target for New Treatments

One promising target is the trypanosomal cysteine protease rhodesain. Rhodesain plays a major role during the parasitic infection by *T. brucei*.⁵³ It is involved in the parasitic crossover of the blood-brain-barrier into the CNS, leading to the late-stage of HAT.⁸⁸ This crossover is initiated by rhodesain-induced stimulation of protease-activated receptors (PARs), which trigger calcium-signaling pathways in their activated form. Thus, changes in the cytoskeleton of the endothelial cells occur, enabling the parasite to migrate from the bloodstream to the CNS.⁸⁹ Moreover, rhodesain influences the synthesis of the VSGs, antigenic proteins, enabling *T. brucei* to elude the host immune response, and destroys anti-VSG immunoglobulins.^{90,91}

The cathepsin L-like cysteine protease rhodesain belongs to the family C1 (papain-family) and comprises a single polypeptide chain of 215 amino acids with a classic papain-like folding, where the catalytic triad (Cys25/His162/Asn182) is embraced by a left (L) and a right (R) domain. Its catalytic mechanism is comparable to other cysteine proteases: the weak nucleophilic thiol group of the Cys25 residue is converted into a highly nucleophilic thiolate ion, involving the His162 and the Asn182 residue. The latter one acts as a H-bond acceptor and stabilizes the required tautomeric form of the His162 imidazole ring, which functions as a base and is involved in deprotonating the thiol group of the Cys25 residue. The so-generated nucleophilic thiolate attacks the carbonyl carbon of the fissile amide bond, and further amino acid residues, situated in the active site, support peptide bond hydrolysis, and thus the recovery of free enzyme.⁵³ Due to its complex and extensive role in the lifecycle of *T. brucei rhodesiense*, rhodesain is regarded as a promising target for the development of

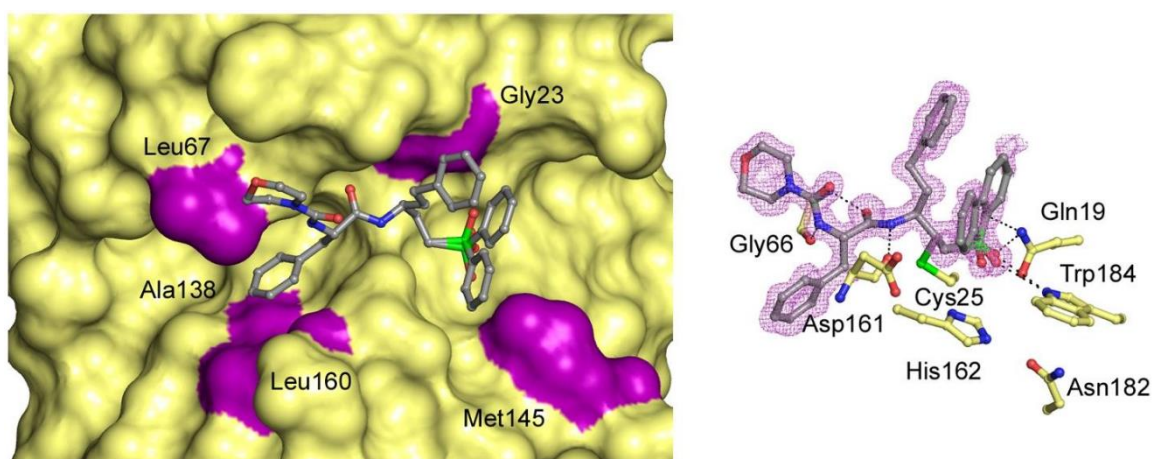


Figure 9. **Surface (left) and ball and stick (right) active site representations of the rhodesain•K11002 complex.** The inhibitor molecule is coloured grey, and the unbiased mFo-DFc electron density is coloured violet. Hydrophobic interactions with neutral/non-polar residues are mapped on the surface and coloured purple.⁹³

novel anti-trypanosomatid drugs.⁵³ The determination of the high-resolution crystal structure of rhodesain in complex with the vinyl sulfone inhibitor K11002 (Figure 9) led to intensive studies on rationally designed inhibitors.^{92,93} Rhodesain shows high structural

similarity to other hCatL-like cysteine proteases, exhibiting crucial roles in various infectious diseases, like malaria, leishmaniasis and trypanosomiasis.^{68,69}

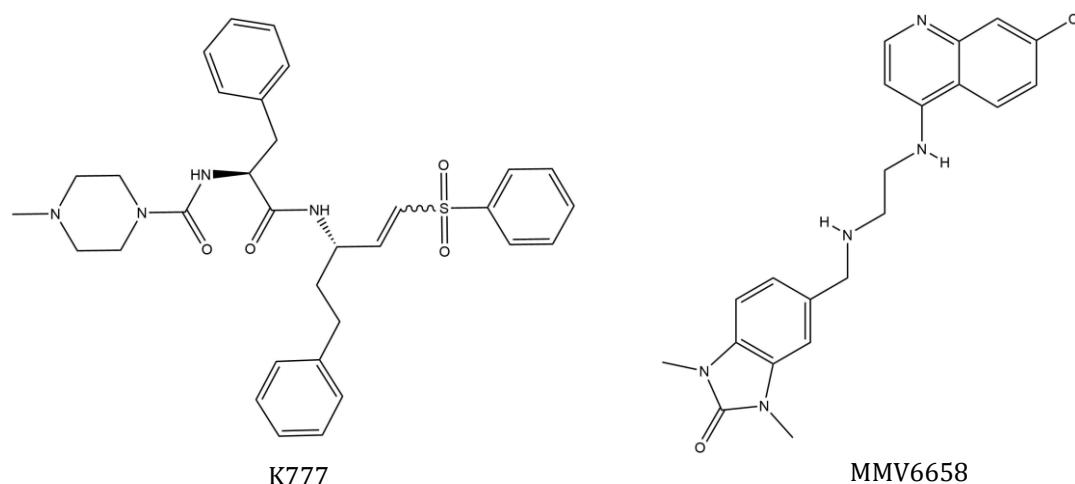


Figure 10. The rhodesain inhibitors K777 and MMV665875.

Thus, it is not surprising that compounds of the Open Access Malaria BOX showed inhibitory activity against rhodesain.⁹⁴ Here, a dimethylbenzimidazol (MMV665875) (Figure 10) was identified as novel mixed rhodesain inhibitor with a K_i of 1.4 mM and an IC_{50} of 0.4 μ M against *T. brucei rhodesiense*.⁹⁵ In the same study, as well as in others by the same research group, a benzimidazole ring was observed in most of the rhodesain inhibitory structures.⁹⁶ Further, various thiosemicarbazones, known as antiparasitic agents against *Plasmodium falciparum* and *Trypanosoma cruzi*, were found to be active against parasitic cysteine proteases, including rhodesain.⁹⁷⁻⁹⁹ Another promising group of rhodesain inhibitors are nitroalkenes,

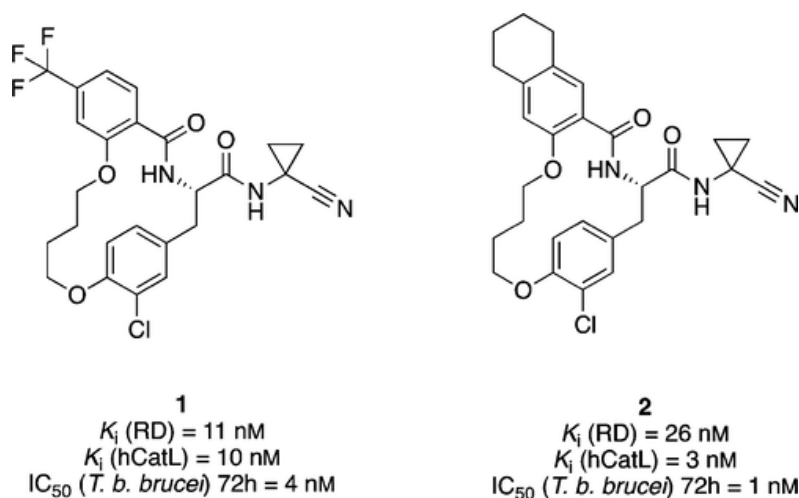


Figure 11. Structure of two rhodesain inhibiting macrocyclic lactams (1, 2). Binding affinities for rhodesain and hCatL, and cell-growth inhibition of *T. b. brucei*.¹⁰²

inspired by K777 (Figure 10), which show prominent activity against rhodesain and cruzain and are potent and safe in rodent, canine and primate models.⁹³

Due to the mentioned high similarity of rhodesain and hCatL,¹⁰⁰ a hCatL ligand library was screened against rhodesain and several macrocyclic lactams (Figure 11) were identified as potent rhodesain inhibitors. Modifications of the most active structure, led to a potent pyrazole derivative ($K_i < 10$ nM), showing as well pronounced trypanocidal activity (IC_{50} (*T. b. rhodesiense*) < 400 nM).¹⁰¹ But, regardless of the efforts in the past decades and many promising rhodesain inhibitors, none could be identified as potential drug candidate. Thus, research is ongoing. Even though cyanobacteria are known to produce structurally diverse protease inhibitors, no screening of cyanobacteria extracts for rhodesain inhibitors has been published yet.

1.5. Research Objective

Cyanobacteria have long been neglected by natural product research,^{30,35,102} and are treasured sources for cytotoxic and antimicrobial metabolites, as well as for protease inhibitors.^{36,48,55-57} Proteases are promising targets for new therapeutic approaches, due to their crucial role in the pathogenesis of many infectious diseases.^{53,54} The cysteine protease rhodesain is a promising target for urgently needed new therapies against HAT, as it plays a major role during the parasitic infection by *T. brucei*.^{53,88-91}

The major aim of my work was to identify and isolate rhodesain inhibitors from cyanobacteria, embedded in the binational Indonesian-German project "Accessing Novel Bacterial Producers from Biodiversity-rich Habitats in Indonesia" (ANoBIn). The three main workpackages comprised: (I) Establishing a cyanobacteria strain and extract collection. (II) Bioactivity screening of the established extract collection, identification and isolation of the active compounds. (III) Screening of a commercial cyanobacteria extract collection against the trypanosomal cysteine protease rhodesain.

(I) Promising habitats in Indonesia and Germany, like ponds, rivers, and biofilms from varying surfaces were sampled, in order to collect a broad diversity of cyanobacteria strains. Different techniques led to the isolation, characterization and biobanking of morphologically distinct cyanobacteria strains. Selected strains were cultivated to generate biomass for extract production.

(II) The resulting biomass extract collection was screened for bioactivities (quorum sensing inhibition, antimicrobial activity, rhodesain inhibition). The most promising hit extracts were analyzed by high-performance liquid chromatography (HPLC) coupled with a diode array detector (DAD) and mass spectrometer (MS). The cyanobacterial extracts were evaluated regarding their chemical composition, in order to identify novel bioactive compounds.

(III) In a third part a cyanobacteria extract collection (kindly provided by Cyano Biotech GmbH, Berlin, Germany) was screened in cooperation with Prof. Dr. Tanja Schirmeister (Johannes Gutenberg University, Mainz) against the trypanosomal cysteine protease rhodesain.

2. Material & Methods

2.1. Instruments

Table 3. **Components of HPLC systems; Tübingen University.**

System	Specification	Component
Agilent 1200 Series	G1379B	Degasser
	G1312A	Binary Pump
	G1367B	Autosampler
	G1330B	Thermostat
	G1316A	Column Compartment
	G1315B	Diode Array Detector
Agilent 1260 Infinity	G4225A	Degasser
	G1312C	Binary Pump
	G1329B	Autosampler
	G1330B	Thermostat
	G1316A	Column Compartment
	G1315D	Diode Array Detector
	G1346C	Fraction Collector
Agilent 6330 IonTrap		Electron Spray Ionization (ESI-) Ion Trap
Sedex LT-ELSD	Model 85LT	ELSD
La Prep, VWR international	P110, P314	Preparative LC System

Table 4. **Components of HPLC systems; Halle University.**

System	Specification	Component
UltiMate 3000 HPLC system, Thermo Scientific	LPG3400SD	Quaternary Pump
	WPS-3000TSL	Autosampler
	TCC-3000SD	Column Oven
	DAD-3000	Diode Array Detector
	AFC-3000	Fraction Collector
UltiMate 3000 HPLC system, Thermo Scientific	DGP-3600A	Quaternary Pump

	WPS-3000TSL	Autosampler
	TCC-3100 1x2P-10P	Column Oven
	PDA-3000	Diode Array Detector
Q Exactive Plus, Thermo Scientific		ESI-quadrupole-Orbitrap
Sedex 85, Sedere	Sedex 85 LT	Evaporative light scattering detector (ELSD)

2.2. Establishing a Cyanobacteria Strain Collection

Environmental samples were collected in Germany and Indonesia, in order to isolate cyanobacteria strains and investigate their secondary metabolite profile. As the project aimed for a diverse cyanobacteria strain collection, samples of various habitats were taken; e.g. biofilms from soil, stone or plastic and water samples from small ponds, lakes and rivers.

2.2.1. Media

For the isolation and cultivation of cyanobacteria, BG11 medium was prepared according to Rippka *et al.* (Table 5) with slight modifications.²⁴ The medium was composed of stock solutions, which were sterilised separately by autoclaving (121 °C, 21 min., 2 bar) or, in case of heat-sensitivity (Table 5: 8, 10, 11) by filtration (0.2 µm). Cycloheximide was solely added during sampling and isolation of new strains, in order to inhibit the growth of eukaryotic microorganisms. For the preparation of solid medium, agarose was used. Depending on the application (sampling, isolation, or maintenance), the amount and composition of stock solutions was varied. In order to favour the growth of nitrogen-fixing cyanobacteria strains, stock solution 1 was omitted and the resulting medium was called BG11-N. For the cultivation of marine cyanobacteria, artificial seawater, instead of deionized water, was used.¹⁰³

Table 5. **BG11 medium composition, modified.**

Stock	Component	Concentration	
		c(stock) [mM]	c(final) [mM]
1	NaNO ₃	3529.83	17.65
2	K ₂ HPO ₄	89.68	0.18
3	MgSO ₄ *7H ₂ O	60.85	0.30
4	CaCl ₂ *2H ₂ O	244.86	0.24
5	EDTA	0.68	0.00
6	Na ₂ CO ₃	75.48	0.38

7	Citric acid		31.23	0.03
	Ammonium ferric citrate (18%)		22.90	0.02
8	Trace Metal Mix	H ₃ BO ₃	46.26	0.0463
		MnCl ₂ *4H ₂ O	9.15	0.0091
		ZnSO ₄ *7H ₂ O	0.77	0.0008
		Na ₂ MoO ₄ *2H ₂ O	1.61	0.0016
		CuSO ₄ *5H ₂ O	0.32	0.0003
		Co(NO ₃) ₂ *6H ₂ O	0.17	0.0002
9	NaHCO ₃		1000.00	1.00
10	TES		1000.00	1.00
11	Cycloheximide*		71.09	1.00
				c(final) [g/L]
12	Agarose [°]			6

* Added for sampling and during the isolation process

[°] Added for preparation of solid medium

2.2.2. Sampling Procedure

2.2.2.1. Blooms and Biofilms

Samples of cyanobacterial blooms and biofilms on stone, soil, bark, or other surfaces were collected with a lab spoon or cotton stick, (A, enrichment culture) transferred directly into 5 mL liquid medium (15 mL centrifuge tube), (B) and streaked on an agar plate (30 mm petri dish), both with and without the main nitrogen source (stock 1). Thus, the isolation of different cyanobacteria strains, depending on their growth behaviour/ physiology could be achieved. In the field, all environmental samples were illuminated either by indirect sunlight or by LED lamps (LUMIstixx, OSRAM GmbH, Munich). As soon as the strains were transferred to the lab, samples were stored in an illuminated climatic chamber at 29°C and 10-25 $\mu\text{mol m}^{-2} \text{s}^{-1}$. Each sample was checked for cyanobacteria colonies, visible by eye, once a week. In case of cyanobacterial growth, which occurred after one week up to several months, the sample was analysed by light microscopy and forwarded to strain isolation and purification (2.2.3).

2.2.2.2. Waterbodies

Water samples were either directly supplied with culture medium, or the phytoplankton was enriched beforehand using a plankton net (mesh width: 25 μm or 50 μm). For this purpose,

the net was thrown into the water body, pulled back and forth for some minutes and pulled out. Each water sample was mixed with BG11 stock solutions to gain a nutrient concentration of 20 %, 50 %, or 100 % of the original BG11 medium. Thus, the isolation of different cyanobacteria strains, depending on their growth behaviour and physiology was attained by enrichment culture.

2.2.3. Strain Isolation and Purification Techniques

For the isolation and purification of cyanobacteria from environmental samples, various techniques were combined depending on the nature of the sample. The condition of each isolate, e.g. contamination and morphology, was checked by microscopy (Axio Lab.A1, ZEISS, Germany). As soon as an unialgal culture was obtained, it was transferred into liquid culture and stored as described in section 2.2.5.

2.2.3.1. Single-Cell Isolation

A single cyanobacteria cell was picked with an extended Pasteur pipette and then transferred into a sterile medium droplet.¹⁰⁴ This procedure was repeated until a single cell, free of any visible contamination, could be placed on a Petri dish with BG11 agar (BG11 mineral nutrient medium containing 1.5 % agarose).²⁴

2.2.3.2. Separation by Filtration

Water samples were filtrated (quantitative filter paper, VWR, 84 g/m², 0,18 mm, pore size: 31-50 µm). The filtrate (I), as well as the filter paper (II) were added to 20 mL BG11 medium (0.1% cycloheximide) in a 50 mL shake flask, and incubated at 28°C with an illumination of 10 to 25 µmol m⁻² s⁻¹ for 5-30 days (enrichment culture). After evaluation under the microscope, a small amount of biomass grown in the liquid culture (I) or on the filter paper (II) was placed on a Petri dish with BG11 solid medium and further processed as described in 2.2.3.3 and 2.2.3.4.

2.2.3.3. Phototaxis

Some cyanobacteria strains grow towards the light. These strains can be isolated via phototaxis by covering the inoculated space over an agarose plate with aluminium foil. The phototaxis-capable strain grows towards the light and can thereby be separated from other cyanobacteria in the sample.¹⁰⁴

2.2.3.4. Streak Plate Method

For the isolation of unialgal strains, aliquots of each sample were spread on BG11 solid medium by three phase streaking. Inoculated plates were incubated (28°C, 10 to 25 $\mu\text{mol m}^{-2} \text{s}^{-1}$) for 2-8 weeks.⁹⁸ Visible cyanobacterial colonies were again spread on BG11 solid medium in order to gain unialgal isolates. The thus purified strains were identified under the light microscope and characterized by their morphology (2.2.4).

2.2.4. Taxonomy

Strain morphology was characterized using a microscope (Axio Lab.A1, ZEISS, Germany) equipped with a digital camera. Filaments, trichomes, cell sizes were measured, and characteristic properties were noted.

In a first step, each cyanobacterium strain was assigned to one of the five sections as described by Rippka *et al.* (Table 1) and further described according to the modern classification system of cyanobacteria.^{21,24}

2.2.5. Strain Maintenance

The isolated, unialgal strains were maintained in glass tubes equipped with SILICOSEN® sterile stoppers, filled with 3 mL BG11 medium, at 28°C with an illumination of 10 to 25 $\mu\text{mol m}^{-2} \text{s}^{-1}$. Depending on the individual growth behaviour, strains were transferred to fresh medium every 4 - 8 weeks. To prevent loss of strains, old cultures were stored at 24°C for at least 3 months as backups.

2.3. Establishing a Cyanobacteria Extract Collection

2.3.1. Biomass Production

In order to investigate the secondary metabolite profile of the newly isolated strains, culturing was performed in different ways to obtain biomass and supernatant. The cultivation method depended on the characteristic growth behaviour of each strain, e.g. its sensibility to shear stress or light.

2.3.1.1. Cultivation in Aerated 50 mL Centrifuge Tubes

Most strains were cultured in 50 mL centrifuge tubes aerated with air or air supplied with 2 % CO₂. Each tube was filled with 10 mL BG11 medium (modified, depending on the strain's requirements), inoculated with a small amount of the maintained culture, and incubated at 28°C and a light intensity of 10 μmol photons s⁻¹ m⁻² for 5 to 10 days.

Next, 15 mL fresh BG11 medium were added, resulting in a volume of 25 mL, and the light intensity was increased to 20-25 μmol photons s⁻¹ m⁻². Depending on the growth of each culture, 10 mL fresh medium were added again after 5 to 10 days, and the aeration was adjusted to air supplied with 2 % CO₂. Due to evaporation losses, the volume was checked every 5 - 10 days and, in case of volume reduction, refilled with sterile Millipore water or fresh BG-11 medium, depending on the growth of the strain. During the cultivation period of at least 21 days, the pH of the cultures was monitored to prevent acidification by the supplied CO₂.

2.3.1.2. Cultivation in Aerated Laboratory Bottles

In order to produce a higher amount of biomass, or in case of insufficient growth in 50 mL centrifuge tubes, strains were cultivated in 250 mL laboratory bottles, aerated with air or air supplied with 2 % to 5 % CO₂. About 50 mL preculture, obtained from cultivation in centrifuge tubes, was filled up with BG11 medium (modified, depending on the cultured strain) up to 200 mL in a 250 mL laboratory bottle. Due to evaporation losses, the volume was adjusted every 5 - 10 days with sterile Millipore water or BG11 medium, depending on the growth of the strain. During a cultivation period of at least 21 days, the pH, optical density (OD) at 750 nm and dry weight (dw) (2.3.1.5) of the culture was monitored, depending on the characteristics of each strain.

2.3.1.3. Cultivation in Shake Flasks

Some strains showed slow or no growth in aerated 50 mL centrifuge tubes, thus they were transferred to 50 or 100 mL shake flasks. In order to optimize their culturing conditions, two light intensities (10 or 25 μmol photons/s/m²), BG11 medium with and without nitrogen source, and a shaking agitation of 50, 100, or 150 rpm was evaluated. Depending on the characteristics of each strain, monitoring was performed as described in (2.3.1.5).

2.3.1.4. Cultivation in High-Density Cultivators

The cultivation in High-Density Cultivators (10 mL or 100 mL), CellDeg GmbH, Berlin, was carried out according to the user manual. Varying light intensities (10 to 50 μmol

photons/s/m²) were applied, depending on each strains properties and growth stage. BG11 medium with and without nitrogen source, and a shaking agitation of 50, 100, or 150 rpm was evaluated. Depending on the characteristics of each strain, monitoring was performed as described in (2.3.1.5).

2.3.1.5. Growth Monitoring

Monitoring of the cultivation was adjusted to each strain, depending on its morphology and growth behaviour; e.g. Chroococcales growing in suspension were monitored by pH, optical density (OD) and dry weight (dw), whereas Stigonematales were only monitored by pH and evaluated via light microscopy (Axio Lab.A1, ZEISS, Germany). Therefore, samples were taken every 2 - 7 days, depending on the growth behaviour of the strain.

The OD was determined at a wavelength of 750 nm (OD₇₅₀) in semi-micro cuvettes with 1mL filling volume using a Biomate 3S spectrometer (Thermo Fischer Scientific). BG11 medium was set as blank value and samples with a high density (OD₇₅₀ ≥ 0.8) were diluted with BG11 medium to 0.2 ≤ OD₇₅₀ ≤ 0.8.

In order to determine the dw biomass, 2 mL test tubes were dried at 80°C for at least 24 h. After cooling down in a desiccator for 15 min the empty test tubes were weighed. For each sample two test tubes were filled with 0.5 mL culture broth and centrifuged at 14,000 rpm for 10 min. While the supernatant was discarded, the pellet was washed two times with deionised (DI) water and dried at 80°C for at least 2 days before weighing.

2.3.1.6. Recovery of Biomass and Medium

After cultivation, 30 mL culture were centrifuged for 10 min at 4,500 rpm and 20 °C. The supernatant was transferred to a 50 mL centrifuge tube for solid phase extraction and stored at -20 °C for later processing. The pellet was washed carefully with 10 mL deionized water and centrifuged again as described above. After discarding the supernatant, the washed pellet was frozen, freeze-dried, and stored at -20 °C.

2.3.2. Preparation of Biomass Extracts

About 0.025 g to 6.5 g of freeze-dried biomass were resuspended in 2 to 100 mL of 50 % (v/v) MeOH in H₂O. The samples were sonicated (Branson sonifier 250; Branson Ultraschall) twice for 2 min (output control 5, duty cycle 50 %) and shaken overhead for at least 20 min. After repeating the sonification and shaking overhead one more time, the samples were centrifuged

for 20 min at 6000 rpm to 14000 rpm (depending on the tube) at 10 °C. The supernatant was transferred into an adequate tube and dried by vacuum centrifugation (EZ-2 Elite; Genevac) or rotary evaporation.

The remaining pellet was resuspended in another 2 to 100 mL of 50 % (v/v) MeOH in H₂O, and the extraction was repeated. The resulting supernatant was combined with the already dried extract and dried again. The two extraction steps were repeated with 80 % (v/v) MeOH, and all supernatants were combined, dried by vacuum centrifugation (EZ-2 Elite; Genevac) or rotary evaporation until the MeOH was evaporated, freeze dried (Lyovac GT2, Oerlikon Leybold Vacuum GmbH) and stored at -20 °C, while the extracted biomass pellet was discarded. During the extraction process, the samples were kept cool on ice, when possible.

2.4. Bioactivity Screening

A collection of 572 cyanobacteria extracts, provided by Cyano Biotech GmbH, Berlin, Germany, was screened for inhibitory activity against rhodesain.

2.4.1. Rhodesain Inhibition Assay

The cyanobacteria extracts were analysed for their inhibitory activity against rhodesain by a fluorimetric enzyme inhibition assay. The assay was based on the ability of rhodesain to cleave the substrate benzyloxycarbonyl-phenylalanylarginine-4-methylcoumaryl-7-amide (Z-Phe-Arg-AMC), resulting in the fluorescent product 7-amino-4-methylcoumarin. The intensity of the fluorescence correlates with the activity of the enzyme.

The assay was performed in white 96 well plates (Lumitrac 600 white 96-well microplates, Greiner Bio-One). Each sample was composed of 185 μ L assay buffer (Table 7), 5 μ L rhodesain solution (Table 6) (received from Prof. Dr. Tanja Schirmeister, Johannes Gutenberg-Universität Mainz Germany), 5 μ L of DMSO as negative control or extract dissolved in DMSO (40 mg/mL, concentration in assay: 0.1 mg/mL for biomass extracts, 0.2 mg/ml for medium extracts), and 5 μ L substrate solution (400 μ M in DMSO). Each sample was measured as duplicate.

A kinetic measurement over ten minutes in intervals of 30 s was performed with a Tecan infinite M200 pro plate reader (Tecan Trading AG, Switzerland) (excitation wavelength: 380nm, emission wavelength: 460nm, ex. slit: 10 nm, em. slit: 20nm, temperature at about 25°C, manual gain: 40, Z-Position: 18400, number of flashes: 20) and analysed with the associated software iControl (Tecan Trading AG).

The following buffers and solutions were used (Table 6; Table 7).

Table 6. **Enzyme buffer composition.**

Component	Amount [g]	Molecular weight [g/mol]	Concentration [mM]
Sodium acetate	4.1	82.03	50
EDTA	1.462	292.3	5
Sodium chloride	11.680	58.4	200
Dithiothreitol (DTT)	0.7725	154.3	5

Add to 1 L distilled water and adjust pH to 5.5 with 1 M acetic acid.

Table 7. Assay buffer composition.

Component	Amount [g]	Molecular weight [g/mol]	Concentration [mM]
Sodium acetate	4.1	82.03	50
EDTA	1.462	292.3	5
Sodium chloride	11.680	58.4	200
Brij 35®	0.012	1199.54	0.01

Add to 1 L distilled water and adjust pH to 5.5 with 1 M acetic acid.

To calculate the increase of the intensity of the fluorescence, the slope of the regression line was calculated taking the x-(time in sec) and y-values (fluorescence intensity) from 0-300 sec into account.

$$b = \frac{\Sigma(x - \bar{x}) * (y - \bar{y})}{\Sigma(x - \bar{x})^2}$$

The slope was then multiplied by 60 to convert the unit to min⁻¹. To calculate the inhibition, the quotient of b(sample) and the control b(DMSO) was first multiplied by 100, and then subtracted from 100.

$$\text{Inhibition [\%]} = 100 - \left(\frac{b \text{ sample}}{b \text{ DMSO}} \right) * 100$$

Measurements were performed in duplicates; the arithmetic mean of the inhibition values were calculated to plot the charts of rhodesain inhibition.

2.4.1.1. Determination of the Inner Filter Effect

The correction factor of the hydrolysis rate (inner filter effect) was determined for varying concentrations of the test compounds as described by Ludewig *et al.* (2010).¹⁰⁵ First, the hydrolysis rate for each inhibitor concentration ($v_{raw}(c_{inh})$) was determined, followed by a measurement of buffer, test compound, and 7-amino-4-methylcoumarin (AMC) without enzyme and substrate, and a measurement of buffer and AMC without test compound, enzyme, and substrate. The final concentration of AMC provided the same fluorescence intensity at $t_0 = 0$ as in the regular assay. The correction factor f_{corr} was calculated by:

$$f_{corr}(c_{inh}) = \frac{F(c_{AMC})}{F(c_{AMC} + c_{inh})}$$

with F as determined fluorescence at a certain AMC concentration c_{AMC} and a certain inhibitor concentration c_{inh} . The resulting correction factor was then applied to correct the regular hydrolysis rate:

$$v_{corr}(c_{inh}) = f_{corr}(c_{inh}) * v_{raw}(c_{inh})$$

with v_{raw} as uncorrected and v_{corr} as corrected, regular hydrolysis rate at a certain concentration of the inhibitor c_{inh} .

2.4.1.2. Determination of IC_{50} and K_i

The IC_{50} and K_i values were calculated using Graph Pad PRISM 6 (Graph Pad Software, USA). To determine the IC_{50} , data were fit by non-linear regression to the following equation.

$$y = y_{min} + \frac{y_{max} - y_{min}}{1 + 10^{(x - \log IC_{50})}}$$

Where y is the observed fluorescence intensity and x the concentration of the test compound. For determination of K_i the data were fit by non-linear regression to the Mixed model enzyme inhibition.

$$y = \frac{v_{max}^{app} * x}{K_m^{app} + x}$$

With v_{max} as maximum enzyme velocity in the same units as y and K_m (Michaelis-Menten constant) in the same units as x , as the substrate concentration where half-maximum enzyme velocity is achieved.

Where K_m^{app} and v_{max}^{app} were defined the following:

$$K_m^{app} = K_m * \frac{1 + I}{\alpha * K_i}$$

$$v_{max}^{app} = \frac{v_{max}}{\alpha * K_i}$$

With α expressing the affinity of the enzyme for the substrate, depending on inhibitor concentration, and K_i as is the inhibition constant, expressed in the same units as I , the inhibitor concentration.

2.4.2. Antimicrobial Activity

The antimicrobial activity of cyanobacterial raw extracts was evaluated as described in section 2.4.2.1, while the antimicrobial activities of compounds isolated from the medium extract M1153 were kindly determined by Jan Straetener (IMIT, University of Tübingen) as described in section 2.4.2.2.

2.4.2.1. Cyanobacterial Extracts

Cyanobacterial raw extracts were tested against *Bacillus subtilis* 168 and *Escherichia coli* K12 in 96 well microtiter plates (flat-bottom, clear, polystyrene, sterile; Greiner Bio-One), reducing the required amount of extract compared to a standard agar diffusion assay.

The test strain was grown in 20 mL KM1 medium in a 100 mL Erlenmeyer flask, inoculated with 40 μ L cryo culture, at 37°C and 120 rpm. After 22 hours, the OD (578 nm) was measured and adjusted to 0.1 with KM1 medium, followed by a further dilution step to an OD of 0.0025 (0.35 mL culture broth OD 0.1 + 13.65 mL KM1).

2.5 μ L of cyanobacterial extract (40 mg/mL solved in DMSO) were transferred to a 96 well microtiter plate and stored at -20°C. Once the test strain mixture (OD 0.0025) was prepared, 97.5 μ L were added to each well containing extract. The microtiter plate was sealed (96-well microplate lid, high profile (9 mm), sterile; Greiner Bio-One) to prevent evaporation and incubated for 24 h at 37 °C and 100 rpm. As growth control, 2.5 μ L DMSO were mixed with 97.5 μ L test strain mixture, while 2.5 μ L gentamicin solution (10 mg/mL in DMSO) represented the positive control. To exclude contamination, 2.5 μ L DMSO mixed with 97.5 μ L sterile KM1 medium served as sterile control.

After 24 h, growth of the test strain in each well was assessed visually. By addition of 10 μ L resazurin solution (0.25 mg/mL resazurin, 9.07 mg/mL KH_2PO_4 9.07, 3.48 mg/mL Na_2HPO_4 , pH 7.0), the viability of the test strain was assessed more accurately. While a blue colour indicated no growth (positive control), pink colouring showed bacterial growth (growth control).

2.4.2.2. Pure Compounds

The antimicrobial activity of selected pure compounds against Gram-negative bacteria was evaluated by determination of their minimal inhibitory concentration (MIC). Serial twofold dilutions of the test compounds from 100 μ M to 0.05 μ M in Mueller-Hinton broth were prepared in 96-well microplates (round bottom, PS, Sarstedt). Each well contained 50 μ L of

test compound solution at twice the desired final concentration and was inoculated with 50 μL of bacterial suspension, yielding a final concentration of 5×10^5 CFU/mL in 100 μL end volume. Microplates were incubated for 16-20 h at 37°C, and the MIC was defined as the lowest concentration of test compound that inhibits visible bacterial growth.

2.4.3. Quorum Sensing Inhibition

The assays of selected cyanobacteria extracts for quorum sensing inhibition were kindly performed by Tomasz Chilczuk, Department of Pharmaceutical Biology/Pharmacognosy, Institute of Pharmacy, University of Halle-Wittenberg, Halle (Saale), Germany, according to sections 2.4.3.1 to 2.4.3.4. All assays were performed in microtiter plates, containing 2.5 μL of biomass extract (40 mg/mL in DMSO), stored at -20°C.

2.4.3.1. Violacein Production Assay^B

An overnight culture of *Chromobacterium violaceum* CV026 was grown in LB medium in a 100 mL Erlenmeyer flask and shaken with 200 rpm at 27 °C. On the following day, the culture was adjusted to OD₆₀₀, and 1 mL of the diluted overnight culture, 1.25 mL of MOPS (1 M, Carl Roth GmbH), 10 μL of a C6-HSL (100 $\mu\text{g}/\text{mL}$ in DMSO) solution and 20 mL LB medium were mixed. 92 μL of the mixture was pipetted with a multichannel pipette (100 – 1200 μL) into each well of a 96 well microtiter plate (flat-bottom, clear, polystyrene, Greiner Bio-One), which included cyanobacteria extracts. The microtiter plate was sealed with a protective sheet (Plate Sealer, 80x150 mm, gas permeable; Greiner Bio-One) to prevent evaporation, and incubated for 24 h at 27 °C. After incubation, the cell density was quantified by measuring the absorption at 600 nm with a microplate reader (Infinite M200, Tecan Trading AG) in order to estimate the cell viability of *C. violaceum* CV026. As positive control, 2.5 μL of a coumarin solution (2 mg/mL in DMSO, Merck KGaA), and as negative control, 2.5 μL DMSO and 2.5 μL H₂O, have been used. The evaluation of the assay was performed by comparing the purple colorization caused by violacein in a well with cyanobacteria extract with the colorization of the positive control coumarin and the negative control DMSO. If a similar reduction in purple colorization and cell density as in the positive control was observed, the extract causing the decrease of violacein production was classified as QS inhibiting extract. An extract was defined as antibacterial if no purple colorization and a lower cell density than the positive control was detected.

^B Paragraph adapted from Chilczuk, Tomasz; Master thesis (2016); “Screening for quorum sensing inhibitors from cyanobacteria”

2.4.3.2. B-Galactosidase Assay^B

An overnight culture of *Staphylococcus aureus* PC322 was grown in TSB medium. The culture was shaken with 200 rpm at 37 °C in a 100 mL Erlenmeyer flask. On the next day, the culture was adjusted to OD₆₀₀ of 0.1 and 1 mL of the diluted culture, 2.5 µL erythromycin (40 mg/mL in ethanol, Sigma-Aldrich), 200 µL X-Gal (40 mg/mL in DMSO) and 25 mL of TSA medium (≈ 45 °C, tryptone soya agar; Oxoid) were quickly mixed. 92 µL of the mixture was pipetted with a multichannel pipette (100 – 1200 µL) into each well of a 96 well microtiter plate (flat-bottom, clear, polystyrene, Greiner Bio-One) containing the cyanobacteria extracts. After sealing the microtiter plate with a protective sheet, the plate was incubated for 24 h at 37 °C. 2.5 µL of a hamamelitannin solution (4 mg/mL in DMSO, Carl Roth GmbH) was used as positive control. 2.5 µL of DMSO and 2.5 µL H₂O served as negative controls. After the incubation period, each well was checked for an activity of the extracts on the expression of hla:lacZ. Extracts were classified as QS inhibiting, if they reduced the blue colour in the same or similar amount as the positive control hamamelitannin. Due to the utilization of agar, no quantification of the cell density has been possible. Extracts were defined as antibacterial, if a clear well and no blue colorization in the microtiter plates could be detected.

2.4.3.3. Prodigiosin Production Assay^B

An overnight culture of *Serratia marcescens* was grown in LB medium in a 100 mL Erlenmeyer flask. The culture was shaken at 200 rpm at 30 °C. On the following day the culture was diluted with LB to OD₆₀₀ of 0.1 and 92 µL of the diluted culture was quickly pipetted with a multichannel pipette (100 – 1200 µL) into each well of a 96 well microtiter plate (flat-bottom, clear, polystyrene, Greiner Bio-One) containing all cyanobacteria extracts. A protective sheet was used to close the microtiter plate. Afterwards the plate was incubated for 24 h at 30 °C. On the following day, each well was checked for prodigiosin production inhibition. 2.5 µL of a coumarin solution (12 mg/mL in DMSO) served as positive control, while 2.5 µL DMSO and 2.5 µL H₂O were used as negative controls. The evaluation was performed by comparing the red colour of each well with the colorization of the positive control and the DMSO control. Extracts that showed a similar reduction of the prodigiosin production as the positive control were classified as QS inhibiting extracts. The classification QS enhancing extract was given to extracts that enhanced the prodigiosin production in *S. marcescens* more than the negative control DMSO. If a culture showed a clear well, the extract was classified as antibacterial.

^B Paragraph adapted from Chilczuk, Tomasz; Master thesis (2016); “Screening for quorum sensing inhibitors from cyanobacteria”

2.4.3.4. Bioluminescence Assay^B

Vibrio harveyi DSMZ6904 was grown in MB medium overnight in a 100 ml Erlenmeyer flask. The culture was shaken with 200 rpm at 27 °C. On the following day, the overnight culture was diluted to OD₆₀₀ of 0.1. The diluted culture was pipetted with a multichannel pipette (100 – 1200 µL) into 96 well microtiter plates (flat-bottom, white, polystyrene, Nunc) containing the cyanobacteria extracts. Each well was filled with 92 µL of diluted culture. The microtiter plate was closed with a clear lid and incubated at 27 °C. Additionally, the microtiter plate was covered with a gas-permeable sheet (pore size 10–50 µm, 0.14 mm thick, rayon fibers coated with acrylate adhesive, Greiner Bio-One) to reduce evaporation. Bioluminescence was measured with a microplate reader (Infinite M200, Tecan Trading AG). Before each measurement, the microtiter plate was shaken for 20 s. For a kinetic measurement, the microtiter plate was incubated for 24 h and the bioluminescence was measured each hour. Since preliminary test showed that *V. harveyi* exhibits a maximum bioluminescence production during an incubation time of 4 - 7 h, endpoint measurements of the bioluminescence were done after 5 h of incubation. After the incubation period the culture was transferred to an empty microtiter plate (flat-bottom, clear, Greiner Bio-One) to measure the cell density at 600 nm. For this assay, no positive control is available. As negative control, 2.5 µL DMSO and 2.5 µL H₂O were used. The DMSO control had a reducing effect on the cell density, while increasing the bioluminescence of *V. harveyi*. The data obtained in the bioluminescence assay are presented as bioluminescence intensity (BI), which was calculated using the following formula:

$$BI = 100 \times \left(\frac{RB_{\text{Extract}}}{RB_{\text{DMSO}}} \right)$$

RB_{DMSO} or RB_{Extract} is the relative bioluminescence of the negative control DMSO or the extract calculated as the ratio between the relative light units (RLU) and the cell density. All extracts that showed at least a 95 % decrease in bioluminescence intensity and had a higher cell density than the negative control were defined as QS inhibiting extracts. Cyanobacteria extracts showing at least a 2-fold increase in bioluminescence of *V. harveyi* and a higher cell density than the negative control were classified as QS enhancing extracts. Furthermore, extracts were defined as antibacterial, if a lower cell density and bioluminescence than the negative control were detected.

^B Paragraph adapted from Chilczuk, Tomasz; Master thesis (2016); “Screening for quorum sensing inhibitors from cyanobacteria”

2.5. Chemical Screening

The cyanobacterial extracts were chemically characterized by analytical HPLC with a diode array detector (DAD) and an evaporative light scattering detector (ELSD), and by HPLC-MS to identify and dereplicate already known compounds prior to the isolation process.

2.5.1. Mass Spectrometry, Tandem Mass Spectrometry and High-Resolution Electrospray Ionisation Mass Spectrometry

LC-MS and MS/MS experiments were performed with an ion trap mass spectrometer (6330 Iontrap LC/MS, Agilent Technologies) and a chromatography system (Agilent 1200, Agilent Technologies) equipped with a C18 column (Nucleosil 100 C18, 100 x 2 mm, Dr. Maisch GmbH). Water + 0.1 % formic acid (FA) (solvent A) and acetonitrile (MeCN) + 0.06 % FA (solvent B), were used as mobile phase (flow rate 0.4 mL/min, linear gradient of 10-100 % solvent B in 17 min) at 40°C. The sample was ionized by electrospray ionization in positive and negative mode. The following general settings were applied: capillary voltage, -3500 V; drying gas flow, 12.0 L/min; drying gas temperature, 350 °C; nebulizing gas pressure, 40 psi. Helium was used as collision gas. MS/MS spectra were generated using the auto MS/MS acquisition mode. Data was analyzed with DataAnalysis (Version 3.4, Bruker Daltonics GmbH). High-resolution electrospray ionization mass spectrometry (HRESIMS) data were acquired on a Q Exactive Plus mass spectrometer (Thermo Fisher Scientific) equipped with a heated ESI interface coupled to an UltiMate 3000 HPLC system (Thermo Fisher Scientific). The following parameters were used for the data acquisition: pos. mode, ESI spray voltage 3.5 kV, scan range 150 – 2000 *m/z*.

2.6. Dereplication of Isolated Compounds

Once bioactivity and chemical screening were completed, the HPLC-MS data of interesting extracts was used for dereplication of known compounds applying the Dictionary of Natural Products (DNP) (CRC Press). The chemical profile was used to find corresponding natural compounds, isolated from cyanobacteria, in the DNP.

2.7. Bioactivity-Guided Isolation

Upon bioactivity testing and chemical characterization, the most promising extracts were subjected to flash-chromatography or time-based fractionation by semi-preparative HPLC, depending on the complexity of the raw extract. Fractionation was followed by further

bioactivity testing, to identify bioactive fractions for the subsequent isolation process of the compounds.

2.7.1. Fractionation with Flash-Chromatography

Cyanobacterial biomass extracts were fractionated with flash- chromatography, prior to semi-preparative HPLC. The raw extracts were resuspended in 50 %, 80 % or 100 % MeOH or MeCN in H₂O (v/v), centrifuged at 10,000 rpm for 10 min, and injected into a flash-chromatography system (Low flow LC system PrepChrom C-700, BÜCHI, Switzerland or Varian, Palo Alto, California, USA) equipped with a reverse phase C18 cartridge (Sepacore Flash cartridge, 12 g, BÜCHI, or Chromabond C18, 16,4 g, Macherey-Nagel). The mobile phase consisted of water + 0.1 % FA (solvent A) and MeOH or MeCN + 0.1 % FA (solvent B). Chromatography was performed with a flow rate of 20 mL/min, while run time and gradient were adjusted individually for each extract. The obtained fractions were analyzed for their inhibitory activity against rhodesain according to section 2.4.1.

2.7.2. Time-based Fractionation with HPLC

To perform a time- and bioactivity based fractionation, dried fractions derived from flash-chromatography (2.7.1) or raw extracts were prepared for HPLC by reconstitution in 100 % MeOH or MeCN, and centrifugation for 5 min at 13000 rpm. The supernatant was transferred to a HPLC vial. Bioactivity-guided fractionation was performed using a HPLC system (Agilent 1260 Infinity, Agilent Technologies) equipped with a C18 column (250 x 4.6 mm, 5 µm, 100 Å, Luna C18, Phenomenex) at 25 °C and an injection volume of 10-15 µL. In order to achieve best possible separation of the target compounds, an optimized gradient was applied, depending on the character of the extract. The fractions were collected time-based every 30 to 60 s, in 96-deep well plates or glass tubes, with a flow rate of 0.95 mL/min, and dried using a vacuum centrifuge (GeneVac EZ-2 Elite, Genevac Ltd). Afterwards, fractions were solved in 50 µL DMSO and tested for inhibitory activity against rhodesain (see 2.4.1). HPLC data were analyzed using Agilent Chemstation (Version B.04.03, Agilent Technologies).

2.7.3. Isolation of Bioactive Compounds

In order to isolate bioactive compounds, either medium extracts or fractions resulting from flash-chromatography or semi-preparative HPLC were subjected to further purification by semi-preparative or preparative HPLC. The resulting purified compounds were analyzed by analytical HPLC-DAD, LC-MS, MS/MS, and HRESIMS experiments (see 2.5.1).

2.7.3.1. Semi-Preparative HPLC

Semi-preparative HPLC was conducted on an UltiMate 3000 HPLC system (Thermo Fisher Scientific) or an Agilent 1260 Infinity (Agilent Technologies) equipped with a C18, PFP, or PH column (250 x 10 mm, 5 μ m, 100 Å, Luna C18, Phenomenex), depending on the chemical properties of the target molecules. Conditions (flowrate, temperature, run time) were optimized to achieve the best separation of the target compounds. The active fractions or raw extracts were resuspended in 100 % MeOH or MeCN, and centrifuged for 5 min at 13000 rpm. The supernatant was transferred to a conical HPLC vial, and 10 to 20 μ L were injected to the HPLC system. Fractions were collected time-based or peak-based in 96-well deep well plates, glass tubes or round bottom flasks, and dried using a vacuum centrifuge (GeneVac EZ-2 Elite, Genevac Ltd.) or a rotary evaporator. Data were analyzed using Agilent Chemstation (Version B.04.03, Agilent Technologies) and Chromeleon 7 (Version 6.8., Thermo Fisher Scientific).

2.7.3.2. Preparative HPLC

Preparative HPLC was performed on a Preparative LC System La Prep, module P110 and P314 (VWR international), equipped with a C18 column (Reprosil-Pur Basic C18, 250x20 mm, Dr. Maisch GmbH). The run was performed with detection wavelength of 230 and 280 nm, a flowrate of 24 mL/min and an optimized gradient of MeCN in H₂O over 25 min. The target fractions were collected manually.

2.8. NMR Analysis and Structure Elucidation of Isolated Compounds

In order to elucidate the structure of unknown compounds, nuclear magnetic resonance (NMR) spectroscopy and high-resolution tandem mass spectrometry (HRMS/MS) were used. For the NMR experiments, pure compounds were dissolved in 0.6 mL *d*₆-DMSO. Spectra were recorded with a Bruker Avance-II spectrometer operating at 600 MHz (¹H) or 150 MHz (¹³C), on an Agilent DD2 spectrometer equipped with a OneNMR probe operating at 400 Mhz (¹H) or on a Varian/Agilent VNMRs spectrometer operating at 600 MHz (¹H). Chemical shifts were referenced to the residual protonated solvent signals of *d*₆-DMSO ($\delta_{\text{H}}= 2.49$ ppm, $\delta_{\text{C}}=39.5$ ppm). All NMR data were analysed by Steffen Breinlinger (Department of Pharmaceutical Biology/Pharmacognosy, Institute of Pharmacy, University of Halle-Wittenberg, Germany) using ACD Structure Elucidator 2017.2.

2.9. Quantification by Evaporative Light Scattering Detection (ELSD)

The concentration of test compound solutions for bioactivity assays were quantified using HPLC coupled with an evaporative light scattering detector (ELSD) (Sedex 85, Sedere, France). Based on the method described by Adnani *et al.*,¹⁰⁶ a calibration curve for quercetin (>99%, Carl Roth) was determined, injecting 0.5 to 50 μL of a 20 $\text{ng}/\mu\text{L}$ solution in 90% MeCN in H_2O . Solutions were injected in triplicate on a C18 column (100 x 3.1 mm, 5 μm , 100 \AA , Kinetex, Phenomenex), eluted with 90% MeCN in H_2O (0.1% formic acid each) (0.85 mL/min) over 2.5 min, and directly conducted to the ELSD. ELSD response areas were averaged and $\log(\text{ELSD response area})$ was plotted against $\log(\text{amount})$ to generate a linear calibration curve (Figure 12).

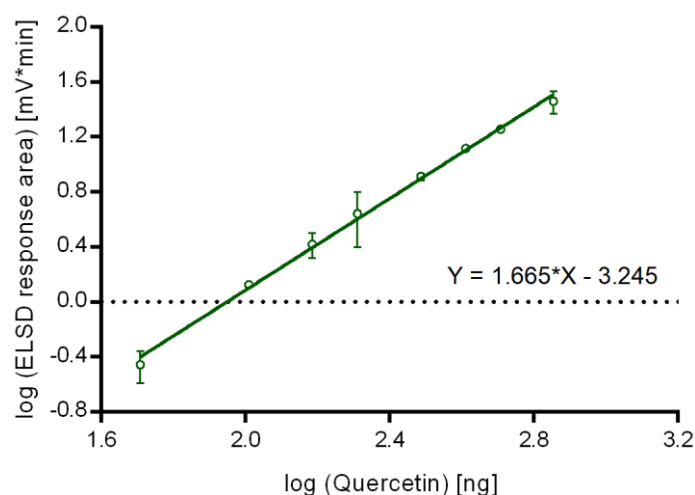


Figure 12. **Quercetin calibration curve, determined after Adnani et al. (2012).**¹⁰² Injecting 0.5 to 50 μL of a 20 $\text{ng}/\mu\text{L}$ solution in 90% MeCN in H_2O .

Solutions of compounds 1 to 5 in 90% MeCN were injected in triplicate, applying the described conditions. ELSD response areas were averaged, and the corresponding amount of compound was calculated applying the quercetin calibration curve.

3. Results and Discussion

As described above, the work within this PhD project can be separated into two parts. Within the first part, a cyanobacteria strain and extract collection was established and screened for rhodesain inhibition, antimicrobial activity and quorum sensing (QS) inhibition.

The focus of the second part was set on a bioactivity guided screening of 572 cyanobacteria extracts (kindly provided by Cyano Biotech GmbH, Berlin) against the trypanosomal cysteine protease rhodesain. Trang Nguyen contributed to some of these results in the context of her master thesis (2017).

3.1. Establishing a Cyanobacteria Strain Collection

3.1.1. Sampling in Germany

In July 2015, various small ponds in the botanical garden of Tübingen, Germany (48°32'20.3"N 9°02'10.8"E), were sampled. The environmental samples were treated as described in section 2.2.2, and grown as enrichment cultures for 18 days followed by streaking across BG-11 agar plates. Additionally, a soil sample from Berlin, Germany (52°36'39.0"N 13°25'47.4"E), and a sample from a biofilm taken from an aquarium situated on the 9th floor, Auf der Morgenstelle 28, Tübingen, Germany (48°32'10.1"N 9°02'10.9"E), were processed as described in section 2.2.2.

In late August 2015, mud, water and plants from a spring close to the Gönninger Seen, Reutlingen, Germany, were sampled and grown for about 4 months in low concentrated BG-11 medium (20 % with and without nitrogen). In September 2015, biofilms from the tropical conservatory in the botanic garden, Tübingen, Germany, were sampled, grown in BG-11 medium (100 % with and without nitrogen), and streaked across BG-11 agar plates (100 % with nitrogen). In June 2016, a biofilm from a mushroom growing in a spruce forest (51°31'03.5"N 7°48'59.9"E) was sampled and streaked across BG-11 agar plates (100% with and without nitrogen). In July 2016, additional samples were taken from the Gönninger Seen, Reutlingen, Germany (48°25'37.8"N 9°10'43.1"E), and grown in BG-11 medium (100 % with and without nitrogen). In February 2017, eight environmental samples from Austria, the Swabian Alps and the Black Forest regions, on BG-11 agar plates or in BG-11 medium, were obtained from Julia Kleinteich, Environmental Systems Analysis, University Tübingen (see Appendix). Out of the environmental samples taken in Germany and Austria, 55 cyanobacteria strains were isolated (Table 8).

All successfully isolated strains are summarized in Table A 1 in the appendix, including further information like sampling site and technique.

Table 8. **Cyanobacteria strains isolated from samples taken in Germany.**

	Section	No. of strains	Share [%]
I	Chroococcales	17	30.9
II	Pleurocapsales	0	-
III	Oscillatoriales	36	65.5
IV	Nostocales	2	3.6
V	Stigonematales	0	-
	Total	55	100

It is noticeable that 65.5% of the cyanobacteria strains belong to section III (Oscillatoriales), 30.9% to section I (Chroococcales) and solely 3.6% to section IV (Nostocales). No cyanobacteria of section II (Pleurocapsales), nor section V (Stigonematales) were isolated. Presumably the applied sampling and isolation techniques favored the growth of section I and III, leading to biased results.

3.1.2. Sampling in Indonesia

In Indonesia, the sampling procedure was slightly modified. Following the advice of our Indonesian cooperation partners, a cotton stick instead of a loop was used for the sampling of biofilms. The cotton stick was kept inside a 15 mL conical centrifugation tube filled with 5 mL BG11 medium, with (BG11+N) and without nitrogen (BG11-N), leading to small colonies entangled inside the threads, which could be easily picked with a pipette. In addition, each sample was directly streaked across BG11 agarose plates with (BG11+N) and without nitrogen (BG11-N), directly in the field. In total 25 sampling sites were probed with varying sampling techniques, resulting in 72 samples from which 92 unialgal strains could be isolated. All successfully isolated strains are summarized in Table A 2, including further information like sampling site and technique.

3.1.3. Exemplary Isolation Procedure

Due to the high number of samples and isolated strains, solely an exemplary isolation procedure will be described in detail. From a waterfall in the Halimun Mountain National Park, Cikaniki, West Java, Indonesia (6°44'76.6"S 106°32'39.6"E), samples from two biofilms (A, B) and water (filtrate, 25 µm plancton net) were collected. Each sample was treated as described in section 2.2.2. The strain morphology and observations of cultures were made according to the procedure described in section 2.2.4. Figure 13 summarizes which sampling method resulted in the isolation of which strains.

	biofilm A		biofilm B		water	
	liquid	solid	liquid	solid	liquid	solid
BG11+N	Chroococcales An-AI012.1	Oscillatoriales An-AI014.1	Chroococcales An-AI016.1.1 Chroococcales An-AI016.1.2.1 Oscillatoriales An-AI016.1.3	Oscillatoriales An-AI018.1.1	Nostocales An-AI034.1	Chroococcales An-AI032
BG11-N	Stigonematales An-AI013.1.1 Oscillatoriales An-AI013.1.2	Nostocales An-AI015.0 Nostocales An-AI015.1		Stigonematales An-AI019.0	Nostocales An-AI035.1 Oscillatoriales An-AI035.2	

Figure 13. **Overview of 3 different samples taken at a water fall (National Park Halimun Mountain, Cikaniki, West Java) and the thereof isolated cyanobacteria strains.** BG11+N: BG11 medium with nitrogen source; BG11-N: BG11 medium without nitrogen source; liquid: 15 mL conical centrifugation tube filled with 5 mL BG11 medium; solid: BG11 agarose plate.

From Biofilm A two strains could be isolated with BG11+N (Figure 14; Figure 13). The strain An-AI012.1 (Figure 14 A), belonging to section I, Chroococcales, could be isolated from a sample collected with a cotton stick and transferred directly into 5 mL BG11+N medium

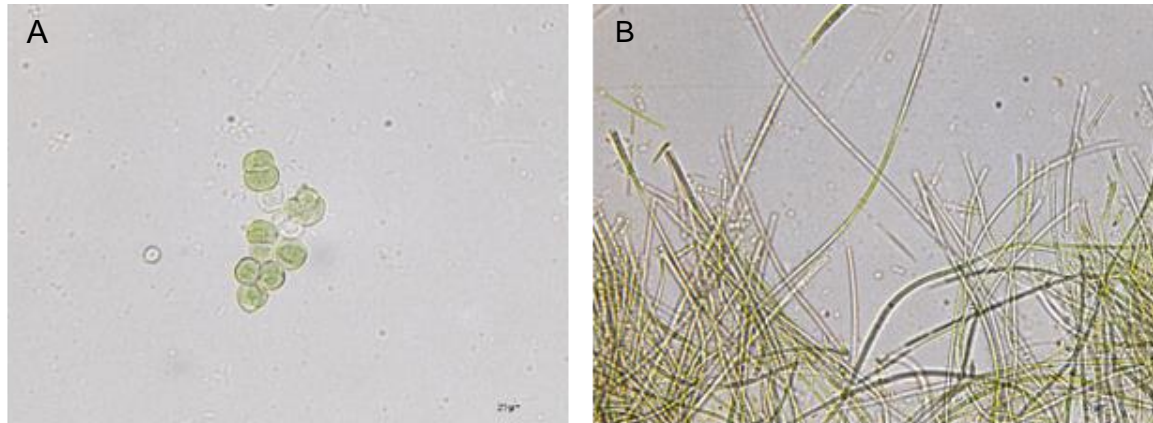


Figure 14. A. An-AI012.1 (Chroococcales) B. An-AI014.1 (Oscillatoriales); Cyanobacteria strains isolated from Biofilm A, water fall (National Park Halimun Mountain, Cikaniki, West Java). BG11+N; liquid: 15 mL conical centrifugation tube filled with 5 mL BG11 medium; solid: BG11 agarose plate.

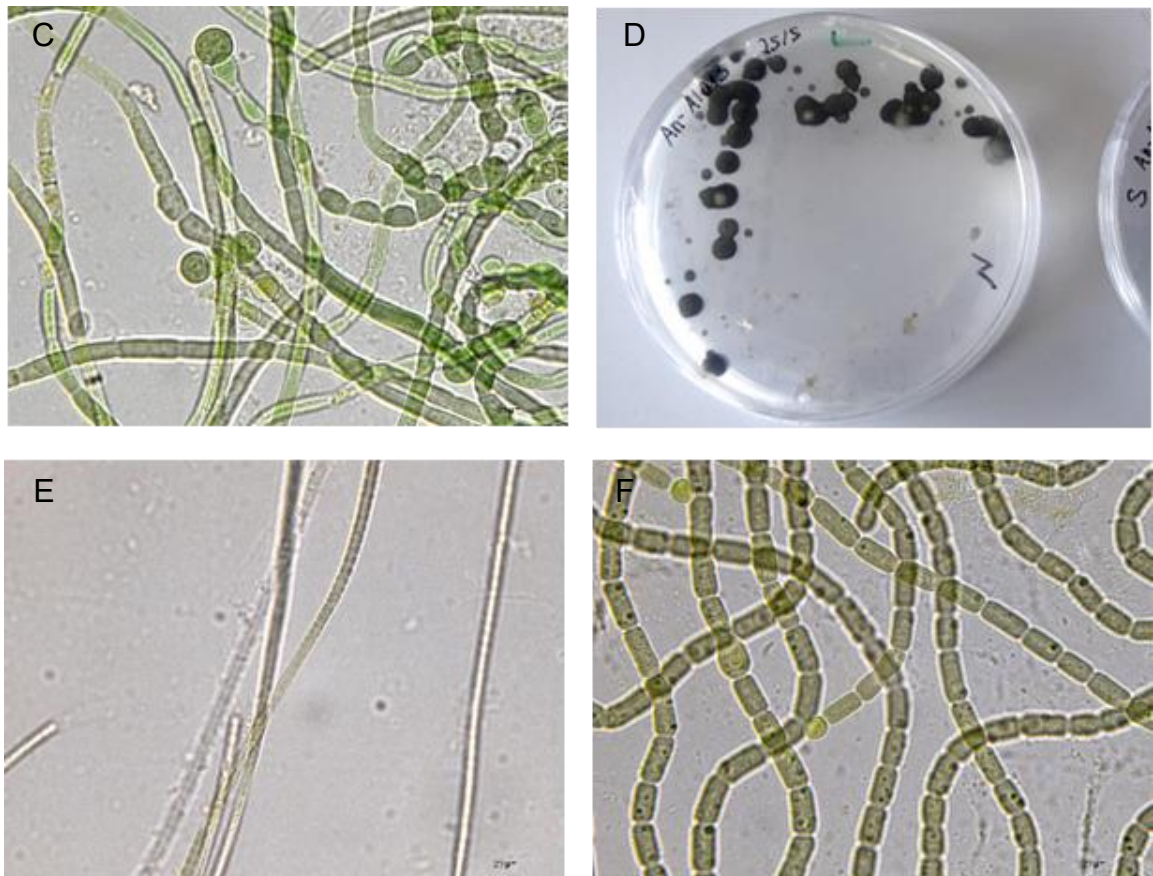


Figure 15. C. An-AI013.1.1 (Stigonematales) D. An-AI015.0 (Nostocales) E. An-AI013.1.2 (Oscillatoriales) F. An-AI015.1 (Nostocales); Cyanobacteria strains isolated from Biofilm A, water fall (National Park Halimun Mountain, Cikaniki, West Java). BG11-N; liquid: 15 mL conical centrifugation tube filled with 5 mL BG11 medium; solid: BG11 agarose plate.

(liquid). From a sample collected with a sterile cotton stick and directly streaked on a BG11 agarose plate (solid) An-AI014.1 (Figure 14 B), belonging to section III, Oscillatoriales, was isolated. From both samples transferred to either liquid or solid BG11-N medium in total four heterocystous cyanobacteria strains were isolated: An-AI013.1.1 (Figure 15 C), belonging to

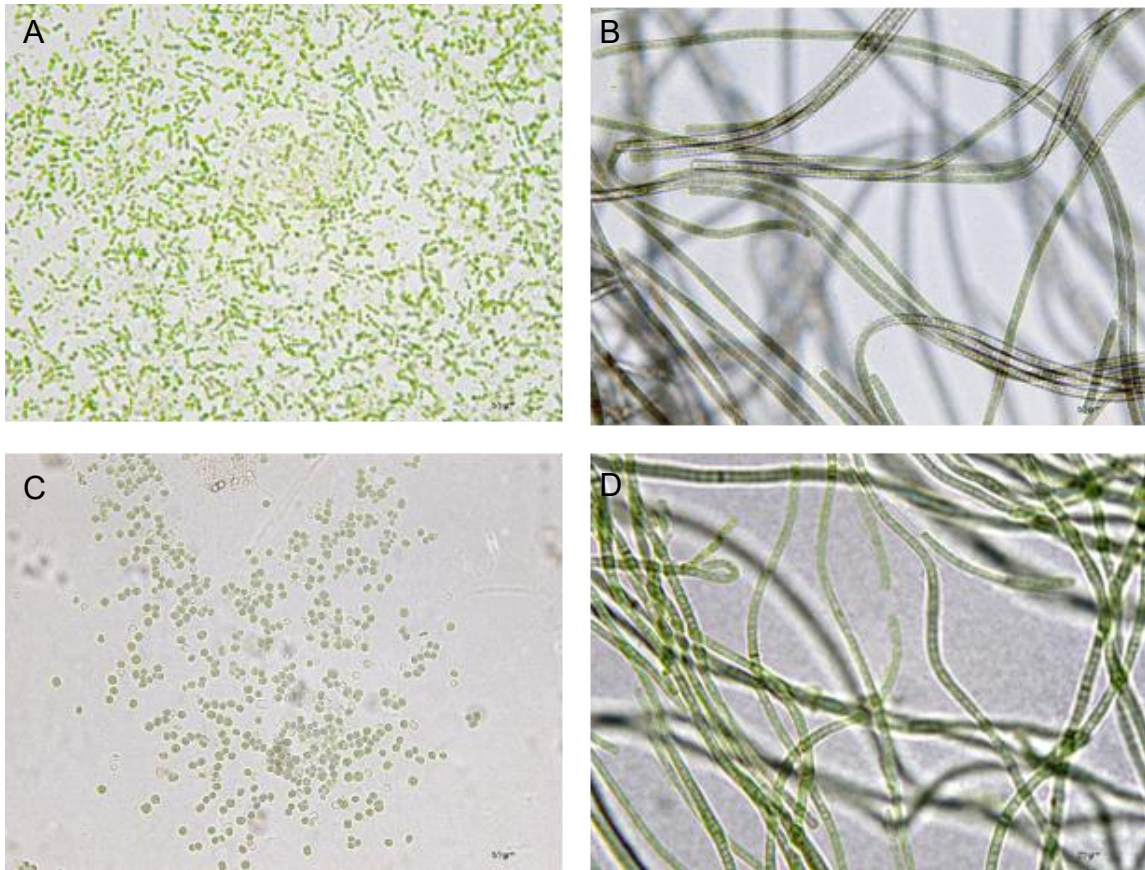


Figure 17. A. An-AI016.1.1 (Chroococcales) B. An-AI018.1.1 (Oscillatoriales) C. An-AI016.1.2.1 (Chroococcales) D. An-AI016.1.3 (Oscillatoriales) Cyanobacteria strains isolated from Biofilm B, water fall (National Park Halimun Mountain, Cikaniki, West Java). BG11+N; liquid: 15 mL conical centrifugation tube filled with 5 mL BG11 medium; solid: BG11 agarose plate.



Figure 16. E. An-AI019 (Stigonematales); Cyanobacteria strains isolated from Biofilm B, water fall (National Park Halimun Mountain, Cikaniki, West Java). BG11-N; liquid: 15 mL conical centrifugation tube filled with 5 mL BG11 medium; solid: BG11 agarose plate.

section V, Stigonematales and An-AI015.0 (Figure 15 D) and An-AI015.1 (Figure 15 F), belonging to section IV, Nostocales. The strain An-AI013.1.2 (Figure 15 E), section III, Oscillatoriales, was as well isolated from BG11-N liquid medium. The sampling of Biofilm B resulted in

the isolation of two strains belonging to section I, Chroococcales (An-Al016.1.1 and An-Al016.1.2, Figure 17 A and C) and one strain belonging to section III, Oscillatoriales (An-Al016.1.3) from BG11+N liquid medium (Figure 17 D). From the sample transferred to BG11+N solid medium one Oscillatoriales strain (An-Al018.1.1) was isolated (Figure 17 B). The heterocystous strain An-Al019.0, section V, Stigonematales, was isolated from the sample

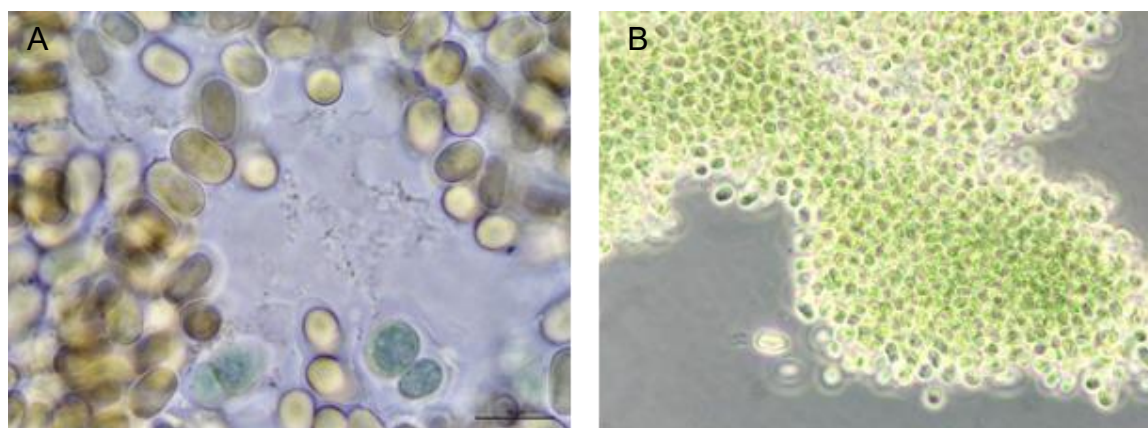


Figure 18. A. An-Al034.1 (Nostocales) B. An-Al032 (Chroococcales) Cyanobacteria strains isolated from water, water fall (National Park Halimun Mountain, Cikaniki, West Java). BG11+N; liquid: 15 mL conical centrifugation tube filled with 5 mL BG11 medium; solid: BG11 agarose plate.

directly streaked on a BG11-N agarose plate (Figure 16 E). Close to the sampling sites of the two biofilms, a water sample was filtrated with a 25 μ m plancton net and treated as previously described.

From BG11+N (liquid) An-Al034.1 (section IV, Nostocales) and BG11+N (solid) An-Al032 (section I, Chroococcales) could be isolated (Figure 18). From the liquid culture with BG11-N An-Al035.1 (section IV, Nostocales) and An-Al035.2 (section III, Oscillatoriales) were isolated (Figure 19). In contrast to biofilm A and B, a heterocystous strain was isolated from medium with a nitrogen source. Nevertheless, in this exemplary sampling procedure most strains,

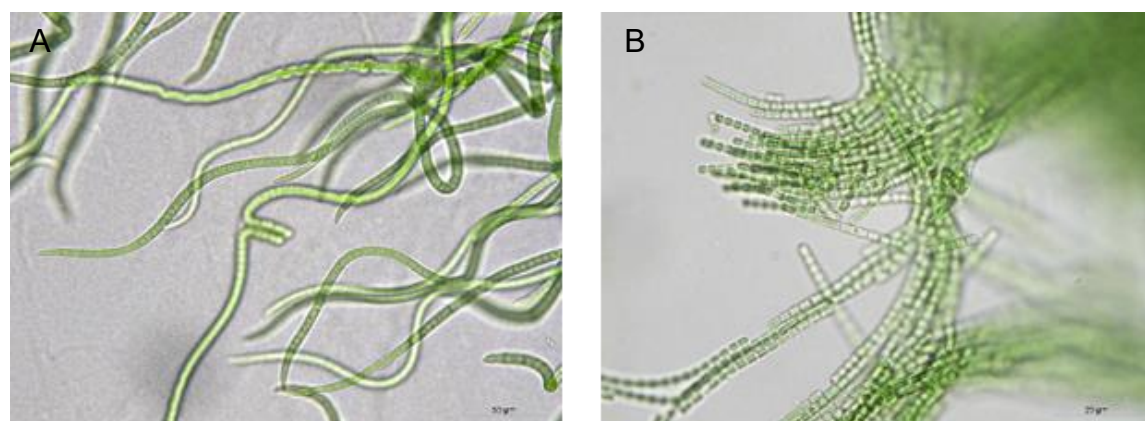


Figure 19. A. An-Al035.1 (Nostocales) B. An-Al035.2 (Oscillatoriales); Cyanobacteria strains isolated from water, water fall (National Park Halimun Mountain, Cikaniki, West Java). BG11-N; liquid: 15 mL conical centrifugation tube filled with 5 mL BG11 medium; solid: BG11 agarose plate.

belonging to Stigonematales or Nostocales, were isolated from samples spread on BG11 solid medium without nitrogen (BG11-N) or incubated in BG11 without nitrogen (BG11-N).

The 92 unialgal strains isolated from Indonesian samples are summarized in Table 9. Comparing the percentage share of section I to V of the strains isolated in Indonesia to those isolated in Germany (Table 8), its conspicuous, that no Stigonematales were isolated from German sampling sites, while 9 from 92 Indonesian strains (9.8 %) belong to this section. Additionally, only 3.6 % of the cyanobacteria strains isolated from samples taken in Germany belong to Nostocales, but 34.8 % of the strains isolated from Indonesian samples. This bias might be explained by different sampling and isolation techniques.

Table 9. Cyanobacteria strains isolated within the Project ANoBlN.

	Section	No. of strains	Share [%]
I	Chroococcales	16	17.4
II	Pleurocapsales	0	-
III	Oscillatoriales	35	38.0
IV	Nostocales	32	34.8
V	Stigonematales	9	9.8
	Total	92	100

Nostocales and Stigonematales belong to the heterocystous cyanobacteria, which are capable of N₂ fixation. When no combined nitrogen is available, 5-10 % of their vegetative cells differentiate into heterocysts. These specialized cells offer the perfect environment for the enzyme catalysing the N₂ fixation, called nitrogenase.²⁷ Thus, heterocystous cyanobacteria are in advantage when no combined nitrogen is available.

Most strains belonging to Stigonematales or Nostocales were isolated from Indonesian samples spread on BG11 solid medium without nitrogen (BG11-N) or incubated in BG11 without nitrogen source (BG11-N). As the German samples were largely processed on BG11 medium including a nitrogen source (BG11+N), heterocystous cyanobacteria within the environmental sample might have been outpaced by non-heterocystous strains.

In addition to the environmental samples taken in Mount Halimun National Park on Java, Indonesia, we received about 46 freshwater and marine cyanobacteria strains from our cooperation partner Dr. Dwi Susilaningsih, Indonesian Institute of Science (LIPI). Those strains were obtained in different medium than BG11, namely in AF6 and IMK medium and in some cases prepared with water taken from the isolates source. Thus, the strains had to be

adapted to BG11 medium with varying nutrient and salt concentrations. Due to some difficulties based on unknown medium ingredients, only 40 of the received strains could be retained (Table 10).

Table 10. Cyanobacteria strains obtained from Dwi Susilaningih within the Project ANoBIn.

	Section	No. of strains	Share [%]
I	Chroococcales	17	42.5
II	Pleurocapsales	0	-
III	Oscillatoriales	18	45
IV	Nostocales	1	2.5
V	Stigonematales	3	7.5
	Total	40	100

No Pleurocapsales could be obtained, neither from German nor Indonesian samples, which corresponds to the assertion of Komárek *et al.*, that strains of this order are very difficult to transfer in pure culture.²¹ This is why Pleurocapsales is regarded as the least studied order within the cyanobacteria, and sequence data is rare.^{107,108}

3.2. Screening of the Cyanobacteria Extract Collection

In order to isolate and identify new anti-infective compounds from cyanobacteria, selected strains were cultivated (see 2.3) in order to generate biomass extracts for subsequent bioactivity testing. Besides the rhodesain inhibiting activity, antimicrobial activity (*Bacillus subtilis* 168, *Staphylococcus aureus* K12) and quorum sensing inhibition (*Vibrio harveyi* DSMZ6904, *Chromobacterium violaceum* CV026, *Staphylococcus aureus* PC322 (hla:lacZ, Eryr)) were evaluated for about 60 cyanobacteria biomass extracts.

3.2.1. Screening for Rhodesain Inhibitory Activity

From 52 cyanobacteria biomass extracts tested for rhodesain inhibiting activity (see section 2.4.1), only 6 showed an inhibition higher than 50% (Figure 20).

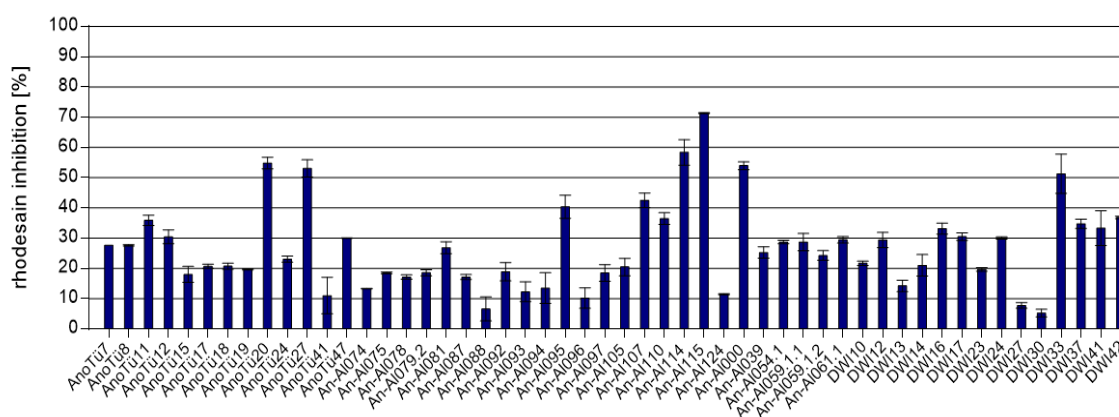


Figure 20. **Rhodesain inhibiting activity of cyanobacteria biomass extracts.** Assay performed as described in section 2.4.1; 5 μ L extract (40 mg/mL) in DMSO (final extract concentration 0.1 mg/mL).

Table 11. **Cyanobacteria biomass extracts with more than 50% inhibition against rhodesain at 0.1 mg/mL.**

Section	Extracts tested		> 50% inhibition	
	No. of strains	[%]	No. of strains	[%]
Chroococcales (I)	13	25.0	2	15.4
Oscillatoriales (III)	27	51.9	2	7.4
Nostocales (IV)	8	15.4	1	12.5
Stigonematales (V)	4	7.7	1	25.0
Total	52	100	6	

Of these six strains, AnoTü20 ($55 \pm 2\%$ inhibition) and DWI33 ($51 \pm 6\%$) belong to Chroococcales (I), AnoTü27 ($53 \pm 3\%$) and An-Al115 ($71 \pm 0\%$) to Oscillatoriales (III), An-Al114 ($59 \pm 4\%$) to Nostocales (IV) and An-Al000 ($54 \pm 1\%$) to Stigonematales (V) (Table 11). Thus, of the tested strains 15.4% of the order Chroococcales, 7.4% of Oscillatoriales, 15% of Nostocales and 25% of Stigonematales revealed inhibition of more than 50%.

3.2.2. Screening for Antimicrobial Activity

From 60 screened cyanobacteria biomass extracts (final concentration 0.1 mg/mL) only seven exhibited antimicrobial activity against *B. subtilis*, and from those extracts only four showed additional activity against *S. aureus*.

Table 12. Cyanobacteria biomass extracts with antimicrobial activity against the Gram-positive bacteria *B. subtilis* and *S. aureus*.

Section			<i>B. subtilis</i> and <i>S. aureus</i>		<i>B. subtilis</i>	
	No. of strains	[%]	No. of strains	[%]	No. of strains	[%]
Chroococcales (I)	16	26.7	1	6.3	2	12.5
Oscillatoriales (III)	27	45.0	2	7.4	4	14.8
Nostocales (IV)	11	18.3	0	0.0	0	0.0
Stigonematales (V)	6	10.0	1	16.7	1	16.7
Total	60	100	4		7	

Thereof, some extracts were active against both Gram-positive bacteria: One (6.3%) belonging to the Chroococcales (AnoTü 41), three (7.4%) to the Oscillatoriales (AnoTü10, An-Al075 and An-Al078), and one (16.7%) belonging to the Stigonematales (An-Al061.1). While one Chroococcales (An-Al072.2.1) and two Oscillatoriales (An-Al054.1 and AnoTü18) extracts were solely active against *B. subtilis*.

3.2.3. Screening for Quorum Sensing Activity

56 cyanobacteria extracts were tested for quorum sensing activity with the three monitor strains *V. harveyi*, *C. violaceum*, and *S. aureus* (see section 2.4.3). A primary screening with the indicator strain *V. harveyi* revealed at least 95% inhibition of bioluminescence intensity for 19 extracts (share of total: 34%). Seven extracts (12.5%) inhibited the violacein production of *C. violaceum*, while 14 extracts (4%) enhanced it.

Table 13. **Cyanobacteria biomass extracts showing either quorum sensing inhibition (QI), quorum sensing enhancement (QSE) or antibacterial activity (AB) against the monitor strains *V. harveyi*, *C. violaceum*, and *S. aureus*.**

section			<i>V. harveyi</i>		<i>C. violaceum</i>				<i>S. aureus</i>			
	no. of strains	[%]	QSI		QSI		QSE		QSI		QSI/AB	
			qty	[%]	qty	[%]	qty	[%]	qty	[%]	qty	[%]
Chroococcales (I)	14	25.0	4	28.6	4	28.6	3	21.4	4	28.6	1	7.1
Oscillatoriales (III)	27	48.2	9	33.3	2	7.4	7	25.9	8	29.6	4	14.8
Nostocales (IV)	10	17.9	3	30.0	1	10.0	0	0.0	3	30.0	0	0.0
Stigonematales (V)	5	8.9	3	60.0	0	0.0	4	80.0	0	0.0	1	20.0
total	56	100.0	19		7		14		15		6	

qyt = quantity

Table 14. **Cyanobacteria biomass extracts with quorum sensing inhibition (QI), quorum sensing enhancement (QSE) or antibacterial activity (AB) against *V. harveyi*, *C. violaceum*, and *S. aureus*.**

Extract	Section	Quorum Sensing		Antibacterial			
		<i>V. harveyi</i>	<i>C. violaceum</i>	<i>S. aureus</i>		<i>B. subtilis</i>	
AnoTü10	III			QSI/AB		AB	AB
AnoTü15	III		QSE	QSI			AB
AnoTü18	III		QSE	QSI		AB	AB
AnoTü20	I	QSI	QSE	QSI			AB
AnoTü27	III	QSI		QSI			
AnoTü41	I		QSI	AB	AB	AB	AB
AnoTü47	IV			QSI			
An-Al078	III			AB	QSI/AB	AB	AB
An-Al081	III	QSI	QSE				
An-Al095	I	QSI		QSI			AB
An-Al097	III	QSI	QSE				
An-Al110	III		QSE	QSI		AB	
An-Al000	V	QSI	QSE				
An-Al039	III	QSI		QSI			
An-Al054.1	III	QSI				AB	AB
An-Al059.1.1	IV	QSI					AB
An-Al059.1.2	IV		QSI	QSI			
An-Al061.1	V		QSE	AB	AB	AB	AB
An-Al072.2.1	I					AB	AB
DWI12	I	QSI		QSI			
DWI41	III		QSE	QSI/AB	QSI		
DWI42	III	QSI	QSE				

Screening with the indicator strain *S. aureus* PC322 showed a decreased *lacZ* activity, indicating QS inhibition, in case of 15 extracts (26.8%). Additionally, six extracts (10.7%) showed antibacterial activity and QS inhibition. Interestingly, 60% of the tested Stigonematales showed QS inhibition against the indicator strain *V. harveyi* and even 80% of Stigonematales showed QS enhancing activity against *C. violaceum*, but no QS inhibition. Table 13 summarizes the affiliation of the active extracts.

Strains showing bioactivity in more than one primary screening are listed in Table 14. Here, five (35.7%) of the extracts belonged to the Chroococcales, 12 (44.4%) to Oscillatoriales, three (30.0%) belonged to Nostocales and two (40.0%) were assigned to Stigonematales. These results match findings in literature, as most known cyanobacterial QS inhibitors were isolated from the order Oscillatoriales, like lyngbyoic acid and malyngolide from *L. majuscula*, and tumonoic acids, isolated from *Blennothrix cantharidosum*.¹⁰⁹⁻¹¹¹

3.2.4. Best-Hit Extracts: Taxonomic Description and Chemical Profiling

All strains revealing QS inhibition, antimicrobial activity or rhodesain inhibition, are listed in Table 15. The chemical profile of each strain was evaluated by HPLC-MS. Bioactivity data of all tested extracts, is presented in Table A 4.

Table 15. Best-hit extracts showing either quorum sensing inhibition (QI), quorum sensing enhancement (QSE) or antibacterial activity (AB) against *V. harveyi*, *C. violaceum*, *S. aureus* and *B. subtilis*, or rhodesain inhibiting activity.

Extract	Section	Quorum Sensing			Antibacterial				Rhodesain Inhibition [%]	
		<i>V. harveyi</i>	<i>C. violaceum</i>	<i>S. marcescens</i>	<i>S. aureus</i>		<i>B. subtilis</i>		SD	SD
AnoTü10	III				QSI/AB		AB	AB	N/A	N/A
AnoTü11	III	QSI							35.9	1.7
AnoTü18	III		QSE		QSI		AB	AB	20.8	1.0
AnoTü20	I	QSI	QSE		QSI			AB	54.9	1.9
AnoTü27	III	QSI			QSI				53.1	2.9
AnoTü41	I		QSI		AB	AB	AB	AB	11.1	6.0
An-Al078	III				AB	QSI/AB	AB	AB	17.2	0.7
An-Al095	I	QSI			QSI			AB	40.4	3.8
An-Al110	III		QSE		QSI		AB		36.5	2.0
An-Al114	IV								58.5	4.2
An-Al115	III	QSI							71.4	0.2
An-Al000	V	QSI	QSE						54.0	1.3
An-Al059.1.2	IV		QSI		QSI				24.3	1.6
An-Al061.1	V		QSE	QSI?	AB	AB	AB	AB	29.5	1.0
DWI33	I		QSE						51.3	6.4
DWI41	III		QSE		QSI/AB	QSI			33.4	5.8

3.2.4.1. AnoTü10: Origin and Morphological Characterization

The cyanobacterium strain AnoTü10 was isolated from a freshwater pond in the Botanical Garden in Tübingen (48°32'20.3"N 9°02'10.8"E). The water sample was treated as described in section 2.2.3.2 (II) and the strains was isolated by phototaxis (see section 2.2.3.3). The strain morphology and observations of cultures were made according to the procedure described in section 2.2.4.

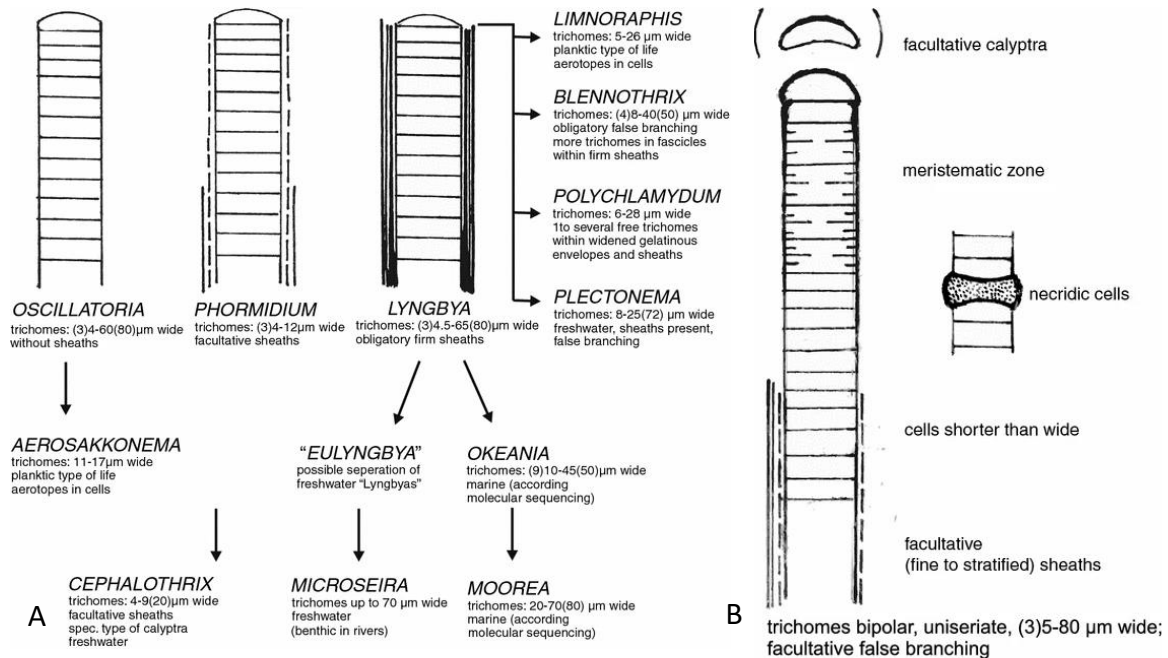


Figure 21. **A. Cytomorphological characteristics of the present revised genera Oscillatoriaceae after polyphasic evaluation; B. Main morphological markers of Oscillatoriaceae.** ³⁰

Thallus macroscopic visible, smooth, layered mats, mostly attached to the substrate, sometimes forming free floating tufts. Trichomes cylindrical, solitary but mostly in clusters, straight or slightly coiled, motile. Without common firm sheaths, but enveloped by wide, colourless, unlamellated, diffluent slime. Trichomes are simple, uniseriate, sometimes heteropolar, not or only slightly constricted at cross-walls, 7–9 µm wide, not attenuated or widened towards ends. Cells are shorter than wide, yellow–green, sometimes with dispersed granules. Terminal cells are rounded after trichome division. Mature trichomes show a thickened outer cell wall at the distal end of the terminal cell (calyptra). Hormogonia separate by help of necridic cells. No false nor true branching observed.

Due to the described morphological features (Figure 22), the strain AnoTü10 was classified as section III (Oscillatoriales), order Oscillatoriales, family Phormidiaceae, subfamily Phormidiodeae, genus Phormidium, and group VIII.^{21,112,113} The species could not be determined by taxonomic criteria. It is noted that this group probably needs revision and belongs to the family Oscillatoriaceae.¹¹³

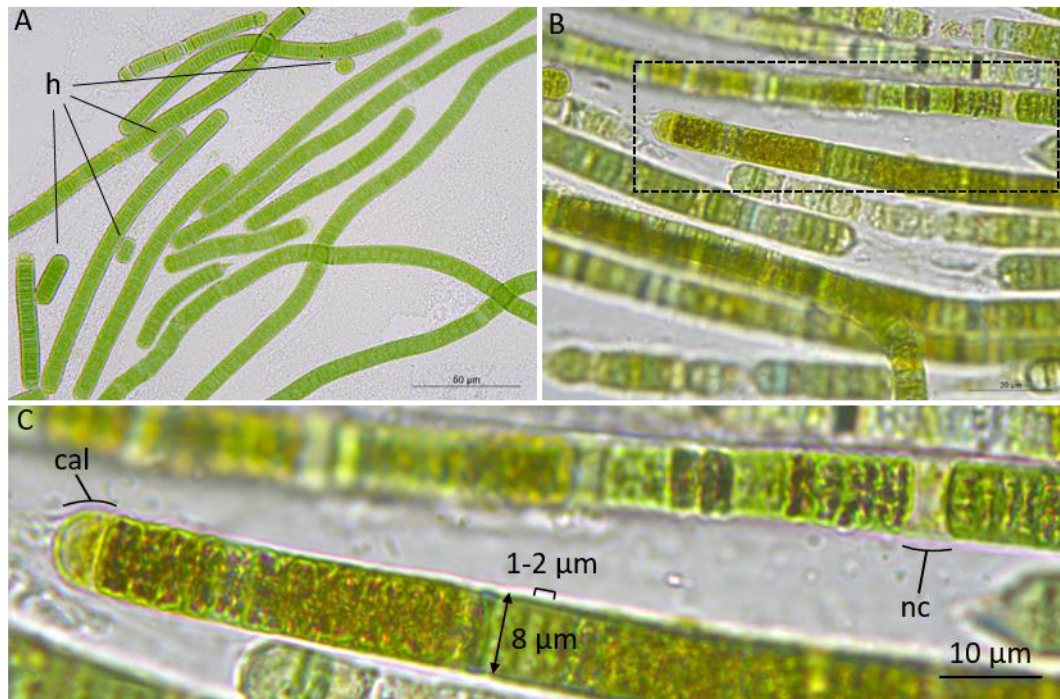


Figure 22. **Morphological characteristics of AnoTü10.** A. Growth of filaments and production of hormogonia (h); B. *overview* and C. *section*: mature trichomes with necrotic cells (nc) and calyptra (cal), width (8 µm) and length (1-2 µm) of common cells.

3.2.4.2. AnoTü10: Chemical Profile

The biomass extract AnoTü10 exhibited antibacterial activity against *S. aureus* and *B. subtilis*. Its HPLC-UV chromatogram shows only one prominent peak between 10.3 and 10.9 min (Figure 23). In the total ion chromatogram (TIC) in positive and negative mode, two compounds with similar retention times can be observed.

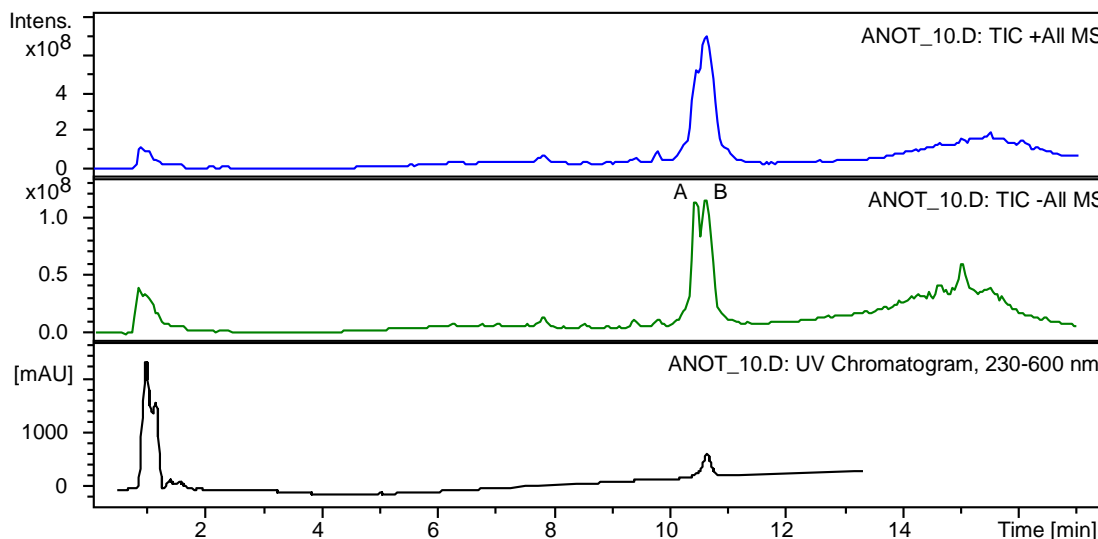


Figure 23. **Chromatogram of compound AnoTü10 biomass extract.** TIC pos. mode (blue), neg. mode (green); HPLC-UV chromatogram (black).

The mass spectra of the compound AnoTü10-A eluting at 10.3 min show a $[M+H]^+$ ion at m/z 843.4 and a $[M-H]^-$ ion at m/z 845.5, hinting a molecular mass of 844.5 Da for AnoTü-A. At 10.7 min the mass spectra show a $[M+H]^+$ ion at m/z 859.5 and a $[M-H]^-$ ion at m/z 857.4 indicating a molecular mass of 858.4 Da for AnoTü-B. Regarding the similar retention time

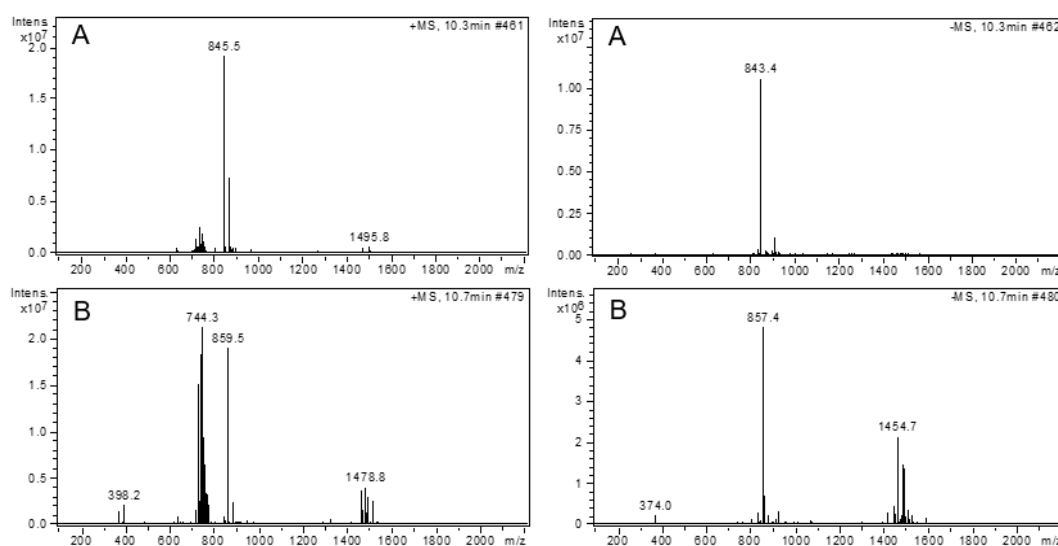


Figure 24. **Mass spectra of compound A and B from AnoTü10 biomass extract.** Pos. mode (left), neg. mode (right).

and molecular mass, the two compounds might be structurally related. The difference of 14 Da indicates an additional methyl group at AnoTü-B. No cyanobacteria-derived compound with a corresponding mass could be found in the DNP for AnoTü10-A nor AnoTü10-B. Thus further investigation of this extract might lead to the isolation of two novel compounds with antibacterial activity.

3.2.4.3. AnoTü20: Origin and Morphological Characterization

The unicellular cyanobacteria strain AnoTü20 was isolated from a fresh water aquarium at the Eberhard Karls University Tübingen (48°32'10.1"N 9°02'10.9"E). The sampled biofilm was enriched in BG11 medium followed by the streak plate method as described in 2.2.3.4. Characterization of the morphology was performed as described in 2.2.4.

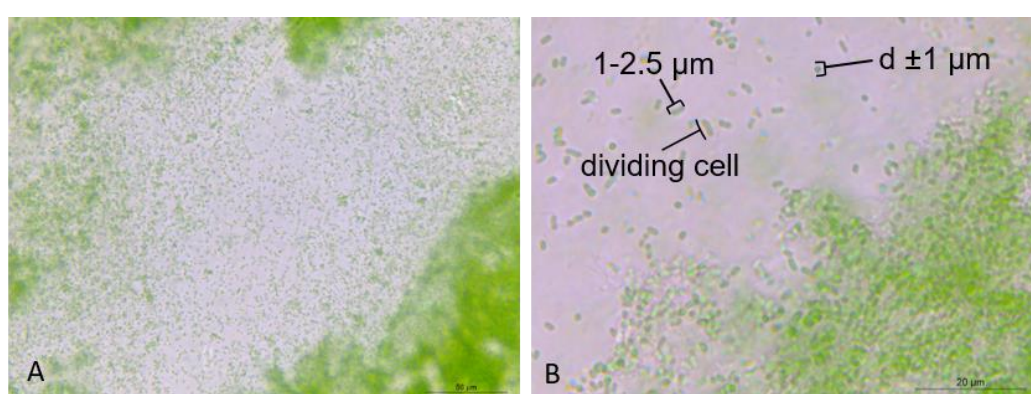


Figure 25. **Morphological characteristics of AnoTü20.** A. *overview*: Irregular growth of colonies without mucilage. B. *dividing cell*: cell division by binary fission, cell width ($\pm 1 \mu\text{m}$) and length (1-2.5 μm).

Solitary cells, thin layer of very fine diffuent mucilage, colonies with irregularly organized cells of variable shape and size, irregular outline, cells slightly elongated to oval, cell content pale blue-green, cell length/ width ratio 1-2.5:1. Cell division by binary fission, dividing the mother cell into two daughter cells, only by one plane. The strains properties agree with *Cyanobium plancticum*,^{114,115} previously described as *Synechococcus plancticus*.¹¹⁶ The strain is classified as section and order Chroococcales (I), family Gloeobacteraceae and subfamily Aphanothecoideae.

Figure 26 shows the genus *Cyanobium*,¹¹⁴ which is described as widely distributed, occurring as plankton, in subaerial and submersed benthic mats, and epiphytic.¹¹⁶⁻¹¹⁸ The common features as solitary cells $< 3 \mu\text{m}$ and cross-wise division match the strain AnoTü20 (Figure 25).

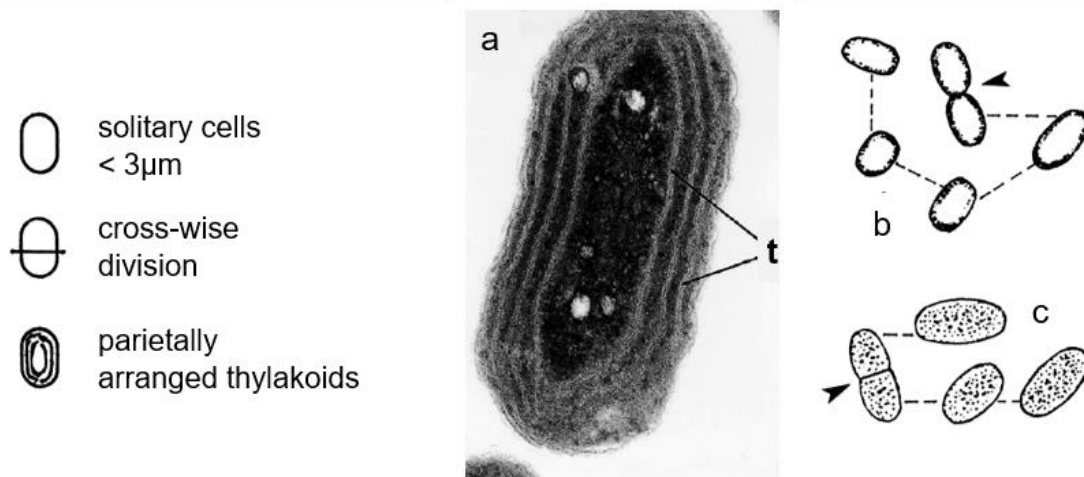


Figure 26. **Cyanobium**; a. *C. gracile*. Cross section through the cell with parietally localized thylakoids (t = thylakoids; bar = 0.3 μm);¹¹³ b. *C. eximium* and c. *C. roseum* (both described from thermal springs in Yellowstone National Park under *Synechococcus*).¹¹⁰

3.2.4.4. AnoTü 20: Chemical Profile

The biomass extract of AnoTü20 showed QS inhibition against *V. harveyi* and *S. aureus*, QS enhancing activity on *C. violaceum*, and antibacterial activity against *B. subtilis*. Additionally, the extract exhibited 55 \pm 2% inhibition of rhodesain. This broad bioactivity spectrum might either be explained by various compounds with individual activities, or by compounds with unspecific activities.

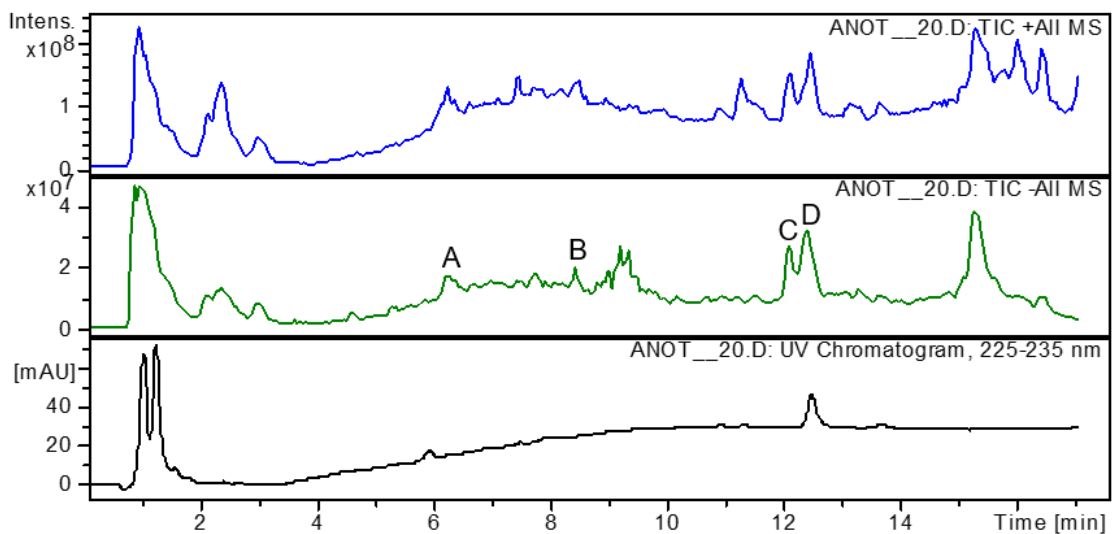


Figure 27. **Chromatogram of AnoTü20 biomass extract**. TIC pos mode (blue), neg. mode (green); HPLC-UV chromatogram (black).

The UV and total ion chromatograms (Figure 27) and the the UV and MS spectra of the detected compounds (Figure 28) show four compounds with strongly differing masses. The mass spectra of compound AnoTü20-A eluting at $t_R = 6.2$ min show a $[M+H]^+$ ion at m/z 1003.5 and a $[M-H]^-$ ion at m/z 1001.4, suggesting a mass of 1002.5 Da. Dereplication with the DNP delivers three already known substances with matching masses, isolated from cyanobacteria. Micropeptin SD1002 ¹¹⁹ and KR1002 ¹²⁰ ($C_{51}H_{70}N_8O_{13}$, M_r 1002.56) share the same molecular formular and were both isolated from *Microcystis* sp., in case of Micropeptin SD1002 more specifically from a hydrophilic extract of *Microcystis aeruginosa*. The linear lipopeptide Apramide D ($C_{54}H_{82}N_8O_8S$, M_r 1002.6) was isolated from the marine cyanobacterium *Lyngbya majuscula*.¹²¹ As the strain AnoTü20 was isolated from freshwater and classified as Chroococcales, Micropeptin SD1002 with serine protease inhibitory activity

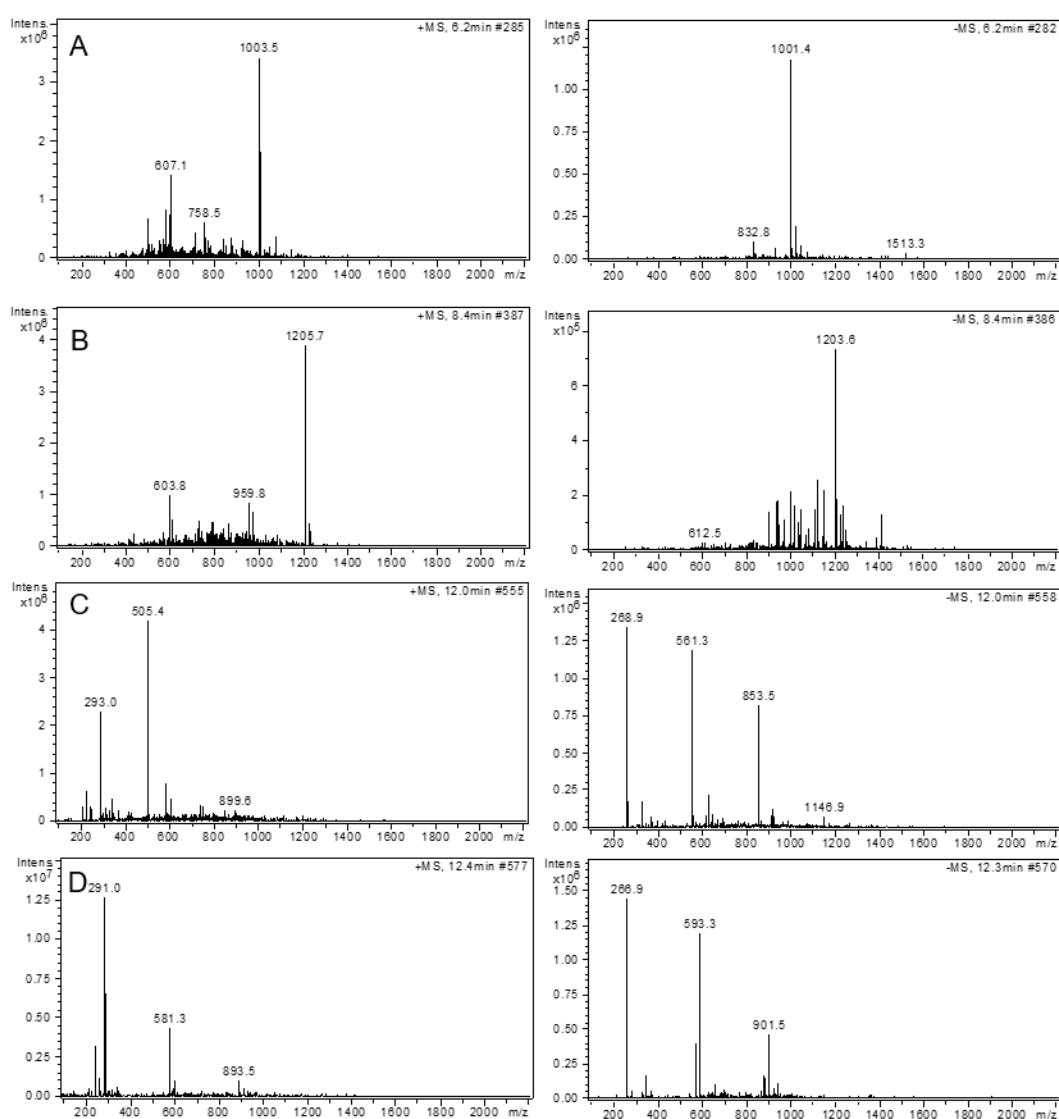


Figure 28. Mass spectra of compound A, B, C and D from AnoTü20 biomass extract. Pos. mode (left), neg. mode (right).

or Micropeptin KR1002 with chymotrypsin and elastase inhibition, seem more likely.^{119,120} Nevertheless, this assumption needs to be verified by MS-MS experiments.

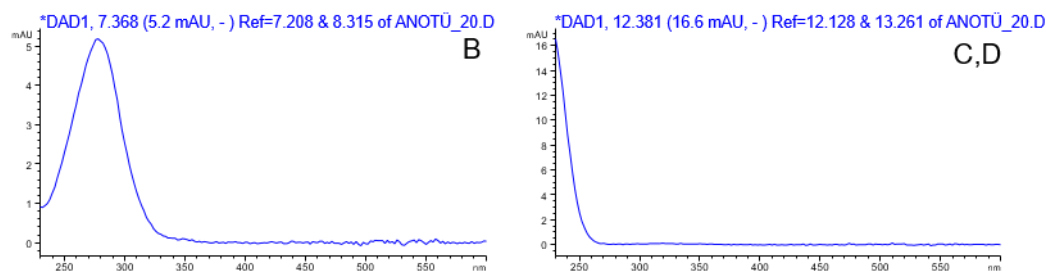


Figure 29. UV spectra of compounds A, B, C and D of biomass extract AnoTü20.

With a $[M+H]^+$ ion at m/z 1205.7 and a $[M-H]^-$ ion at m/z 1203.6 at 8.4 min, compound AnoTü20-B has a molecular mass of 1204.6 Da, for which no cyanobacteria derived substance could be found in the DNP. Though, the UV-spectrum of AnoTü 20-B with λ_{\max} 278 nm features high similarity with the UV spectra of compounds An-A1000-C, F and I (3.2.4.5). The MS spectra of AnoTü20-C at 12.0 min shows an intense ion peak at m/z 505.4 for $[M+H]^+$, but no corresponding mass in the spectra in negative mode. From the MS spectra of AnoTü20-D at 12.4 min no mass could be concluded.

The biomass extract of AnoTü20 showed QS inhibition against *V. harveyi* and *S. aureus*, QS enhancing activity on *C. violaceum*, and antibacterial activity against *B. subtilis*. Additionally, the extract exhibited $55 \pm 2\%$ inhibition of rhodesain. The inhibition of rhodesain might be caused by the compound AnoTü20-A, which mass resembles the micropeptines SD1002 and KR1002 and the linear lipopeptide Apramide D. Regarding its broad bioactivity spectrum and interesting chemical profile, further investigation by MS-MS analysis might result in the identification of novel, bioactive compounds with either varying, individual, or unspecific activities.

3.2.4.5. An-Al000: Origin and Morphological Characterization

The strain An-Al000 exhibits a polymorphic life cycle and varying morphology, depending on the presence of a nitrogen source in the medium (Figure 30). This cyanobacterium was isolated from a biofilm on stone in Cibinong, West Java, Indonesia (6°29'34.8"S 106°50'59.3"E) collected on the 25th of April 2016 by Delicia Yunita Rahman, Indonesian Institute of Sciences (LIPI), Research Center for Biotechnology, Bogor, Java. The sample was processed according to 2.2.2.1, and An-Al000 was isolated from a BG11 agarose plate with nitrogen source. Figure 30 A gives an overview of the polymorphic life cycle of a population cultivated in HD-Cultivator-Modules (10 mL) with CO₂ supply, in BG11 medium, including a nitrogen source.

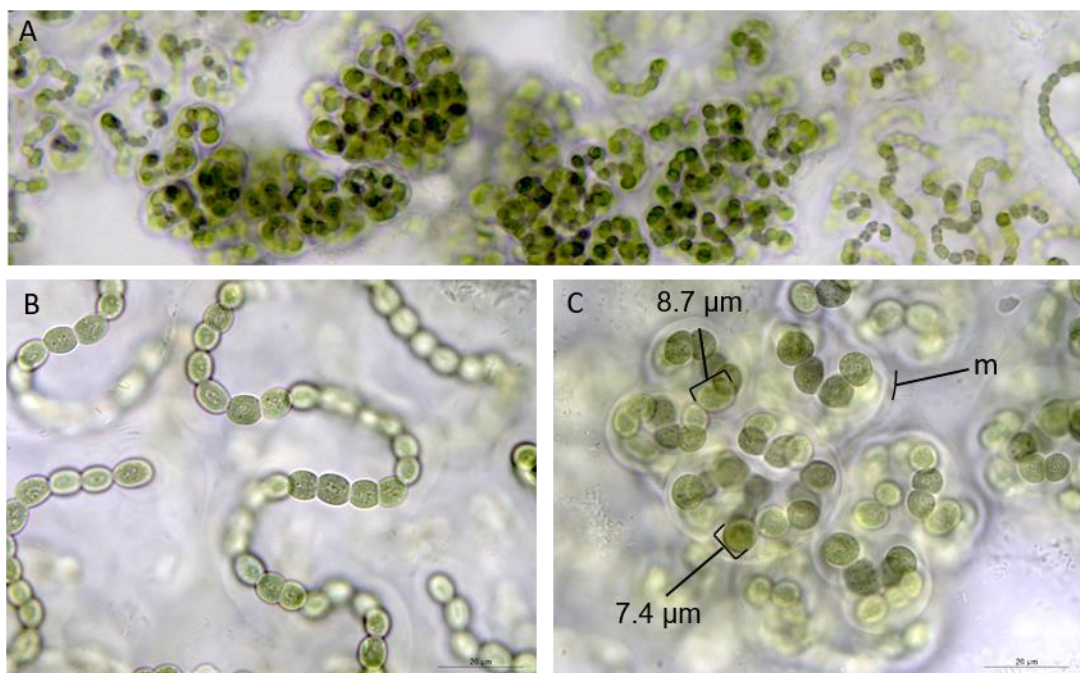


Figure 30. **Morphological variability of An-Al000.** BG11 (incl. nitrogen source), HD-Cultivator-Modules (10 mL) (2.3.1.4). A. *Overview:* varying morphology in one population, displaying a polymorphic life cycle. *Detail:* B. *Nostoc*-like stage C. *Chlorogloeopsis*-like stage, irregularly arranged in filaments with colorless sheaths (sh).

On the right side of the macroscopic picture, young filaments are shown, while mature filaments appear in the middle and on the left side. Figure 30 B and C show immature and mature filaments respectively, in more detail. Young filaments (B) show isodiametric to cylindrical cells, constricted at cross-walls, 5-6 µm wide, 5-8.5 µm long, with apical cells mostly longer than wide, oval to conical, sheath absent. Intercalary and terminal heterocysts are not present. Mature filaments (C), cells oval or irregularly shaped, 7-9 µm in diameter, cells irregularly arranged in filaments with colourless sheaths (sh), rarely cell division in two planes, neither heterocysts nor typical akinetes present. Though, the mature stage might

present akinete-like cells with thickened cell walls (arthrospores) as typical for the genus *Chlorogloeopsis*.¹²²

In order to evaluate the dependence of the morphology on nitrogen content of the media, two different media, one with the normal nitrogen supply and one without nitrogen, were applied. Figure 31 A and B show the morphological characteristics of a population grown in BG11 without a nitrogen source. Here, cells are oval or spherical light blue green with dark granules (gr). Intercalary heterocysts (ihc) 5-6 μm wide, 7-8 μm long, terminal heterocysts (thc) significantly smaller, 2-3 μm wide, 3-4 μm long, both types light yellow-green and solitary. Filaments straight to slightly coiled.

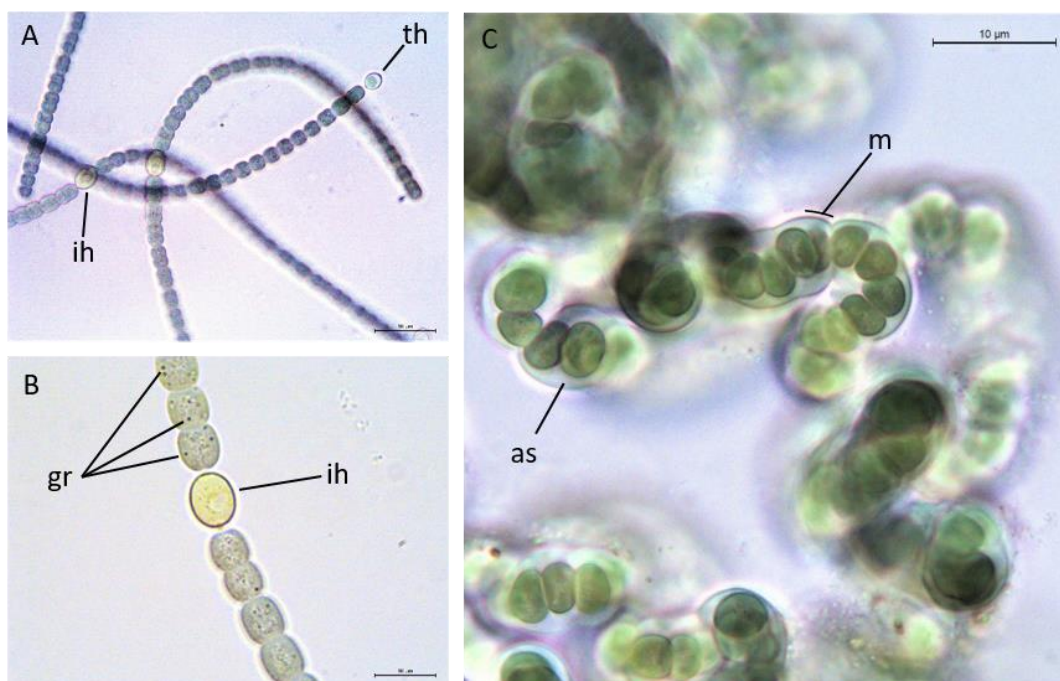


Figure 31. **Morphological variability of An-A1000 depending on the presence of a nitrogen source.** A. BG11 without nitrogen source; *overview*: *Nostoc*-like filaments with intercalary heterocysts (ih) and terminal heterocysts (thc). B. BG11 without nitrogen source; *detail*: *Nostoc*-like filament with intercalary heterocyst (ihc) and granules (gr). C. BG11 with nitrogen source; *Chlorogloeopsis*-like stage with muscilogous sheaths (m), multiple branching, germination of arthrospores (as).

Figure 31 C shows a population grown in BG11 without nitrogen supply. Here, the filaments remind of the *Chlorogloeopsis*-like stage, as previously described for mature filaments. Cells irregularly shaped, 7-9 μm in diameter, dark blue green, irregularly arranged in filaments with colourless sheaths (sh), cell division in two planes, neither heterocysts nor typical akinetes present. Cells seem to develop in arthrospores (as).

The physiology of An-A1000 reminds of *Chlorogloeopsis fritschii*, though the morphological properties of mature filaments do not exactly fit the descriptions.^{24,123,124} *Chlorogloeopsis*

fritschii represents the only member of the genus *Chlorogloeopsis*, classified in the family Chlorogloeocapsaceae.¹²⁴ Due to its special morphology, it is not easily recognised in natural samples, but probably widely distributed from thermal springs to hypersaline lakes. *Chlorogloeopsis fritschii* is also known to grow in freshwater media.¹²³ In order to clarify the taxonomic classification of An-Al000, further characterization as well as using a polyphasic approach are needed.¹²⁵

3.2.4.6. An-Al000: Chemical Profile

The biomass extract of An-Al000 not only show 54.0 ± 1.3 % inhibition of rhodesain, but also QS inhibiting and enhancing activity (Table 15). Additionally, the chemical screening by HPLC-DAD and HPLC-MS (Figure 32, Figure 33) revealed various compounds with interesting UV-spectra (Figure 34).

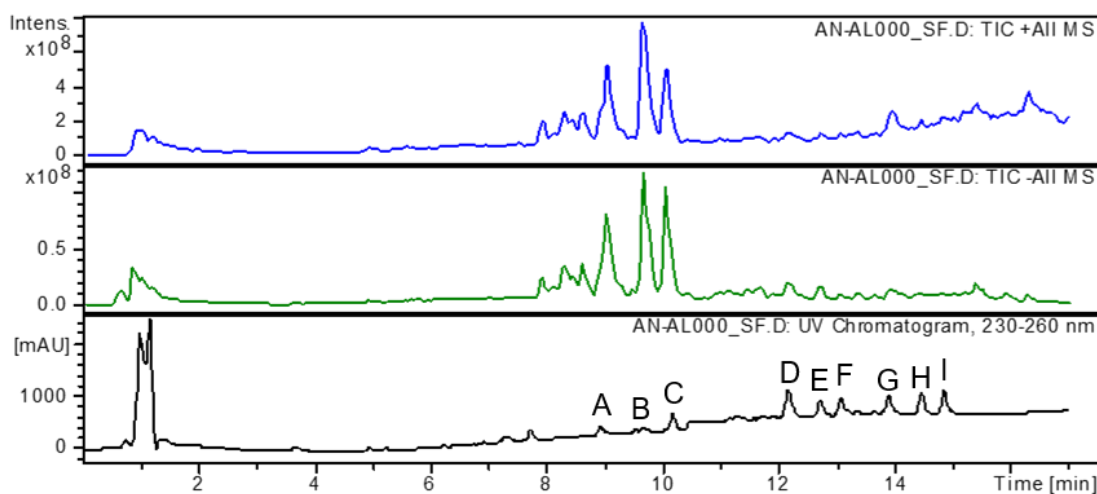


Figure 32. **Chromatogram of An-Al000 biomass extract.** TIC pos mode (blue), neg. mode (green); HPLC-UV chromatogram (black).

The three main compounds observed in the total ion chromatograms in positive and negative mode eluted after 9.1 min (An-Al000-A), 9.6 min (An-Al000-B), and 10 min (An-Al000-C). The mass spectra of the compound eluting at 9.1 min show a $[M-H]^-$ ion at $m/z = 940.5$ and a $[M+Na]^+$ ion at $m/z = 964.5$, hinting a mass of 941.5 Da for An-Al000-A. The $[M-H]^-$ ion at $m/z = 968.5$ in negative mode as well as the ions at $m/z = 992.5$ ($[M+Na]^+$) and $m/z = 952.5$ ($[M-H_2O]^+$) in positive mode at 9.6 min suggest a molecular mass of 969.5 Da for An-Al000-B.

An-Al000-C, eluting after 10.0 min, has a molecular mass of 1004.5 Da with $m/z = 1003.5$ $[M-H]^-$ in negative, and an adduct at $m/z = 1027.5$ $[M+Na]^+$ in positive mode. For the later eluting compounds between 12.1 min and 14.8 min, no molecular masses could unambiguously be

determined from the MS data (Figure 33). The UV-spectra of the compounds (Figure 34) might indicate 3 different basic structures occurring in the extract.

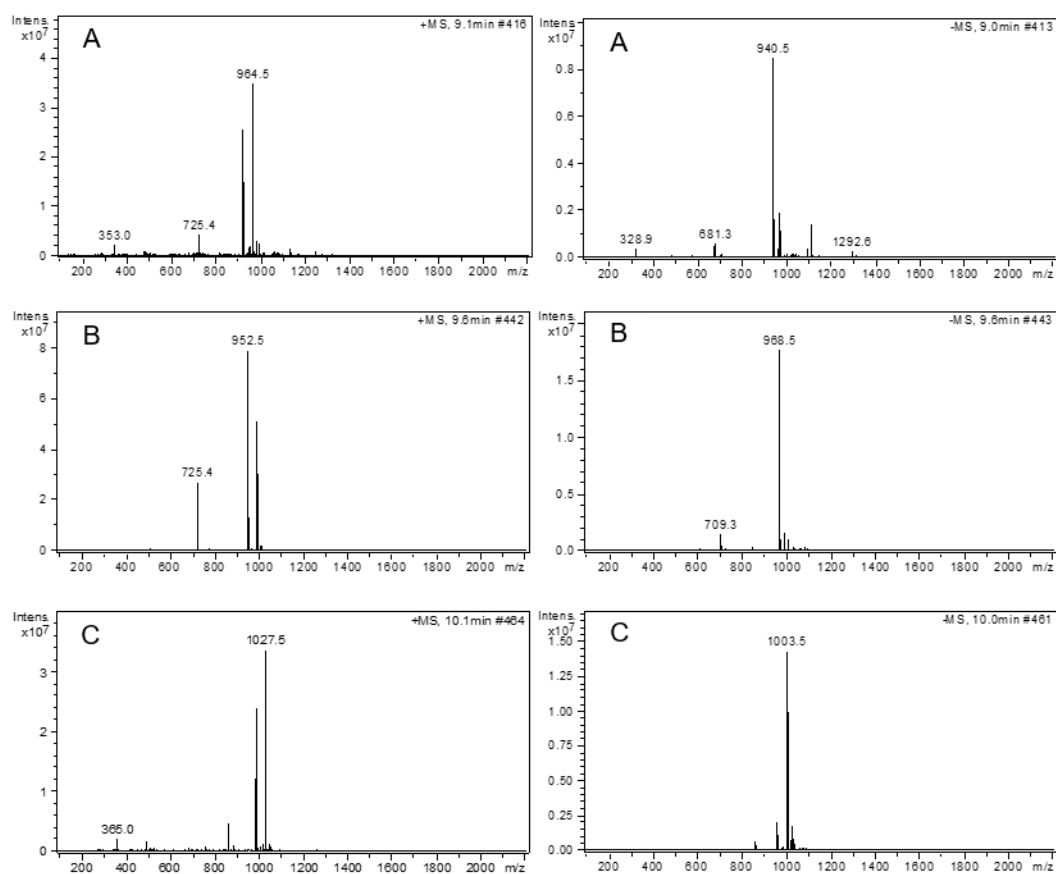


Figure 33. Mass spectra of compound A, B and C from An-Al000 biomass extract. Pos. mode (left), neg. mode (right).

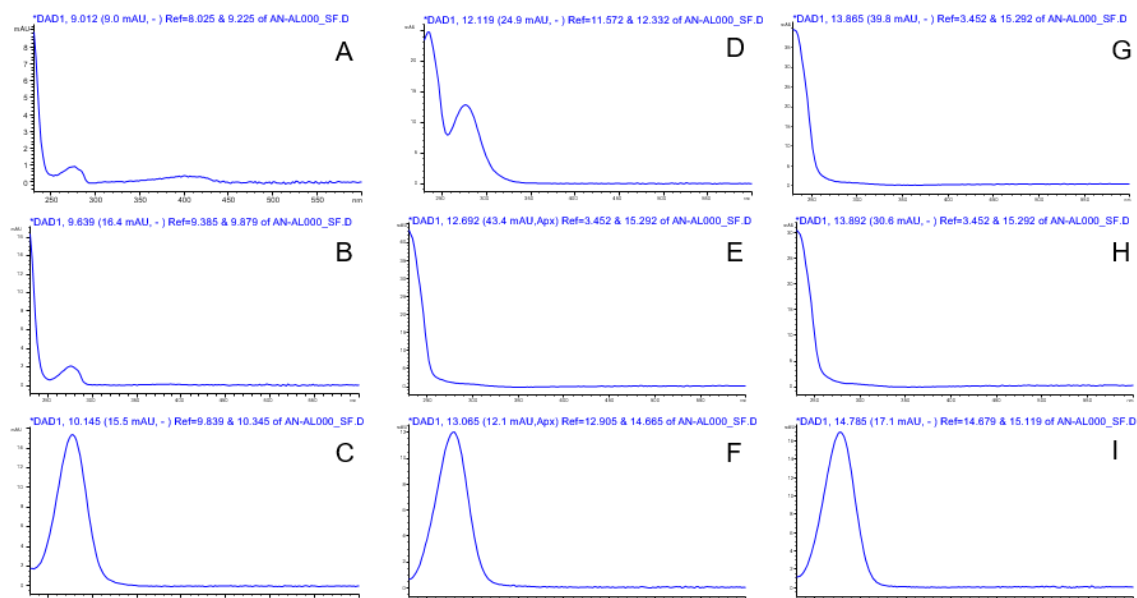


Figure 34. UV-spectra of compounds A to I of biomass extract An-Al000.

While An-Al000-A and B show similar UV-spectra with λ_{\max} at 275 nm, An-Al000-C, F, and I exhibit a λ_{\max} of 277 nm. Compound An-Al000-D shows a unique UV-spectrum with λ_{\max} 234 nm and λ_{\max} 276 nm, while An-Al000-E, G, and H exhibit a maximum at λ_{\max} 234 nm.

The mass of compound An-Al000-B corresponds to Microcystin LM (M_r 969.5, $C_{48}H_{72}N_7O_{12}S$) and Microcystin EE (M_r 969.4, $C_{46}H_{63}N_7O_{16}$),^{126,127} but the UV spectrum is not similar to those of microcystins. Insulapeptolide D also has a molecular mass of 969.6 ($C_{48}H_{75}N_9O_{12}$). This metabolite has been isolated from *Nostoc insulare* as a potent inhibitor of human leukocyte elastase.¹²⁸ Its UV λ_{\max} of 277 nm in MeOH is similar to the absorption maximum of An-Al000-B. Thus, An-Al000-B might be Insulapeptolide D, and An-Al000-A Insulapeptolide A (M_r 941.5, $C_{46}H_{71}N_9O_{12}$). The rhodesain inhibiting activity of the extract might therefore be based on the Insulapeptolides, which are known to be potent inhibitors of the serine protease human leukocyte elastase (HLE). As rhodesain belongs to the cysteine proteases, its active site is similar to the one of HLE. This assumption needs to be evaluated by MS-MS experiments.

An-Al000-C has a similar molecular mass as the depsipeptide Wewakpeptin C (M_r 1004.6, $C_{54}H_{84}N_8O_8S$), isolated from *Lyngbya semiplena*,¹²⁹ hinting that An-Al000-F and I might present further Wewakpeptins, known for cytotoxic activity. This presumption as well, needs to be confirmed by MS-MS experiments. Though some substances might be known, the biomass extract An-Al000 counts to the most promising extracts, investigated within this project, regarding its bioactivity profile and chemical composition.

3.2.4.7. An-Al115: Origin and Morphological Characterization

The strain An-Al115 was isolated from a biofilm on soil in a tea garden, Halimun Mountain National Park, Cikaniki, West Java, Indonesia ($6^{\circ}44'64.3''S$ $106^{\circ}32'39.7''E$), collected on the

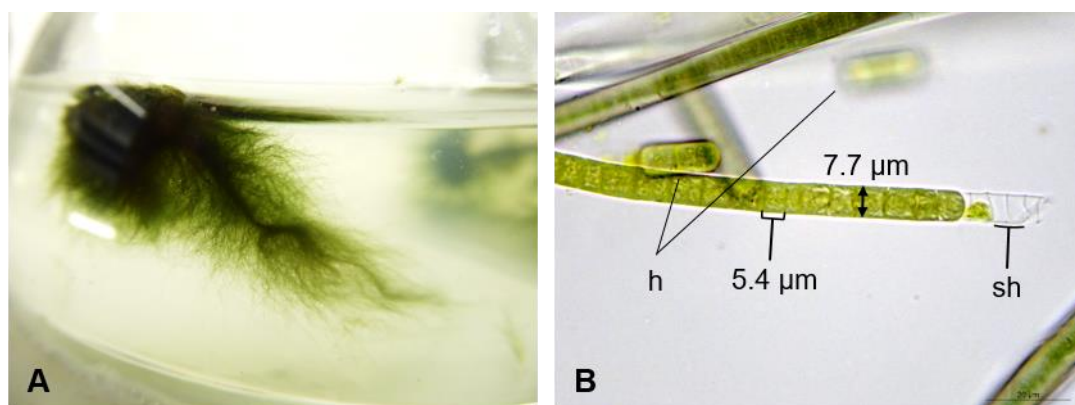


Figure 35. **Morphological characteristics of An-Al115.** A. Overview: Macroscopic appearance in HD-cultivator 100 mL. B. Detail: Trichomes straight with colorless sheaths (sh); reproduction by hormogonia (h).

21st of April 2016 by Ronja Kossack. The sample was processed according to 2.2.1, and An-Al115 was isolated from a BG11 agarose plate with nitrogen source.

An-Al115 is a filamentous, non-heterocystous cyanobacterium, forming a dark green macroscopic thallus mostly attached to the substrate, but sometimes forming free floating tufts. Filaments are solitary and straight, enclosed in a firm colourless sheath (sh). Trichomes are simple, uniseriate and isopolar, not constricted at cross-walls, 7–8 μm wide, not attenuated or widened towards ends. Cells are shorter (5–6 μm) than wide, light to dark green, sometimes with granules. Terminal cells are rounded after trichome division. Hormogonia (h) separate by fragmentation of trichomes and stay with sheaths, necridic cells occasionally present. No false nor true branching observed.

Due to the described morphological features (Figure 35), the strain AnOTü10 was classified as section III (Oscillatoriales), order Oscillatoriales, family Oscillatoriaceae, subfamily Oscillatorioideae, genus *Lyngbya*.¹¹³ The species needs to be determined by polyphasic approach. The genus *Lyngbya* is found in various morphologies and ecotypes, especially in tropical regions,¹¹³ though most studies deal with marine *Lyngbya* sp.^{130–132}

The genus was first described by Gomont (1892) and further defined and characterized by modern classification systems (Komárek, 2014).^{21,22} It roused attention due to its conspicuous secondary metabolite profile, especially regarding the benthic, marine species *Lyngbya majuscula*.^{133–135} Nevertheless, this seemingly chemical richness is based on polyphyly. In the past, morphologically similar but evolutionarily divergent species have been grouped together. In the past strains of the cyanobacterial genus *Moorea* gen. nov. have been misidentified as *Lyngbya*, leading to the assumption, that *Lyngbya* produces a rich diversity of secondary metabolites.¹³⁵

3.2.4.8. An-Al115: Chemical Profile

The biomass extract of the strain An-Al115 showed the highest rhodesain inhibiting activity of $71.4 \pm 0.2\%$, and QS inhibition on the indicator strain *V. harveyi* (Table 15). The MS data and UV spectra are shown in Figure 37, Figure 38, and Figure 36. The MS spectra of An-Al115-A provides no reliable information. For An-Al115-B, the mass spectra at 8.1 min show a $[\text{M}-\text{H}]^-$ ion at $m/z = 974.4$ and a $[\text{M}+\text{Na}]^+$ ion at $m/z = 998.4$, indicating a mass of 975.4 Da, which resembles Micropeptin 478A (M_r 975.3 Da, $\text{C}_{40}\text{H}_{62}\text{ClN}_9\text{O}_{15}\text{S}$), a potent plasmin inhibitor isolated from *Microcystis aeruginosa*.¹³⁶

The MS spectra at 8.8 min (An-Al115-C) show a $[M-H]^-$ ion at $m/z = 1002.5$ and a $[M+Na]^+$ ion at $m/z = 1026.4$, indicating a mass of 1003.5 Da. The mass of An-Al115-C corresponds to Wewakpeptin A (M_r 1003.6, $C_{54}H_{81}N_7O_{11}$),¹²⁹ which was isolated from *Lyngbya semiplena*, and is known for its cytotoxic activity. The UV spectra of An-Al115-C, indicates a similarity with the potential Insulapeptolides An-Al000-A and B, with λ_{max} ($\log \epsilon$): 277 nm (Figure 34) and not with the potential Wewakpeptin An-Al000-C. In case of An-Al115-D, a $[M+H]^+$ ion at $m/z = 869.4$, as well as a $[M-H]^-$ ion at $m/z = 867.3$ could be detected, suggesting a molecular mass of 868.4 Da, which suits the known protein phosphatase inhibitor Oscillamide B (M_r 868.4, $C_{41}H_{60}N_{10}O_9S$), isolated from *Planktothrix agardhii* and *P. rubescens*.¹³⁷ All assumptions need to be varified by MS-MS experiments, but the identification of rhodesain inhibiting substances

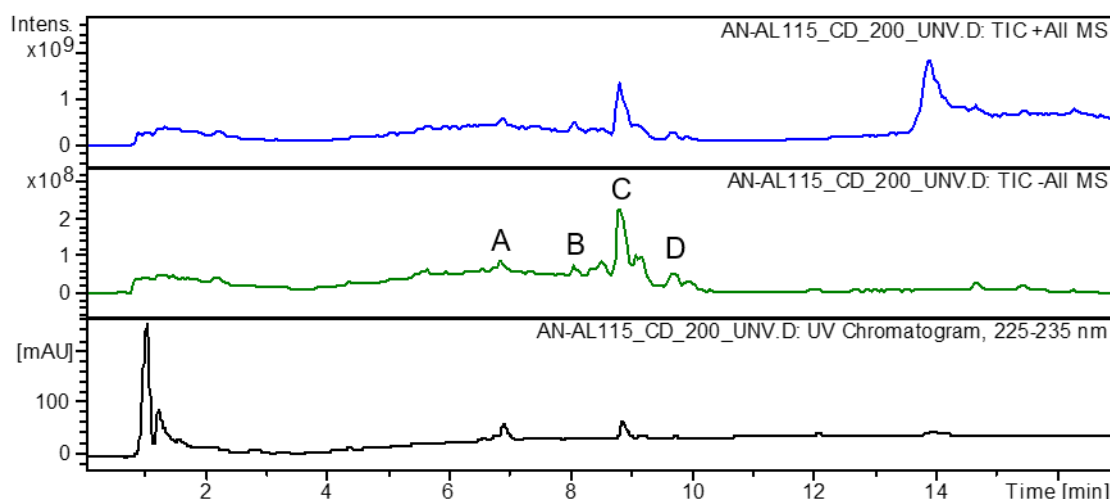


Figure 37. **Chromatogram of An-Al115 biomass extract.** TIC pos mode (blue), neg. mode (green); HPLC-UV chromatogram (black).

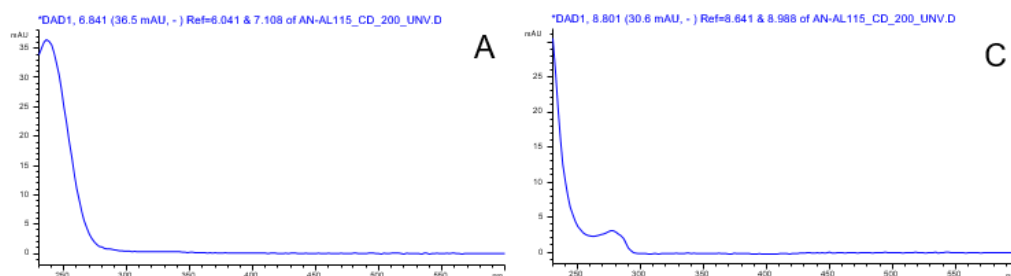


Figure 36. **UV-spectra of compounds-A and B of biomass extract An-Al115.**

in the biomass extract An-A115 could be beneficial for our endeavour to find novel rhodesain inhibitors.¹³⁷

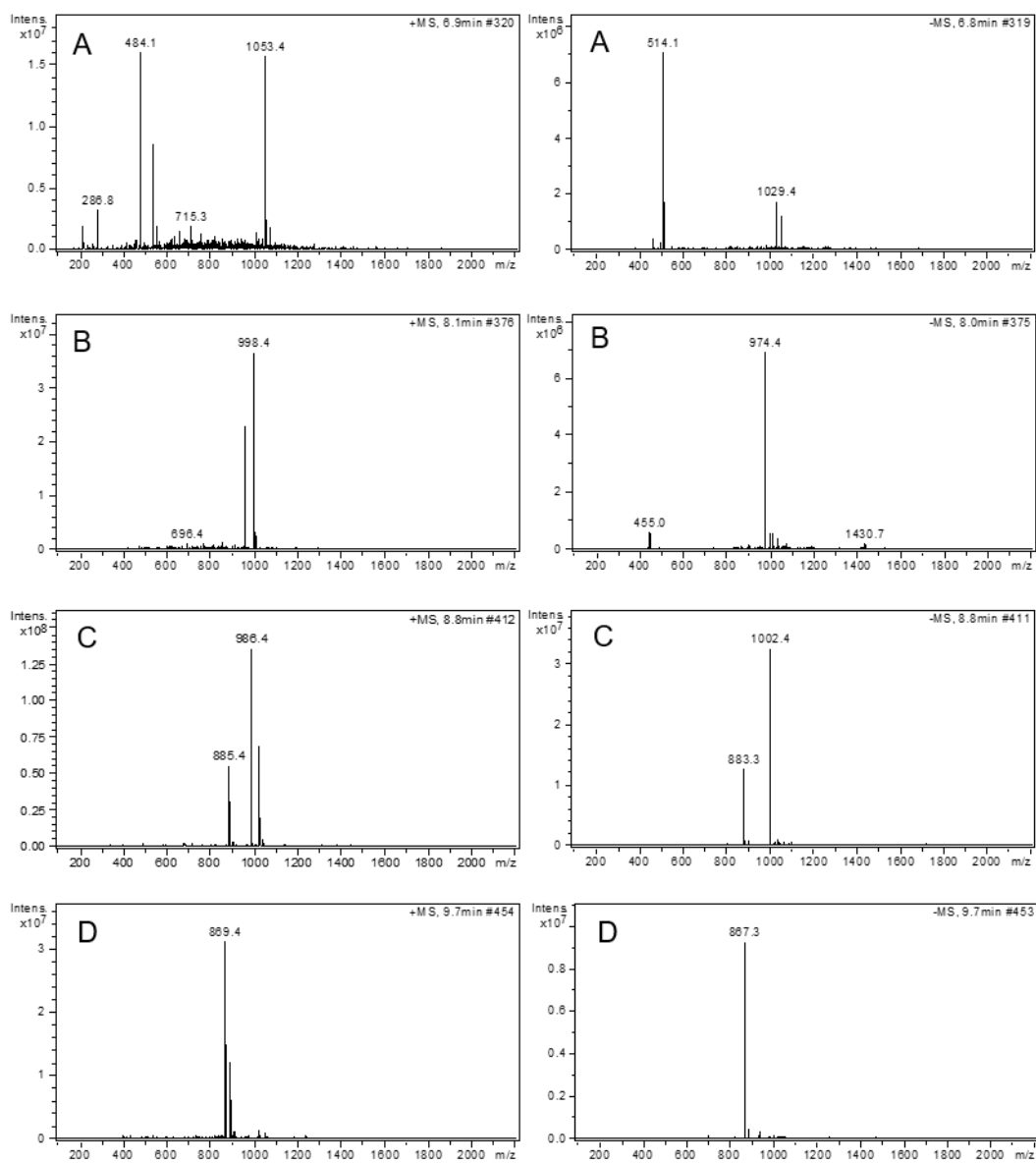


Figure 38. Mass spectra of compound A to D from An-A115 biomass extract. Pos. mode (left), neg. mode (right).

3.2.4.9. An-Al061.1: Origin and Morphological Characterization

This cyanobacterium was isolated from a soil biofilm collected in Cibinong, West Java, Indonesia (6°29'59.6"S 106°49'44.2"E) on the 19th of April 2016 by Delicia Yunita Rahman, Indonesian Institute of Sciences (LIPI), Research Center for Biotechnology, Bogor, Java. The sample was processed according to 2.2.2.1 (A), and An-Al061.1 was isolated from a BG11 agarose plate without nitrogen source.

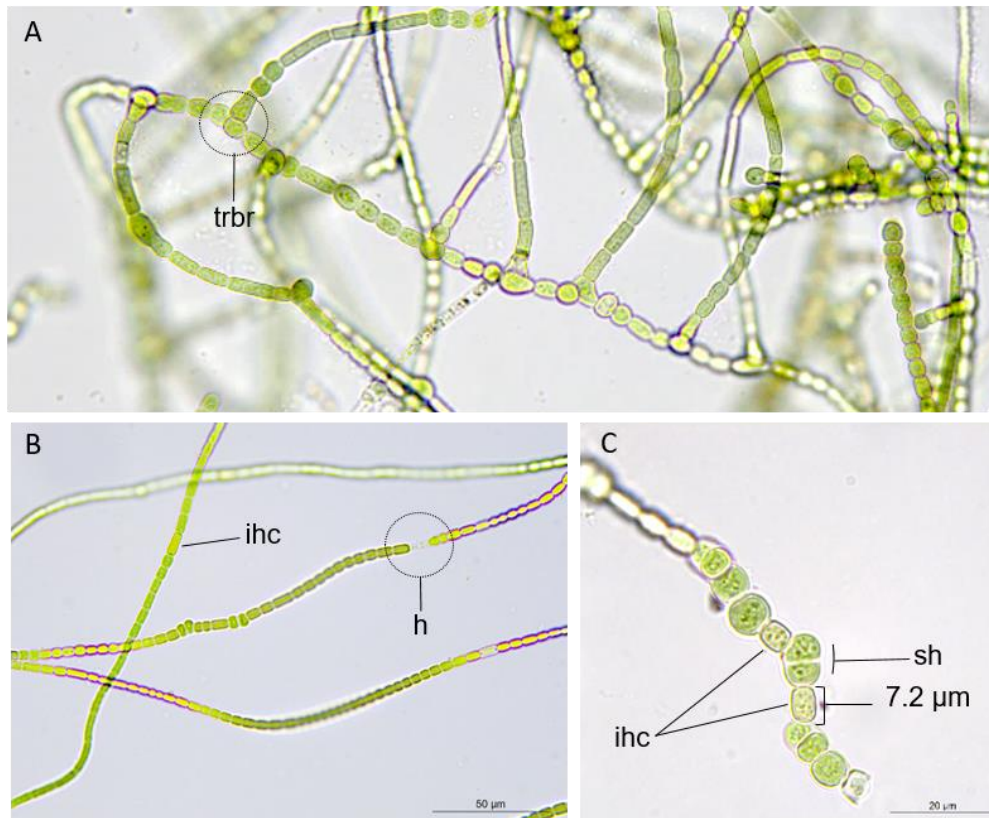


Figure 39. **Morphological characteristics of An-Al061.1.** A. *Overview*: Polymorphic population; true branching (trbr). B. *Detail*: Intercalary heterocysts (ihc), and formation of hormogonia resp. hormocytes (h). C. *Detail*: Intercalary heterocysts (ihc), colorless sheath (sh).

The filamentous cyanobacterium grows as small colonies consisting of intertwined, branched filaments, in liquid and on solid medium with and without nitrogen source. The filaments show extensive true-branching (T-like, rarely Y-like) (Figure 39 A). Trichomes uniseriate, composed of polymorphic cells, from slightly to clearly constricted at crosswalks, (3)-5-8-(12) µm wide, with a thin colourless sheath, up to 1 µm wide. Lateral filaments are more or less of the same width as the main filaments. The cells are short to long, 5-12-(20) µm in length and as wide as the main filaments, mostly barrel-shaped, but some oval. Heterocysts occur intercalary and lateral, cylindrical, of the same length as vegetative cells (Figure 39 B, C). Hormogonia (h) originate at the apical part of lateral branches (Figure 39 B), where they

are separated from the vegetative cells without the formation of necrotic cells as hormocytes (sheathed hormogonia).

Evaluation of the described morphological features suggest a classification in the family Hapalosiphonaceae within the order Nostocales. Here, An-AL061.1 might either belong to the genus *Chondrogloea*¹³⁸ or *Hapalisophon*.²³ For the genus *Chondrogloea*, only two species are described, and as no phylogeny is known, the whole genus needs revision.¹²² The species *Chondrogloea flagelliformis* was found on wet rocks in Indonesia, Java, and is as well-known under the pseudonyms *Mastigocladus flagelliforme*¹³⁹ and *Hapalisophon flagelliforme*,¹⁴⁰ indicating taxonomic difficulties.¹²²

3.2.4.10. An-AL061.1: Chemical Profile

The biomass extract An-AL061.1 was counted as hit extract due to its antimicrobial activity against *S. aureus* and *B. subtilis*, as well as its QS enhancing activity on *C. Violaceum*. HPLC-DAD and HPLC-MS experiments revealed a complex composition (Figure 40), but dereplication using the DNP, revealed that most of the detected compounds might already be known, as summarized in Table 16. The corresponding mass spectra are shown in the Appendix (Figure A 1).

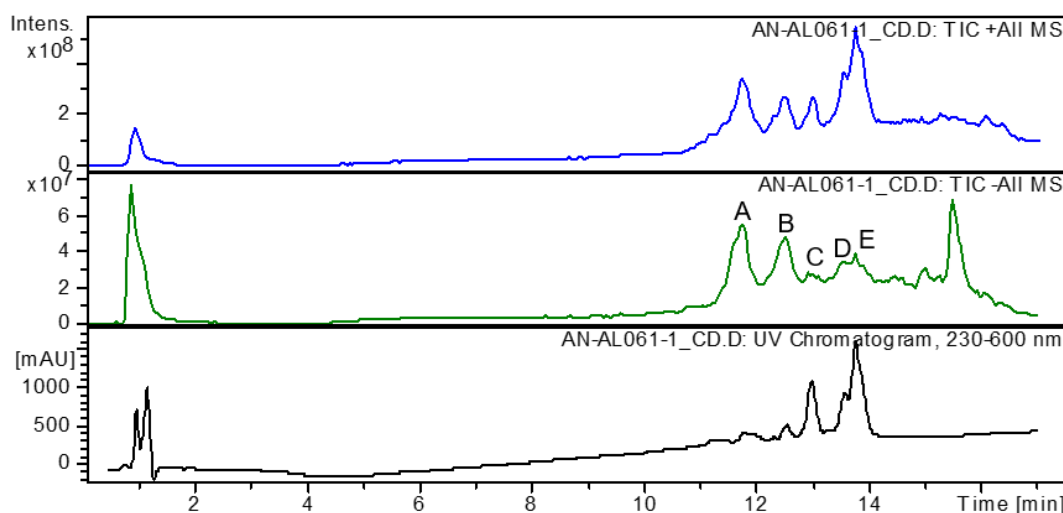


Figure 40. **Chromatogram of An-AL061.1 biomass extract.** TIC pos mode (blue), neg. mode (green); HPLC-UV chromatogram (black).

In the MS data at least five different main components were recognized. Compound An-AL061.1-A showed an $(M+H)^+$ ion at 11.7 min with $m/z = 1032.6$, resembling the peptide Oscillapeptilide 97B (M_r 1031.5, $C_{52}H_{73}N_9O_{13}$) with inhibitory activity against trypsin (IC_{50} 0.2 mg/mL).¹⁴¹ Compound Al061.1-B with an $(M+H)^+$ ion at 12.5 min with $m/z = 998.7$ matches

the mass and UV-spectra of the Trypsin inhibitor Micropeptin SF995 (M_r 995.5, $C_{48}H_{73}N_{11}O_{12}$) with λ_{max} 206; 280 (MeOH).¹⁴²

With an (M+H)⁺ ion at 13.0 min with m/z = 609.4, compound Al061.1-C equals Microcin SF 608 (M_r 608.3, $C_{32}H_{44}N_6O_6$), isolated from the same water bloom of *Microcystis* sp. as Micropeptin SF995. It also inhibited trypsin (IC₅₀ 0.5 mg/mL).¹⁴¹ Additionally, the mass fits the dechlorinated form of Microginin 91A (Microginin 91B, M_r 608.3, $C_{28}H_{50}Cl_2N_4O_6$), for which no UV data is available.¹⁴³

The (M+H)⁺ ion at 13.5 min with m/z = 305.0 (Al061.1-D) resembles a derivate of Fischerindole L,¹⁴⁴ and three derivatives of Hapalindole A and Hapalindole E each (M_r 304.2, $C_{21}H_{24}N_2$) (Table 16).^{145,146} These results fit to the (M+H)⁺ ion at 13.8 min with m/z = 339.1 (Al061.1-E), which could be assigned to either Fischerindole L, Hapalindole A, or Hapalindole E (M_r 338.2, $C_{21}H_{23}ClN_2$), all exhibiting similar UV-spectra with λ_{max} 220; 278; 290 and λ_{max} 222; 280; 291 respectively.

Table 16. Compounds isolated from *Hapalisophon* sp. or *Fischerella* sp., which fit the MS data and UV spectra of molecules in the biomass extract An-Al061.1.

no.	t_R [min]	m/z [M+H] ⁺	chemical name	molecular formula	accurate mass	source
A	11.7	1032.6	Oscillapeptilide 97B	$C_{52}H_{73}N_9O_{13}$	1031.532786	<i>Oscillatoria agardhii</i> ¹⁴¹
B	12.5	998.7	Micropeptin SF995	$C_{48}H_{73}N_{11}O_{12}$	995.544019	<i>Microcystis</i> sp. ¹⁴²
C	13	609.4	Microcin SF 608	$C_{32}H_{44}N_6O_6$	608.332234	<i>Microcystis</i> sp. ¹⁴²
			Microginin 91A, dechloro	$C_{28}H_{50}Cl_2N_4O_6$	608.310742	<i>Microcystis aeruginosa</i> ¹⁴³
D	13.5	305.0	Fischerindole L, 10- Epimer, dechloro	$C_{21}H_{24}N_2$	304.193948	<i>Hapalosiphon welwitschii</i> ¹⁴⁴
			Hapalindole A, dechloro	-	-	<i>Hapalosiphon fontinalis</i> ATCC 39964 ^{145,146}
			Hapalindole A, 9- Epimer, dechloro,	-	-	<i>Fischerella</i> ATCC 43239 ^{145,146}
			Hapalindole A, 10a- Epimer, dechloro,	-	-	<i>Hapalosiphon fontinalis</i> ATCC 39964 ^{145,146}
			Hapalindole E, dechloro	-	-	<i>Hapalosiphon fontinalis</i> ¹⁴⁶

			Hapalindole E, 5'- Epimer, dechloro	-	-	<i>Hapalosiphon welwitschii, Westiella intricata, H. laingii</i> ¹⁴⁶
			Hapalindole E, 1',2',5'- Triepimer, dechloro,	-	-	<i>Hapalosiphon laingii</i> ¹⁴⁶
E	13.8	339.1	Fischerindole L	C ₂₁ H ₂₃ ClN ₂	338.154976	<i>Fischerella muscicola</i> ¹⁴⁴
			Hapalindole E	-	-	<i>Hapalosiphon fontinalis</i> ¹⁴⁵
			Hapalindole A	-	-	<i>Hapalosiphon fontinalis</i> ¹⁴⁵

Regarding the UV-spectra of the identified compounds (Figure 41), compound Al061.1-B and Al061.1-C, as well as Al061.1-D and Al061.1-E seem to be structurally related. The assumptions referring An-Al061.1-A, -B, and -C need to be further analysed by MS-MS experiments, as all matching compounds were isolated from different genera than *Hapalosiphon*. An-Al061.1-D and -E seem to resemble either the Fischerindoles or the

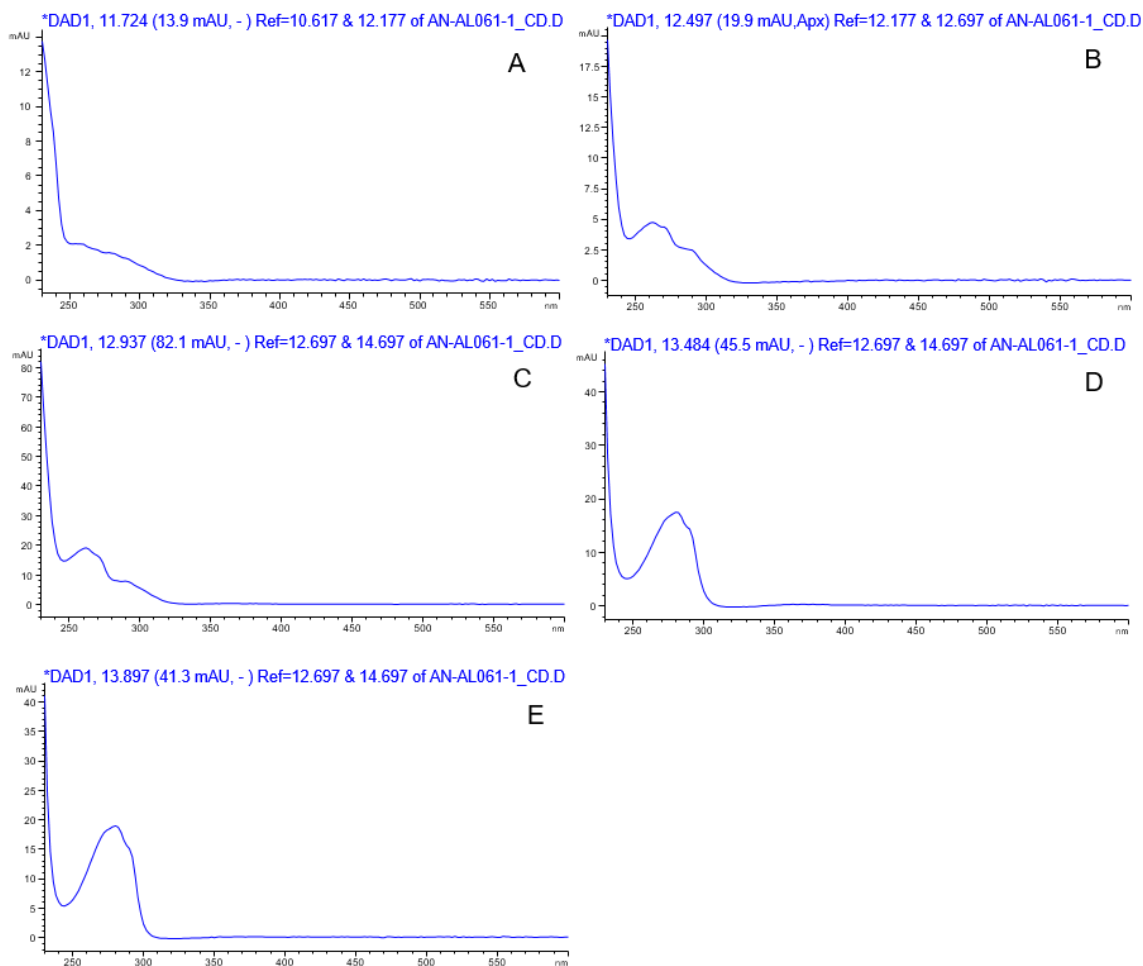


Figure 41. UV spectra of compounds A, B, C, D, and E of biomass extract An-Al061.1.

Hapalindoles, as An-AI061.1 was classified in the family Hapalosiphonaceae within the order Nostocales.

3.2.4.11. An-AI006.1: Origin and Morphological Characterization

The strain An-AI006.1 was isolated from a biofilm on soil in the Halimun Mountain National Park, Citalahab, West Java, Indonesia (6°44'34.3"S 106°31'82.8"E), collected on the 20th of April 2016 by Ronja Kossack. The sample was processed according to 2.2.1, and An-AI006.1 was isolated from a BG11 agarose plate without nitrogen source. Due to its distinct morphological characteristics (Figure 42), the strain could easily be identified as *Cylindrospermum* sp. (Nostocales (III), Nostocaceae).

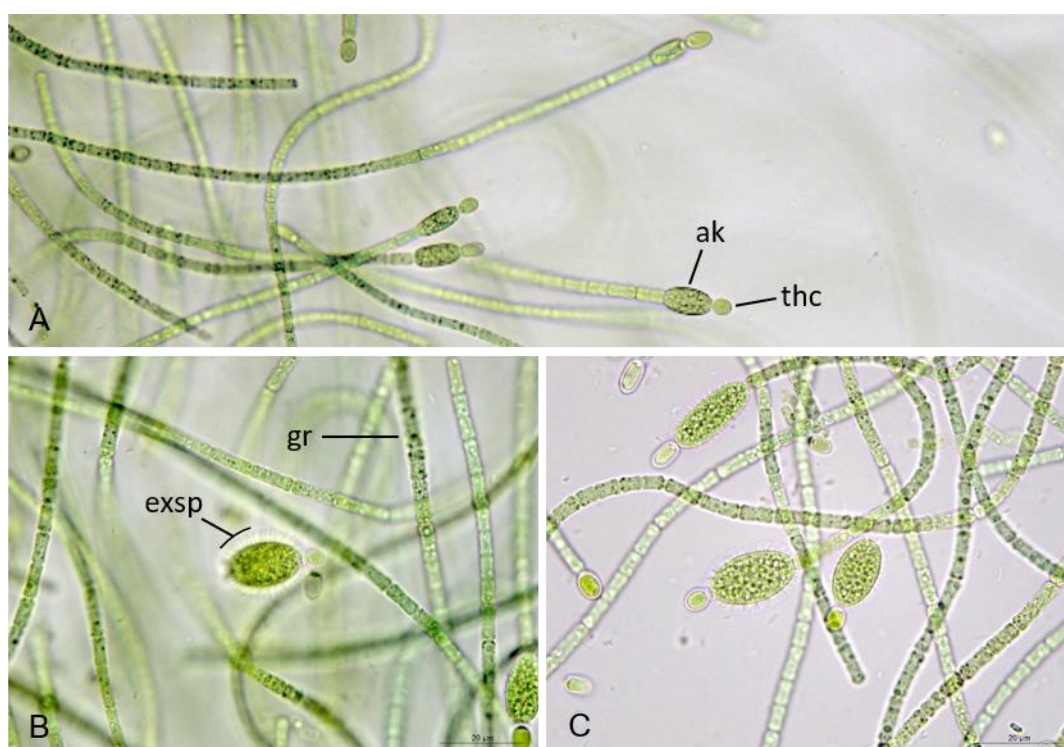


Figure 42. **Morphological characteristics of An-AI006.1** BG11 without nitrogen source; A. overview: Slightly curved filaments with terminal heterocysts (th) and immature paraheterocytic akinetes (ak). B. and C. detail: Trichomes with granules (gr) and mature akinetes with exospores (exsp).

Thallus gelatinous, with shiny wet surface, blue green to green or olive-green when old, air bubbles forming in liquid culture and on solid medium. Filaments motile and slightly curved. Trichomes long, cells constricted at cross walls, 3.5–4.5 µm wide, barrel shaped, longer than wide, with blue-green, granulated cytoplasm, without aerotypes, 3.5–8 µm long. End cells rounded. Terminal heterocysts with always paraheterocytic akinetes. Heterocysts always terminal, rounded, almost spherical to ellongate-ellipdial, light green, 3.5–7 µm long, 3.5–4.5

μm wide. Akinetes single, oval to cylindrical, with bright green strongly granulated content, 16-20 μm long, 8-10 μm wide, with smooth, thin, colourless exospores, 3.5 μm long.

Most *Cylindrospermum* species are benthic, epiphytic or epilithic.¹⁴⁷ They are known to be found as biofilm on moist and flooded grounds, especially in rice fields where they serve as biofertilizer.^{148,149} There are species described from Europe, as well as from subtropical and tropical habitats.¹²² This isolate does not resemble any found description for a known *Cylindrospermum* species, though it would need to be confirmed by a polyphasic approach whether this is a novel species.¹²⁵

3.2.4.12. An-AL006.1: Chemical Profile

Even though the biomass extract An-AL006.1 showed no activity in the bioactivity screening, the main compound in this extract might be interesting. The HPLC-UV chromatogram and TIC in Figure 44 reveal a lipophilic compound ($t_R = 15.7$ min).

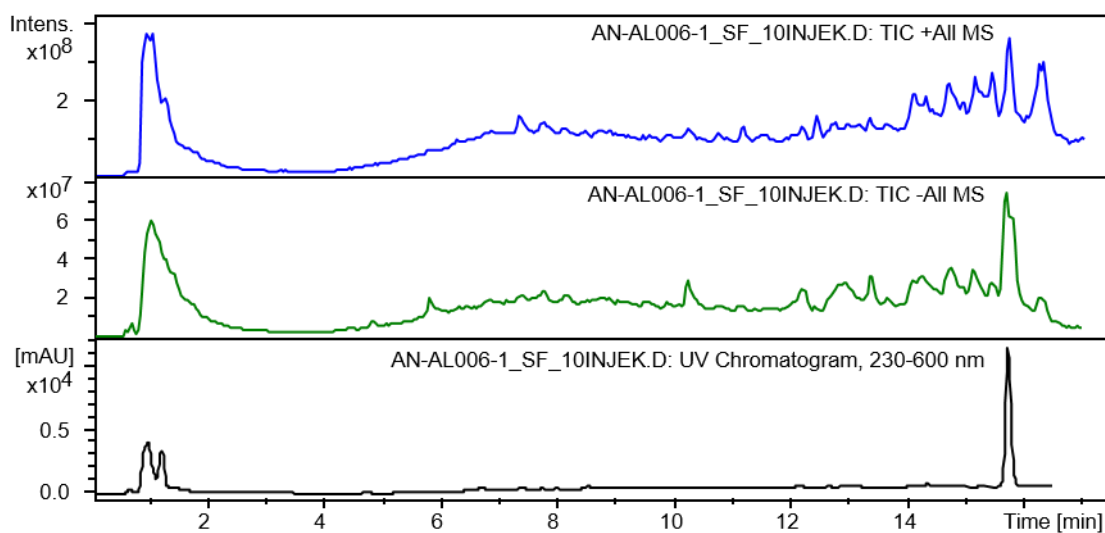


Figure 44. **Chromatogram of An-AL006.1 biomass extract.** TIC pos mode (blue), neg. mode (green); HPLC-UV chromatogram (black).

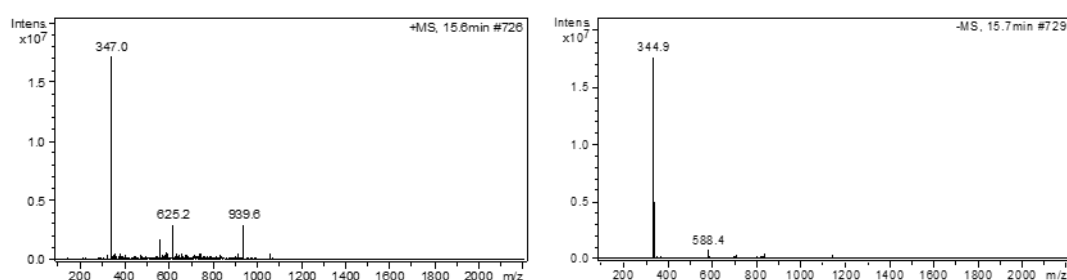


Figure 43. **Mass spectra of compound A of An-AL006.1 biomass extract.** Pos. mode (left), neg. mode (right).

The corresponding mass spectra (Figure 43) featured an $(M+H)^+$ ion with $m/z = 347.0$ and a $(M-H)^-$ ion with $m/z = 345.9$. For the corresponding mass range no resembling known

compound, isolated from cyanobacteria sp. could be found in the Dictionary of Natural products. Additionally, the UV spectrum with λ_{max} 228.0 and 299.6 showed no similarity to any other compound identified within this study (Figure 45). The following attempts to isolate this unknown lipophilic compound An-AI006.1-A by Flash Chromatography from 250 mg biomass extract yielded a not weighable amount. Due to the low concentration, the subsequent ^1H NMR experiment did not lead to any insight into the structure of this substance.

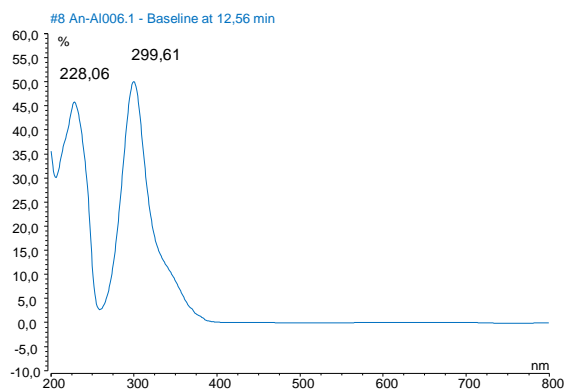


Figure 45. UV spectrum of compound A of biomass extract An-AI006.1.

3.3. Screening of the Cyano Biotech GmbH Extract Collection for Rhodesain Inhibitory Activity

In cooperation with the company Cyano Biotech GmbH, Berlin, Germany, and Prof. Dr. Tanja Schirmeister (Institute of Pharmacy und Biochemistry, Johannes Gutenberg-Universität Mainz, Germany), a primary screening of 450 biomass and 122 medium extracts was performed (2.4.1). To our surprise, 69 of the 450 screened biomass extracts showed an inhibition of more than 90% at 0.33 mg/mL. These extracts were subjected to a second screening with lower extract concentration (0.1 mg/ mL), resulting in twelve extracts (2.7%) with an inhibition equal or higher than 70% (Table 17).

Table 17. Cyanobacteria biomass extracts with an inhibition of rhodesain equal or higher than 70%, and corresponding media extracts.

Strain	rhodesain inhibition [%]			
	biomass extract [mg/mL]		medium extract [mg/mL]	
	0.1	0.33	0.2	0.33
<i>Nostoc</i> 1	81	99	-	55
<i>Cylindrospermum</i> 1	100	100	-	-
<i>Cylindrospermum</i> 2	95	100	98	99
<i>Fischerella</i> 1	97	99	-	-
<i>Fischerella</i> 2	96	99	-	-
<i>Nostoc</i> 2	86	96	-	-
<i>Cylindrospermum</i> 3	99	100	-	-
<i>Oscillatoria</i> 1	93	100	-	66
<i>Nostoc</i> 3	98	100	-	94
<i>Calothrix</i> 1	70	99	-	48
<i>Aphanizomenon</i> 1	74	99	-	-
<i>Stigonematales</i> 1	70	98	-	-

Interestingly, only *Cylindrospermum* 2 showed prominent inhibitory activity for both medium und biomass extracts, though some medium extracts were not available. From the twelve most active extracts, eight belong to the section Nostocales, three to the section Stigonematales, and one to the section Oscillatoriales, while none of the strains belonging to the Chroococcales showed pronounced inhibitory activity. Based on their bioactivity and chemical profiles, the five most promising biomass extracts (*Cylindrospermum* 2, *Cylindrospermum* 3, *Oscillatoria* 1, *Nostoc* 3, *Aphanizomenon* 1) were chosen for fractionation

using Flash Chromatography and semi-preparative HPLC in order to identify and isolate the rhodesain inhibitory compounds (Master thesis, Trang Nguyen, 2017). As most attempts to isolate the active compounds were unsuccessful, solely the processing of biomass extract *Nostoc* 3 is reported within this thesis.

Table 18. **Medium extracts with an inhibition of rhodesain equal or higher than 70%.**

strain	rhodesain inhibition [%]			
	biomass extract [mg/mL]		medium extract [mg/mL]	
	0.1	0.33	0.2	0.33
<i>Anabaena</i> 1	-	86	78	85
<i>Fischerella</i> 3	-	67	83	95
<i>Calothrix</i> 2	-	86	97	100
<i>Cylindrospermum</i> 2	95	100	98	99
<i>Microcystis</i> 1	-	64	88	92
<i>Nostoc</i> 4	-	66	89	94
<i>Tolypothrix</i> 1	-	19	79	95
<i>Oscillatoriales</i> 2	60	93	85	91
<i>Microcystis</i> 2	-	86	86	86
<i>Nostoc</i> 5	-	-	81	86
<i>Planktothrix</i> 1	60	90	98	97
<i>Microcystis</i> 3	-	74	96	99
<i>Anabaena</i> 2	-	81	87	98
<i>Nostoc</i> 6	-	89	93	100
<i>Pseudanabaena</i> 1	-	87	70	83
<i>Limnothrix</i> 1	38	96	75	86
<i>Stigonematales</i> 2	-	58	81	84
<i>Scytonema</i> 1	45	90	80	95

Of the screened medium extracts 21 of 122 showed an inhibition of more than 80% at 0.33 mg/mL (17.2%) (Table 18). A second screening of these active extracts was performed with lower extract concentration (0.2 mg/mL) to narrow down the number of promising extracts. Surprisingly, the screening with 0.2 mg/mL still resulted in 18 extracts (10%) with an inhibition higher than 70 %, though in case of some extracts there was not enough amount

left to perform a second screening. From these most active extracts, ten belonging to the section Nostocales, two to the section Stigonematales, three to the section Oscillatoriales, and three *Microcystis* strains belonging to the Chroococcales showed pronounced inhibitory activity.

Based on their chemical profile and rhodesain inhibition, two medium extracts were chosen for further processing (medium extracts of *Fischerella* 3 and *Nostoc* 6). As not all approaches led to the successful isolation of bioactive compounds, solely the analysis of the medium extract of *Nostoc* 6 is described in this thesis.

3.3.1. Isolation of Inhibitory Compounds from the Biomass Extract *Nostoc* 3

The first isolation of bioactive compounds from *Nostoc* 3 was performed by Trang Nguyen under my supervision (Master thesis, Trang Nguyen, 2017). The results are summarized in the following, for more details refer to the mentioned thesis.

Analysis of the biomass extract by HPLC-DAD revealed minor peaks eluting after 3 to 4.5 min, and 3 prominent peaks between 6.5 and 8 min (Figure 46).

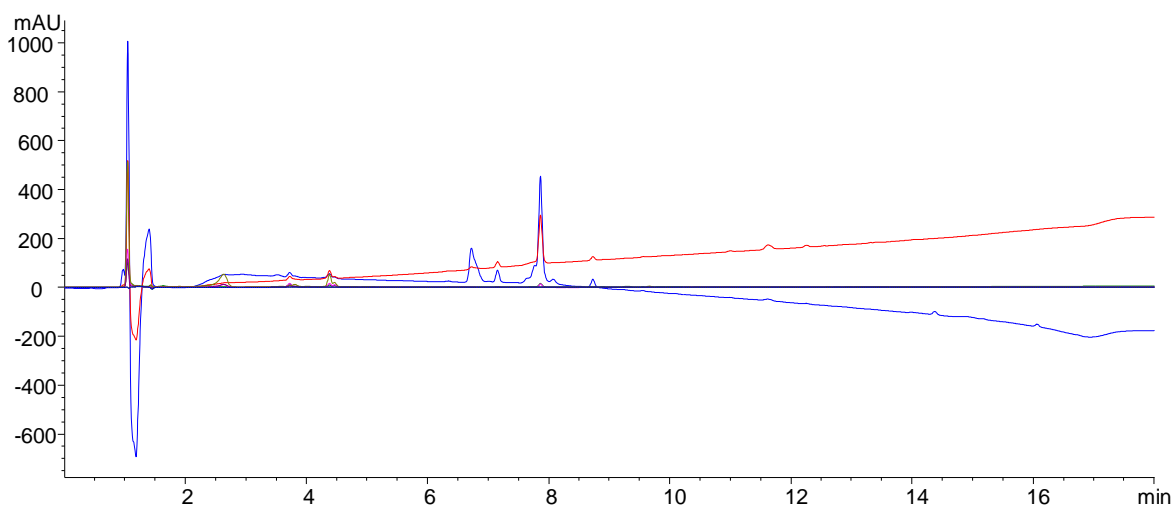


Figure 46. **HPLC-UV chromatogram of biomass extract *Nostoc* 3.** Blue: 210 nm, red: 230 nm, green: 260 nm, pink: 280 nm, green: 310 nm.

The subsequent pre-fractionation of 0.3 g biomass extract with Flash Chromatography (see section 2.7.1) accompanied by bioactivity testing of the resulting fractions, showed that the main inhibitory activity of the extract was due to the compounds eluting with 12% to 24% MeOH in H₂O. Thus, fractions 7 to 14 were combined (80 mg yield), and subjected to further analysis by semi-preparative HPLC (time-based fractionation, see section 2.7.2). The major compounds of the biomass extract showed considerably less inhibitory activity with 10-15%.

Time based fractionation at a gradient of 5% to 30% MeCN in H₂O (0.1% FA) and a subsequent rhodesain assay with the resulting fractions, assigned the bioactivity to compounds eluting with $t_R = 13-14$ min (Figure 47).

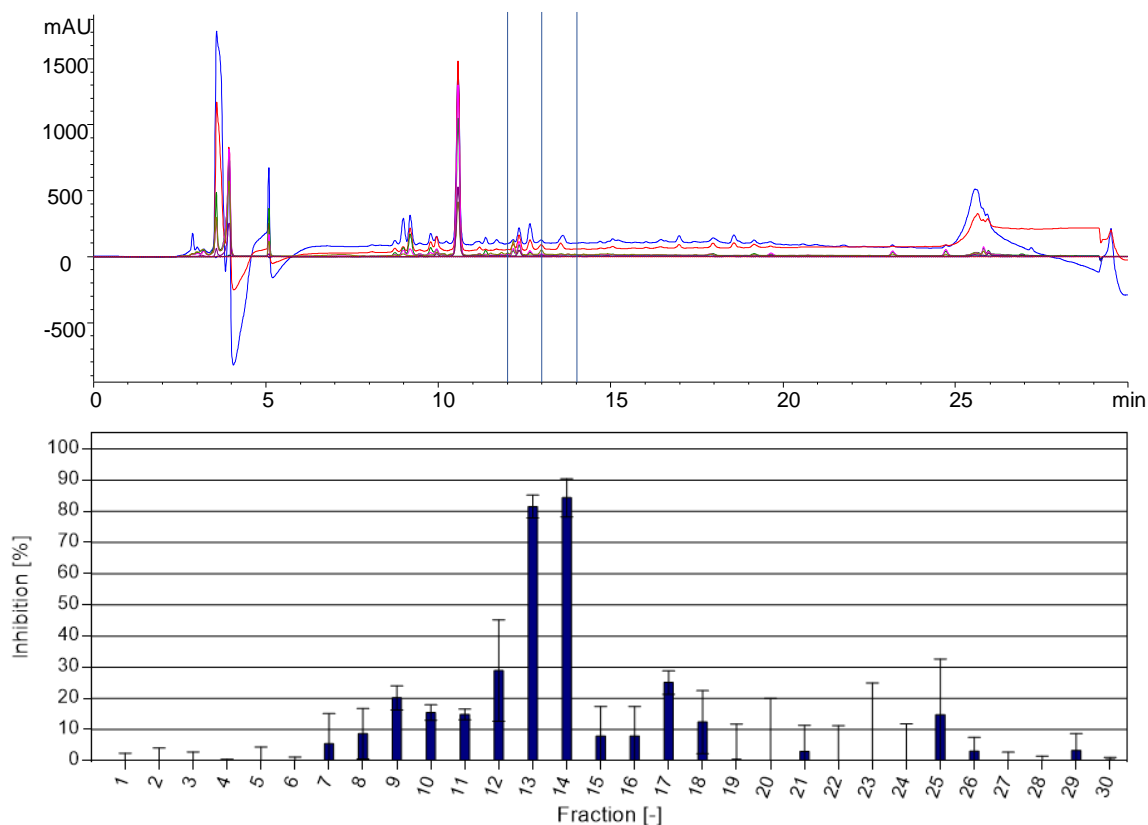
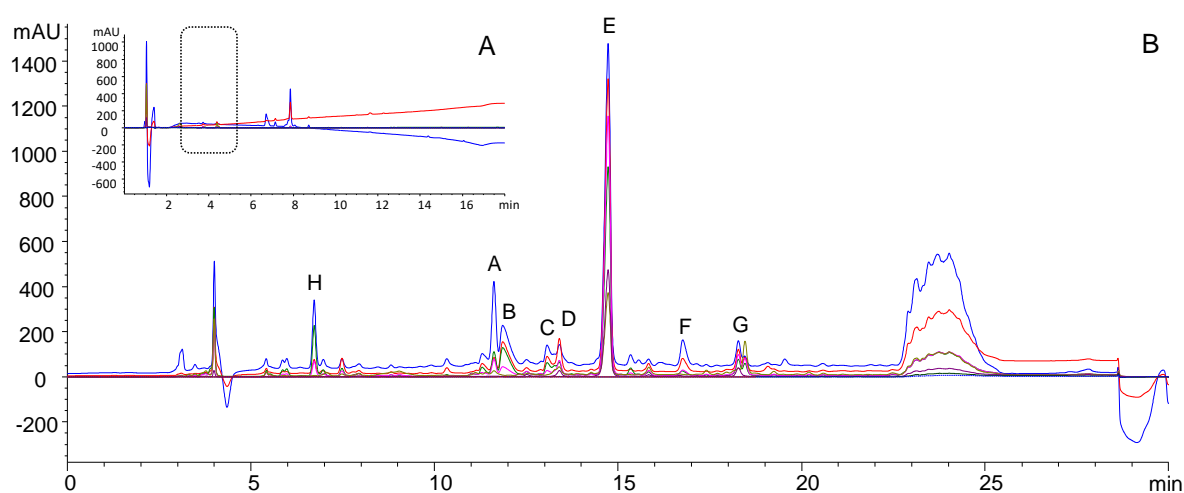


Figure 47. **HPLC-UV chromatogram of the combined flash fractions 7-14 from *Nostoc 3* and respective results of the rhodesain assay performed with the collected fractions from time-based HPLC.** Blue: 250 nm, red: 254.4 nm, green: 210 nm, pink: 230 nm, light green: 280 nm. Assay performed as described in section 2.4.1.

Due to the observed inhibitory activity, the gradient was further optimized to 5% to 20% MeCN in H₂O (0.1% FA) in 20 min, gaining a better peak resolution. Fractionation by semi-preparative HPLC (see 2.7.3.1) resulted in the isolation of 8 compounds with varying inhibitory activity (Figure 48). While *Nostoc 3-A*, -B, -C, -D and G revealed over 90% inhibition and *Nostoc 3-F* about 71%, *Nostoc 3-H* showed only about 43% and 5 nearly no inhibitory activity (see 2.4.2.2).



compound Nostoc 3-	retention time [min]	yield [mg]	monoisotopic mass m/z $[M+H]^+$	inhibition at 0.1 mg mL^{-1} [%]
A	10.5	0.32	622.2	91.7 ± 0.6
B	12.0	0.51	622.3	97.8 ± 0.0
C	13.1	0.21	604.2	98.3 ± 0.1
D	13.4	0.26	606.3	99.7 ± 2.7
E	14.6	7.5	604.2	4.5 ± 0.0
F	16.9	0.32	622.3	71.3 ± 6.0
G	18.3	0.24	618.2	100.4 ± 1.0
H	6.7	0.15	n. d.	$43.4 \pm 6.5^*$

Figure 48. **A. HPLC-UV chromatogram overview of the raw biomass extract *Nostoc* 3** **B. HPLC-UV chromatogram of the inhibitory active fractions 7 to 14.** Blue: 210 nm, red: 230 nm, green: 260 nm, pink: 280 nm, light green: 310 nm.

LC-MS-analysis (see section 2.5.1) resulted in $[M+H]^+$ ions with m/z 604.2 and 622.3, indicating a structural relationship between the compounds. Dereplication of the isolated compounds with the “Dictionary of Natural products”, regarding the source (*Nostoc* sp.), revealed no matches (see Master thesis, Trang Nguyen, 2017). Therefore, the isolated substances were considered to not be yet described. As the inhibitory active compounds *Nostoc* 3-A, B, C, D, F and G were not isolated in sufficient amounts nor had the required purity to perform NMR experiments, solely *Nostoc* 3-E was subjected to $^1\text{H-NMR}$ and $^{13}\text{C-NMR}$ measurements (see section 2.8).

In order to isolate higher amounts of the rhodesain inhibiting compounds discovered in *Nostoc* 3, 0.9 g biomass extract were fractionated by reversed phase Flash Chromatography (see section 2.7.1). In Figure 49, the UV-chromatogram ($\lambda=210$ nm) is shown, revealing one distinct peak eluting with 59% MeOH (28-30 min), four poorly separated peaks eluting between 68% and 96% MeOH (32-47 min), and 5 minor peaks eluting with 100% MeOH at 51 min, 53 min, 57 min and 59 min.

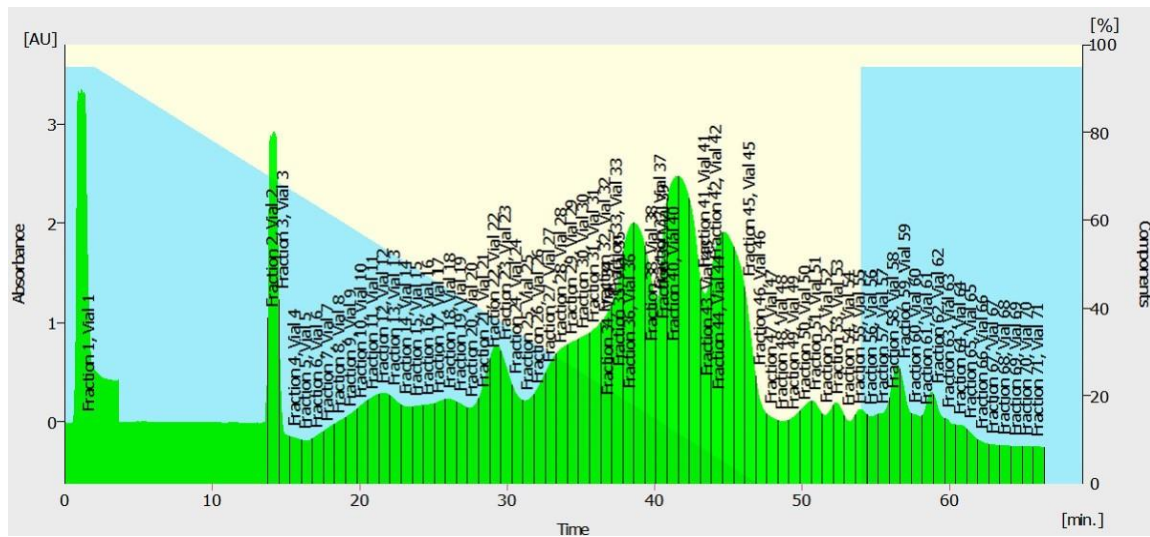


Figure 49. UV-chromatogram ($\lambda=210$ nm) of biomass raw extract *Nostoc* 3, fractionation by reversed phase Flash Chromatography. 0.9 g biomass extract in 3 mL MeOH 80% in H₂O (v/v), 20 mL/min, blue shade: proportion of solvent A (H₂O), light yellow shade: proportion of solvent B (MeOH).

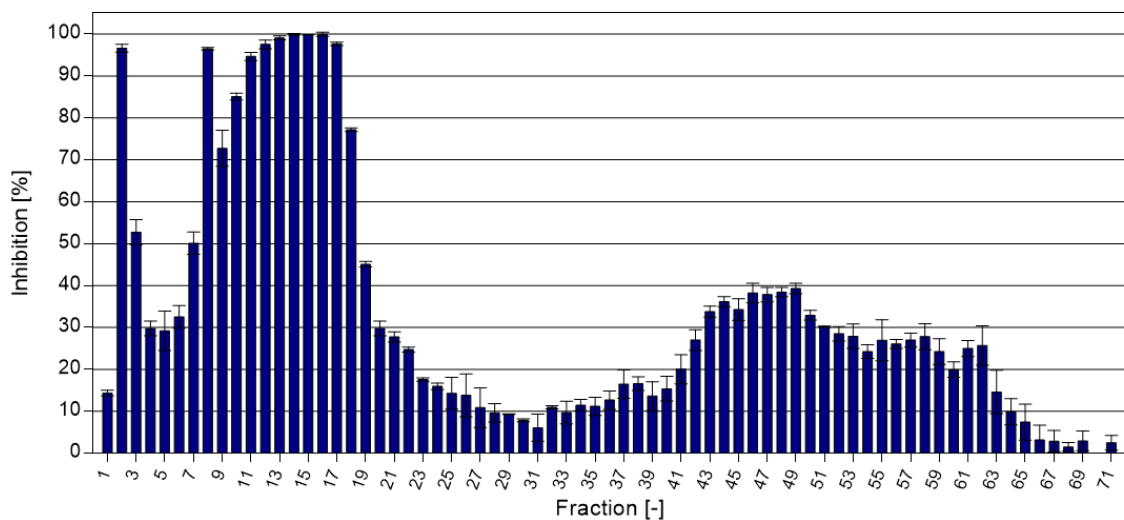


Figure 50. Rhodesain inhibition [%] of fraction one to 72, generated by reversed phase Flash Chromatography of biomass extract *Nostoc* 3.

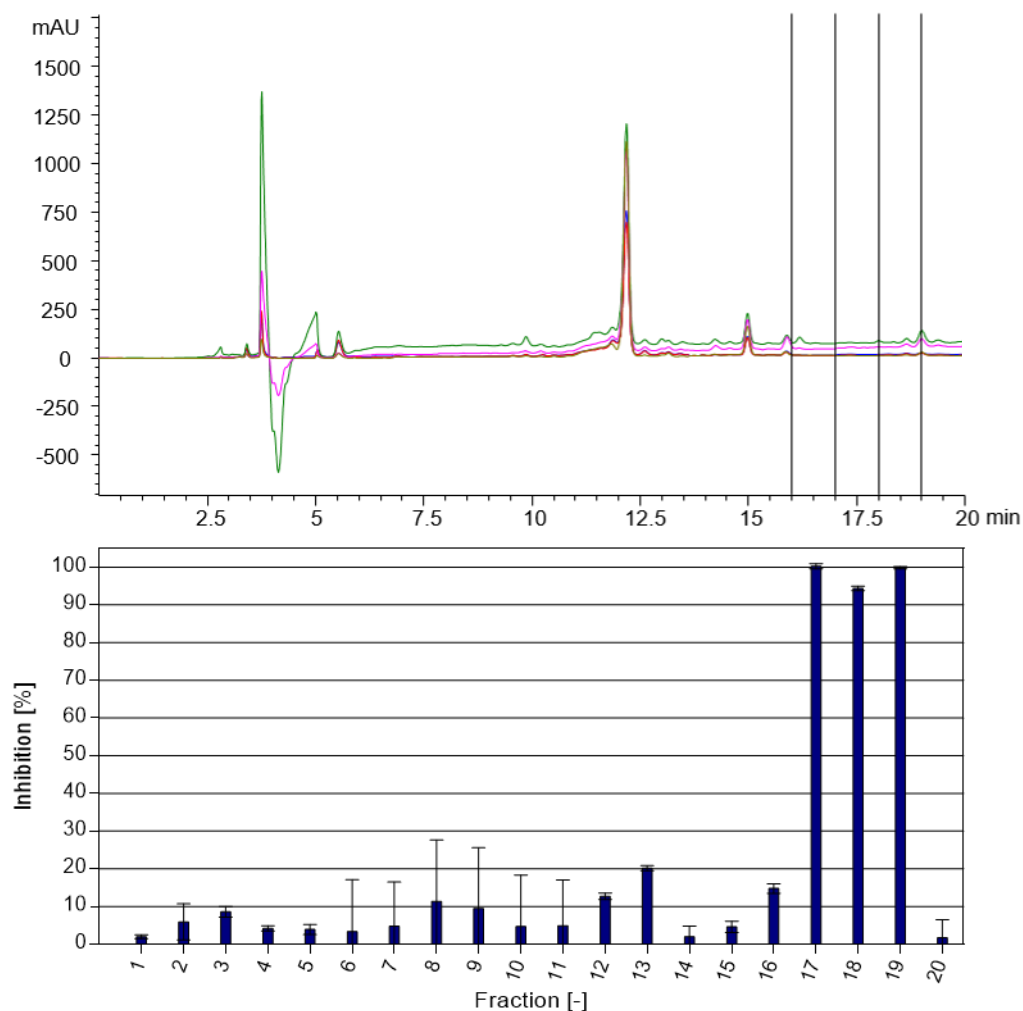


Figure 51. **HPLC-UV chromatogram of combined fractions 7-19 from biomass extract *Nostoc 3* and rhodesain inhibition [%] of the collected fractions.** 5-20 % MeCN in H₂O (0.1% FA), blue: 250 nm, red: 254.4 nm, green: 210 nm, pink: 230 nm, light green: 280 nm. Assay performed as described in section 2.4.1.

A rhodesain inhibition assay was conducted with each fraction (Figure 50) (see 2.4.1), connecting the main inhibitory activity (70% to 100% inhibition) with fractions 7 to 19 (40 mg yield), and lower inhibitory activity (30% to 40% inhibition) with fractions 43 to 54 (23 mg yield). Due to their high inhibitory activity, and based on the corresponding prior results of the first isolation described above, fractions 7 to 19 were combined and subjected to time-based fractionation with HPLC-DAD (Figure 51) (see 2.7.2). The results of the fractionation deviated slightly from the previous separation. The main inhibition of rhodesain is achieved by fractions 17 to 19, which correspond to no compound visible in the HPLC-UV chromatogram. In addition to HPLC-DAD, HPLC-MS measurements with a gradient of 10-100% MeCN in H₂O were conducted (see 2.5.1). The HPLC-UV chromatogram ($\lambda=250-270$ nm) of the combined fractions 7-19 showed one distinct peak eluting after 1.8 min with a $[M+H]^-$ ion at m/z 602.1 and a $[M+H]^+$ ion at m/z 604.2, indicating a molecular mass of 603

(Figure 52). This mass corresponded to *Nostoc* 3-E isolated from *Nostoc* 3 in prior experiments, while the molecular mass of 617, calculated from $[M+H]^-$ m/z 616.1 and $[M+H]^+$ with m/z 618.2 corresponded to compound *Nostoc* 3-G (Figure 53). Thus, the combined fractions 7-19 were subjected to further processing in order to isolate *Nostoc* 3-E and G.

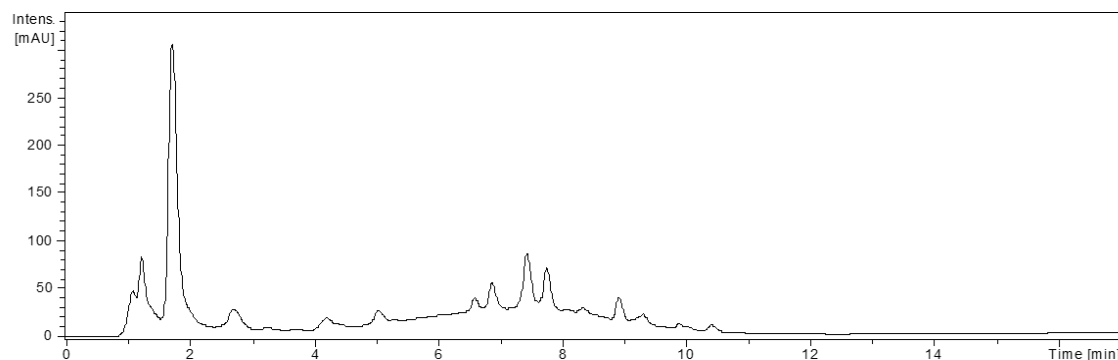


Figure 52. HPLC-UV chromatogram ($\lambda=250-270$ nm) of combined fractions 7-19 from biomass extract *Nostoc* 3. 0.4 mL/min, 17 min, 10-100% MeCN (0.06% FA) in H₂O (0.1% FA).

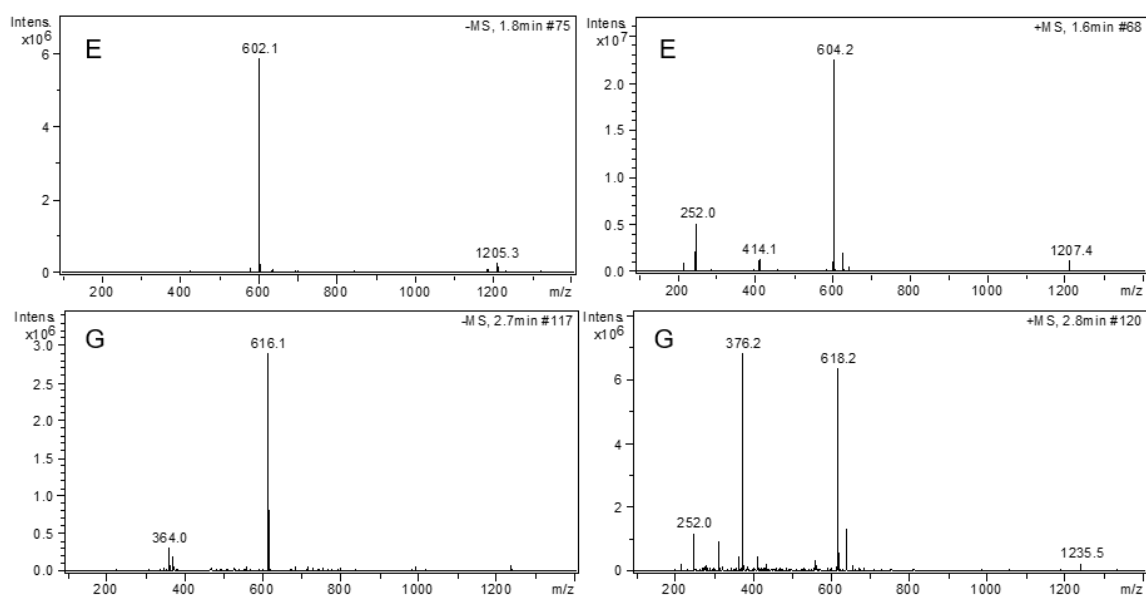


Figure 53. Mass spectra of compound *Nostoc* 3-E and G. Neg. mode (left), Pos. mode (right).

3.3.1.1. Compound Isolation and Characterization

About 40 mg inhibitory active combined fractions 7-19 were dissolved in 20% MeOH in H₂O, and subjected to further purification by semi-preparative HPLC (see section 2.7.3.2) using an optimized gradient of 5-25 % MeCN in H₂O. Two runs resulted in three fractions containing the target compound *Nostoc* 3-E, two fractions containing *Nostoc* 3-G and two containing the potentially inhibitory active compound *Nostoc* 3-I, eluting around 25% MeCN in H₂O, later than the previously isolated compounds *Nostoc* 3-A to H.

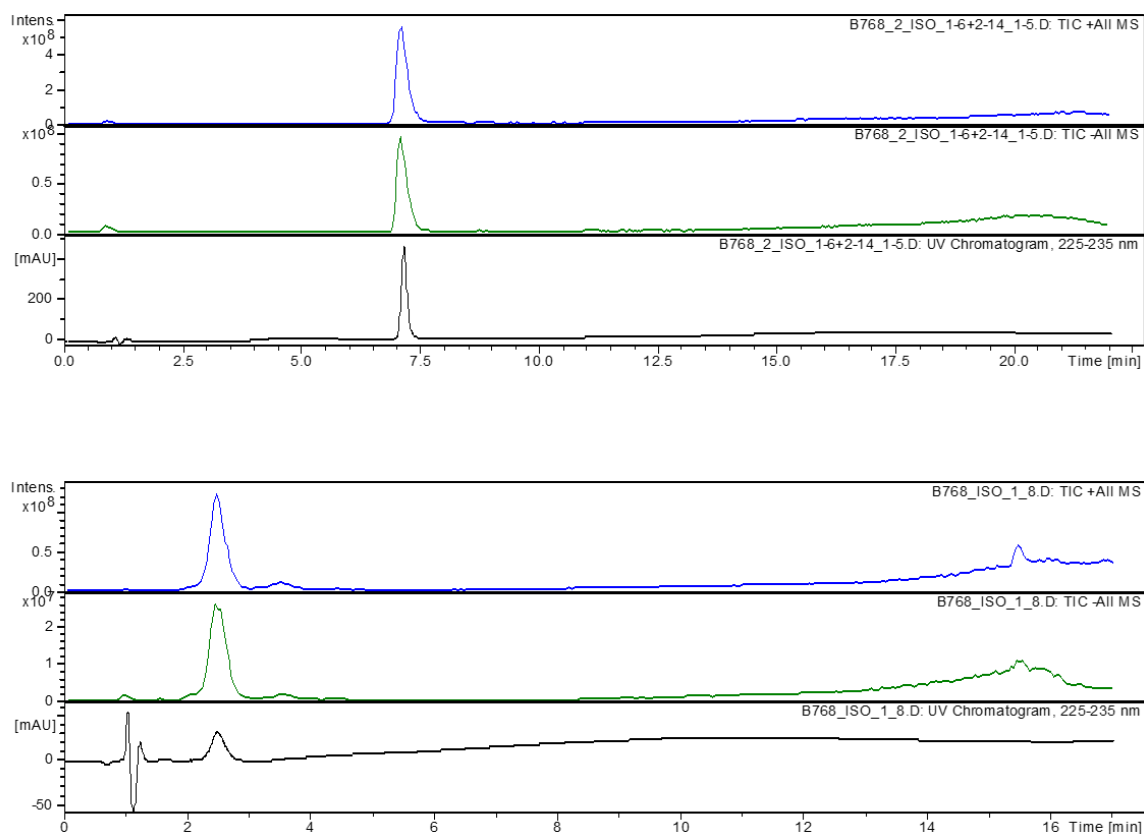


Figure 54. **Chromatogram of compound *Nostoc* 3-E and G from *Nostoc* 3 biomass extract.** TIC pos. mode (blue), neg. mode (green), HPLC-UV chromatogram (black).

A second preparative isolation step with 5-18% MeCN in H₂O (0.1% FA) led to the final isolation of *Nostoc* 3-E (yield 3 mg) and *Nostoc* 3-G (1.2 mg). Figure 54 and Figure 55 show the respective chromatograms of the compounds, proving sufficient purity for NMR measurements. In addition to compounds *Nostoc* 3-E and G, compound *Nostoc* 3-I with a

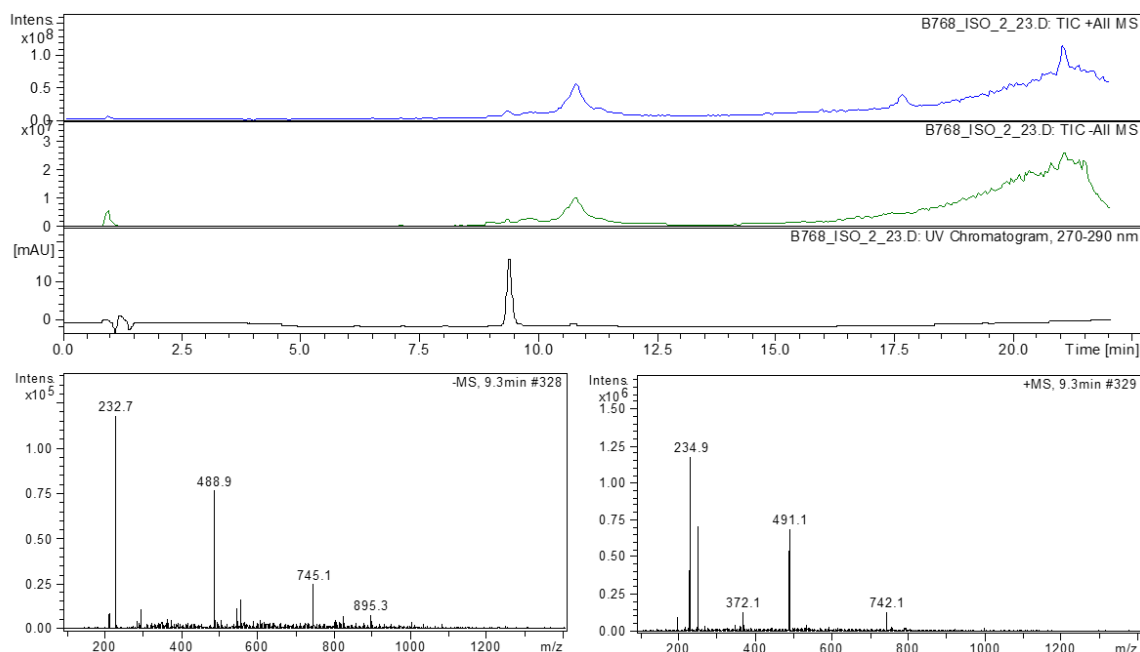


Figure 55. **Chromatogram and mass spectra of compound *Nostoc 3-I* from *Nostoc 3* biomass extract.** TIC pos. mode (blue), neg. mode (green), HPLC-UV chromatogram (black), mass spectra: Neg. mode (left), pos. mode (right).

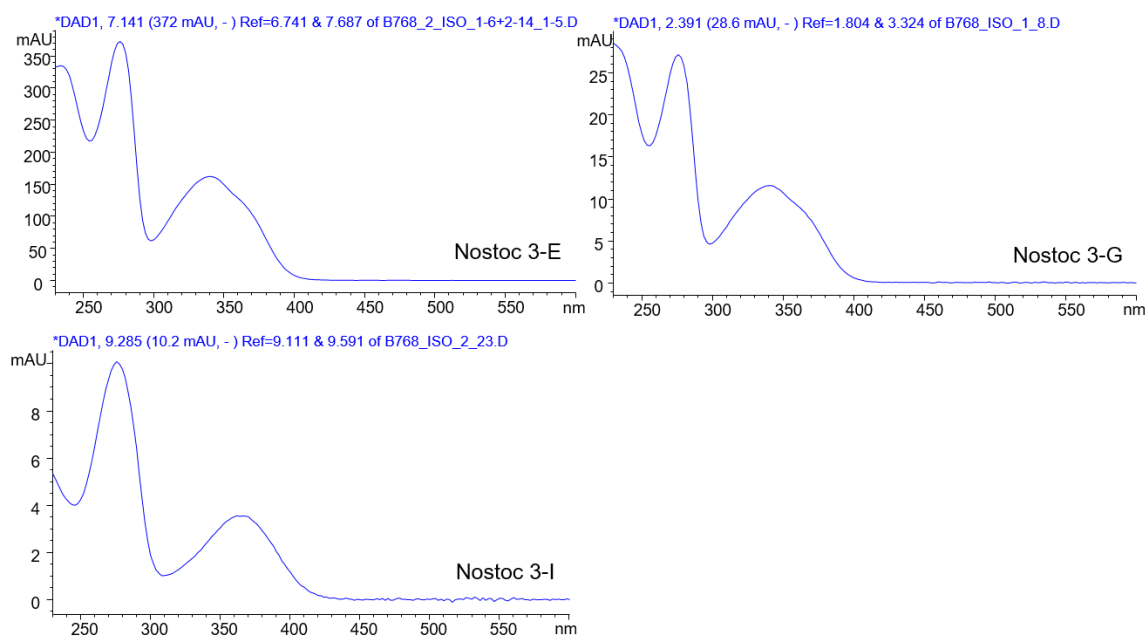


Figure 56. **UV-spectra of compounds *Nostoc 3-E*, *G* and *I*.** Maxima at 280 and 335 (E, G) or 335 (I) respectively.

molecular mass of 490, calculated from $[M+H]^-$ m/z 491.1 and $[M+H]^+$ m/z 488.9 (Figure 55). The similar mass- and UV spectra of *Nostoc 3-E* and *G* (Figure 56) combined with the similar molecular masses of 603 and 617 suggest a structural relationship between the isolated compounds. The mass difference of 14 might be explained by an additional methylene group.

As *Nostoc* 3-E, in contrast to *Nostoc* 3-G, showed no rhodesain inhibition, first structure-activity relationships of this compound family could be deduced after completed structure elucidation. Based on NMR and HRMS data (Table A 5), evaluated by Steffen Breinlinger, a partial structure of *Nostoc* 3-E was deduced (Figure 57).

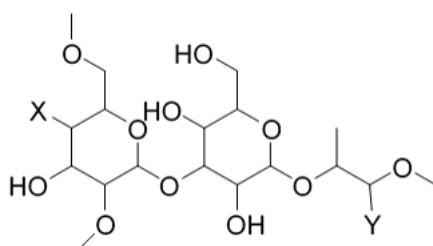


Figure 57. **Partial structure of *Nostoc* 3-E from *Nostoc* 3 biomass extract.** X and Y present unidentified residues.

The structure of *Nostoc* 3-E consists of a sugar backbone, comprising two C6 sugars, bound by a 1,4-glycosidic linkage. An aliphatic side chain is linked to the sugar backbone. The residues X and Y could not be identified yet, though X might be a hydroxyl group. As the whole structure could not be elucidated by NMR, additional experiments were needed. Remarkably, *Nostoc* 3-E readily crystallized, when pure MeOH was added to the dried compound. Thus, about 5 mg of *Nostoc* 3-E were sent to the company Crystallise! (Dr. Gunther Steinfeld and Dr. Gustavo Santiso-Quñones) in order to determine the complete structure via X-ray crystallography. Unfortunately, no adequate crystals could be grown and most of *Nostoc* 3-E was lost while trying. As no more biomass nor biomass extract of *Nostoc* 3 was available, the structure could not be fully elucidated.

3.3.1.2. *Nostoc* 3 Biomass Extract - Summary and Future Perspectives

From the biomass extract *Nostoc* 3, five of nine isolated compounds showed an inhibitory activity higher than 90 % at 1 mg/mL concentration. The yield was low, except for *Nostoc* 3-E, indicating that the inhibitors were minor compounds. From 6 g cyanobacterial biomass (0.3 g biomass extract), only 0.21 mg to 0.51 mg of the compounds could be isolated. Thus, only in case of *Nostoc* 3-E structure elucidation by NMR spectroscopy and HRMS could be attempted. The data were evaluated by Steffen Breinlinger, leading to the partial structure shown in Figure 57. Since more material was needed to complete the structure elucidation, a 2nd isolation round was performed using 1 g biomass extract, which led to the isolation of higher amounts of *Nostoc* 3-E (3 mg) and *Nostoc* 3-G (1.5 mg). Unfortunately, compounds *Nostoc* 3-A to D, F and H could not be isolated again during the 2nd isolation. In addition to *Nostoc* 3-E and *Nostoc* 3-G, the more lipophilic potentially inhibitory active compound *Nostoc*

3-I could be isolated. Compound *Nostoc* 3-I possesses a molecular weight of 490 Da, and a UV-spectrum similar to *Nostoc* 3-E and *Nostoc* 3-G. As, except for *Nostoc* 3-E, the isolated compounds purity was too low to achieve exploitable NMR spectra, structure elucidation was focused on the inactive compound *Nostoc* 3-E. Unfortunately, neither NMR spectroscopy nor X-ray crystallography led to a complete elucidation of the structure. As no more biomass or raw extract of *Nostoc* 3 were available, the structure elucidation could not be completed. Isolation of additional amounts of the compounds from more biomass extract might lead to the isolation of sufficient inhibitory active compounds for structure elucidation and clarification of structure-activity relationships.

3.3.2. Isolation of Inhibitory Compounds from the Medium Extract *Nostoc* 6

From 122 screened medium extracts, *Nostoc* 6 showed not only the strongest inhibitory activity against the cysteine protease rhodesain, but also the most interesting chemical profile. Thus, the raw extract was subjected to further processing with semi-preparative HPLC, in order to identify and isolate the inhibitory active substances. The results are summarized in the following publication.

Reprinted with permission from Kossack, R.; Breinlinger, S.; Nguyen, T.; Moschny, J.; Straetener, J.; Berscheid, A.; Brötz-Oesterhelt, H.; Enke, H.; Schirmeister, T.; Niedermeyer, T. H. J. Nostotrebin 6 related cyclopentenediones and δ -lactones with broad activity spectrum isolated from the cultivation medium of the cyanobacterium *Nostoc* sp. CBT1153. *J. Nat. Prod.* 2020. Copyright (2020) American Chemical Society. doi: 10.1021/acs.jnatprod.9b00885

3.3.2.1. Nostotrebin 6 Related Cyclopentenediones and δ -lactones with Broad Activity Spectrum Isolated from the Cultivation Medium of the Cyanobacterium *Nostoc* sp. CBT1153

Nostotrebin 6 Related Cyclopentenediones and δ -Lactones with Broad Activity Spectrum Isolated from the Cultivation Medium of the Cyanobacterium *Nostoc* sp. CBT1153

Ronja Kossack, Steffen Breinlinger, Trang Nguyen, Julia Moschny, Jan Straetener, Anne Berscheid, Heike Brötz-Oesterhelt, Heike Enke, Tanja Schirmeister, and Timo H. J. Niedermeyer*



Cite This: <https://dx.doi.org/10.1021/acs.jnatprod.9b00885>



Read Online

ACCESS |



Metrics & More

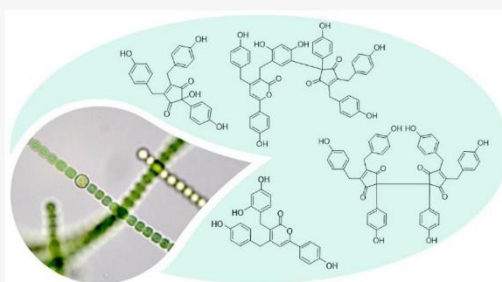


Article Recommendations



Supporting Information

ABSTRACT: Cyanobacteria are an interesting source of biologically active natural products, especially chemically diverse and potent protease inhibitors. On our search for inhibitors of the trypanosomal cysteine protease rhodesain, we identified the homodimeric cyclopentenedione (CPD) nostotrebin 6 (**1**) and new related monomeric, dimeric, and higher oligomeric compounds as the active substances in the medium extract of *Nostoc* sp. CBT1153. The oligomeric compounds are composed of two core monomeric structures, a trisubstituted CPD or a trisubstituted unsaturated δ -lactone. Nostotrebin 6 thus far has been the only known cyanobacterial CPD. It has been found to be active in a broad variety of assays, indicating that it might be a pan-assay interference compound (PAIN). Thus, we compared the antibacterial and cytotoxic activities as well as the rhodesain inhibition of selected compounds. Because a compound with a δ -lactone instead of a CPD core structure was equally active as nostotrebin 6, the bioactivities of these compounds seem to be based on the phenolic substructures rather than the CPD moiety. While the dimers were roughly equally potent, the monomer displayed slightly weaker activity, suggesting that the compounds show unspecific activity depending upon the number of free phenolic hydroxy groups per molecule.



Neglected by natural product researchers for a long time, cyanobacteria are nowadays recognized as a prolific source of structurally diverse and pharmacologically active natural products.^{1–6} Several cyanobacterial specialized metabolites have served as potent lead structures inspiring drug development programs, e.g., the dolastatins,^{7–9} the cryptophycins,^{10–12} the saxitoxins,^{13,14} and the anabaenopeptins.^{15,16} One of the better studied cyanobacteria genera is *Nostoc*, from which numerous compounds have been isolated.^{6,17} These are mainly non-ribosomal peptides and depsipeptides, but a variety of other chemically diverse structures, such as, e.g., polyketides, alkaloids, or terpenoids, were also found.

About 100 natural cyclopentenediones (CPDs) were isolated from various sources, like higher plants,^{18,19} fungi,^{20,21} and bacteria.^{22,23} Most of those CPDs are based on a cyclopent-4-ene-1,3-dione, varying in the side chains. The biosynthesis of CPDs has not yet been explored, but several synthetic routes were described.^{24–26} The only cyanobacterial CPD known to date is the *Nostoc* metabolite nostotrebin 6 (**1**), a homodimer built of two identical 4,5-bis(4-hydroxybenzyl)-2-(4-hydroxyphenyl)cyclopent-4-ene-1,3-dione units. Compound **1** was discovered in a *Nostoc* sp. biomass extract as a result of its acetylcholinesterase (AChE) and butyrylcholinesterase (BChE) inhibitory activities.^{27,28} In addition, cytotoxicity and pro-

apoptotic activity on mouse fibroblasts as well as antimicrobial activity, especially against Gram-positive bacteria, have been reported for the compound.^{29,30}

Often, cyanobacterial specialized metabolites show pronounced cytotoxicity, but another activity that is frequently observed for cyanobacterial non-ribosomal peptides is the inhibition of proteases.^{31–36} The cathepsin L-like cysteine protease rhodesain plays an important role during human infection with *Trypanosoma brucei*, known as human African trypanosomiasis (HAT).³⁷ It is involved in the parasitic crossing of the blood–brain barrier, leading to the late stage of HAT.³⁸ Furthermore, rhodesain is involved in the synthesis of variant surface glycoproteins (VSGs) of the trypanosomes, enabling *T. brucei* to elude the host immune response.³⁹ Because of its essential physiological role in the metabolism of the parasite, rhodesain is regarded as a promising target for the development of urgently needed new therapeutics.³⁷

Received: September 13, 2019

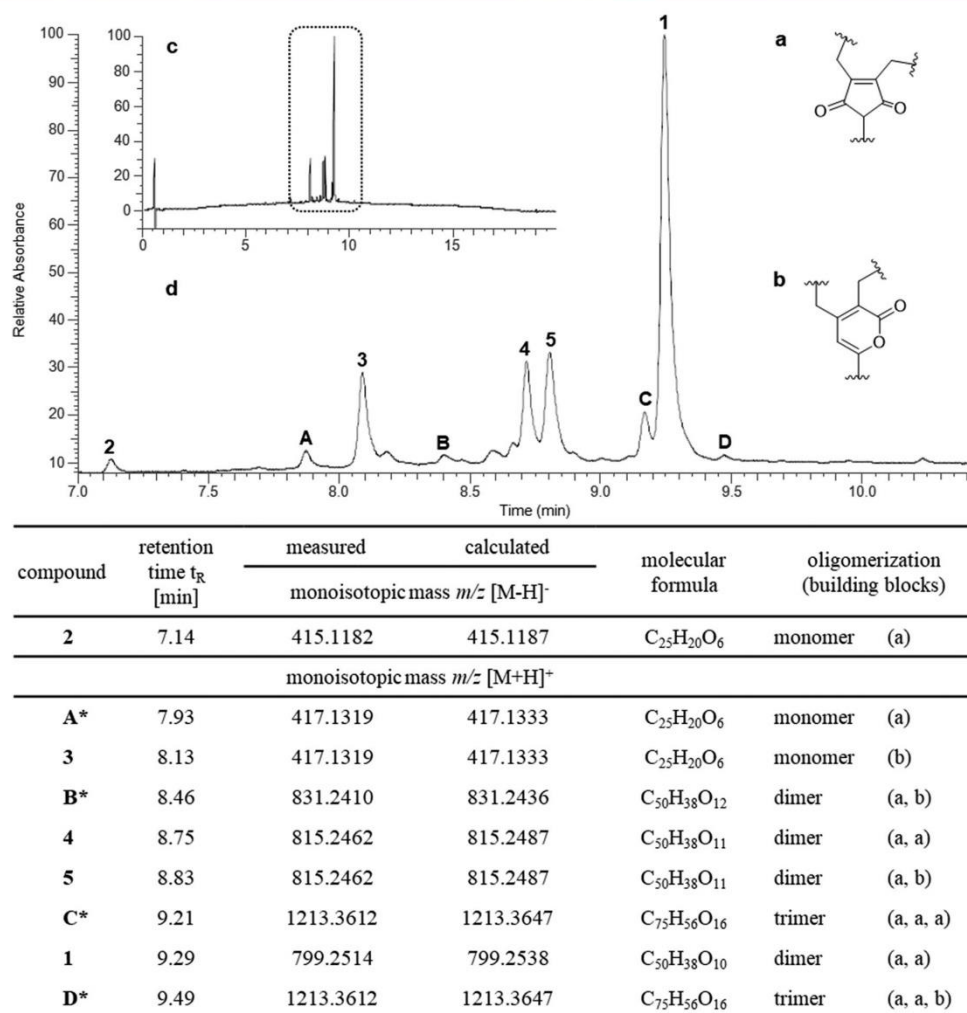
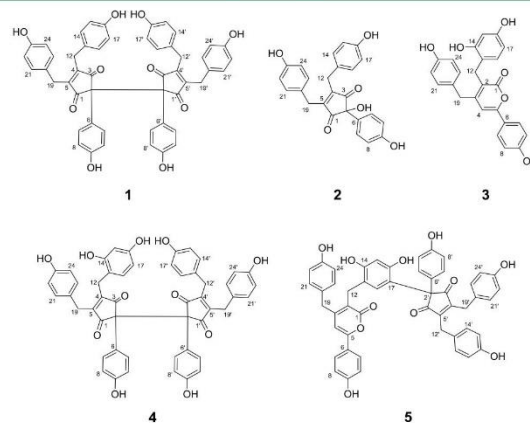


Figure 1. Nostotrebin 6 (**1**) and derivatives based on a (a) CPD or (b) δ -lactone core structure, biosynthesized by *Nostoc* sp. CBT1153. (c) HPLC–UV chromatogram overview ($\lambda = 230$ nm) of the *Nostoc* sp. CBT1153 medium extract. (d) HPLC–UV chromatogram, with t_R of 7.0–10.5 min. (*) Not fully structure-elucidated compounds; the structures were proposed on the basis of HRMS² and UV spectroscopy data.

Our ongoing search for specialized metabolites from cyanobacteria combined with our interest in finding novel anti-infective natural products prompted us to screen a library of 572 cyanobacteria extracts for inhibitors of the trypanosomal protease rhodesain. A medium extract from *Nostoc* sp. CBT1153 revealed not only high biological activity against rhodesain but also a rather simple chemical composition. Until today, most cyanobacterial natural products were isolated from biomass and only few compounds from cyanobacteria cultivation media are known.^{40–43} Therefore, we set out to isolate and characterize the rhodesain-inhibiting compounds found in this medium extract, identifying compound **1** and several new biosynthetically related compounds as active substances.



B

<https://dx.doi.org/10.1021/acs.jnatprod.9b00885>
J. Nat. Prod. XXXX, XXX, XXX–XXX

RESULTS AND DISCUSSION

Isolation and Structure Elucidation. Our screening of a cyanobacteria extract collection (450 biomass extracts and 122 medium extracts) against the cysteine protease rhodesain resulted in 9 biomass extracts with an inhibitory activity of more than 80% at 0.1 mg/mL and 14 medium extracts with an inhibition higher than 80% at 0.2 mg/mL. With inhibition of >90%, an extract from the culture medium of *Nostoc* sp. CBT1153 revealed prominent activity, while the corresponding biomass extract showed inhibition of 89% at 0.33 mg/mL. This raised our interest, because only few compounds have been isolated from cyanobacteria cultivation media to date. A comparison of the chromatographic profiles showed that the biomass and medium extracts contained the same major compounds (Figure S1 of the Supporting Information). However, because the medium extract did not contain any hydrophilic metabolites or chlorophylls, we decided to proceed with the medium extract. The main substance present in the medium extract as well as in the biomass extract of this *Nostoc* strain could quickly be dereplicated by high-resolution tandem mass spectrometry (HRMS²) to the CPD homodimer nostotrebin 6 (1), which was first isolated from a *Nostoc* sp. biomass extract by Zelik et al. in 2010.³⁰ Because we later isolated the compound for comparative bioactivity testing, the dereplication was also confirmed by one-dimensional (1D) and two-dimensional (2D) nuclear magnetic resonance (NMR) data.

Fractionation and subsequent bioactivity testing showed that the inhibitory activity was caused by not only compound 1, but also the other substances present in the extract. Intriguingly, the molecular masses and the respective calculated sum formulas as well as the tandem mass spectrometry (MS²) spectra of these compounds indicated a structural relationship with the homodimeric CPD 1 and hinted at the presence of monomeric, dimeric, and higher oligomeric forms of a common core structure (Figure 1). More detailed evaluation of the high-performance liquid chromatography–mass spectrometry (HPLC–MS) data showed that the extract contained at least four putative monomeric, eight dimeric, and three trimeric compounds (Figure S3 of the Supporting Information). Trace amounts of tetrameric structures could be detected. Four new mono- and dimeric derivatives were isolated in sufficient yield for structure elucidation by 1D and 2D NMR experiments.

Compound 2 was isolated as a yellow amorphous powder. The molecular formula C₂₅H₂₀O₆ was calculated from the [M – H][–] ion at *m/z* 415.1182. The ¹H NMR spectrum showed only five distinct proton signals, indicating a highly symmetric structure. Four signals were found in the aromatic region (integrals of 4, 4, 2, and 2), and two doublets were observed around δ_H 3.75 (integral of 4). On the basis of the sum formula and the ¹H NMR spectrum, we assumed compound 2 to be related to the monomeric building block of compound 1 (core structure a), with an additional hydroxy group being present. Structure elucidation via 2D NMR experiments was straightforward. Heteronuclear multiple-bond correlations (HMBCs) and the ¹³C chemical shifts were similar to compound 1 (see Figure 2 and Table 1), except C-2 as well as C-6, which were deshielded by more than 15 and 7 ppm, respectively. The NMR data thus confirmed the presence of a hydroxy group at C-2 (instead of the second monomer in compound 1). Similar intramolecular interactions as in compound 1 can be expected in compound 2 (intramolecular hydrogen bonds and stacking interactions

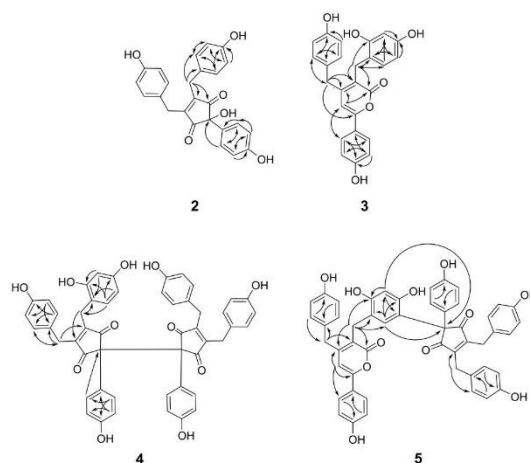


Figure 2. HMBC correlations of compounds 2, 3, 4, and 5, indicated by arrows.

between the aromatics),²⁸ resulting in a restricted rotation of the substituents of the CPD. Thus, as in compound 1, the methylene protons at C-12 and C-19 in compound 2 are magnetically inequivalent, showing geminal coupling. Being the monomer of nostotrebin 6 with an additional hydroxy group, compound 2 was named nostotrebinol 3.

Compound 3 was isolated as a yellow amorphous powder. HRMS analysis resulted in a [M + H]⁺ ion at *m/z* 417.1319 from which the molecular formula C₂₅H₂₀O₆ was calculated, suggesting this compound to be composed of just one of the monomers present in compound 1, carrying an additional hydroxy group. Four singlet signals in the region near δ_H 9 were observed in the ¹H spectrum, and one of these broad singlets was further deshielded, indicating increased acidity. ¹³C chemical shifts were determined via heteronuclear single-quantum correlation (HSQC) and HMBC experiments. The data indicated that compound 3 was not simply a hydroxylated monomer of compound 1, because the ¹³C signals for the keto groups of the CPD substructure (δ_C >200) were missing. Instead, the ¹³C shift for C-1 (δ_C 170) and HMBCs pointed to a δ-lactone core structure (core structure b). The conjugation of the *p*-hydroxyphenyl group with the lactone via the C-5–C-6 bond accounts for the broad singlet at δ_H ~9.5 (vinylogous phenylogous carboxylic acid). Similar to compound 1, two hydroxybenzyl substituents are attached to the δ-lactone at C-2 and C-3. Chemical shifts differ slightly as a result of the additional *m*-hydroxy group in one of the hydroxyphenyl substituents but are similar to compound 1 overall (Table 1). HMBC key correlations are depicted in Figure 2. In comparison to compound 1, the ultraviolet (UV) spectrum of compound 3 features an additional maximum at 360 nm with equal intensity as the maximum at 223 nm (Figure S2 of the Supporting Information). Because compound 3 contains a lactone core structure and four hydroxy groups, it was named nostolactone 4.

Compound 4 was isolated as an orange amorphous solid. The detected protonated molecule [M + H]⁺ at *m/z* 815.2462 suggested a molecular formula of C₅₀H₃₈O₁₁, indicating the presence of an additional hydroxy group in comparison to compound 1. Indeed, the ¹H NMR spectrum of compound 4 showed that the compound is not symmetrical, featuring three

C

<https://dx.doi.org/10.1021/acs.jnatprod.9b00885>
J. Nat. Prod. XXXX, XXX, XXX–XXX

Table 1. ^1H (600 MHz) and ^{13}C (150 MHz) NMR Spectroscopic Data of Monomeric Compounds 2 and 3 in $\text{DMSO-}d_6$

position	2		3	
	δ_{C} , type	δ_{H} (J in Hz)	δ_{C} , type	δ_{H} (J in Hz)
1	202.0, C		169.7, C	
2	75.2, C		125.1, C	
3	202.0, C		151.7, C	
4	156.2, C		109.7, CH	6.26, s
5	156.2, C		145.5, C	
6	127.3, C		124.2, C	
7	126.9, CH	6.84, m	131.7, CH	7.55, d (8.8)
8	114.9, CH	6.59, m	115.7, CH	6.80, d (8.8)
9	157.2, C		158.3, C	
10	114.9, CH	6.59, m	115.7, CH	6.80, d (8.8)
11	126.9, CH	6.84, m	131.7, CH	7.55, d (8.8)
12a	28.5, CH_2	3.74, d (14.5)	22.6, CH_2	3.49 (s)
12b		3.77, d (14.5)		
13	126.4, C		114.4, C	
14	129.7, CH	6.91, d (8.6)	155.3, C	
15	115.3, CH	6.62, m	102.2, CH	6.28, d (1.0)
16	156.2, C		156.5, C	
17	115.3, CH	6.62, m	105.9, CH	6.11, dd (8.2, 2.5)
18	129.7, CH	6.91, d (8.6)	129.8, CH	6.76, d (8.2)
19a	28.5, CH_2	3.74, d (14.5)	28.4, CH_2	3.86, s
19b		3.77, d (14.5)		
20	126.4, C		128.0, C	
21	129.7, CH	6.91, d (8.6)	129.1, CH	7.01, m
22	115.3, CH	6.62, m	115.2, CH	6.65, m
23	156.2, C		155.8, C	
24	115.3, CH	6.62, m	115.2, CH	6.65, m
25	129.7, CH	6.91, d (8.6)	129.1, CH	7.01, m
OH		OH 9.45, br s		OH 9.07
OH		OH 9.45, br s		OH 9.27
OH		OH 9.45, br s		OH 9.41
OH		OH 9.45, br s		OH 9.92

doublets in the aromatic region with an integral of 1 each. Coupling constants of 8.25 and 2.4 Hz indicated a *m*-dihydroxy-substituted phenyl residue. This substitution pattern was confirmed via correlations in the HMBC spectrum (Figure 2). The remaining proton and carbon signals are in good accordance with the data for compound 1 (Table 2). The UV spectrum of compound 5 is virtually identical to the spectrum of compound 1. Because the only structural difference between compounds 1 and 4 is the presence of one additional hydroxy group (7 instead of 6), compound 4 was named nostotrebin 7.

Compound 5, isolated as a yellow amorphous solid, has the same molecular formula as compound 4 ($[\text{M} + \text{H}]^+$ ion at m/z 815.2462). Intriguingly, evaluation of the ^1H and ^{13}C NMR spectra revealed that this compound contains both the monomer 3 (core structure b) and the CPD monomer (core structure a) found in compound 1, forming a heterodimer. Evaluation of the 2D NMR data showed a strong HMBC of H-18 and C-2' (Figure 2), indicating that the two monomeric building blocks are not, as expected, connected by a covalent bond between the monomer cores but that the CPD monomer is an additional substituent at the dihydroxy-substituted phenyl group of the δ -lactone monomer (covalent bond between C-17 and C-2'). The presence of monomer 3 in compound 5 is confirmed by the UV spectrum of compound 5, which also shows an absorption maximum at 360 nm. Interestingly, because the dimer 5 only contains one δ -lactone monomer, the maximum at 360 nm is only about half as intense as the

maximum at 230 nm. As a result of its dimeric structure, comprising one lactone and one CPD monomer, with in total seven hydroxy groups, compound 5 was named nostotrebinlactone 7.

Compounds A, B, C, and D could not be isolated in sufficient amounts for unambiguous structure elucidation. However, their HRMS² and UV spectra clearly showed that they are composed of the basic core structures a and b (Figure 1 and the Supporting Information). Their deduced structural features are discussed in the Supporting Information.

In addition to the compounds discussed above, several additional monomers, dimers, and trimers could be detected by HPLC–MS (Figure S3 of the Supporting Information). These compounds mainly differ in the number of hydroxy groups. Intriguingly, we could also detect minor amounts of two tetramers ($\text{C}_{100}\text{H}_{76}\text{O}_{22}$ and $\text{C}_{100}\text{H}_{74}\text{O}_{22}$; Figure S3 of the Supporting Information). We suspect that the oligomerization of the two monomers is not enzyme-catalyzed but due to their general chemical reactivity, resulting in an array of compounds differing mainly in the monomers that reacted and the extent of hydroxylation. This non-enzymatic oligomerization is also supported by the fact that compounds 4 and 5 are not optically active.

Bioactivity Characterization. Nostotrebin 6 (1) was first isolated from the extract of *Nostoc* sp. str. Lukešová 27/97, which was highly active in a screening for AChE inhibitors (Table 3).²⁷ Although HPLC analysis of this extract revealed compound 1 as

D

<https://dx.doi.org/10.1021/acs.jnatprod.9b00885>
J. Nat. Prod. XXXX, XXX, XXX–XXX

Table 2. ¹H (600 MHz) and ¹³C (150 MHz) NMR Spectroscopic Data of Dimeric Compounds 1, 4, and 5 in DMSO-*d*₆

position	1		4		5	
	δ_C	δ_H (J in Hz)	δ_C type	δ_H (J in Hz)	δ_C type	δ_H (J in Hz)
1	nd ^a		nd		169.6, C	nd
2	61.2, C		58.1, C		125.0, C	61.2, C
3	nd		nd		151.5, C	nd
4	155.0, C		155 ^b , C		109.7, CH	152.9, CH
5	155.0, C		155 ^b , C		145.5, C	152.9, C
6	120.3, C		120.3, C		124.2, C	124.6, C
7	130.5, CH	6.457, m	130.8, CH	6.46, m	131.9, CH	129.2, CH
8	113.6, CH	6.46, m	113.9, CH	6.46, d (1.5)	115.8, CH	115.3, CH
9	156.9, C		157.2, C		158.1, C	156.9, C
10	113.6, CH	6.46, m	113.9, CH	6.46, d (1.5)	115.8, CH	115.3, CH
11	130.5, CH	6.457, m	130.8, CH	6.46, m	131.9, CH	129.2, CH
12	28.0, CH ₂	3.56, br d (14.3)	22.4, CH ₂	3.46, br d (3.3)	22.7, CH ₂	28.0, CH ₂
13	126.4, C		112.8, C		113.6, C	126.8, C
14	129.4, CH	6.72, d (8.4)	156.9, C	6.72, m	155.0, CH	129.4, CH
15	115.1, CH	6.52, d (8.4)	102.3, CH	6.22, d (2.4)	101.7, CH	115.1, CH
16	155.7, C		155.7, C		153.7, C	155.7, C
17	115.1, CH	6.52, d (8.4)	106.0, CH	5.96, m	117.3, C	115.1, CH
18	129.4, CH	6.72, d (8.4)	129.9, CH	6.42, d (8.25)	132.6, CH	129.4, CH
19	28.0, CH ₂	3.56, br d (14.3)	28.0, CH ₂	3.55, m	28.6, CH ₂	28.0, CH ₂
20	126.4, C		112.8, C		127.8, C	126.8, C
21	129.4, CH	6.72, d (8.4)	129.4, CH	6.72, m	129.2, C	129.4, CH
22	115.1, CH	6.52, d (8.4)	115.1, CH	6.52, m	115.4, CH	115.1, CH
23	155.7, C		155.8, C		155.8, C	155.7, C
24	115.1, CH	6.52, d (8.4)	115.1, CH	6.52, m	115.4, CH	115.1, CH
25	129.4, CH	6.72, d (8.4)	129.4, CH	6.72, m	129.2, CH	129.4, CH
OH		2xOH 9.47, br s		2xOH 9.0–9.7 ^b , m		2xOH 9.25, br s
OH		4xOH 9.21, br s		3xOH 9.0–9.7 ^b , m		3xOH 9.46, br s
OH				OH 9.0–9.7 ^b , m		OH 9.90, br s
OH				OH 9.0–9.7 ^b , m		OH 10.13, br s

^and = not detected. ^bOverlapping ¹³C and ¹H resonances.

Table 3. Inhibitory Effects of Compounds 1, 3, and 5^a

compound	IC ₅₀ (μM)		MIC (μM)		
	rhodesain	HeLa cells	<i>B. subtilis</i> 168	<i>E. faecium</i> BM4147-1	<i>S. aureus</i> ATCC29213
1	15 ± 2	16 ± 9	13	13	13
5	33 ± 4	33 ± 9	3	13	3
3	63 ± 3	84 ± 13	50	100	50

^ahalf maximal inhibitory concentrations (IC₅₀) of compounds 1, 3, and 5 against rhodesain and HeLa cells (*n* = 3) and minimal inhibitory concentrations (MICs) of compounds 1, 3, and 5 against selected Gram-positive bacteria (*n* = 3).

the main compound, several minor peaks were detected as well but not characterized at that time.²⁸ Compound 1 was also found to be cytotoxic and pro-apoptotic on mouse fibroblasts (BALB/c)²⁹ as well as antibacterial against Gram-positive bacteria (Table S1 of the Supporting Information)³⁰ and suggested as lead structure for drug development.²⁴ However, because compound 1 is a polyphenolic compound, caution might be appropriate. Showing such a broad variety of bioactivities in seemingly unrelated assays, the compound can be suspected to be a pan-assay interference compound (PAIN).^{44,45} To either confirm compound 1 and its derivatives are PAINs or to establish structure–activity relationships for this compound family, we performed a comparative activity testing with compound 3 as the monomer, compound 1 as the homodimer, and compound 5 as the heterodimer. Therefore, we assessed the cytotoxicity on HeLa cells, the antibacterial activity against *Bacillus subtilis*, *Enterococcus faecium*, and *Staphylococcus aureus*, and the rhodesain inhibition potency. Results are summarized in Table 3.

The IC₅₀ of compound 1 against HeLa cells (16 μM) was comparable to published data,²⁹ while compounds 5 (IC₅₀ = 33 μM) and 3 (IC₅₀ = 84 μM) were slightly less active. Our results also confirmed published data concerning the antimicrobial activity of compound 1 against selected Gram-positive bacteria.³⁰ Compound 1 and the two tested derivatives were active against *B. subtilis* 168, *E. faecium* BM4147-1, and *S. aureus* ATCC29213, with MICs of 13 μM for compound 1, 3–13 μM for compound 6, and 50–100 μM for compound 3 (Table 3).

Inhibition of rhodesain was tested in a standard fluorescence assay⁴⁶ by measuring the fluorescence increase as a result of the hydrolysis of Cbz-Phe-Arg-AMC in the absence or presence of inhibitor. To investigate the inhibition mechanism (time dependency, unspecific thiol reactivity, and unspecific inhibition by aggregation^{46,47}), more detailed experiments were performed with compound 1 as the major representative of this compound family. The residual activity of rhodesain after 5, 10, and 30 min incubation time of enzyme and compound 1 prior to substrate addition ([S] = 10 μM) was measured. The inhibition was found to be not time-dependent.⁴⁸ The presence of the low-molecular-weight sulfur nucleophile dithiothreitol (DTT, 4.75 mM) did not have any influence on the inhibition of rhodesain by compound 1 (Figure S5 of the Supporting Information). Therefore, it can be excluded that the compound reacts unspecifically with thiols.^{46,49} Unspecific inhibition by aggregation was excluded by the addition of the non-ionic detergent Brij 35 (0.005 and 0.025%; Supporting Information).^{46,47} Thus, prominent error sources in fluorometric assays⁴⁷ could be discarded. Additionally, the inner filter effects for compounds 1, 3, and 5 were calculated and included in the calculations of IC₅₀

values, because in fluorometric assays, yellow-colored substances are known to potentially absorb light at the wavelength of interest. Slight differences in the inhibitory activity of compounds became apparent (Table 3). While compound 1 revealed an IC₅₀ of 15 μM against rhodesain (comparable to the IC₅₀ against BChE and AChE²⁸), compound 5 showed a higher IC₅₀ value of 33 μM and compound 3 again was less active (IC₅₀ = 66 μM). Interestingly, the IC₅₀ values against HeLa cells of each compound are in line with their rhodesain inhibitory activity. Hence, despite their structural similarity, the bioactivity seems to vary slightly between the monomeric and dimeric derivatives.

Although all three compounds are active in a comparable concentration range, in all assays, the monomer 3 (3 hydroxy groups; *M_r* ~ 400 Da) is slightly less active than the dimers 5 and 1 (7/6 hydroxy groups; *M_r* ~ 800 Da). This agrees with the observation in other polyphenolic natural products that the bioactivity increases with the number of hydroxy groups per molecule,^{50–55} suggesting that the activity of the nostotrebins/nostolactones is indeed due to unspecific, polyphenol-like activity on proteins.

The broad bioactivity spectrum, which has been reported for CPDs in general, was postulated to be based on the chemically reactive CPD substructure.²⁴ For example, the antifungal activity of coruscaneone A was at first attributed to the 2-methoxymethylenecyclopent-4-ene-1,3-dione moiety, assuming an irreversible covalent addition to its target by Michael addition,¹⁸ while the side chain styryl-like moiety was suspected to contribute to target binding. However, subsequent evaluation of synthesized 2-cinnamyliden-1,3-diones related to coruscaneone A showed that the CPD core structure was not essential for bioactivity but, instead, highlighted the importance of the styryl side chain.⁵⁶ Furthermore, CPDs isolated from *Lindera aggregata*, comprising one or two CPD moieties but no hydroxy groups, were found to be inactive against *B. subtilis*.⁵⁷ Compound 1, containing two CPD subunits, and compound 5, containing just one CPD substructure, were roughly equally active in our assays. Hence, as discussed above, it is likely that the bioactivities of the nostotrebins compound family are not due to the CPD moiety but the phenolic hydroxy groups.

Although the physiological role of CPDs has not yet been studied in detail, a protective function for the producing organisms, especially against bacterial and fungal pathogens, was assumed.²⁴ In the case of compound 1, a protective role against biotic stress was suggested as well.³⁰ Our study might affirm this reasoning, as the nostotrebins/nostolactones were found to be present in the cultivation medium. Another potential ecological role of the CPDs might be protection against UV irradiation. The structures of the nostotrebins show some resemblance with the structures of the scytonemins, known UV protectants or photon dissipators.⁵⁸ However, in contrast to the scytonemins, which absorb strongly over the entire UV range (100–380 nm), the nostotrebins absorb UV light strongly only in the UV-C range (100–280 nm), while their absorption in the UV-B range (280–315 nm) is comparably weaker and low in the UV-A range (315–380 nm).

EXPERIMENTAL SECTION

General Experimental Procedures. Optical rotations were obtained on a Jasco P-2000 polarimeter. UV spectra were obtained on a GeneQuant 1300 spectrophotometer (GE Healthcare Bio-Sciences). Infrared–attenuated total reflection (IR–ATR) spectra were obtained on a Bruker FTIR IFS 28 spectrometer, equipped with a

F

<https://dx.doi.org/10.1021/acs.jnatprod.9b00885>
J. Nat. Prod. XXXX, XXX, XXX–XXX

deuterated triglycine sulfate (DTGS) detector and a ZnSe crystal (1.3 mm). The incidence angle was 45°. NMR experiments were performed in DMSO-*d*₆ on a Bruker Avance II spectrometer operating at 600 MHz (¹H) or 150 MHz (¹³C) on an Agilent DD2 spectrometer equipped with a OneNMR probe at 400 MHz (¹H) or on a Varian/Agilent VNMRs spectrometer operating at 600 MHz (¹H). Chemical shifts were referenced to the residual solvent signals (δ_{H} 2.49, δ_{C} 39.5). NMR data were analyzed with ACD/Structure Elucidator Suite 2018.2. High-resolution electrospray ionization mass spectrometry (HRESIMS) data were acquired on a Q-Exactive Plus mass spectrometer (Thermo Fisher Scientific) equipped with a heated ESI interface coupled to an UltiMate 3000 HPLC system (Thermo Fisher Scientific). The following parameters were used for the data acquisition: positive ion mode, ESI spray voltage of 3.5 kV, and scan range of *m/z* 150–2000. Analytical and semi-preparative HPLC were performed on an UltiMate 3000 HPLC system (Thermo Fisher Scientific).

Cyanobacterial Material: Generation of Medium Extract.

Nostoc sp. CBT1153 (CCY0508) was classified as *Nostoc* based on its morphology and is deposited in the culture collection of the Cyano Biotech GmbH, Germany. The strain was cultivated in BG11 medium⁵⁹ at 28 °C, illuminated continuously by Sylvania GROLUX fluorescent lamps (50–200 $\mu\text{mol photons m}^{-2} \text{s}^{-1}$), and aerated with 0.5–5% CO₂ in sterile filtered air in 20 L polycarbonate carboys. To minimize cell death and lysis, the cultures were harvested weekly and diluted with fresh medium (semi-continuous cultivation to avoid entering into the stationary phase). Frequent microscopic examination of the cultures did not show significant amounts of sheath fragments that would indicate dead or lysed cells. XAD-16 adsorption resin was present during the whole cultivation duration to adsorb organic compounds present in the cultivation medium, and the adsorbed compounds were subsequently extracted with MeOH. Sufficient amounts of cyanobacteria biomass and medium extract for further processing were obtained after a cultivation duration of about 10 weeks. After separation of the biomass from the medium by centrifugation, the biomass was lyophilized. The dried biomass was resuspended in 50% MeOH (v/v), treated with an ultrasonication rod (Bandelin), and extracted on a shaker for 30 min at room temperature. After centrifugation, the biomass was subsequently extracted using 80% MeOH (v/v). The solutions were combined and dried *in vacuo* to yield the biomass extract.

Bioassay-Guided Fractionation and Isolation of Compound 1 and Its Derivatives. The medium extract was dissolved in MeOH and fractionated by HPLC using a Luna C18 column (250 \times 10 mm, 5 μm , 100 Å, Phenomenex) and a gradient of 30–75% MeCN in H₂O (0.1% formic acid each) at 4.5 mL/min over 23 min. Fractions were collected every 0.5 min, resulting in five fractions inhibiting rhodesain. These fractions contained all of the major compounds detectable in the extract. A total of 140 mg of medium extract was dissolved in 1.4 mL of MeCN and subjected to semi-preparative HPLC using a Luna C18 column (250 \times 10 mm, 5 μm , 100 Å, Phenomenex) and a gradient of 40–46% MeCN in H₂O (0.1% formic acid each) at 4.5 mL/min over 30 min, yielding compounds **2** (0.5 mg, *t_R* of 4.7 min), **A** (<0.1 mg, *t_R* of 6.2 min), **3** (9.5 mg, *t_R* of 8.8 min), **B** (0.1 mg, *t_R* of 9.7 min), **4** (4.3, *t_R* of 12.0 min), **5** (9.4 mg, *t_R* of 13.1 min), **C** (3.6 mg, *t_R* of 16.7 min), **I** (40.5 mg, *t_R* of 17.5 min), and **D** (<0.1 mg, *t_R* of 21.1 min). The compounds were found to be not optically active.

Nostotrebin 6 (1): yellow amorphous powder; UV (MeCN) λ_{max} (log ϵ), 226 (4.75) nm; IR (ATR) ν_{max} 3393, 1734, 1686, 1610, 1510, 1437, 1337, 1224, 1171, 821 cm^{-1} ; ¹H and ¹³C NMR data, Table 2; HRESIMS, *m/z* 799.2514 [M + H]⁺ (calculated for C₅₀H₃₉O₁₀, 799.2538).

Nostotrebino 3 (2): yellow amorphous powder; UV (MeCN) λ_{max} (log ϵ), 225 (4.02), 277 (3.61) nm; IR (ATR) ν_{max} 3196, 2917, 1701, 1594, 1513, 1445, 1241, 1172, 1022, 998, 825 cm^{-1} ; ¹H and ¹³C NMR data, Table 1; HRESIMS, *m/z* 415.1182 [M – H][–] (calculated for C₂₅H₁₉O₆, 415.1182).

Nostolactone 4 (3): yellow amorphous powder; UV (MeCN) λ_{max} (log ϵ), 226 (4.28), 279 (3.92), 359 (4.33) nm; IR (ATR) ν_{max} 3342, 1722, 1601, 1513, 1445, 1372, 1229, 1173, 1104, 974, 823 cm^{-1} ; ¹H and ¹³C NMR data, Table 1; HRESIMS, *m/z* 417.1319 [M + H]⁺ (calculated for C₂₅H₂₁O₆, 417.1333).

Nostotrebin 7 (4): orange amorphous powder; UV (MeCN) λ_{max} (log ϵ), 225 (4.49), 275 (3.99) nm; IR (ATR) ν_{max} 3172, 2918, 1735, 1691, 1612, 1513, 1447, 1375, 1242, 1023, 824 cm^{-1} ; ¹H and ¹³C NMR data, Table 2; HRESIMS, *m/z* 815.2462 [M + H]⁺ (calculated for C₅₀H₃₉O₁₁, 815.2487).

Nostotrebino 7 (5): yellow amorphous powder; UV (MeCN) λ_{max} (log ϵ), 227 (4.59), 278 (4.05), 357 (4.32) nm; IR (ATR) ν_{max} 3350, 1273, 1690, 1599, 1512, 1441, 1350, 1241, 1173, 832 cm^{-1} ; ¹H and ¹³C NMR data, Table 2; HRESIMS, *m/z* 815.2462 [M + H]⁺ (calculated for C₅₀H₃₉O₁₁, 815.2487).

Quantification by Evaporative Light Scattering Detection (ELSD). To avoid weighing inaccuracies, the concentrations of test compound solutions for bioactivity testing were quantified using HPLC coupled with ELSD (Sedex 85, Sedere) according to Adnani et al.⁶⁰ Quercetin (>99%, Carl Roth) was used as a standard substance to establish the calibration curve (injection of 0.5 to 50 μL of a 20 ng/ μL solution in 90% MeCN in H₂O). Solutions were injected in triplicate on a Kinetex C18 column (100 \times 3.1 mm, 5 μm , 100 Å, Phenomenex), eluted with 90% MeCN in H₂O (0.1% formic acid each) at 0.85 mL/min over 2.5 min. ELSD response areas were averaged, and log(ELSD response area) was plotted against log(amount) to generate a linear calibration curve. Solutions of the compounds in 90% MeCN in H₂O were injected in triplicate under identical conditions. ELSD response areas were averaged, and the corresponding compound concentration was calculated using the quercetin calibration curve.

Rhodesain Assay: General Procedure. Rhodesain was recombinantly expressed as described previously.⁶¹ The hydrolysis of Cbz-Phe-Arg-AMC by rhodesain was detected by a kinetic measurement over 10 min in intervals of 30 s with a Tecan infinite M200 pro plate reader according to Breuning et al.⁴⁶ (excitation wavelength, 380 nm; excitation bandwidth, 9 nm; detection wavelength, 460 nm; detection bandwidth, 20 nm; and *z* position, 18 400 μm). The assay was performed in white 96-well plates (Lumitrac 600 white 96-well microplates, Greiner Bio-One). As the assay buffer, 50 mM sodium acetate at pH 5.5 with 5 mM ethylenediaminetetraacetic acid (EDTA), 200 mM NaCl, and 0.005% Brij 35 was used. The following solution was applied as the enzyme buffer: 50 mM sodium acetate at pH 5.5 containing rhodesain, 5 mM EDTA, 200 mM NaCl, and 5 mM DTT. Substrate (10 mM final concentration) and inhibitor stock solutions were prepared in dimethyl sulfoxide (DMSO) and diluted with assay buffer to a final DMSO concentration of 5%. DMSO alone (5% final concentration) served as the negative control. The determination of the inner filter effect is described in the Supporting Information.

Studies on the Rhodesain Inhibition Mechanism. For more detailed studies on the inhibition mechanism of the compounds on rhodesain, the assays were adjusted as follows: To study a time-dependent inhibition, enzyme and test compound were incubated 0, 5, and 30 min prior to substrate addition.⁴⁸ Subsequently, the standard kinetic measurement over 10 min in intervals of 30 s was performed. To evaluate unspecific electrophilic reactions of the test compounds with the target enzyme, the assay buffer was supplemented with a concentration of 1 and 5 mM DTT (0.125 and 4.75 mM final concentration; see the Supporting Information) and influence on the inhibition was evaluated.^{46,49} The formation of aggregates by the test compound and target enzyme was investigated by the addition of Brij 35 to the assay buffer (final concentration of 0.01 and 0.025%; see the Supporting Information).^{46,47} The inner filter effect was determined as described by Ludewig et al.⁴⁷ IC₅₀ was calculated using Graph Pad PRISM 6. Data were fit by nonlinear regression, applying the equation “log(inhibitor) versus response – variable slope (four parameters)”.

Cell Culture and Cell Survival Rate. HeLa cells were maintained in RPMI 1640 medium supplemented with 10% fetal bovine serum, which was heat-inactivated at 60 °C for 30 min, and 1% penicillin/streptomycin mixture. Cells were cultured at 37 °C in a humidified atmosphere containing 5% CO₂. For estimation of the cell viability against compound **1** and its derivatives, a serial dilution of the test compounds from 100 to 0.05 μM in RPMI 1640 medium supplemented with 10% fetal bovine serum was prepared in 96-well flat-bottom polystyrene microplates (Sarstedt). Cycloheximide was used as a control. A total of 100 μL of cell culture was added to a 96-well plate

containing the serial dilution of the test compounds, achieving a final cell concentration of 1×10^4 cells/well. A growth control (cells in medium but no inhibitor) and a sterility control (medium only) were added. After 24 h of incubation with test compounds at 37 °C, 10 μ L of resazurin solution (1 mg/mL) was added to each well, followed by 24 h of further incubation at 37 °C and 5% CO₂. Fluorescence was measured in a TECAN infinite M200 plate reader at 560 nm excitation and 600 nm emission. The cell viability was estimated in relation to the growth control. All experiments were performed at least in triplicate.

Antimicrobial Activity. The antimicrobial activity of compound **1** and its derivatives against the Gram-positive bacteria *B. subtilis*, *S. aureus*, and *E. faecium* was evaluated by determination of their MIC according to the guidelines of the Clinical and Laboratory Standards Institute (CLSI).⁶² Serial 2-fold dilutions of the test compounds from 100 to 0.05 μ M in cation-adjusted Mueller–Hinton broth were prepared in 96-well round-bottom polystyrene microplates (Sarstedt). Each well contained 50 μ L of test compound solution at twice the desired final concentration and was inoculated with 50 μ L of bacterial suspension, yielding a final inoculum of 5×10^5 colony-forming units (CFU)/mL in 100 μ L final volume. Microplates were incubated for 16–20 h at 37 °C, and the MIC was determined as the lowest concentration of the test compound that inhibited visible bacterial growth.

■ ASSOCIATED CONTENT

Supporting Information

The Supporting Information is available free of charge at <https://pubs.acs.org/doi/10.1021/acs.jnatprod.9b00885>.

UV, IR, MS, MS/MS, ¹H, ¹³C, HSQC, and HMBIC spectra of compounds **1–5** and additional information about the rhodesain assays (PDF)

■ AUTHOR INFORMATION

Corresponding Author

Timo H. J. Niedermeyer – Department of Pharmaceutical Biology/Pharmacognosy, Institute of Pharmacy, University of Halle-Wittenberg, 06120 Halle (Saale), Germany; German Center for Infection Research (DZIF), Partner Site Tübingen, 72076 Tübingen, Germany; orcid.org/0000-0003-1779-7899; Email: timo.niedermeyer@pharmazie.uni-halle.de

Authors

Ronja Kossack – Department of Pharmaceutical Biology/Pharmacognosy, Institute of Pharmacy, University of Halle-Wittenberg, 06120 Halle (Saale), Germany

Steffen Breinlinger – Department of Pharmaceutical Biology/Pharmacognosy, Institute of Pharmacy, University of Halle-Wittenberg, 06120 Halle (Saale), Germany

Trang Nguyen – Department of Microbiology/Biotechnology, Interfaculty Institute for Microbiology and Infection Medicine (IMIT), University of Tübingen, 72076 Tübingen, Germany

Julia Moschny – Department of Pharmaceutical Biology/Pharmacognosy, Institute of Pharmacy, University of Halle-Wittenberg, 06120 Halle (Saale), Germany

Jan Straetener – Department of Microbial Bioactive Compounds, Interfaculty Institute for Microbiology and Infection Medicine (IMIT), University of Tübingen, 72076 Tübingen, Germany; German Center for Infection Research (DZIF), Partner Site Tübingen, 72076 Tübingen, Germany

Anne Berscheid – Department of Microbial Bioactive Compounds, Interfaculty Institute for Microbiology and Infection Medicine (IMIT), University of Tübingen, 72076 Tübingen, Germany; German Center for Infection Research (DZIF), Partner Site Tübingen, 72076 Tübingen, Germany

Heike Brötz-Oesterhelt – Department of Microbial Bioactive Compounds, Interfaculty Institute for Microbiology and Infection Medicine (IMIT), University of Tübingen, 72076 Tübingen, Germany; German Center for Infection Research (DZIF), Partner Site Tübingen, 72076 Tübingen, Germany

Heike Enke – Cyano Biotech GmbH, 12489 Berlin, Germany

Tanja Schirmeister – Institute of Pharmacy and Biochemistry, University of Mainz, 55128 Mainz, Germany

Complete contact information is available at:

<https://pubs.acs.org/doi/10.1021/acs.jnatprod.9b00885>

Notes

The authors declare the following competing financial interest(s): Heike Enke is CSO and co-owner of Cyano Biotech GmbH, but the company does not have any financial interest in the research presented here. The authors declare no competing financial interest.

■ ACKNOWLEDGMENTS

This work was financially supported by the Federal Ministry of Education and Research (BMBF, Project ANoBin, FKZ 16GW0115, to Ronja Kossack), the German Research Foundation (DFG, INST 271/388-1, to Timo H. J. Niedermeyer), and the German Center for Infection Research (DZIF Partner Site Tübingen; to Jan Straetener, Anne Berscheid, Heike Brötz-Oesterhelt, and Timo H. J. Niedermeyer). The authors thank Dr. A. Porzel (Leibniz Institute of Plant Biochemistry, Halle, Germany) and Dr. P. Schmieder (Leibniz Institute of Molecular Pharmacology, Berlin, Germany) for recording the NMR spectra.

■ REFERENCES

- (1) Salvador-Reyes, L. A.; Luesch, H. *Nat. Prod. Rep.* **2015**, *32*, 478–503.
- (2) Niedermeyer, T. H. *Planta Med.* **2015**, *81*, 1309–1325.
- (3) Tan, L. T. J. *Appl. Phycol.* **2010**, *22*, 659–676.
- (4) Nunnery, J. K.; Mevers, E.; Gerwick, W. H. *Curr. Opin. Biotechnol.* **2010**, *21*, 787–793.
- (5) Niedermeyer, T.; Brönstrup, M. In *Microalgal Biotechnology: Integration and Economy*; Posten, C., Walter, C., Eds.; de Gruyter: Berlin, Germany, 2012; pp 169–200.
- (6) Tidgewell, K.; Clark, B. R.; Gerwick, W. H. *Comprehensive Natural Products II*; Elsevier: Amsterdam, Netherlands, 2010; pp 141–188.
- (7) Younes, A.; Yasothan, U.; Kirkpatrick, P. *Nat. Rev. Drug Discovery* **2012**, *11*, 19–20.
- (8) Flahive, E.; Srirangam, J. The Dolastatins: Novel Antitumor Agents from *Dolabella auricularia*. In *Anticancer Agents from Natural Products*; Kingston, D., Cragg, G., Newman, D., Eds.; CRC Press: Boca Raton, FL, 2005; pp 191–214.
- (9) Luesch, H.; Harrigan, G. G.; Goetz, G.; Horgen, F. D. *Curr. Med. Chem.* **2002**, *9*, 1791–1806.
- (10) Bouchard, H.; Brun, M.-P.; Commerçon, A.; Zhang, J. Novel conjugates, preparation thereof, and therapeutic use thereof. WO Patent WO/2011/001052, Jan 6, 2011.
- (11) Rohr, J. *ACS Chem. Biol.* **2006**, *1*, 747–750.
- (12) Hirsch, C. F.; Liesch, J. M.; Salvatore, M. J.; Schwartz, R. E.; Sesin, D. F. Antifungal fermentation product and method. U.S. Patent 4,946,835, Aug 7, 1990.
- (13) Llewellyn, L. E. *Nat. Prod. Rep.* **2006**, *23*, 200–222.
- (14) Rodriguez-Navarro, A. J.; Lagos, N.; Lagos, M.; Braghetto, I.; Csendes, A.; Hamilton, J.; Figueroa, C.; Truan, D.; Garcia, C.; Rojas, A.; Iglesias, V.; Brunet, L.; Alvarez, F. *Anesthesiology* **2007**, *106*, 339–345.
- (15) Halland, N.; Brönstrup, M.; Czech, J.; Czechitzky, W.; Evers, A.; Follmann, M.; Kohlmann, M.; Schiell, M.; Kurz, M.; Schreuder, H. A.; Kallus, C. J. *Med. Chem.* **2015**, *58*, 4839–4844.

- (16) Schreuder, H.; Liesum, A.; Lönze, P.; Stump, H.; Hoffmann, H.; Schiell, M.; Kurz, M.; Toti, L.; Bauer, A.; Kallus, C.; Klemke-Jahn, C.; Czech, J.; Kramer, D.; Enke, H.; Niedermeyer, T. H. J.; Morrison, V.; Kumar, V.; Brönstrup, M. *Sci. Rep.* **2016**, *6*, 32958.
- (17) Dittmann, E.; Gugger, M.; Sivonen, K.; Fewer, D. P. *Trends Microbiol.* **2015**, *23*, 642–652.
- (18) Babu, K. S.; Li, X.-C.; Jacob, M. R.; Zhang, Q.; Khan, S. I.; Ferreira, D.; Clark, A. M. *J. Med. Chem.* **2006**, *49*, 7877–7886.
- (19) Wang, S.-Y.; Lan, X.-Y.; Xiao, J.-H.; Yang, J.-C.; Kao, Y.-T.; Chang, S.-T. *Phytother. Res.* **2008**, *22*, 213–216.
- (20) Antkowiak, R.; Antkowiak, W. Z.; Banczyk, I.; Mikolajczyk, L. *Can. J. Chem.* **2003**, *81*, 118–124.
- (21) Wijeratne, E. M. K.; Turbyville, T. J.; Zhang, Z.; Bigelow, D.; Pierson, L. S.; van Etten, H. D.; Whitesell, L.; Canfield, L. M.; Gunatilaka, A. A. L. *J. Nat. Prod.* **2003**, *66*, 1567–1573.
- (22) Hayashi, M.; Kim, Y.-P.; Takamatsu, S.; Enomoto, A.; Shinose, M.; Takahashi, Y.; Tanaka, H.; Komiyama, K.; Omura, S. *J. Antibiot.* **1996**, *49*, 1091–1095.
- (23) Noble, M.; Noble, D.; Fletton, R. A. *J. Antibiot.* **1978**, *31*, 15–18.
- (24) Sevcikova, Z.; Pour, M.; Novak, D.; Ulrichova, J.; Vacek, J. *Mini-Rev. Med. Chem.* **2014**, *14*, 322–331.
- (25) Clemo, N. G.; Gedge, D. R.; Pattenden, G. J. *Chem. Soc., Perkin Trans. 1* **1981**, 1448.
- (26) Li, X.-C.; Ferreira, D.; Jacob, M. R.; Zhang, Q.; Khan, S. I.; ElSohly, H. N.; Nagle, D. G.; Smillie, T. J.; Khan, I. A.; Walker, L. A.; Clark, A. M. *J. Am. Chem. Soc.* **2004**, *126*, 6872–6873.
- (27) Zelik, P.; Lukesova, A.; Voloshko, L. N.; Stys, D.; Kopecky, J. *J. Enzyme Inhib. Med. Chem.* **2009**, *24*, 531–536.
- (28) Zelik, P.; Lukesova, A.; Cejka, J.; Budesinsky, M.; Havlicek, V.; Cegan, A.; Kopecky, J. *J. Enzyme Inhib. Med. Chem.* **2010**, *25*, 414–420.
- (29) Vacek, J.; Hrbáč, J.; Kopecký, J.; Vostálová, J. *Molecules* **2011**, *16*, 4254–4263.
- (30) Cheel, J.; Bogdanová, K.; Ignatova, S.; Garrard, I.; Hewitson, P.; Kolář, M.; Kopecký, J.; Hrouzek, P.; Vacek, J. *Algal Res.* **2016**, *18*, 244–249.
- (31) Radau, G. *Curr. Enzyme Inhib.* **2005**, *1*, 295–307.
- (32) Chlipala, G.; Mo, S.; Carcache de Blanco, E. J.; Ito, A.; Bazarek, S.; Orjala, J. *Pharm. Biol.* **2009**, *47*, 53–60.
- (33) Miller, B.; Friedman, A. J.; Choi, H.; Hogan, J.; McCammon, J. A.; Hook, V.; Gerwick, W. H. J. *J. Nat. Prod.* **2014**, *77*, 92–99.
- (34) Mazur-marzec, H.; Fidor, A.; Ceglowska, M.; Wieczerek, E.; Kropidłowska, M.; Goua, M.; Macaskill, J.; Edwards, C. *Mar. Drugs* **2018**, *16*, 220.
- (35) Liu, L.; Jokela, J.; Wahlsten, M.; Nowruzi, B.; Permi, P.; Zhang, Y. Z.; Xhaard, H.; Fewer, D. P.; Sivonen, K. *J. Nat. Prod.* **2014**, *77*, 1784–1790.
- (36) Jokela, J.; Heinilä, L. M. P.; Shishido, T. K.; Wahlsten, M.; Fewer, D. P.; Fiore, M. F.; Wang, H.; Haapaniemi, E.; Permi, P.; Sivonen, K. *Front. Microbiol.* **2017**, *8*, 1963.
- (37) Ettari, R.; Tamborini, L.; Angelo, I. C.; Micale, N.; Pinto, A.; de Micheli, C.; Conti, P. *J. Med. Chem.* **2013**, *56*, 5637–5658.
- (38) Lonsdale-Eccles, J. D.; Grab, D. J. *Trends Parasitol.* **2002**, *18*, 17–19.
- (39) Overath, P.; Chaudhri, M.; Steverding, D.; Ziegelbauer, K. *Parasitol. Today* **1994**, *10*, 53–58.
- (40) Volk, R.-B.; Girreser, U.; Al-Refai, M.; Laatsch, H. *Nat. Prod. Res.* **2009**, *23*, 607–612.
- (41) Jaki, B.; Orjala, J.; Sticher, O. *J. Nat. Prod.* **1999**, *62*, 502–503.
- (42) Caicedo, N. H.; Kumirska, J.; Neumann, J.; Stolte, S.; Thöming, J. *Mar. Biotechnol.* **2012**, *14*, 436–445.
- (43) Hirata, K.; Takashina, J.; Nakagami, H.; Ueyama, S.; Murakami, K.; Kanamori, T.; Miyamoto, K. *Biosci., Biotechnol., Biochem.* **1996**, *60*, 1905–1906.
- (44) Baell, J. B.; Holloway, G. A. *J. Med. Chem.* **2010**, *53*, 2719–2740.
- (45) Baell, J.; Walters, M. A. *Nature* **2014**, *513*, 481–483.
- (46) Breuning, A.; Degel, B.; Schulz, F.; Buchhold, C.; Stempka, M.; Machon, U.; Heppner, S.; Gelhaus, C.; Leippe, M.; Leyh, M.; Kisker, C.; Rath, J.; Stich, A.; Gut, J.; Rosenthal, P. J.; Schmuck, C.; Schirmeister, T. *J. Med. Chem.* **2010**, *53*, 1951–1963.
- (47) Ludewig, S.; Kossner, M.; Schiller, M.; Baumann, K.; Schirmeister, T. *Curr. Top. Med. Chem.* **2010**, *10*, 368–382.
- (48) Han, H.; Yang, Y.; Olesen, S. H.; Becker, A.; Betzi, S.; Schönbrunn, E. *Biochemistry* **2010**, *49*, 4276–4282.
- (49) Blanchard, J. E.; Elowe, N. H.; Huitema, C.; Fortin, P. D.; Cechetto, J. D.; Eltis, L. D.; Brown, E. D. *Chem. Biol.* **2004**, *11*, 1445–1453.
- (50) Wang, L.-K.; Lin-Shiau, S.-Y.; Lin, J.-K. *Eur. J. Cancer* **1999**, *35*, 1517–1525.
- (51) Shimoi, K.; Masuda, S.; Furugori, M.; Esaki, S.; Kinae, N. *Carcinogenesis* **1994**, *15*, 2669–2672.
- (52) Son, S.; Lewis, B. A. *J. Agric. Food Chem.* **2002**, *50*, 468–472.
- (53) Li, K.; Li, X.-M.; Ji, N.-Y.; Wang, B.-G. *J. Nat. Prod.* **2008**, *71*, 28–30.
- (54) Masella, R.; Cantafora, A.; Modesti, D.; Cardilli, A.; Gennaro, L.; Bocca, A.; Coni, E. *Redox Rep.* **1999**, *4*, 113–121.
- (55) Sroka, Z.; Cisowski, W. *Food Chem. Toxicol.* **2003**, *41*, 753–758.
- (56) Riveira, M. J.; Tekwani, B. L.; Labadie, G. R.; Mischne, M. P. *MedChemComm* **2012**, *3*, 1294–1298.
- (57) Chen, L.; Liu, B.; Deng, J.-J.; Zhang, J.-S.; Li, W.; Ahmed, A.; Yin, S.; Tang, G.-H. *RSC Adv.* **2018**, *8*, 17898–17904.
- (58) Simeonov, A.; Michaelian, K. *Biol. Phys.* **2017**, 1–38.
- (59) Andersen, R. A. *Algal Culturing Techniques*; Elsevier Academic Press: Burlington, MA, 2005.
- (60) Adnani, N.; Michel, C. R.; Bugni, T. S. *J. Nat. Prod.* **2012**, *75*, 802–806.
- (61) Caffrey, C. R.; Hansell, E.; Lucas, K. D.; Brinen, L. S.; Alvarez Hernandez, A.; Cheng, J.; Gwaltney, S. L.; Roush, W. R.; Stierhof, Y.-D.; Bogyo, M.; Steverding, D.; Mckerrow, J. H. *Mol. Biochem. Parasitol.* **2001**, *118*, 61–73.
- (62) Clinical and Laboratory Standards Institute (CLSI). *Methods for Dilution Antimicrobial Susceptibility Tests for Bacteria that Grow Aerobically: Approved Standard*, 10th ed.; CLSI: Wayne, PA, 2015; Vol. 35.

3.3.2.2. Studies on Rhodesain Inhibition Mechanism

In addition to the mechanistic studies reported in Kossack *et al.* with regard to time dependency, unspecific electrophilic reactions, and the formation of aggregates,¹⁵⁰ steady state experiments were performed with Nostotrebin 6 in order to investigate the inhibition mechanism. Therefore, the initial velocity of the enzymatic reaction was determined using the slopes of the first minutes of the progress curves, obtained without preincubation of enzyme and inhibitor, and at varying inhibitor (Nostotrebin 6) and substrate concentrations. The resulting data were fit by non-linear regression to the mixed model enzyme inhibition in Graph Pad PRISM (see 2.4.1.2), illustrated in Figure 58. The resulting parameters are summarized in Table 19.

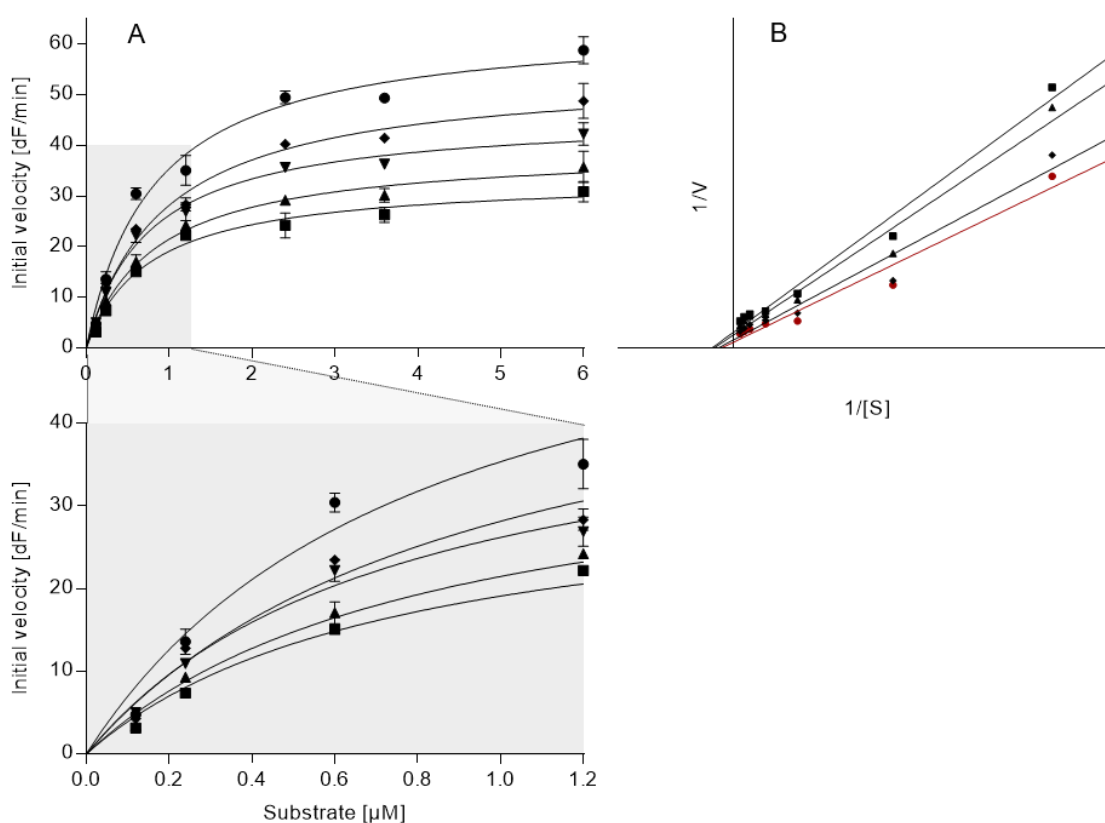


Figure 58. **Steady state experiments with Nostotrebin 6.** (A) Initial velocity of rhodesain at varying substrate and inhibitor concentrations [I]: 0 μM (\bullet), 3.125 μM (\blacklozenge), 6.25 μM (\blacktriangledown), 12.5 μM (\blacktriangle), and 20 μM (\blacksquare). Shaded in gray: 0-1.2 μM substrate. (B) Lineweaver-Burk plot: 0 μM (\bullet), 3.125 μM (\blacklozenge), 12.5 μM (\blacktriangle), and 20 μM (\blacksquare).

The initial velocity in presence of varying inhibitor concentrations [I] was plotted against the substrate concentration [S]. v_{max} is reduced by the inhibitor, indicating either a noncompetitive or an uncompetitive inhibition. As K_m changes only slightly and within the standard deviation, a noncompetitive inhibition is more likely. With an alpha value of 0.74, it is unclear which type of inhibition can be assumed. But with alpha=1 a noncompetitive inhibition is more likely. In case of an uncompetitive inhibition, the alpha value would be very

small, but greater than zero, whereas a competitive inhibition results in a very large alpha value.¹⁵¹

Table 19. **Best-fit values for the parameters of mixed-model inhibition.**

v_{\max}	Alpha	K_i	K_m
63.15 dF/min	0.74	25.9 μM	0.86 μM

Noncompetitive inhibitors do not affect the binding of the substrate, but bind equally well to the enzyme and enzyme–substrate complex. Thus, there is no effect on k_m but on v_{\max} .¹⁵² The K_i value is a measure of the affinity of the inhibitor for the enzyme, the smaller the K_i the higher the affinity of the inhibitor to the enzyme. Here, the K_i was determined as 25.9 μM . This value is high compared to other rhodesain inhibitors like the macrocyclic lactams identified as potent rhodesain inhibitors, with $K_i < 500$ nM, by Giroud *et al.*¹⁰¹ Combined with the results shown in Kossack *et al.*,¹⁵⁰ nostotrebin 6 can be assumed to be a time-independent inhibitor, which does neither react unspecifically with thiols, nor by aggregation. Presumably, nostotrebin 6 and the structurally related oligomers act as noncompetitive inhibitors due to their phenol groups.

Unspecific Reactivity due to Phenolic Hydroxy Groups ^A

It was observed for other polyphenolic natural products, that the bioactivity increases with the number of hydroxy groups per molecule,^{153–158} suggesting that the activity of the nostotrebins/ nostolactones is indeed due to unspecific, polyphenol-like activity on proteins. The broad bioactivity spectrum, which has been reported for CPDs in general, was postulated to be based on the chemically reactive CPD substructure.¹⁵⁹ For example, the antifungal activity of coruscanone A was at first attributed to the 2- methoxymethylenecyclopent-4-ene-1,3-dione moiety, assuming an irreversible covalent addition to its target by Michael addition,¹⁶⁰ while the side chain styryl-like moiety was suspected to contribute to target binding. However, subsequent evaluation of synthesized 2-cinnamyliden-1,3-diones related to coruscanone A showed that the CPD core structure was not essential for bioactivity but, instead, highlighted the importance of the styryl side chain.¹⁶¹ Furthermore, CPDs isolated from *Lindera aggregata*, comprising one or two CPD moieties but no hydroxy groups, were found to be inactive against *B. subtilis*.¹⁶² Compound **1**, containing two CPD subunits, and

^A Paragraph adapted from Kossack, R.; Breinlinger, S.; Nguyen, T.; Moschny, J.; Straetener, J.; Berscheid, A. *et al.* (2020) Nostotrebin 6 Related Cyclopentenediones and δ -Lactones with Broad Activity Spectrum Isolated from the Cultivation Medium of the Cyanobacterium *Nostoc* sp. CBT1153. *J. Nat. Prod.* DOI: 10.1021/acs.jnatprod.9b00885

compound **5**, containing just one CPD substructure, were roughly equally active in our assays. Hence, as discussed above, it is likely that the bioactivities of the nostotrebin compound family are not due to the CPD moiety but the phenolic hydroxy groups.

4. Conclusions and Future Perspectives

The major aim of my work was to isolate and characterize anti-infective metabolites from cyanobacteria, especially inhibitors of the trypanosomal cysteine protease rhodesain, as part of the binational Indonesian-German project "Accessing Novel Bacterial Producers from Biodiversity-rich Habitats in Indonesia" (ANoBIIn). Cyanobacteria are valuable sources for cytotoxic and antimicrobial metabolites, as well as for protease inhibitors.^{36,48,55-57} Proteases are promising targets for new therapeutic approaches, due to their crucial role in the pathogenesis of many infectious diseases.^{53,54} The cysteine protease rhodesain plays a major role during the parasitic infection by *T. brucei*, and is thus regarded as an auspicious target for urgently needed new medications against human African trypanosomiasis.^{53,88-91}

(I) In total 147 cyanobacteria strains were successfully isolated from diverse habitats in Indonesia and Germany. Different sampling as well as isolation techniques led to the isolation of morphologically distinct strains, which were classified into the five sections described by Rippka *et al.*²⁴ In the future, a polyphasic approach, as described by Komárek *et al.*, which mirrors evolutionary history and includes monophyletic taxa, should be applied for further characterization.²¹ From German sites, a total of 55 cyanobacteria strains were isolated. Most strains belonged to the Oscillatoriales (65.5%), whereas 30.9% belonged to the Chroococcales, and only 3.6% to the Nostocales. Compared to the sampling in Indonesia, which led to the isolation of 92 cyanobacteria strains (38.0% Oscillatoriales, 34.8% Nostocales, 17.4% Chroococcales, 9.8% Stigonematales), these results might indicate a higher cyanobacterial diversity in the Indonesian samples. However, different sampling techniques could have led to biased results.

(II) From the newly established strain collection, about 60 biomass extracts were screened for rhodesain inhibition, antimicrobial activity (*Bacillus subtilis*, *Staphylococcus aureus*) and QS inhibition and enhancement (*Vibrio harveyi*, *Chromobacterium violaceum*, *Staphylococcus aureus*, *Serratia marcescens*). Of 52 tested extracts, 11.5% showed more than 50% inhibition of rhodesain at 0.1 mg/mL and 2% more than 70% inhibition. Five of the screened extracts, revealing interesting bioactivities combined with a promising chemical profile, were selected for closer examination. The HPLC-DAD and HPLC-MS profiles of the strains indicated several bioactive, potentially novel compounds, though these findings need to be verified by additional MS-MS experiments. Rhodesain inhibiting substances were found in at least three biomass extracts, thus the hypothesis that cyanobacteria could serve as a source for rhodesain inhibitors was confirmed. The rhodesain inhibiting substances need to be identified, isolated and characterized, and might serve as lead-structures for therapies against

HAT in the future. This newly established strain collection provides a valuable source for bioactive compounds, as cyanobacterial metabolites are known for their antifungal, antiviral and anticancer activities.^{31,35}

(III) A cyanobacteria extract collection, kindly provided by the Cyano Biotech GmbH, was screened against the trypanosomal cysteine protease rhodesain in cooperation with Prof. Dr. Tanja Schirmeister (Johannes Gutenberg University, Mainz). 2.7% of the screened biomass extracts exhibited an inhibition of 70-100% at 0.1 mg/mL, which resembles the screening results of our in-house extract collection. Processing of the biomass extract from a *Nostoc* sp. strain led to the successful isolation of rhodesain inhibiting substances. Five of the nine structurally related compounds showed an inhibitory activity higher than 90% at 0.1 mg/mL. The partial structure of an inactive derivative was successfully characterized. As soon as the complete structures of the active derivatives are elucidated, they might serve as new lead structures for the treatment of HAT. Additionally, structure-activity relationships could be deduced from the structure of inhibitory inactive derivatives, which would be beneficial for the design and structure optimization of new inhibitors.

In the medium extract of another *Nostoc* sp. strain, we identified the homodimeric cyclopentenedione (CPD) nostotrebin 6 and novel related monomeric, dimeric, and higher oligomeric compounds as active substances. The oligomeric compounds are composed of two core monomeric structures, a trisubstituted CPD or a trisubstituted unsaturated δ -lactone. Nostotrebin 6 so far has been the only known cyanobacterial CPD and has been found to be active in a broad variety of assays, indicating that it might be a pan-assay interference compound (PAIN). Thus, we compared the antibacterial and cytotoxic activity, as well as the rhodesain inhibition of selected compounds. As a compound with a δ -lactone instead of a CPD core structure was equally active as nostotrebin 6, the bioactivities of these compounds seem to be based on the phenolic substructures, rather than on the CPD moiety. While the dimers were roughly equally potent, the monomer displayed slightly weaker activity, suggesting that the compounds show unspecific activity depending on the number of free phenolic hydroxyl groups per molecule.^A

The isolation of nostotrebin 6 shows that it is important to keep in mind that 5-12% of a typical academic screening library are PAINS.¹⁶³ Therefore, it is crucial to familiarize with the most common PAIN structures, conduct intensive literature search and perform various

^A Paragraph adapted from Kossack, R.; Breinlinger, S.; Nguyen, T.; Moschny, J.; Straetener, J.; Berscheid, A. et al. (2020) Nostotrebin 6 Related Cyclopentenediones and δ -Lactones with Broad Activity Spectrum Isolated from the Cultivation Medium of the Cyanobacterium *Nostoc* sp. CBT1153. *J. Nat. Prod.* DOI: 10.1021/acs.jnatprod.9b00885

assays that detect activities with different readouts while screening for new lead structures.¹⁶⁴ To our knowledge, this work is the first to consider cyanobacteria as a source for rhodesain inhibitors. Until today, most cyanobacterial natural products were isolated from biomass, and only few compounds from cyanobacteria cultivation media are known.¹⁶⁵⁻¹⁶⁸ The present findings show that cyanobacteria medium extracts provide a valuable source for biologically active natural products.

5. References

- (1) Gans, J.; Wolinsky, M.; Dunbar, J. Computational improvements reveal great bacterial diversity and high metal toxicity in soil. *Science* **2005**, *309* (5739), 1387–1390. DOI: 10.1126/science.1112665.
- (2) Sengupta, S.; Chattopadhyay, M. K.; Grossart, H.-P. The multifaceted roles of antibiotics and antibiotic resistance in nature. *Front. Microbiol.* **2013**, *4*, 47. DOI: 10.3389/fmicb.2013.00047.
- (3) Overmann, J.; Scholz, A. H. Microbiological research under the Nagoya Protocol: facts and fiction. *Trends Microbiol* **2017**, *25* (2), 85–88. DOI: 10.1016/j.tim.2016.11.001.
- (4) Myers, N.; Mittermeier, R. A.; Mittermeier, C. G.; da Fonseca, G. A.; Kent, J. Biodiversity hotspots for conservation priorities. *Nature* **2000**, *403* (6772), 853–858. DOI: 10.1038/35002501.
- (5) Molinski, T. F.; Dalisay, D. S.; Lievens, S. L.; Saludes, J. P. Drug development from marine natural products. *Nat. Rev. Drug Discovery* **2009**, *8* (1), 69–85. DOI: 10.1038/nrd2487.
- (6) Fusetani, N.; Matsunaga, S. Bioactive sponge peptides. *Chem. Rev.* **1993**, *93* (5), 1793–1806. DOI: 10.1021/cr00021a007.
- (7) Harrigan, G. G.; Goetz, G. Symbiotic and dietary marine microalgae as a source of bioactive molecules – experience from natural products research. *J Appl Phycol* **2002**, *14* (2), 103–108.
- (8) Kobayashi, J.; Ishibashi, M. Bioactive metabolites of symbiotic marine microorganisms. *Chem. Rev.* **1993**, *93* (5), 1753–1769. DOI: 10.1021/cr00021a005.
- (9) Piel, J. Metabolites from symbiotic bacteria. *Nat. Prod. Rep.* **2004**, *21* (4), 519–538. DOI: 10.1039/b310175b.
- (10) Griffin, D. W. Atmospheric movement of microorganisms in clouds of desert dust and implications for human health. *Clinical microbiology reviews* **2007**, *20* (3), 459–477. DOI: 10.1128/CMR.00039-06.
- (11) Speth, D.; Hu, B.; Bosch, N.; Keltjens, J.; Stunnenberg, H.; Jetten, M. Comparative genomics of two independently enriched “Candidatus Kuenenia Stutgartiensis” anammox bacteria. *Front. Microbiol.* **2012**, *3*, 307. DOI: 10.3389/fmicb.2012.00307.
- (12) Thole, S.; Kalhoefer, D.; Voget, S.; Berger, M.; Engelhardt, T.; Liesegang, H.; Wollherr, A.; Kjelleberg, S.; Daniel, R.; Simon, M.; Thomas, T.; Brinkhoff, T. *Phaeobacter gallaeciensis* genomes from globally opposite locations reveal high similarity of adaptation to surface life. *ISME J.* **2012**, *6* (12), 2229–2244. DOI: 10.1038/ismej.2012.62.

- (13) Whitaker, R. J.; Grogan, D. W.; Taylor, J. W. Geographic barriers isolate endemic populations of hyperthermophilic archaea. *Science* **2003**, *301* (5635), 976–978. DOI: 10.1126/science.1086909.
- (14) Glaeser, J.; Overmann, J. Biogeography, evolution, and diversity of epibionts in phototrophic consortia. *Appl. Environ. Microbiol.* **2004**, *70* (8), 4821–4830. DOI: 10.1128/AEM.70.8.4821-4830.2004.
- (15) Curtis, T. P.; Sloan, W. T.; Scannell, J. W. Estimating prokaryotic diversity and its limits. *PNAS* **2002**, *99* (16), 10494–10499. DOI: 10.1073/pnas.142680199.
- (16) Overmann, J. Principles of enrichment, isolation, cultivation, and preservation of prokaryotes. In *The prokaryotes*; Springer, 2013; pp 149–207.
- (17) Niedermeyer, T.; Brönstrup, M. Natural-product drug discovery from microalgae. In *Microalgal Biotechnology: Integration and Economy*; Posten, C., Walter, C., Eds.; de Gruyter, 2012; pp 169–200.
- (18) Schopf, J. W.; Packer, B. M. Early archean (3.3-billion to 3.5-billion-year-old) microfossils from warrawoona group, australia. *Science* **1987**, *237* (4810), 70–73.
- (19) Schopf, W. J. The development and diversification of Precambrian life. *Origins of life* **1974**, *5* (1-2), 119–135. DOI: 10.1007/BF00927018.
- (20) Whitton, B. A. *Ecology of cyanobacteria II: Their diversity in space and time*; Springer Science & Business Media, 2012.
- (21) Komárek, J.; Kastovsky, J.; Mares, J.; Johansen, J. R. Taxonomic classification of cyanoprokaryotes (cyanobacterial genera) 2014, using a polyphasic approach. *Preslia* **2014** (86), 295–335.
- (22) Gomont, M. Monographie des Oscillatoriées (Nostocacées homocystées). *Ann Sci. Nat. Bot. Ser.* **1892**, *7* (15), 263–368.
- (23) Bornet, É. *Revision des nostocacées hétérocystées contenues dans les principaux herbier de France*, 1886.
- (24) Rippka, R.; Deruelles, J.; Waterbury, J. B.; Herdman, M.; Stanier, R. Y. Generic assignments, strain histories and properties of pure cultures of cyanobacteria. *J. Gen. Microbiol.* **1979**, *111*, 1–61.
- (25) Boone, D. R.; Castenholz, R. W.; Garrity, G. M., Eds. *Bergey's Manual of Systematic Bacteriology: Volume one: the Archaea and the deeply branching and phototrophic bacteria*, 2nd ed.; Springer, 2012. DOI: 10.1007/978-0-387-21609-6.
- (26) Waterbury, J. B.; Stanier, R. Y. Patterns of growth and development in pleurocapsalean cyanobacteria. *Microbiological Reviews* **1978**, *42* (1), 2–44.
- (27) Bergman, B.; Gallon, J. R.; Rai, A. N.; Stal, L. J. N₂ Fixation by nonheterocystous cyanobacteria. *FEMS Microbiol. Rev.* **1997**, *1997* (19), 139–185.

- (28) Stanier, R. Y.; Cohen-Bazire, G. Phototrophic prokaryotes: the cyanobacteria. *Annu Rev Microbiol* **1977**, *31*, 225–274. DOI: 10.1146/annurev.mi.31.100177.001301.
- (29) Geitler, L. *Dr. L. Rabenhorst's Kryptogamen-Flora von Deutschland, Österreich und der Schweiz*, Reprint [d.] 2., vollst. neu bearb. Aufl., [Leipzig, Akad. Verl.-Ges.], 1930 - 1932; Koeltz; Bishen Singh Mahendra Pal Singh, 1985.
- (30) Nagle, D. G.; Paul, V. J. Production of secondary metabolites by filamentous tropical marine cyanobacteria: ecological functions of the compounds. *J. Phycol.* **1999**, *35*, 1412–1421.
- (31) Niedermeyer, T. H. Anti-infective natural products from cyanobacteria. *Planta Med* **2015**, *81* (15), 1309–1325. DOI: 10.1055/s-0035-1546055.
- (32) Salvador-Reyes, L. A.; Luesch, H. Biological targets and mechanisms of action of natural products from marine cyanobacteria. *Nat. Prod. Rep.* **2015**, *32* (3), 478–503.
- (33) Tan, L. T. Filamentous tropical marine cyanobacteria: a rich source of natural products for anticancer drug discovery. *J. Appl. Phycol.* **2010**, *22* (5), 659–676.
- (34) Nunnery, J. K.; Mevers, E.; Gerwick, W. H. Biologically active secondary metabolites from marine cyanobacteria. *Current Opinion in Biotechnology* **2010**, *21*, 787–793.
- (35) Tidgewell, K.; Clark, B. R.; Gerwick, W. H. The natural products chemistry of cyanobacteria. In *Comprehensive Natural Products II*; Elsevier, 2010; pp 141–188. DOI: 10.1016/B978-008045382-8.00041-1.
- (36) Miller, B.; Friedman, A. J.; Choi, H.; Hogan, J.; McCammon, J. A.; Hook, V.; Gerwick, W. H. The marine cyanobacterial metabolite gallinamide A is a potent and selective inhibitor of human cathepsin L. *J. Nat. Prod.* **2014**, *77* (1), 92–99. DOI: 10.1021/np400727r.
- (37) Younes, A.; Yasothan, U.; Kirkpatrick, P. Brentuximab vedotin. *Nat. Rev. Drug Discovery* **2012**, *11* (1), 19–20.
- (38) Flahive, E.; Srirangam, J. 11: The dolastatins: novel antitumor agents from *Dolabella auricularia*. In *Anticancer agents from natural products*; Kingston, D., Cragg, G., Newman, D., Eds.; CRC Press, 2005; pp 191–214.
- (39) Luesch, H.; Harrigan, G. G.; Goetz, G.; Horgen, F. D. The cyanobacterial origin of potent anticancer agents originally isolated from sea hares. *Curr. Med. Chem.* **2002**, *9*, 1791–1806.
- (40) Bouchard, H.; Brun, M.-P.; Commerçon, A.; Zhang, J. Novel conjugates, preparations thereof, and therapeutic use thereof.
- (41) Rohr, J. Cryptophycin anticancer drugs revisited. *ACS Chem. Biol.* **2006**, *1* (12), 747–750.
- (42) Hirsch, C. F.; Liesch, J. M.; Salvatore, M. J.; Schwartz, R. E.; Sesin, D. F. Antifungal fermentation product and method. 219,942.

- (43) Llewellyn, L. E. Saxitoxin, a toxic marine natural product that targets a multitude of receptors. *Nat. Prod. Rep.* **2006**, *23* (2), 200–222.
- (44) Rodriguez-Navarro, A. J.; Lagos, N.; Lagos, M.; Braghetto, I.; Csendes, A.; Hamilton, J.; Figueroa, C.; Truan, D.; Garcia, C.; Rojas, A.; Iglesias, V.; Brunet, L.; Alvarez, F. Neosaxitoxin as a local anesthetic: preliminary observations from a first human trial. *Anesthesiology* **2007**, *106* (2), 339–345.
- (45) Halland, N.; Brønstrup, M.; Czech, J.; Czechtizky, W.; Evers, A.; Follmann, M.; Kohlmann, M.; Schiell, M.; Kurz, M.; Schreuder, H. a.; Kallus, C. Novel small molecule inhibitors of activated thrombin activatable fibrinolysis inhibitor (TAFIa) from natural product anabaenopeptin. *J. Med. Chem.* **2015**, *58* (11), 4839–4844.
- (46) Schreuder, H.; Liesum, A.; Lönze, P.; Stump, H.; Hoffmann, H.; Schiell, M.; Kurz, M.; Toti, L.; Bauer, A.; Kallus, C.; Klemke-Jahn, C.; Czech, J.; Kramer, D.; Enke, H.; Niedermeyer, T. H. J.; Morrison, V.; Kumar, V.; Brønstrup, M. Isolation, co-crystallization and structure-based characterization of anabaenopeptins as highly potent inhibitors of activated thrombin activatable fibrinolysis inhibitor (TAFIa). *Sci. Rep.* **2016**, *6* (August), 32958.
- (47) Dittmann, E.; Gugger, M.; Sivonen, K.; Fewer, D. P. Natural product biosynthetic diversity and comparative genomics of the cyanobacteria. *Trends Microbiol.* **2015**, *23* (10), 642–652. DOI: 10.1016/j.tim.2015.07.008.
- (48) Radau, G. Cyanopeptides: A new and nearly inexhaustible natural resource for the design and structure-activity relationship studies of new inhibitors of trypsin-like serine proteases. *CEI* **2005**, *1* (3), 295–307. DOI: 10.2174/157340805774580510.
- (49) Chlipala, G.; Mo, S.; Carcache de Blanco, E. J.; Ito, A.; Bazarek, S.; Orjala, J. Investigation of antimicrobial and protease-inhibitory activity from cultured cyanobacteria. *Pharm. Biol.* **2009**, *47* (1), 53–60. DOI: 10.1080/13880200802415483.
- (50) Mazur-marzec, H.; Fidor, A.; Cegłowska, M.; Wieczerek, E.; Kropidłowska, M.; Goua, M.; Macaskill, J.; Edwards, C. Cyanopeptolins with trypsin and chymotrypsin inhibitory activity from the cyanobacterium *Nostoc edaphicum* CCNP1411. *Mar. Drugs* **2018**, *16* (7). DOI: 10.3390/md16070220.
- (51) Liu, L.; Jokela, J.; Wahlsten, M.; Nowruzi, B.; Permi, P.; Zhang, Y. Z.; Xhaard, H.; Fewer, D. P.; Sivonen, K. Nostosins, trypsin inhibitors isolated from the terrestrial cyanobacterium *Nostoc* sp. Strain FSN. *J. Nat. Prod.* **2014**, *77* (8), 1784–1790. DOI: 10.1021/np500106w.
- (52) Jokela, J.; Heinilä, L. M. P.; Shishido, T. K.; Wahlsten, M.; Fewer, D. P.; Fiore, M. F.; Wang, H.; Haapaniemi, E.; Permi, P.; Sivonen, K. Production of high amounts of hepatotoxin nodularin and new protease inhibitors Pseudospumigins by the Brazilian Benthic *Nostoc* sp. CENA543. *Front. Microbiol.* **2017**, *8*, 1963. DOI: 10.3389/fmicb.2017.01963.

- (53) Ettari, R.; Tamborini, L.; Angelo, I. C.; Micale, N.; Pinto, A.; Micheli, C. de; Conti, P. Inhibition of rhodesain as a novel therapeutic modality for human African trypanosomiasis. *J. Med. Chem.* **2013**, *56* (14), 5637–5658. DOI: 10.1021/jm301424d.
- (54) Turk, B. Targeting proteases: successes, failures and future prospects. *Nat. Rev. Drug Discovery* **2006**, *5* (9), 785–799. DOI: 10.1038/nrd2092.
- (55) Linington, R. G.; Edwards, D. J.; Shuman, C. F.; McPhail, K. L.; Matainaho, T.; Gerwick, W. H. Symplocamide A, a potent cytotoxin and chymotrypsin inhibitor from the marine Cyanobacterium *Symploca* sp. *J. Nat. Prod.* **2008**, *71* (1), 22–27. DOI: 10.1021/np070280x.
- (56) Gunasekera, S. P.; Miller, M. W.; Kwan, J. C.; Luesch, H.; Paul, V. J. Molassamide, a depsipeptide serine protease inhibitor from the marine cyanobacterium *Dichothrix utahensis*. *J. Nat. Prod.* **2010**, *73* (3), 459–462. DOI: 10.1021/np900603f.
- (57) Kwan, J. C.; Eksioglu, E. A.; Liu, C.; Paul, V. J.; Luesch, H. Grassystatins A-C from marine cyanobacteria, potent cathepsin E inhibitors that reduce antigen presentation. *J. Med. Chem.* **2009**, *52* (18), 5732–5747. DOI: 10.1021/jm9009394.
- (58) Murakami, M.; Okita, Y.; Matsuda, H.; Okino, T.; Yamaguchi, K. Aeruginosin 298-A, a thrombin and trypsin inhibitor from the blue-green alga *Microcystis aeruginosa* (NIES-298). *Tetrahedron Lett.* **1994**, *35* (19), 3129–3132. DOI: 10.1016/S0040-4039(00)76848-1.
- (59) Matsuda, H.; Okino, T.; Murakami, M.; Yamaguchi, K. Aeruginosins 102-A and B, New Thrombin Inhibitors from the Cyanobacterium *Microcystis viridis* (NIES-102). *Tetrahedron* **1996**, *52* (46), 14501–14506.
- (60) Boudreau, P. D.; Miller, B. W.; McCall, L.-I.; Almaliti, J.; Reher, R.; Hirata, K.; Le, T.; Siqueira-Neto, J. L.; Hook, V.; Gerwick, W. H. Design of Gallinamide A Analogs as Potent Inhibitors of the Cysteine Proteases Human Cathepsin L and *Trypanosoma cruzi* Cruzain. *J. Med. Chem.* **2019**, *62* (20), 9026–9044. DOI: 10.1021/acs.jmedchem.9b00294.
- (61) Stoye, A.; Juillard, A.; Tang, A. H.; Legac, J.; Gut, J.; White, K. L.; Charman, S. A.; Rosenthal, P. J.; Grau, G. E. R.; Hunt, N. H.; Payne, R. J. Falcipain Inhibitors Based on the Natural Product Gallinamide A are Potent in Vitro and in Vivo Antimalarials. *J. Med. Chem.* **2019**, *62* (11), 5562–5578. DOI: 10.1021/acs.jmedchem.9b00504.
- (62) Shin, H. J.; Matsuda, H.; Murakami, M.; Yamaguchi, K. Circinamide, a novel papain inhibitor from the cyanobacterium *Anabaena circinalis* (NIES-41). *Tetrahedron* **1997**, *53* (16), 5747–5754. DOI: 10.1016/S0040-4020(97)00285-8.
- (63) Bonjouklian, R.; Smitka, T. A.; Hunt, A. H.; Occolowitz, J. L.; Perun Jr, T. J.; Doolin, L.; Stevenson, S.; Knauss, L.; Wijayarathne, R.; Szewczyk, S.; Patterson, G. M. L. A90720A, a Serine Protease Inhibitor Isolated from a Terrestrial Blue-Green Alga *Microchaete loktakensis*. *Tetrahedron* **1996**, *52* (2), 395–404.

- (64) Jakobi, C.; Oberer, L.; Quiquerez, C.; König, W. A.; Weckesser, J. Cyanopeptolin S, a sulfate-containing depsipeptide from a water bloom of *Microcystis* sp. *FEMS Microbiol. Lett.* **1995**, *129* (2-3), 129–133. DOI: 10.1111/j.1574-6968.1995.tb07569.x.
- (65) Weckesser, J.; Martin, C.; Jakobi, C. Cyanopeptolins, depsipeptides from cyanobacteria. *Syst. Appl. Microbiol.* **1996**, *19* (2), 133–138. DOI: 10.1016/S0723-2020(96)80038-5.
- (66) Hanada, K.; Tamai, M.; Yamagishi, M.; Ohmura, S.; Sawada, J.; Tanaka, I. Isolation and Characterization of E-64, a New Thiol Protease Inhibitor. *Agr Biol Chem* **1978**, *42* (3), 523–528. DOI: 10.1080/00021369.1978.10863014.
- (67) Taori, K.; Liu, Y.; Paul, V. J.; Luesch, H. Combinatorial strategies by marine cyanobacteria: symplostatin 4, an antimitotic natural dolastatin 10/15 hybrid that synergizes with the coproduced HDAC inhibitor largazole. *ChemBioChem* **2009**, *10* (10), 1634–1639. DOI: 10.1002/cbic.200900192.
- (68) Lankelma, J. M.; Voorend, D. M.; Barwari, T.; Koetsveld, J.; van der Spek, A. H.; Porto, A. P. N. A. de; van Rooijen, G.; van Noorden, C. J. F. Cathepsin L, target in cancer treatment? *Life Sciences* **2010**, *86* (7-8), 225–233. DOI: 10.1016/j.lfs.2009.11.016.
- (69) Robinson, M. W.; Dalton, J. P. *Cysteine Proteases of Pathogenic Organisms*, Vol. 712; Springer US, 2011. DOI: 10.1007/978-1-4419-8414-2.
- (70) Holmes, P. On the road to elimination of Rhodesiense human African trypanosomiasis: first WHO meeting of stakeholders. *PLoS Negl. Trop. Dis.* **2015**, *9* (4), e3244. DOI: 10.1371/journal.pntd.0003571.
- (71) Picozzi, K.; Fevre, E. M.; Odiit, M.; Carrington, M.; Eisler, M. C.; Maudlin, I.; Welburn, S. C. Sleeping sickness in Uganda: a thin line between two fatal diseases. *BMJ (Clinical research ed.)* **2005**, *331* (7527), 1238–1241. DOI: 10.1136/bmj.331.7527.1238.
- (72) Simarro, P. P.; Cecchi, G.; Franco, J. R.; Paone, M.; Diarra, A.; Ruiz-Postigo, J. A.; Fèvre, E. M.; Mattioli, R. C.; Jannin, J. G. Estimating and Mapping the Population at Risk of Sleeping Sickness. *PLoS Negl. Trop. Dis.* **2012**, *6* (10), e1859. DOI: 10.1371/journal.pntd.0001859.
- (73) Lindner, A. K.; Lejon, V.; Chappuis, F.; Seixas, J.; Kazumba, L.; Barrett, M. P.; Mwamba, E.; Erphas, O.; Akl, E. A.; Villanueva, G.; Bergman, H.; Simarro, P.; Kadima Ebeja, A.; Priotto, G.; Franco, J. R. New WHO guidelines for treatment of gambiense human African trypanosomiasis including fexinidazole: substantial changes for clinical practice. *Lancet Infect. Dis.* **2020**, *20* (2), e38-e46. DOI: 10.1016/S1473-3099(19)30612-7.
- (74) Simarro, P. P.; Franco, J. R.; Cecchi, G.; Paone, M.; Diarra, A.; Ruiz Postigo, J. A.; Jannin, J. G. Human African Trypanosomiasis in Non-Endemic Countries (2000–2010). *J. Travel Med.* **2011**, *19* (1), 44–53. DOI: 10.1111/j.1708-8305.2011.00576.x.
- (75) Kennedy, P. G. E. Update on Human African Trypanosomiasis (Sleeping Sickness). *J. Neurol.* **2019**, *266* (9), 2334–2337.

- (76) WHO Expert Committee on the Control; Surveillance of African Trypanosomiasis; World Health Organization. *Control and Surveillance of African Trypanosomiasis: Report of a WHO Expert Committee*, 881-884; World Health Organization, 1998.
- (77) Kennedy, P. G. E. Clinical features, diagnosis, and treatment of human African trypanosomiasis (sleeping sickness). *The Lancet Neurology* **2013**, *12* (2), 186–194. DOI: 10.1016/S1474-4422(12)70296-X.
- (78) Bisser, S.; Lumbala, C.; Nguertoum, E.; Kande, V.; Flevaud, L.; Vatunga, G.; Boelaert, M.; Büscher, P.; Josenando, T.; Bessell, P. R.; Biéler, S.; Ndung'u, J. M. Sensitivity and specificity of a prototype rapid diagnostic test for the detection of *Trypanosoma brucei gambiense* infection: a multi-centric prospective study. *PLoS Negl. Trop. Dis.* **2016**, *10* (4), e0004608. DOI: 10.1371/journal.pntd.0004608.
- (79) Blum, J.; Schmid, C.; Burri, C. Clinical aspects of 2541 patients with second stage human African trypanosomiasis. *Acta Trop.* **2006**, *97* (1), 55–64. DOI: 10.1016/j.actatropica.2005.08.001.
- (80) Division of Parasitic Disease (DPDx), of the Centers for Disease Control and Prevention. *Life Cycle of Trypanosoma brucei gambiense and Trypanosoma brucei rhodesiense*. <https://www.cdc.gov/parasites/sleepingsickness/biology.html> (accessed 2020-07-29).
- (81) Tiberti, N.; Matovu, E.; Hainard, A.; Enyaru, J. C.; Lejon, V.; Robin, X.; Turck, N.; Ngoyi, D. M.; Krishna, S.; Bisser, S. New biomarkers for stage determination in *Trypanosoma brucei rhodesiense* sleeping sickness patients. *Clin. Transl. Med.* **2013**, *2* (1), 1.
- (82) Brun, R.; Don, R.; Jacobs, R. T.; Wang, M. Z.; Barrett, M. P. Development of novel drugs for human African trypanosomiasis. *Future Microbiol.* **2011**, *6* (6), 677–691. DOI: 10.2217/fmb.11.44.
- (83) Burri, C. Chemotherapy against human African trypanosomiasis: is there a road to success? *Parasitology* **2010**, *137* (14), 1987–1994. DOI: 10.1017/S0031182010001137.
- (84) Chatelain, E.; Ioset, J.-R. Drug discovery and development for neglected diseases: the DNDi model. *Drug Des. Devel. Ther.* **2011**, *5*, 175–181. DOI: 10.2147/DDDT.S16381.
- (85) Nagle, A. S.; Khare, S.; Kumar, A. B.; Supek, F.; Buchynskyy, A.; Mathison, C. J. N.; Chennamaneni, N. K.; Pendem, N.; Buckner, F. S.; Gelb, M. H.; Molteni, V. Recent developments in drug discovery for leishmaniasis and human African trypanosomiasis. *Chem. Rev.* **2014**, *114* (22), 11305–11347. DOI: 10.1021/cr500365f.
- (86) Koning, H. P. de; Gould, M. K.; Sterk, G. J.; Tenor, H.; Kunz, S.; Luginbuehl, E.; Seebeck, T. Pharmacological validation of *Trypanosoma brucei* phosphodiesterases as novel drug targets. *J. Infect. Dis.* **2012**, *206* (2), 229–237. DOI: 10.1093/infdis/jir857.

- (87) McKerrow, J. Cysteine protease inhibitors as chemotherapy for parasitic infections. *Bioorg. Med. Chem.* **1999**, 7 (4), 639–644. DOI: 10.1016/S0968-0896(99)00008-5.
- (88) Lonsdale-Eccles, J. D.; Grab, D. J. Trypanosome hydrolases and the blood–brain barrier. *Trends Parasitol.* **2002**, 18 (1), 17–19. DOI: 10.1016/S1471-4922(01)02120-1.
- (89) Nikolskaia, O. V.; A Lima, A. P. C. de; Kim, Y. V.; Lonsdale-Eccles, J. D.; Fukuma, T.; Scharfstein, J.; Grab, D. J. Blood-brain barrier traversal by African trypanosomes requires calcium signaling induced by parasite cysteine protease. *J. Clin. Invest.* **2006**, 116 (10), 2739–2747. DOI: 10.1172/JCI27798.
- (90) Overath, P.; Chaudhri, M.; Steverding, D.; Ziegelbauer, K. Invariant surface proteins in bloodstream forms of *Trypanosoma brucei*. *Parasitol. Today* **1994**, 10 (2), 53–58. DOI: 10.1016/0169-4758(94)90393-X.
- (91) Santos, C. C.; Coombs, G. H.; Lima, A. P. C. A.; Mottram, J. C. Role of the *Trypanosoma brucei* natural cysteine peptidase inhibitor ICP in differentiation and virulence. *Mol. Microbiol.* **2007**, 66 (4), 991–1002. DOI: 10.1111/j.1365-2958.2007.05970.x.
- (92) Kerr, I. D.; Wu, P.; Marion-Tsukamaki, R.; Mackey, Z. B.; Brinen, L. S. Crystal Structures of TbCatB and rhodesain, potential chemotherapeutic targets and major cysteine proteases of *Trypanosoma brucei*. *PLoS Negl. Trop. Dis.* **2010**, 4 (6), e701. DOI: 10.1371/journal.pntd.0000701.
- (93) Rocha, D. A.; Silva, E. B.; Fortes, I. S.; Lopes, M. S.; Ferreira, R. S.; Andrade, S. F. Synthesis and structure-activity relationship studies of cruzain and rhodesain inhibitors. *Eur. J. Med. Chem.* **2018**, 157, 1426–1459. DOI: 10.1016/j.ejmech.2018.08.079.
- (94) Spangenberg, T.; Burrows, J. N.; Kowalczyk, P.; McDonald, S.; Wells, T. N. C.; Willis, P. The open access malaria box: a drug discovery catalyst for neglected diseases. *PLoS ONE* **2013**, 8 (6), e62906. DOI: 10.1371/journal.pone.0062906.
- (95) Pereira, G. A. N.; da Silva, E. B.; Braga, S. F. P.; Leite, P. G.; Martins, L. C.; Vieira, R. P.; Soh, W. T.; Villela, F. S.; Costa, F. M. R.; Ray, D.; Andrade, S. F. de; Brandstetter, H.; Oliveira, R. B.; Caffrey, C. R.; Machado, F. S.; Ferreira, R. S. Discovery and characterization of trypanocidal cysteine protease inhibitors from the 'malaria box'. *Eur. J. Med. Chem.* **2019**, 179, 765–778. DOI: 10.1016/j.ejmech.2019.06.062.
- (96) Pereira, G. an; Santos, L. H.; Wang, S. C.; Martins, L. C.; Villela, F. S.; Liao, W.; Dessoy, M. A.; Dias, L. C.; Andricopulo, A. D.; Costa, M. af; Nagem, R. A.; Caffrey, C. R.; Liedl, K. R.; Caffarena, E. R.; Ferreira, R. S. Benzimidazole inhibitors of the major cysteine protease of *Trypanosoma brucei*. *Future Med. Chem.* **2019**, 11 (13), 1537–1551. DOI: 10.4155/fmc-2018-0523.
- (97) Greenbaum, D. C.; Mackey, Z.; Hansell, E.; Doyle, P.; Gut, J.; Caffrey, C. R.; Lehrman, J.; Rosenthal, P. J.; Mckerrow, J. H.; Chibale, K. Synthesis and structure-activity relationships of

parasiticidal thiosemicarbazone cysteine protease inhibitors against *Plasmodium falciparum*, *Trypanosoma brucei*, and *Trypanosoma cruzi*. *J. Med. Chem.* **2004**, *47* (12), 3212–3219. DOI: 10.1021/jm030549j.

(98) Klayman, D. L.; Bartosevich, J. F.; Griffin, T. S.; Mason, C. J.; Scovill, J. P. 2-Acetylpyridine thiosemicarbazones. 1. A new class of potential antimalarial agents. *J. Med. Chem.* **1979**, *22* (7), 855–862.

(99) Wilson, H. R.; Revankar, G. R.; Tolman, R. L. In vitro and in vivo activity of certain thiosemicarbazones against *Trypanosoma cruzi*. *J. Med. Chem.* **1974**, *17* (7), 760–761. DOI: 10.1021/jm00253a025.

(100) Siklos, M.; BenAissa, M.; Thatcher, G. R. J. Cysteine proteases as therapeutic targets: does selectivity matter? A systematic review of calpain and cathepsin inhibitors. *Acta Pharm. Sin. B* **2015**, *5* (6), 506–519. DOI: 10.1016/j.apsb.2015.08.001.

(101) Giroud, M.; Dietzel, U.; Anselm, L.; Banner, D.; Kuglstatler, A.; Benz, J.; Blanc, J.-B.; Gaufreteau, D.; Liu, H.; Lin, X.; Stich, A.; Kuhn, B.; Schuler, F.; Kaiser, M.; Brun, R.; Schirmeister, T.; Kisker, C.; Diederich, F.; Haap, W. Repurposing a library of Human Cathepsin L ligands: identification of macrocyclic lactams as potent rhodesain and *Trypanosoma brucei* inhibitors. *J. Med. Chem.* **2018**, *61* (8), 3350–3369. DOI: 10.1021/acs.jmedchem.7b01869.

(102) Berry, J. P.; Gantar, M.; Perez, M. H.; Berry, G.; Noriega, F. G. Cyanobacterial toxins as allelochemicals with potential applications as algaecides, herbicides and insecticides. *Mar. Drugs* **2008**, *6*, 117–146. DOI: 10.3390/md20080007.

(103) Morel, F. M. M.; Rueter, J. G.; Anderson, D. M.; Guillard, R. R. L. Aquil: A chemically defined phytoplankton culture medium for trace metal studies. *J. Phycol.* **1979**, *15* (2), 135–141. DOI: 10.1111/j.1529-8817.1979.tb02976.x.

(104) Andersen, R. A. *Algal Culturing Techniques*; Elsevier Academic Press, 2005.

(105) Ludewig, S.; Kossner, M.; Schiller, M.; Baumann, K.; Schirmeister, T. Enzyme kinetics and hit validation in fluorimetric protease assays. *Curr. Top. Med. Chem.* **2010**, *10* (3), 368–382. DOI: 10.2174/156802610790725498.

(106) Adnani, N.; Michel, C. R.; Bugni, T. S. Universal quantification of structurally diverse natural products using an evaporative light scattering detector. *J. Nat. Prod.* **2012**, *75* (4), 802–806. DOI: 10.1021/np300034c.

(107) Oliveira Alvarenga, D.; Rigonato, J.; Henrique Zanini Branco, L.; Soares Melo, I.; Fatima Fiore, M. *Phyllonema aviceniicola* gen. nov., sp. nov. and *Foliisarcina bertioagensis* gen. nov., sp. nov., epiphyllic cyanobacteria associated with *Avicennia schaueriana* leaves. *Int. J. Syst. Evol. Microbiol.* **2016**, *66* (2), 689–700. DOI: 10.1099/ijsem.0.000774.

- (108) Shalygin, S.; Kavulic, K. J.; Pietrasiak, N.; Bohunická, M.; Vaccarino, M. A.; Chesarino, N. M.; Johansen, J. R. Neotypification of *Pleurocapsa fuliginosa* and epitypification of *P. minor* (Pleurocapsales): resolving a polyphyletic cyanobacterial genus. *Phytotaxa* **2019**, *392* (4), 245.
- (109) Kwan, J. C.; Meickle, T.; Ladwa, D.; Teplitski, M.; Paul, V.; Luesch, H. Lyngbyoic acid, a "tagged" fatty acid from a marine cyanobacterium, disrupts quorum sensing in *Pseudomonas aeruginosa*. *Mol. BioSyst.* **2011**, *7* (4), 1205–1216. DOI: 10.1039/c0mb00180e.
- (110) Dobretsov, S.; Teplitski, M.; Alagely, A.; Gunasekera, S. P.; Paul, V. J. Malyngolide from the cyanobacterium *Lyngbya majuscula* interferes with quorum sensing circuitry. *Environ. Microbiol. Rep.* **2010**, *2* (6), 739–744. DOI: 10.1111/j.1758-2229.2010.00169.x.
- (111) Clark, B. R.; Engene, N.; Teasdale, M. E.; Rowley, D. C.; Matainaho, T.; Valeriote, F. A.; Gerwick, W. H. Natural products chemistry and taxonomy of the marine cyanobacterium *Blennothrix cantharidosmum*. *J. Nat. Prod.* **2008**, *71* (9), 1530–1537. DOI: 10.1021/np800088a.
- (112) Komárek, J. Delimitation of the family Oscillatoriaceae (Cyanobacteria) according to the modern polyphasic approach (introductory review). *Braz. J. Bot* **2018**, *41* (2), 449–456. DOI: 10.1007/s40415-017-0415-y.
- (113) Komárek, J.; Anagnostidis, K.; Pascher, A.; Büdel, B. *Oscillatoriales*, Unaltered reprint; Süßwasserflora von Mitteleuropa Cyanoprokaryota, / Jiří Komárek; Konstantinos Anagnostidis ; Teil 2; Spektrum Akad. Verl., 2007.
- (114) Komárek, J. Coccoid and colonial cyanobacteria. In *Freshwater Algae of North America*; Elsevier, 2003; pp 59–116. DOI: 10.1016/B978-012741550-5/50004-0.
- (115) Komárek, J.; Anagnostidis, K.; Pascher, A.; Ettl, H.; Büdel, B. *Chroococcales*; Süßwasserflora von Mitteleuropa Cyanoprokaryota, / Jiří Komárek; Konstantinos Anagnostidis ; Teil 1; Spektrum Akad. Verl., 2000.
- (116) Drews, G.; Prauser, H.; Uhlmann, D. Massenvorkommen von *Synechococcus plancticus* nov. spec., einer solitären, planktischen Cyanophyceae, in einem Abwasserteich. *Archiv für Mikrobiologie* **1961**, *39* (2), 101–115.
- (117) Komárek, J. Intergeneric characters in unicellular cyanobacteria, living in solitary cells. *Algo Stud* **1999**, 195–205.
- (118) Copeland, J. J. Yellowstone thermal myxophyceae. *Ann N Y Acad Sci* **1936**, *36* (1), 4–223.
- (119) Reshef, V.; Carmeli, S. Protease inhibitors from a water bloom of the cyanobacterium *Microcystis aeruginosa*. *Tetrahedron* **2001**, *57* (14), 2885–2894. DOI: 10.1016/S0040-4020(01)00141-7.

- (120) Thorskov Bladt, T.; Kalifa-Aviv, S.; Ostefeld Larsen, T.; Carmeli, S. Micropeptins from *Microcystis* sp. collected in Kabul Reservoir, Israel. *Tetrahedron* **2014**, *70* (4), 936–943. DOI: 10.1016/j.tet.2013.12.009.
- (121) Luesch, H.; Yoshida, W. Y.; Moore, R. E.; Paul, V. J. Apramides A-G, novel lipopeptides from the marine cyanobacterium *Lyngbya majuscula*. *J. Nat. Prod.* **2000**, *63* (8), 1106–1112. DOI: 10.1021/np000078t.
- (122) Komárek, J.; Pascher, A.; Büdel, B. *Heterocytous Genera; Süßwasserflora von Mitteleuropa Cyanoprokaryota*, / Jiří Komárek ; Teil 3; Springer Spektrum, 2013.
- (123) Hindák, F. On *Chlorogloeopsis fritschii* (Cyanophyta/Cyanobacteria) from thermal springs in Slovakia and from a saline lake in Tunisia. *Algo Stud* **2008**, *126*, 47–64. DOI: 10.1127/1864-1318/2008/0126-0047.
- (124) Anagnostidis, K.; Komárek, J. Modern approach to the classification system of Cyanophytes. 5 - Stigonematales. *Algo Stud* **1990**, *59*, 1–73.
- (125) Komárek, J. A polyphasic approach for the taxonomy of cyanobacteria: principles and applications. *Eur. J. Phycol.* **2016**, *51* (3), 346–353. DOI: 10.1080/09670262.2016.1163738.
- (126) Namikoshi, M.; Yuan, M.; Sivonen, K.; Carmichael, W. W.; Rinehart, K. L.; Rouhiainen, L.; Sun, F.; Brittain, S.; Otsuki, A. Seven new microcystins possessing two L-glutamic acid units, isolated from *Anabaena* sp. strain 186. *Chem. Res. Toxicol.* **1998**, *11*, 143–149.
- (127) Craig, M.; McCready, T. L.; Luu, H. A.; Smillie, M. A.; Dubord, P.; Holmes, C. F. B. Identification and characterization of hydrophobic microcystins in canadian freshwater cyanobacteria. *Toxicon* **1993**, *31* (12), 1541–1549.
- (128) Mehner, C.; Müller, D.; Kehraus, S.; Hautmann, S.; Gütschow, M.; König, G. M. New peptolides from the cyanobacterium *Nostoc insulare* as selective and potent inhibitors of human leukocyte elastase. *ChemBioChem* **2008**, *9* (16), 2692–2703. DOI: 10.1002/cbic.200800415.
- (129) Han, B.; Goeger, D.; Maier, C. S.; Gerwick, W. H. The wewakpeptins, cyclic depsipeptides from a Papua New Guinea collection of the marine cyanobacterium *Lyngbya semiplena*. *J. Am. Chem. Soc.* **2005**, *70* (8), 3133–3139. DOI: 10.1021/jo0478858.
- (130) Lundgren, P.; Bauer, K.; Lugomela, C.; Söderbäck, E.; Bergman, B. Reevaluation of the nitrogen fixation behaviour in the marine non-heterocystous cyanobacterium *Lyngbya Majuscula* 1. *J. Phycol.* **2003**, *39* (2), 310–314.
- (131) Rana, L.; Chhikara, S.; Dhankhar, R. Physiological studies of native cyanobacterial species *Lyngbya contorta* and *Phormidium foveolarum* in sewage waste water. *J. Environ. Biol.* **2014**, *35* (3), 595.
- (132) Curren, E.; Leong, S. C. Y. *Lyngbya regalis* sp. nov. (Oscillatoriales, Cyanophyceae), a new tropical marine cyanobacterium. *Phytotaxa* **2018**, *367* (2), 120–132.

- (133) Esquenazi, E.; Coates, C.; Simmons, L.; Gonzalez, D.; Gerwick, W. H.; Dorrestein, P. C. Visualizing the spatial distribution of secondary metabolites produced by marine cyanobacteria and sponges via MALDI-TOF imaging. *Mol. Biosyst.* **2008**, *4* (6), 562–570. DOI: 10.1039/b720018h.
- (134) Thacker, R. W.; Paul, V. J. Morphological, chemical, and genetic diversity of tropical marine cyanobacteria *Lyngbya* spp. and *Symploca* spp. (Oscillatoriales). *Appl. Environ. Microbiol.* **2004**, *70* (6), 3305–3312. DOI: 10.1128/AEM.70.6.3305-3312.2004.
- (135) Engene, N.; Choi, H.; Esquenazi, E.; Rottacker, E. C.; Ellisman, M. H.; Dorrestein, P. C.; Gerwick, W. H. Underestimated biodiversity as a major explanation for the perceived rich secondary metabolite capacity of the cyanobacterial genus *Lyngbya*. *Environ. Microbiol.* **2011**, *13* (6), 1601–1610. DOI: 10.1111/j.1462-2920.2011.02472.x.
- (136) Ishida, K.; Matsuda, H.; Murakami, M. Four new microginins, linear peptides from the cyanobacterium *Microcystis aeruginosa*. *Tetrahedron* **1998**, *54* (44), 13475–13484. DOI: 10.1016/S0040-4020(98)00826-6.
- (137) Sano, T.; Usui, T.; Ueda, K.; Osada, H.; Kaya, K. Isolation of new protein phosphatase inhibitors from two cyanobacteria species, *Planktothrix* spp. *J. Nat. Prod.* **2001**, *64* (8), 1052–1055.
- (138) Schmidle, W. *Schizophyceae, Conjugatae, Chlorophyceae*; éditeur non identifié, 1901.
- (139) Schmidle, W. Algologische Notizen IV. Einige neue von Prof. Dr. Hansgirg in Vorderindien gesammelte Süswasseralegen. *Allg. Bot. Ztschr* **1900**, *6*, 17–19.
- (140) Forti, A. Sylloge Myxophycearum omnium hucusque cognitarum. *De Toni, Sylloge Algarum* **1907**, *5*.
- (141) Kiyonaga Fujii; Kaarina Sivonen; Emiko Naganawa; Ken-ichi Harada. Non-Toxic Peptides from Toxic Cyanobacteria, *Oscillatoria agardhii*. *Tetrahedron* **2000**, *56* (5), 725–733. DOI: 10.1016/S0040-4020(99)01017-0.
- (142) Ronny Banker; Shmuel Carmeli. Inhibitors of serine proteases from a waterbloom of the cyanobacterium *Microcystis* sp. *Tetrahedron* **1999**, *55* (35), 10835–10844. DOI: 10.1016/S0040-4020(99)00597-9.
- (143) Ishida, K.; Kato, T.; Murakami, M.; Watanabe, M.; Watanabe, M. F. Microginins, Zinc Metalloproteases Inhibitors from the Cyanobacterium *Microcystis aeruginosa*. *Tetrahedron* **2000**, *56* (44), 8643–8656. DOI: 10.1016/S0040-4020(00)00770-5.
- (144) Aeri Park; Richard E. Moore; Gregory M.L. Patterson. Fischerindole L, a new isonitrile from the terrestrial blue-green alga *Fischerella muscicola*. *Tetrahedron Lett.* **1992**, *33* (23), 3257–3260. DOI: 10.1016/S0040-4039(00)92061-6.
- (145) Moore, R. E.; Cheuk, C.; Patterson, G. M. L. Hapalindoles: New Alkaloids from the Blue-Green Alga *Hapalosiphon fontinalis*. *J Am Chem Soc* **1984**, *106*, 6456–6457.

- (146) Moore, R. E.; Cheuk, C.; Yang, X.-q. G.; Patterson, G. M. L.; Bonjouklian, R.; Smitka, T. A.; Mynderse, J. S.; Foster, R. S.; Jones, N. D.; Swartzendruber, J. K.; Deeter, J. B. Hapalindoles, Antibacterial and Antimycotic Alkaloids from the Cyanophyte *Hapalosiphon fontinalis*. *J. Am. Chem. Soc.* **1987**, *52*, 1036–1043.
- (147) Komárek, J.; Kling, H.; Komárková, J. Filamentous Cyanobacteria. In *Freshwater Algae of North America*; Elsevier, 2003; pp 117–196. DOI: 10.1016/B978-012741550-5/50005-2.
- (148) Venkataraman, G. S.; Neelakantan, S. Effect of the cellular constituents of the nitrogen-fixing blue-green alga, *Cylindrospermum muscicola*, on the root growth of rice plants. *J. Gen. Appl. Microbiol.* **1967**, *13* (1), 53–61.
- (149) A. Vaishampayan; R. P. Sinha; D.-P. Häder; T. Dey; A. K. Gupta; U. Bhan; A. L. Rao. Cyanobacterial biofertilizers in rice agriculture. *Bot. Rev.* **2001**, *67* (4), 453–516.
- (150) Kossack, R.; Breinlinger, S.; Nguyen, T.; Moschny, J.; Straetener, J.; Berscheid, A.; Brötz-Oesterhelt, H.; Enke, H.; Schirmeister, T.; Niedermeyer, T. H. J. Nostotrebins 6 related cyclopentenediones and δ -lactones with broad activity spectrum isolated from the cultivation medium of the cyanobacterium *Nostoc* sp. CBT1153. *J. Nat. Prod.* **2020**.
- (151) Copeland, R. A. *Evaluation of enzyme inhibitors in drug discovery: A guide for medicinal chemists and pharmacologists*, 2nd ed.; Wiley, 2013.
- (152) Kenakin, T. P. *Pharmacology in drug discovery and development: Understanding drug response*, Second edition; Academic Press, 2017.
- (153) I.-K. Wang; S.-Y. Lin-Shiau; J.-K. Lin. Induction of apoptosis by apigenin and related flavonoids through cytochrome C release and activation of caspase-9 and caspase-3 in leukaemia HL-60 cells. *Eur. J. Cancer* **1999**, *35* (10), 1517–1525. DOI: 10.1016/S0959-8049(99)00168-9.
- (154) Shimoi, K.; Masuda, S.; Furugori, M.; Esaki, S.; Kinae, N. Radioprotective effect of antioxidative flavonoids in Y-Ray irradiated mice. *Carcinogenesis* **1994**, *15* (11), 2669–2672.
- (155) Son, S.; Lewis, B. A. Free radical scavenging and antioxidative activity of caffeic acid amide and ester analogues: structure-activity relationship. *J. Agric. Food Chem.* **2002**, *50* (3), 468–472. DOI: 10.1021/jf010830b.
- (156) Li, K.; Li, X.-M.; Ji, N.-Y.; Wang, B.-G. Bromophenols from the marine red alga *Polysiphonia urceolata* with DPPH radical scavenging activity. *J. Nat. Prod.* **2008**, *71* (1), 28–30. DOI: 10.1021/np070281p.
- (157) Masella, R.; Cantafora, A.; Modesti, D.; Cardilli, A.; Gennaro, L.; Bocca, A.; Coni, E. Antioxidant activity of 3,4-DHPEA-EA and protocatechuic acid: a comparative assessment with other olive oil biophenols. *Redox Report* **1999**, *4* (3), 113–121. DOI: 10.1179/135100099101534792.

- (158) Sroka, Z.; Cisowski, W. Hydrogen peroxide scavenging, antioxidant and anti-radical activity of some phenolic acids. *Food Chem Toxicol* **2003**, *41* (6), 753–758.
- (159) Sevcikova, Z.; Pour, M.; Novak, D.; Ulrichova, J.; Vacek, J. Chemical properties and biological activities of cyclopentenediones: a review. *Mini Rev. Med. Chem.* **2014**, *14* (4), 322–331. DOI: 10.2174/1389557514666140306130207.
- (160) Babu, K. S.; Li, X.-C.; Jacob, M. R.; Zhang, Q.; Khan, S. I.; Ferreira, D.; Clark, A. M. Synthesis, antifungal activity, and structure-activity relationships of coruscanone A analogues. *J. Med. Chem.* **2006**, *49* (26), 7877–7886. DOI: 10.1021/jm061123i.
- (161) Riveira, M. J.; Tekwani, B. L.; Labadie, G. R.; Mischne, M. P. Synthesis and biological activity profile of novel 2-cinnamylidene-1, 3-diones related to coruscanone A: promising new antileishmanial agents. *MedChemComm* **2012**, *3* (10), 1294–1298.
- (162) Chen, X.-L.; Liu, F.; Xiao, X.-R.; Yang, X.-W.; Li, F. Anti-inflammatory abietanes diterpenoids isolated from *Tripterygium hypoglaucum*. *Phytochemistry* **2018**, *156*, 167–175.
- (163) Baell, J. B.; Holloway, G. A. New substructure filters for removal of pan assay interference compounds (PAINS) from screening libraries and for their exclusion in bioassays. *J. Med. Chem.* **2010**, *53* (7), 2719–2740. DOI: 10.1021/jm901137j.
- (164) Baell, J.; Walters, M. A. Chemistry: chemical con artists foil drug discovery. *Nature* **2014**, *513* (7519), 481–483. DOI: 10.1038/513481a.
- (165) Volk, R.-B.; Mundt, S. Cytotoxic and non-cytotoxic exometabolites of the cyanobacterium *Nostoc insulare*. *J. Appl. Phycol.* **2007**, *19* (1), 55–62. DOI: 10.1007/s10811-006-9110-2.
- (166) Jaki, B.; Orjala, J.; Sticher, O. A novel extracellular diterpenoid with antibacterial activity from the cyanobacterium *Nostoc commune*. *J. Nat. Prod.* **1999**, *62*, 502–503. DOI: 10.1021/np980444x.
- (167) Caicedo, N. H.; Kumirska, J.; Neumann, J.; Stolte, S.; Thöming, J. Detection of bioactive exometabolites produced by the filamentous marine cyanobacterium *Geitlerinema* sp. *Mar. Biotechnol.* **2012**, *14* (4), 436–445. DOI: 10.1007/s10126-011-9424-1.
- (168) Hirata, K.; Takashina, J.; Nakagami, H.; Ueyama, S.; Murakami, K.; Kanamori, T.; Miyamoto, K. Growth inhibition of various organisms by a violet pigment, nostocine A, produced by *Nostoc spongiaeforme*. *Biosci. Biotechnol., Biochem.* **1996**, *60* (11), 1905–1906.

6. Appendix: Supplementary Data

6.1. List of Abbreviations

AMC	7-Amino-4-methylcoumarin
ANoBIIn	Accessing Novel Bacterial Producers from Biodiversity-rich Habitats in Indonesia
CFU	Colony forming unit
CNS	Central nervous system
CSF	Cerebrospinal fluid
CPD	Cyclopentenedione
DAD	Diode array detector
DMSO	Dimethylsulfoxid
EDTA	Ethylenediaminetetraacetic acid
ELSD	Evaporative light scattering detector
FA	Formic acid
HAT	Human African Trypanosomiasis
HPLC	High performance liquid chromatography
HPLC-MS	High performance liquid chromatography coupled to a mass spectrometer
HRMS	High resolution mass spectrometry
hCatL	Human cathepsin L
K_i	Inhibition constant
K_m	Michaelis-Menten constant
LC	Liquid chromatography
LED	Light-emitting diode
MeCN	Acetonitrile
MeOH	Methanol
MIC	Minimal inhibitory concentration
NaOH	Sodium hydroxide
NECT	Nifurtimox-eflornithine combination therapy
NGOs	Non-governmental organisations
NMR	Nuclear magnetic resonance spectroscopy
NRPS	Nonribosomal peptide synthetase
OD	Optical density
PAIN	Pan-assay interference compound

PKS	Polyketide synthase
PARs	Protease-activated receptors
PTRE	Post-treatment reactive encephalopathy
QS	Quorum sensing
QSI	Quorum sensing inhibition
QSE	Quorum sensing enhancement
RDTs	Rapid diagnostic tests
RLU	Relative light units
rpm	Revelations per minute
t_R	Relative retention time
TPP	Target product profile
VSG	Variable surface glycoproteins
WBC	White blood cells
WHO	World Health Organisation

6.2. Supporting Data

Content of the Supporting Data

Figure A 1. Mass spectra of compound A to E of An-Al061.1 biomass extract. Pos. mode (left), neg. mode (right).....	133
Figure A 2. Biomass extract <i>Nostoc</i> 3; Preparative isolation; first run. 40 mg in 4 mL MeOH 20%, 0.1% FA, 24 mL/min, 0-25 min: 5-25%, 27-32: 100%, Reprosil Pure Basic C18 10 μ m, 240 und 340 nm.	134
Figure A 3. Biomass extract <i>Nostoc</i> 3; Preparative isolation; second run. 40 mg in 4 mL MeOH 20%, 0.1% FA, 24 mL/min, 0-25 min: 5-25%, 27-32: 100%, Reprosil Pure Basic C18 10 μ m, 220 und 340 nm.	134
Table A 1. Cyanobacterial Strains isolated from samples taken in Germany	120
Table A 2. Cyanobacterial Strains isolated from samples taken in Indonesia	123
Table A 3. Cyanobacteria strains obtained from Dwi Susilaningsih within the Project ANoBIn	129
Table A 4. Bioactivity data of all tested extracts from the established cyanobacteria strain collection.	130
Table A 5. ¹H- and ¹³C-NMR data of compound 5 from biomass extract <i>Nostoc</i> 3	135

Supporting information reprinted with permission from Kossack, R.; Breinlinger, S.; Nguyen, T.; Moschny, J.; Straetener, J.; Berscheid, A.; Brötz-Oesterhelt, H.; Enke, H.; Schirmeister, T.; Niedermeyer, T. H. J. Nostotrebin 6 related cyclopentenediones and δ -lactones with broad activity spectrum isolated from the cultivation medium of the cyanobacterium *Nostoc* sp. CBT1153. J. Nat. Prod. 2020. Copyright (2020) American Chemical Society. doi: 10.1021/acs.jnatprod.9b00885

Status in publication process: Published; 24.01.2020

Table A 1. Cyanobacterial Strains isolated from samples taken in Germany.

Ano Tü	Taxonomy					Sampling						
	Sec.	Order	Family	Subfamily	Genus	Sampling Date	Location	GPS	Substrate		Medium	Method
1	III	Oscillatoria	Pseudanabaenaceae	Pseudanabaenoideae	<i>Geitlerinema</i>	09.07.2015	Palm house, Botanical Garden, Tübingen, Germany	48°32'20.3"N 9°02'10.8"E	pond	biofilm	BG11 + N	Filtrate, Phototaxis
2	III	Oscillatoriales	Pseudanabaenaceae	Pseudanabaenoideae	<i>Geitlerinema</i>	09.07.2015			pond	biofilm	BG11 + N	ER, Phototaxis
3	III	Oscillatoriales	Pseudanabaenaceae	Pseudanabaenoideae	<i>Geitlerinema</i>	09.07.2015			pond	biofilm	BG11 + N	Filtrate
4	III	Oscillatoriales	Pseudanabaenaceae			09.07.2015			pond	biofilm	BG11 + N	Filtrate, Phototaxis
6	III	Oscillatoriales	Pseudanabaenaceae			09.07.2015			pond	biofilm	BG11 + N	Filter, Phototaxis
7	I	Microcystis or Cloeothece				09.07.2015			pond	biofilm	BG11 + N	Filter
8	III	Oscillatoriales				10.07.2015			pond	biofilm	BG11 + N	Filtrate
9	III	Oscillatoriales	Pseudanabaenaceae	Pseudanabaenoideae	<i>Limnothrix or Jaaginema</i>	10.07.2015			pond	biofilm	BG11 + N	Filtrate
10	III	Oscillatoriales	Oscillatoriaceae	Oscillatorioideae	<i>Phormidium</i>	10.07.2015			pond	biofilm	BG11 + N	Filter, Phototaxis
11	III	Oscillatoriales	Pseudanabaenaceae			10.07.2015			pond	biofilm	BG11 + N	ER
12	III	Oscillatoriales				10.07.2015			pond	biofilm	BG11 + N	ER, Phototaxis
13	III	Oscillatoriales	Pseudanabaenaceae	Pseudanabaenoideae		10.07.2015			pond	biofilm	BG11 + N	ER, Phototaxis
14	III	Oscillatoriales				10.07.2015			Ground, Berlin	52°36'39.0"N 13°25'47.4"E	garden	ground
15	III	Oscillatoriales	Pseudanabaenaceae	Pseudanabaenoideae		10.07.2015	garden	ground			BG11 + N	ER
16	I	Microcystis or Cloeothece				10.07.2015	Aquarium, University Tübingen	48°32'10.1"N 9°02'10.9"E	aquarium	biofilm	BG11 + N	ER
17	I	Chroococcales	Aphanothece or Cyanothece			10.07.2015			aquarium	biofilm	BG11 + N	ER
18	III	Oscillatoriales	Phormidiaceae	Phormidioideae	<i>Psuedophormidium</i>	10.07.2015			aquarium	biofilm	BG11 + N	Phototaxis

19	III	Oscillatoriales				10.07.2015			aquarium	biofilm	BG11 + N	ER
20	I	Chroococcales				10.07.2015			aquarium	biofilm	BG11 + N	ER
21	III	Oscillatoriales				07.09.2015	Palm house, Botanical Garden, Tübingen, Germany	48°32'22.5"N 9°02'09.4"E	pond	biofilm	BG11 + N	Filtrate
22	I	Oscillatoriales	Oscillatoriaceae		08.09.2015	pond			biofilm	BG11 + N	Filtrate	
23	III	Oscillatoriales	Pseudanabaenaceae	Leptolyngbyoideae		09.09.2015			pond	biofilm	BG11 + N	ER
24	I	Synechococcales/ Chroococcales				31.08.2015	Gönninger Seen, Tübingen, Germany	48°25'37.8"N 9°10'43.1"E	clean pool	mud	BG11 - N	ER
25	I	Synechococcales/ Chroococcales				31.08.2015			clean pool	mud	BG11 - N	ER
26	III	Oscillatoriales	Pseudanabaenaceae	Pseudanabaenoideae		31.08.2015			clean pool	mud	BG11 + N	ER
27	I	Chroococcales/ Synechococcales	Microcystaceae/ Synechococcaceae		<i>Radiocystis or Cyanocatena</i>	31.08.2015			clean pool	sediment	BG11 + N	ER
28	III	Oscillatoriales	Pseudanabaenaceae			31.08.2015			clean pool	sediment	BG11 + N	ER
29	III	Oscillatoriales	Pseudanabaenaceae	Pseudanabaenoideae	<i>Pseudanabenana or Arthronema</i>	31.08.2015			clean pool	water	BG11 + N	ER
30	III	Oscillatoriales	Pseudanabaenaceae			31.08.2015			clean pool	water	BG11 + N	ER
32	III	Oscillatoriales	Pseudanabaenaceae	Pseudanabaenoideae		09.09.2015	Palm house, Botanical Garden, Tübingen, Germany	48°32'20.3"N 9°02'10.8"E	pond	water	BG11 + N	ER
33	III	Oscillatoriales	Pseudanabaenaceae			31.08.2015	Gönninger Seen, Tübingen, Germany	48°25'34.4"N 9°10'42.8"E	clean pool	mud	BG11 + N	ER
34	III	Oscillatoriales	Pseudanabaenaceae	Leptolyngbyoideae		31.08.2015			clean pool	water	BG11 + N	ER
37	I	Chroococcales	Synechococcaceae	Aphanotheoideae	<i>Cyanobium</i>	09.07.2015			pond	water	BG11 + N	Filter
39	III	Oscillatoriales				09.07.2015			pond	water	BG11 + N	ER
40	III	Oscillatoriales				09.07.2015			pond	water	BG11 + N	ER, Phototaxis
41	I	Chroococcales				31.08.2015	Gönninger Seen,	48°25'34.4"N 9°10'42.8"E	clean pool	aquatic plant	BG11 - N	ER

							Tübingen, Germany						
42	III	Oscillatoriales	Pseudanabaenaceae			07.07.2016	Mountainlake, Swiss		clean pool	biofilm	BG11 + N	ER	
43	I	Chroococcales	Chroococcaceae		<i>Chroococcus</i>	07.07.2016			clean pool	biofilm	BG11 + N	ER	
44	I	Chroococcales/ Synechococcales	Synechococcaceae	Aphanothecoideae	<i>Lemmermanniella</i>	18.06.2016	Spruce forest, Unna, Germany	51°31'03.5"N 7°48'59.9"E	mushroom	biofilm	BG11 + N	ER	
45	III	Oscillatoriales	Pseudanabaenaceae	Leptolyngbyoideae or Heteroleibleinioideae		09.07.2016	Gönninger Seen, Tübingen, Germany	48°25'37.8"N 9°10'43.1"E	clean pool	biofilm	BG11 + N	ER	
46	III	Oscillatoriales	Oscillatoriaceae	Oscillatorioideae	<i>Oscillatoria</i>	09.07.2016			clean pool	biofilm	BG11 - N	ER	
47	IV	Nostocales	Rivulariaceae			21.03.2016	Pond, Tübingen, Germany	48°32'16.8"N 9°02'42.0"E	pond	biofilm	BG11 + N	ER	
48	I	Chroococcales	Dermocarpellaeae	Staniera?		18.06.2016	Spruce forest, Unna, Germany	51°31'03.5"N 7°48'59.9"E	mushroom	biofilm	BG11 + N	ER	
49	III	Oscillatoriales	Pseudanabaenaceae			09.07.2015	Pool Botanical Garden, Tübingen, Germany	48°32'20.3"N 9°02'10.8"E	pond	biofilm	BG11 + N	ER	
50	IV	Nostocales	Microchaetaceae	Tolypothrix		14.03.2017			stone wall	biofilm	BG11 - N	ER	
51	I	Chroococcales	Microcystaceae		<i>Gloeocapsa</i>	15.03.2017	Bärenhöhle, Germany	48°22'15.0"N 9°12'54.9"E	stone wall	biofilm	BG11 - N	ER	
52	I	Chroococcales				16.03.2017			stone wall	biofilm	BG11 - N	ER	
53	I	Chroococcales				18.08.2015	Steinlach, Tübingen, Germany	48°30'35.2"N 9°03'20.1"E	river	water	BG11 + N	ER	
54	III	Oscillatoriales	Pseudanabaenaceae			18.08.2015			river	water	BG11 + N	ER	
55	III	Oscillatoriales	Pseudanabaenaceae			20.08.2015	Bieringen, Germany	48°26'55.5"N 8°51'11.3"E	stone	biofilm	BG11 + N	ER	
56	III	Oscillatoriales	Pseudanabaenaceae			27.09.2015	Ehrenberg, Austria		lake	biofilm	BG11 + N	ER	
57	III	Oscillatoriales	Pseudanabaenaceae			27.09.2015			lake	biofilm	BG11 + N	ER	
58	III	Oscillatoriales				18.08.2015	Talheimer Wasserfall,	48°22'39.6"N 9°05'57.1"E	waterfall	water	BG11 + N	ER	

							Tübingen, Germany,						
59	I	Chroococcales					27.09.2015	Ehrenberg, Austria		lake	biofilm	BG11 + N	ER
60	I	Chroococcales					18.08.2015	Hirschauer Baggersee, Germany	48°29'41.3"N 9°00'19.8"E	river	water	BG11 + N	ER

Table A 2. Cyanobacterial Strains isolated from samples taken in Indonesia.

Strain	Sec.	Order	Family	Subfamily	Genus	Col,	Sampling Date	Substrate		Location		Additional information	
										City	GPS	Meth.	Med.
An-AI001.1	IV	Oscillatoriales				Ronja, Dwi	2016.04.19	Soil	Rice field	Citalahab	6°44'34.9"S 106°30'44.9"E	cotton stick	BG11 + N
An-AI002.1.1	IV	Nostocales	Nostocaceae		<i>Cylindro spermu m</i>	Ronja, Dwi	2016.04.20	Soil	Rice field	Citalahab		cotton stick	BG11 + N
An-AI002.1.2	IV	Nostocales	Rivulariaceae		<i>Rivulari a</i>	Ronja, Dwi	2016.04.20	Soil	Rice field	Citalahab		cotton stick	BG11 + N
An-AI002.2.1	III	Oscillatoriales				Ronja, Dwi	2016.04.20	Soil	Rice field	Citalahab		cotton stick	BG11 + N
An-AI006.1	IV	Nostocales	Nostocaceae		<i>Cylindro spermu m</i>	Ronja, Dwi	2016.04.20	Soil	Backyard	Citalahab	6°44'34.3"S 106°31'82.8"E	cotton stick	BG11 - N, solid
An-AI006.2.4	IV	Nostocales	Nostocaceae		<i>Cylindro spermu m</i>	Ronja, Dwi	2016.04.20	Soil	Backyard	Citalahab		cotton stick	BG11 - N, solid
An-AI006.3.2	IV	Nostocales	Rivulariaceae		<i>Rivulari a</i>	Ronja, Dwi	2016.04.20	Soil	Backyard	Citalahab		cotton stick	BG11 - N, solid
An-AI009.0	III	Oscillatoriales				Ronja, Dwi	2016.04.20	Biofilm	Bark	Citalahab		cotton stick	BG11 + N, solid
An-AI009.1.1	III	Oscillatoriales				Ronja, Dwi	2016.04.20	Bark	Bark	Citalahab		cotton stick	BG11 + N, solid
An-AI010.1	III	Oscillatoriales				Ronja, Dwi	2016.04.20	Water	River	Cikaniki	6°44'32.8"S 106°31'85.0"E	water, 5 µm pl. n.	BG11 + N

An-AI011.1	IV	Nostocales	Nostocaceae		<i>Cylindrospermopsis</i>	Ronja, Dwi	2016.04.20	Water	River	Cikaniki		water, 5 µm pl. n.	BG11 - N
An-AI012.1	I	Chroococcales				Ronja, Dwi	2016.04.21	Biofilm	Biofilm Waterfall A	Cikaniki	6°44'76.6"S 106°32'39.6"E	cotton stick	BG11 + N
An-AI013.1.1	V	Stigonematales				Ronja, Dwi	2016.04.21	Biofilm	Biofilm Waterfall A	Cikaniki		cotton stick	BG11 - N
An-AI013.1.2	I	Oscillatoriales				Ronja, Dwi	2016.04.21	Biofilm	Biofilm Waterfall A	Cikaniki		cotton stick	BG11 - N
An-AI014.1	I	Oscillatoriales				Ronja, Dwi	2016.04.21	Biofilm	Biofilm Waterfall A	Cikaniki		cotton stick	BG11 + N, solid
An-AI015.0	IV	Nostocales				Ronja, Dwi	2016.04.21	Biofilm	Biofilm Waterfall A	Cikaniki		cotton stick	BG11 - N, solid
An-AI015.1	IV	Nostocales				Ronja, Dwi	2016.04.21	Biofilm	Biofilm Waterfall A	Cikaniki		cotton stick	BG11 - N, solid
An-AI016.1.1	I	Chroococcales				Ronja, Dwi	2016.04.21	Biofilm	Biofilm Waterfall B	Cikaniki		cotton stick	BG11 + N
An-AI016.1.2.1	I	Chroococcales				Ronja, Dwi	2016.04.21	Biofilm	Biofilm Waterfall B	Cikaniki		cotton stick	BG11 + N
An-AI016.1.3	III	Oscillatoriales				Ronja, Dwi	2016.04.21	Biofilm	Biofilm Waterfall B	Cikaniki		cotton stick	BG11 + N
An-AI018.1.1	III	Oscillatoriales				Ronja, Dwi	2016.04.21	Biofilm	Biofilm Waterfall B	Cikaniki		cotton stick	BG11 + N, solid
An-AI019.0	V	Stigonematales				Ronja, Dwi	2016.04.21	Biofilm	Biofilm Waterfall B	Cikaniki	cotton stick	BG11 - N, solid	
An-AI020.1.2.1	IV	Nostocales				Ronja, Dwi	2016.04.21	Biofilm	Biofilm Stone	Cikaniki	6°44'83.7"S 106°32'27.9"E	cotton stick	BG11 + N
An-AI021.1	I	Chroococcales				Ronja, Dwi	2016.04.21	Biofilm	Biofilm Stone	Cikaniki		cotton stick	BG11 - N
An-AI023.1.4.1	IV	Nostocales				Ronja, Dwi	2016.04.21	Water	Running water	Cikaniki	6°43'11.9"S 106°33'17.6"E	cotton stick	BG11 + N
An-AI026.1	III	Oscillatoriales				Ronja, Dwi	2016.04.21	Soil	Soil Teagarden	Cikaniki	6°44'64.3"S 106°32'39.7"E	cotton stick	BG11 + N, solid

An-AI029.1.1.1	III	Oscillatoriales				Ronja, Dwi	2016.04.21	Biofilm	Soil Teagarden	Cikaniki	6°44'76.6"S 106°32'39.6"E	cotton stick	BG11 + N
An-AI029.1.1	IV	Nostocales				Ronja, Dwi	2016.04.21	Biofilm	Soil Teagarden	Cikaniki		cotton stick	BG11 - N
An-AI029.2.2	III	Nostocales				Ronja, Dwi	2016.04.21	Biofilm	Soil Teagarden	Cikaniki		cotton stick	BG11 - N
An-AI029.2.4	III	Nostocales				Ronja, Dwi	2016.04.21	Biofilm	Soil Teagarden	Cikaniki		cotton stick	BG11 - N
An-AI029.3.2	III	Nostocales				Ronja, Dwi	2016.04.21	Biofilm	Soil Teagarden	Cikaniki		cotton stick	BG11 - N
An-AI030.1	III	Oscillatoriales				Ronja, Dwi	2016.04.21	Biofilm	Soil Teagarden	Cikaniki		cotton stick	BG11 + N, solid
An-AI030.2	III	Oscillatoriales				Ronja, Dwi	2016.04.21	Biofilm	Soil Teagarden	Cikaniki		cotton stick	BG11 + N, solid
An-AI032	I	Chroococcales				Ronja, Dwi	2016.04.21	Water	Waterfall	Cikaniki	6°44'76.6"S 106°32'39.6"E	cotton stick	BG11 + N, solid
An-AI034.1	V	Nostocales	Chlorogloeopsidaceae	Chlorogloeopsis		Ronja, Dwi	2016.04.21	Water	Waterfall	Cikaniki		water, 25 µm pl. n.	BG11 + N
An-AI035.1	IV	Nostocales	Scytonemaceae	Microchaetaceae		Ronja, Dwi	2016.04.21	Water	Waterfall	Cikaniki		water, 25 µm pl. n.	BG11 - N
An-AI035.2	III	Oscillatoriales	Pseudanabeaenaceae	Pseudanabeaenoidae	<i>Pseudanabaena</i>	Ronja, Dwi	2016.04.21	Water	Waterfall	Cikaniki		water, 25 µm pl. n.	BG11 - N
An-AI036	III	Oscillatoriales	Pseudanabeaenaceae	Pseudanabeaenoidae	<i>Geitlerinema</i>	Ronja, Dwi	2016.04.22	Biofilm	Biofilm on wall	Cikaniki	6°44'32.0"S 106°31'86.7"E	cotton stick	BG11 pH 7
An-AI037	I	Chroococcales				Ronja, Dwi	2016.04.22	Biofilm	Biofilm on wall	Cikaniki		cotton stick	BG11 - N
An-AI039.0	III	Oscillatoriales				Ronja, Dwi	2016.04.22	Biofilm	Biofilm on wall	Cikaniki		cotton stick	BG11 + N, solid
An-AI039.1	III	Oscillatoriales	Coleofasciculaceae		<i>Geitlerinema</i>	Ronja, Dwi	2016.04.22	Biofilm	Biofilm on wall	Cikaniki		cotton stick	BG11 + N, solid
An-AI041.1	III	Oscillatoriales	Pseudanabeaenaceae			Ronja, Dwi	2016.04.22	Biofilm	Biofilm on bark	Cikaniki	6°44'35.4"S 106°31'89.4"E	cotton stick	BG11 pH 7
An-AI047.1.1	I	Chroococcales				Ronja, Dwi	2016.04.22	Biofilm	Biofilm on plastic	Cikaniki	6°44'34.2"S 106°31'82.9"E	cotton stick	BG11 + N, solid
An-AI054.1	III	Oscillatoriales				Ronja, Dwi	2016.04.22	Biofilm	Biofilm on soil	Cikaniki	6°44'30.5"S 106°31'85.2"E	cotton stick	BG11 + N, solid
An-AI055.1	IV	Nostocales				Ronja, Dwi	2016.04.22	Biofilm	Biofilm on soil	Cikaniki		cotton stick	BG11 - N, solid
An-AI059.1.1	IV	Nostocales				Delicia, Dwi	2016.04.25	Biofilm	Stone	Cibinong	6°29'35.2"S 106°50'59.3"E	cotton stick	BG11 + N, solid

An-AI059.1.2	III	Oscillatoriales				Delicia, Dwi	2016.04.25	Biofilm	Stone	Cibinong		cotton stick	BG11 + N, solid
An-AI059.2	IV	Nostocales				Delicia, Dwi	2016.04.25	Biofilm	Stone	Cibinong		water, 5 µm pl. n.	BG11 - N
An-AI059.3.2	I	Chroococcales				Delicia, Dwi	2016.04.25	Biofilm	Stone	Cibinong		cotton stick	BG11 + N, solid
An-AI059.3.3.1.2	IV	Nostocales				Delicia, Dwi	2016.04.25	Biofilm	Stone	Cibinong		cotton stick	BG11 + N, solid
An-AI059.3.3.2	III	Oscillatoriales				Delicia, Dwi	2016.04.25	Biofilm	Stone	Cibinong		cotton stick	BG11 + N, solid
An-AI061.1	V	Nostocales	Hapalosiphonaceae		<i>Mastigo cladus</i>	Delicia, Dwi	2016.04.19	Biofilm	Biofilm on Soil	Cibinong	6°29'59.6"S 106°49'44.2"E	cotton stick	BG11 - N
An-AI061.4	IV	Nostocales	Scytonemataceae			Delicia, Dwi	2016.04.19	Biofilm	Biofilm on Soil	Cibinong		cotton stick	BG11 - N
An-AI063.1	I	Chroococcales				Delicia, Dwi	2016.04.19	Biofilm	Biofilm on Soil	Cibinong		cotton stick	BG11 - N, solid
An-AI063.2	IV	Nostocales				Delicia, Dwi	2016.04.19	Biofilm	Biofilm on Soil	Cibinong		cotton stick	BG11 - N, solid
An-AI063.3	IV	Nostocales				Delicia, Dwi	2016.04.19	Biofilm	Biofilm on Soil	Cibinong		cotton stick	BG11 - N, solid
An-AI063.4	V	Stigonematales				Delicia, Dwi	2016.04.19	Biofilm	Biofilm on Soil	Cibinong		cotton stick	BG11 - N, solid
An-AI063.5	I	Chroococcales				Delicia, Dwi	2016.04.19	Biofilm	Biofilm on Soil	Cibinong		cotton stick	BG11 - N, solid
An-AI063.6	III	Nostocales				Delicia, Dwi	2016.04.19	Biofilm	Biofilm on Soil	Cibinong		cotton stick	BG11 - N, solid
An-AI063.7	V	Nostocales	Hapalosiphonaceae			Delicia, Dwi	2016.04.19	Biofilm	Biofilm on Soil	Cibinong		cotton stick	BG11 - N, solid
An-AI071.1.1	IV	Nostocales				Delicia, Dwi	2016.05.07	Biofilm	Biofilm on root	Cibinong		6°29'35.2"S 106°50'59.3"E	cotton stick
An-AI071.1.1.4.1	IV	Nostocales				Delicia, Dwi	2016.05.07	Biofilm	Biofilm on root	Cibinong	cotton stick		BG11 - N
An-AI071.1.2	IV	Nostocales				Delicia, Dwi	2016.05.07	Biofilm	Biofilm on root	Cibinong	cotton stick		BG11 - N
An-AI071.1.3.3	IV	Nostocales				Delicia, Dwi	2016.05.07	Biofilm	Biofilm on root	Cibinong	cotton stick		BG11 - N
An-AI071.1.4.1	IV	Nostocales				Delicia, Dwi	2016.05.07	Biofilm	Biofilm on root	Cibinong	cotton stick		BG11 - N
An-AI071.1.5.1	IV	Nostocales				Delicia, Dwi	2016.05.07	Biofilm	Biofilm on root	Cibinong	cotton stick		BG11 - N

An-AI071.1.6.1	IV	Nostocales				Delicia, Dwi	2016.05.07	Biofilm	Biofilm on root	Cibinong		cotton stick	BG11 - N
An-AI072	I	Chroococcales				Delicia, Dwi	2016.05.08	Biofilm	Biofilm on root	Cibinong		cotton stick	BG11 + N, solid
An-AI072.2.1	I	Chroococcales				Delicia, Dwi	2016.05.08	Biofilm	Biofilm on root	Cibinong		cotton stick	BG11 + N, solid
LIP116-An-AI074	III					Ronja, Dwi	2016.04.20	Soil	Backyard	Citalahab	6°44'34.3"S 106°31'82.8"E	cotton stick	BG11 + N
LIP116-An-AI078	III					Ronja, Dwi	2016.04.21	Soil	Soil Teagarden	Cikaniki	6°44'64.3"S 106°32'39.7"E	cotton stick	BG11 + N, solid
LIP116-An-AI079	III					Ronja, Dwi	2016.04.22	Biofilm	Biofilm on wall	Cikaniki	6°44'32.0"S 106°31'86.7"E	cotton stick	BG11 + N, solid
LIP116-An-AI081	III					Ronja, Dwi	2016.04.22	Biofilm	Biofilm on soil	Cikaniki	6°44'30.5"S 106°31'85.2"E	cotton stick	BG11 + N, solid
LIP116-An-AI087	III					Ronja, Dwi	2016.04.20	Soil	Backyard	Citalahab		cotton stick	BG11 + N, solid
LIP116-An-AI088	III					Ronja, Dwi	2016.04.20	Biofilm	Biofilm on bark	Citalahab	6°44'34.3"S 106°31'82.8"E	cotton stick	BG11 + N, solid
LIP116-An-AI090	III					Ronja, Dwi	2016.04.20	Biofilm	Biofilm on bark	Citalahab		cotton stick	BG11 + N, solid
LIP116-An-AI092	V	Nostocales	Chlorogloeopsidaceae	Chlorogloeopsis		Delicia, Dwi	2016.04.25	Biofilm	Stone	Cibinong	6°29'35.2"S 106°50'59.3"E	cotton stick	BG11 + N, solid
LIP116-An-AI093	III					Delicia, Dwi	2016.04.19	Biofilm	Biofilm on Soil	Cibinong	6°29'59.6"S 106°49'44.2"E	cotton stick	BG11 + N, solid
LIP116-An-AI094	I					Delicia, Dwi	2016.05.08	Biofilm	Biofilm on root	Cibinong		cotton stick	BG11 + N, solid
LIP116-An-AI095	I					Delicia, Dwi	2016.05.08	Biofilm	Biofilm on root	Cibinong	6°29'35.2"S 106°50'59.3"E	cotton stick	BG11 + N, solid
LIP116-An-AI096	IV					Ronja, Dwi	2016.04.21	Biofilm	Biofilm Waterfall B	Cikaniki		cotton stick	BG11 + N, solid
LIP116-An-AI097	III					Ronja, Dwi	2016.04.21	Biofilm	Biofilm Waterfall B	Cikaniki		cotton stick	BG11 + N, solid
LIP116-An-AI099	V					Ronja, Dwi	2016.04.21	Biofilm	Biofilm Waterfall B	Cikaniki	6°44'76.6"S 106°32'39.6"E	cotton stick	BG11 - N, solid
LIP116-An-AI101	IV	Nostocales	Nostocaceae			Ronja, Dwi	2016.04.21	Biofilm	Biofilm Waterfall B	Cikaniki		cotton stick	BG11 - N, solid

LIP16-An-AI105	IV				Ronja, Dwi	2016.04.21	Biofilm	Biofilm Waterfall A	Cikaniki		cotton stick	BG11 - N, solid
LIP16-An-AI107	IV				Ronja, Dwi	2016.04.21	Biofilm	Biofilm Waterfall A	Cikaniki		cotton stick	BG11 - N, solid
LIP16-An-AI110	III				Delicia, Dwi	2016.04.25	Biofilm	Stone	Cibinong	6°29'35.2"S 106°50'59.3"E	cotton stick	BG11 - N
LIP16-An-AI114	IV				Ronja, Dwi	2016.04.21	Biofilm	Biofilm Waterfall A	Cikaniki	6°44'76.6"S 106°32'39.6"E	cotton stick	BG11 - N, solid
LIP16-An-AI115	III				Ronja, Dwi	2016.04.21	Biofilm	Soil Teagarden	Cikaniki	6°44'64.3"S 106°32'39.7"E	cotton stick	BG11 + N, solid
LIP16-An-AI118	III				Ronja, Dwi	2016.04.21	Biofilm	Biofilm on plastic	Cikaniki	6°44'34.2"S 106°31'82.9"E	cotton stick	BG11 + N, pH3
LIP16-An-AI124	III				Delicia, Dwi	2016.04.25	Biofilm	Stone	Cibinong	6°29'35.2"S 106°50'59.3"E	cotton stick	BG11 + N
LIP16-An-AI000	V	Nostocales	Chlorogloeopsidaceae	Chlorogloeopsis	Information lost during isolation process.							

Table A 3. Cyanobacteria strains obtained from Dwi Susilaningsih within the Project ANoBI.

DWI	Accession number	Sec.	Sampling Date	Substrate	Location		
2	LIP11-2-AI008	III	29.10.2011	surface	Bendungan Batujai	Lombok	NTB
4	LIP112-2-AI007	III	08.06.2012	Surface of wood	Mahakam river	Balikpapan	East Borneo
5	LIP112-2-AI008	III	08.06.2012	surface of soil	Mahakam river	Balikpapan	East Borneo
8	LIP112-2-AI014	III	02.05.2012	water	Gunung Pancar	Bogor	West Jawa
10	LIP112-2-AI027	IV	22.11.2011	surface	midle lake giak siam kecil	Giak siam kecil, bukit batu	Riau
11	LIP112-2-AI056	III	05.07.2012	surface of sediment	Gili Meno	Lombok	NTB
12	LIP113-2-AI003	I	17.05.2013	sediment	Lembah Anai	Bukit Tinggi	West Sumatera
13	LIP113-2-AI004	I	17.05.2013	water sediment	hotspring; Aia Angek;	Solok	West Sumatera
14	LIP113-2-AI009	III	12.06.2013	water, hot spring	Cangar		East Jawa
15	LIP113-2-AI011	V	12.06.2013	water, hot spring	Cangar		East Jawa
16	LIP113-2-AI012	V	12.06.2013	water, hot spring	Cangar		East Jawa
17	LIP113-2-AI021	I	21.06.2013	water	Cave, Kapota,	Wakatobi	South East Sulawesi
18	LIP113-2-AI022	III	22.06.2013	surface of starfish tentackel	Numana Beach, Wangi-wangi	Wakatobi	South East Sulawesi
19	LIP113-2-AI023	III	22.06.2013	surface of clamp	Numana Beach, Wangi-wangi	Wakatobi	South East Sulawesi
20	LIP113-2-AI025	I	23.06.2013	water	Numana, Wangi-wangi	Wakatobi	South East Sulawesi
21	LIP113-2-AI028	V	23.06.2013	surface of stone	PDAM. Wangi-wangi	Wakatobi	South East Sulawesi
22	LIP113-2-AI035	I	23.06.2013	water	Pia-pia, Wangi-wangi	Wakatobi	South East Sulawesi
23	LIP113-2-AI036	III	23.06.2013	water	Pia-pia, Wangi-wangi	Wakatobi	South East Sulawesi
24	LIP113-2-AI037	I	23.06.2013	surface of shell	wisata beach hotel, wangi-wangi	Wakatobi	South East Sulawesi
25	LIP113-2-AI041	I	23.06.2013	surface of shell	wisata beach hotel, wangi-wangi	Wakatobi	South East Sulawesi
26	LIP113-2-AI042	I	23.06.2013	surface of shell	wisata beach hotel, wangi-wangi	Wakatobi	South East Sulawesi
27	LIP113-2-AI048	I	29.05.2013	water	Dock, Pramuka island	Thousand island	Jakarta
28	LIP113-2-AI050	I	29.05.2013	water	Dock, Pramuka island	Thousand island	Jakarta
29	LIP113-2-AI053	III	29.05.2013	water	Mangrove, Rambut island	Thousand island	Jakarta
30	LIP113-2-AI004	I	20.06.2013	water	Liya Sampora, Wangi-wangi	wangi-wangi	South East Sulawesi
31	LIP113-2-AI009	I	20.06.2013	surface of stone	Kohondao, Wangi-wangi	wangi-wangi	South East Sulawesi
32	LIP113-2-AI012	I	20.06.2013	water	Patuno, Wangi-wangi	wangi-wangi	South East Sulawesi

33	LIP113-2-AI021	I	20.06.2013	surface of stone	Patuno,Wangi-wangi	wangi-wangi	South East Sulawesi
34	LIP113-2-AI036	III	22.06.2013	surface of stone	Patuno resort, Wangi-wangi	wangi-wangi	South East Sulawesi
35	LIP113-2-AI037	I	07.03.2013	water	DKP Belitung	Belitung	Bangka-Belitung
36	LIP113-2-AI048	I	07.03.2013	water	DKP Belitung	Belitung	Bangka-Belitung
37	LIP113-2-AI054	III	07.03.2013	water	Pantai Nyiur Melambai	Belitung	Bangka-Belitung
39	LIP113-2-AI069	I	08.03.2013	water	Pantai Tanjung Tinggi	Belitung	Bangka-Belitung
40	LBB 13-AL012	III	07.03.2013	water	Pantai Tanjung Mudong	Belitung	Bangka-Belitung
41	LBB 13-AL043	III	09.06.2013	water	Gunung pancar	Bogor	West Java
42	LBB 13-AL044	III	09.06.2013	water	Gunung pancar	Bogor	West Java

Sec. = Section

Table A 4. Bioactivity data of all tested extracts from the established cyanobacteria strain collection.

Extract	Section	Quorum sensing				Antibacterial				Rhodesain nhibition	
		<i>V. harveyi</i>	<i>C. violaceum</i>	<i>S. marcescens</i>		<i>S. aureus</i>		<i>B. subtilis</i>		inhibition [%]	SD [%]
AnoTü7	I									27.7	0.0
AnoTü8	III		QSI							27.7	0.2
AnoTü10	III					QSI/AB		AB	AB	N/A	N/A
AnoTü11	III	QSI								35.9	1.7
AnoTü12	III									30.5	2.3
AnoTü15	III		QSE			QSI			AB	18.1	2.6
AnoTü17	I		QSE							20.7	0.7
AnoTü18	III		QSE			QSI		AB	AB	20.8	1.0
AnoTü19	III									19.7	0.2
AnoTü20	I	QSI	QSE			QSI			AB	54.9	1.9
AnoTü24	I					QSI				23.1	1.0
AnoTü25	I	N/A	N/A	N/A	N/A	N/A	N/A	N/A	AB	N/A	N/A
AnoTü27	III	QSI				QSI				53.1	2.9
AnoTü41	I		QSI			AB	AB	AB	AB	11.1	6.0
AnoTü47 (O2)	IV			QSI?		QSI				23.8	0.3
AnoTü47 (CO2)	IV									30.0	0.1
An-Al074	III					QSI				13.4	0.1
An-Al075	III					QSI/AB			AB	18.6	0.2

An-AI078	III					AB	QSI/AB	AB	AB	17.2	0.7
An-AI079.2	III					QSI				18.6	1.0
An-AI081	III	QSI	QSE							26.9	2.0
An-AI087	III					QSI				17.2	0.8
An-AI088	III	QSI								6.7	4.0
An-AI092	V	QSI								19.0	3.0
An-AI093	III									12.3	3.3
An-AI094	IV									13.6	5.1
An-AI095	I	QSI				QSI			AB	40.4	3.8
An-AI096	IV									10.2	3.4
An-AI097	III	QSI	QSE							18.6	2.7
An-AI105	IV									20.5	2.9
An-AI107	IV	QSI								42.5	2.4
An-AI110	III		QSE			QSI		AB		36.5	2.0
An-AI114	IV									58.5	4.2
An-AI115	III	QSI								71.4	0.2
An-AI124	III								AB	11.6	0.2
An-AI000	V	QSI	QSE							54.0	1.3
An-AI000_SF	V	N/A	N/A	N/A	N/A	N/A	N/A	N/A	AB	N/A	N/A
An-AI013.1.1	V	N/A	N/A	N/A	N/A	N/A	N/A	N/A	AB	N/A	N/A
An-AI019	V	N/A	N/A	N/A	N/A	N/A	N/A	N/A		N/A	N/A
An-AI039	III	QSI				QSI				25.3	1.9
An-AI054.1	III	QSI						(AB)	AB	28.8	0.6
An-AI059.1.1	IV	QSI		QSI?					AB	28.8	2.9
An-AI059.1.2	IV		QSI			QSI				24.3	1.6
An-AI061.1_CD (I)	V		QSE	QSI?		AB	AB	AB	AB	29.5	1.0
An-AI061.1_F (I)	V	QSI	QSE					(AB)	AB	25.0	4.9
An-AI061.1.1_F (II)	V	N/A	N/A	N/A	N/A	N/A	N/A	N/A	AB	N/A	N/A
An-AI061.1.1_CD (II)	V	N/A	N/A	N/A	N/A	N/A	N/A	N/A	AB	N/A	N/A
An-AI071.1.5.1	IV	QSI								N/A	N/A
An-AI071.1.1.3	IV	N/A	N/A	N/A	N/A	N/A	N/A	N/A		N/A	N/A
An-AI072.2.1 (I)	I								AB	N/A	N/A
An-AI072.2.1 (II)	I	N/A	N/A	N/A	N/A	N/A	N/A	N/A	AB	N/A	N/A

An-AI072	I	N/A	N/A	N/A	N/A	N/A	N/A	N/A		N/A	N/A
DWI10	IV					QSI				21.8	0.7
DWI12	I	QSI				QSI				29.5	2.5
DWI13	I	QSI								14.3	1.9
DWI14	III									21.1	3.5
DWI16	V		QSE							33.2	1.8
DWI17	I									30.5	1.3
DWI23	III		QSI							19.7	0.6
DWI24	I		QSI							30.1	0.4
DWI27	I		QSI							7.8	0.9
DWI30	I		QSI							5.3	1.2
DWI33	I		QSE							51.3	6.4
DWI37	III									34.8	1.5
DWI41	III		QSE			QSI/AB	QSI			33.4	5.8
DWI42	III	QSI	QSE							36.9	0.4

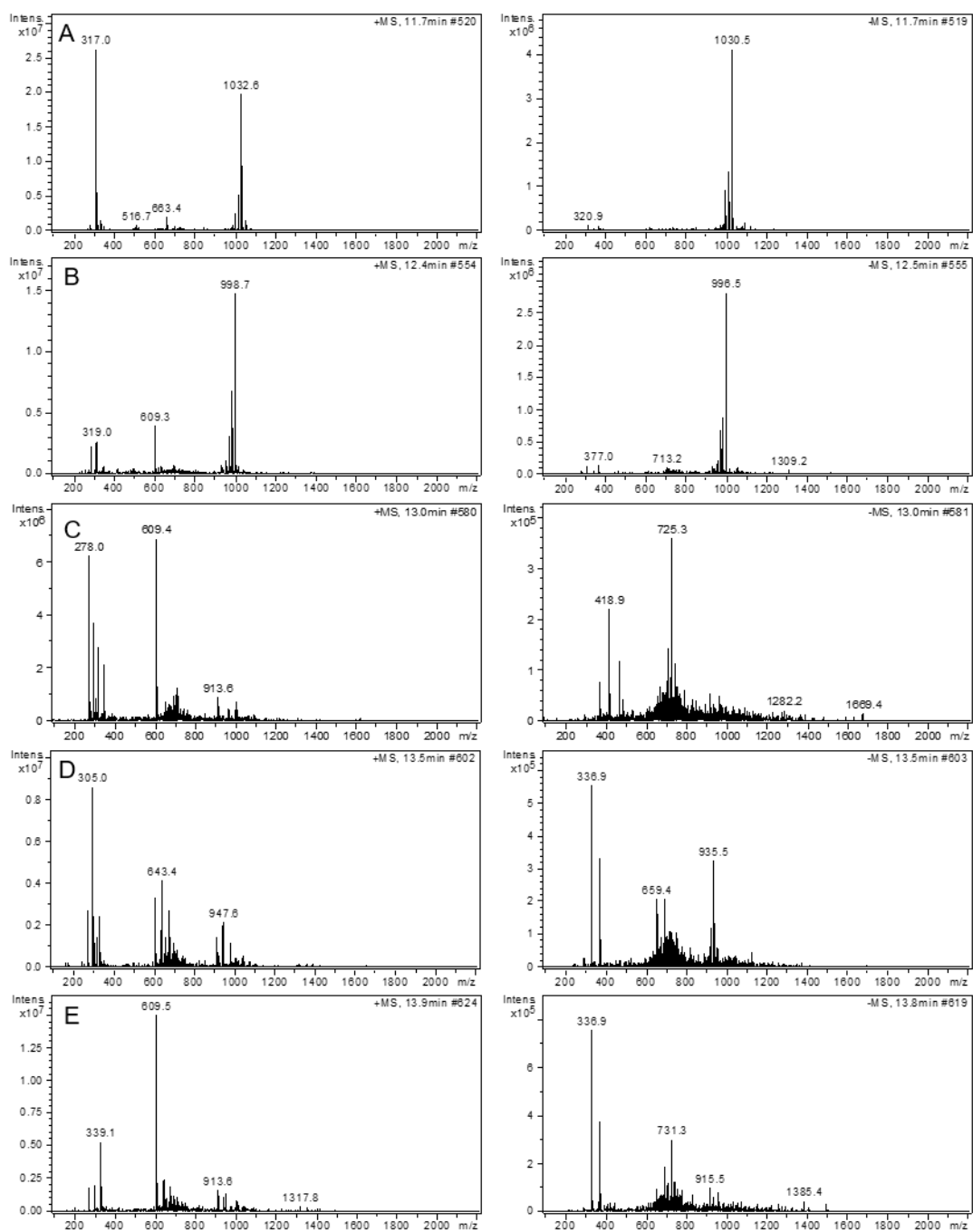


Figure A 1. Mass spectra of compound A to E of An-AI061.1 biomass extract. Pos. mode (left), neg. mode (right).

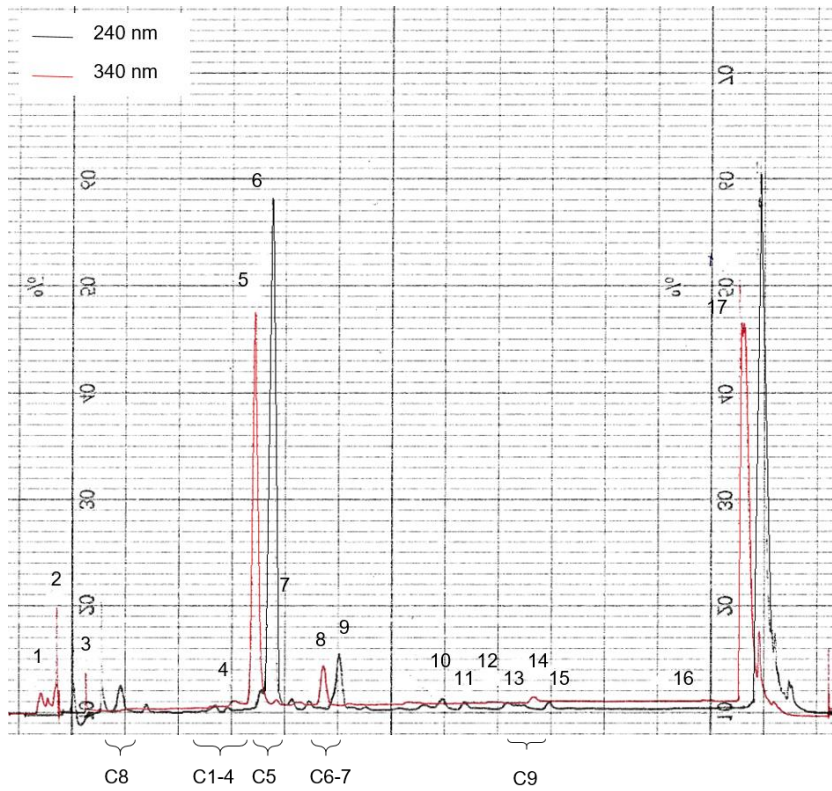


Figure A 2. **Biomass extract *Nostoc* 3; Preparative isolation; first run.** 40 mg in 4 mL MeOH 20%, 0.1% FA, 24 mL/min, 0-25 min: 5-25%, 27-32: 100%, Reprosil Pure Basic C18 10 μ m, 240 und 340 nm.

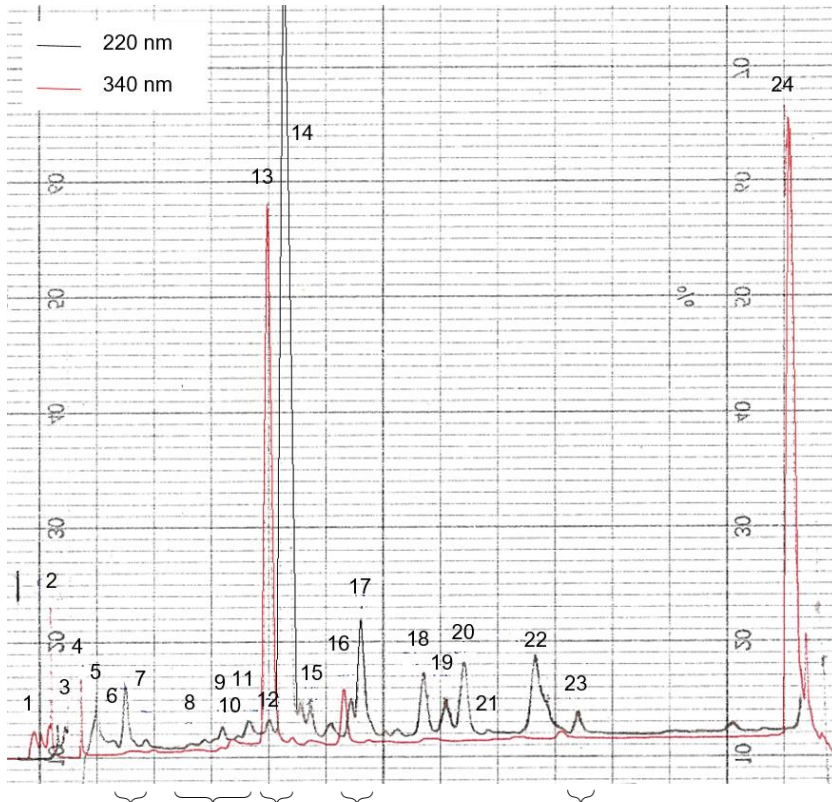


Figure A 3. **Biomass extract *Nostoc* 3; Preparative isolation; second run.** 40 mg in 4 mL MeOH 20%, 0.1% FA, 24 mL/min, 0-25 min: 5-25%, 27-32: 100%, Reprosil Pure Basic C18 10 μ m, 220 und 340 nm.

Table A 5. **¹H- and ¹³C-NMR data of compound 5 from biomass extract *Nostoc 3*.**

position	H Shift [ppm]	H Multiplicity	C Shift [ppm]	XHn
1	3.44	m	79.1	CH
2	3.79	M	68.8	CH
3			78.7	CH
4	5.40	d (3.66)	95.9	CH
6	4.10	t (7.02, 7.02)	70.2	CH
7	3.24	m	70.7	CH
8	3.40	m	81.4	CH
9	2.97	m	72.2	CH
10	4.44	d (7.78)	102.9	CH
12	3.13	m	76.5	CH
15	4.75	d (5.49)		OH
17	3.37	s	57.2	CH3
18	3.44	m	59.4	CH2
20	3.44	m	60.8	CH3
21	3.65	Br dd (11.83,3.13)	60.7	CH2
22	4.48	br t (5.65, 5.65)		OH
23/24	4.83	t (5.42, 5.42)		
26	4.21	qd (6.43, 6.43, 6.43, 3.59)	76.3	CH
27	1.06	d (6.56)	17.0	CH3
28	4.42	d (3.36)	85.3	CH
30	3.28	s	57.3	CH3
n. d.			127.7	?
n. d.			147.6	?
n. d.			149.3	?
n. d.	6.97	m		
n. d.	8.41	s		
n. d.	8.80	s		

6.3. Supporting Information “Nostotrebins 6 Related Cyclopentenediones and δ -Lactones with Broad Activity Spectrum Isolated from the Cultivation Medium of the Cyanobacterium *Nostoc* sp. CBT1153”

Supporting Information

Nostotrebins 6 related Cyclopentenediones and δ -Lactones with Broad Activity Spectrum Isolated from the Medium Extract of the Cyanobacterium *Nostoc* sp. CBT1153

Ronja Kossack[†], Steffen Breinlinger[‡], Trang Nguyen[‡], Julia Moschny[‡], Jan Straetener^{§,∇},
Anne Berscheid^{§,∇}, Heike Brötz-Oesterhelt^{§,∇}, Heike Enke[⊥], Tanja Schirmeister^{||}, Timo H. J.
Niedermeyer^{‡,∇,*}

[†]Department of Pharmaceutical Biology/Pharmacognosy, Institute of Pharmacy, University of Halle-Wittenberg, 06120 Halle (Saale), Germany

[‡]Department of Microbiology/Biotechnology, Interfaculty Institute for Microbiology and Infection Medicine (IMIT), University of Tübingen, 72076 Tübingen, Germany

[§]Department of Microbial Bioactive Compounds, Interfaculty Institute for Microbiology and Infection Medicine (IMIT), University of Tübingen, 72076 Tübingen, Germany

[⊥]Cyano Biotech GmbH, 12489 Berlin, Germany

^{||}Institute of Pharmacy and Biochemistry, University of Mainz, 55128 Mainz, Germany

[∇] German Center for Infection Research (DZIF), Partner Site Tübingen, Tübingen, Germany

*Corresponding author

Fig S1 - Comparison of medium and biomass extract.....	3
Fig S2 - UV spectra of compounds 1 – 9.....	4
Fig S3 – IR spectra of compounds 1 – 5	5
Fig S4 - MS and MS/MS spectra.....	10
Monomers.....	11
Dimers.....	14
Trimers.....	19
Tetramers.....	22
NMR spectra of compounds 1, 3, 5, 6, and 8.....	24
Fig S5.1 - NMR spectra of compound 2 (Nostotrebinol 3).....	24
Fig S5.2 - NMR spectra of compound 3 (Nostolactone 4).....	28
Fig S5.3 - NMR spectra of compound 4 (Nostotrebin 7)	32
Fig S5.4 - NMR spectra of compound 5 (Nostotrebinlactone 7).....	37
Fig S5.5 - NMR spectra of compound 1 (Nostotrebin 6)	42
Discussion of structural features of A, B, C, and D	46
Bioactivity characterization.....	47
Determination of the inner filter effect	47
Table S1 - Bioactivity of Nostotrebin 6 (1) as described in the literature...	48
Fig S5 - Rhodesain Assay.....	49

Fig. S1 - Comparison of medium and biomass extract

Nostoc sp. CBT1153 medium extract (a) and biomass extract (b), HPLC-UV chromatogram (210 nm), overview and t_R 7.0-10.5 min.

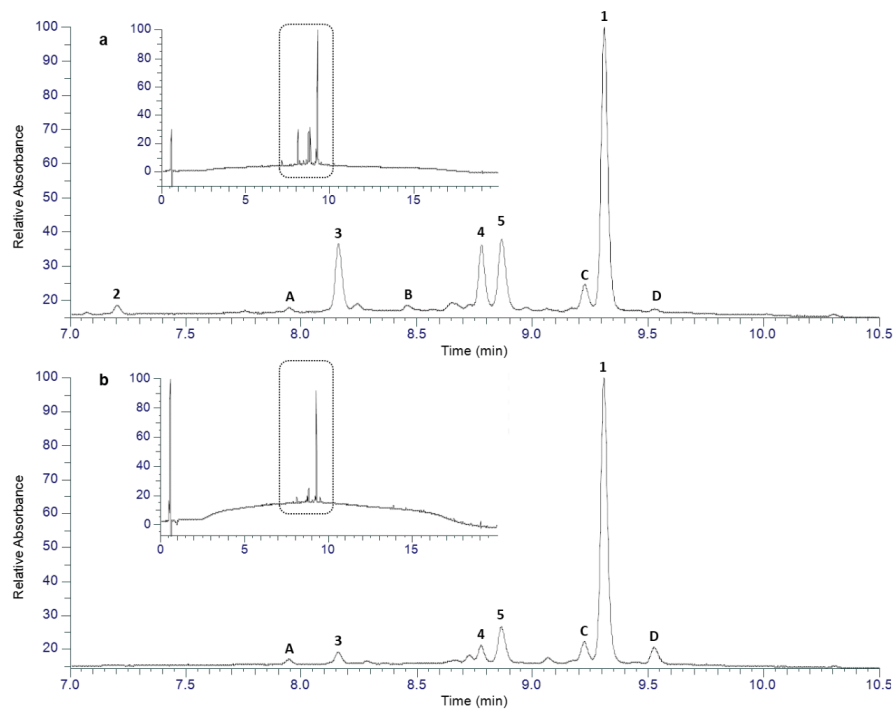
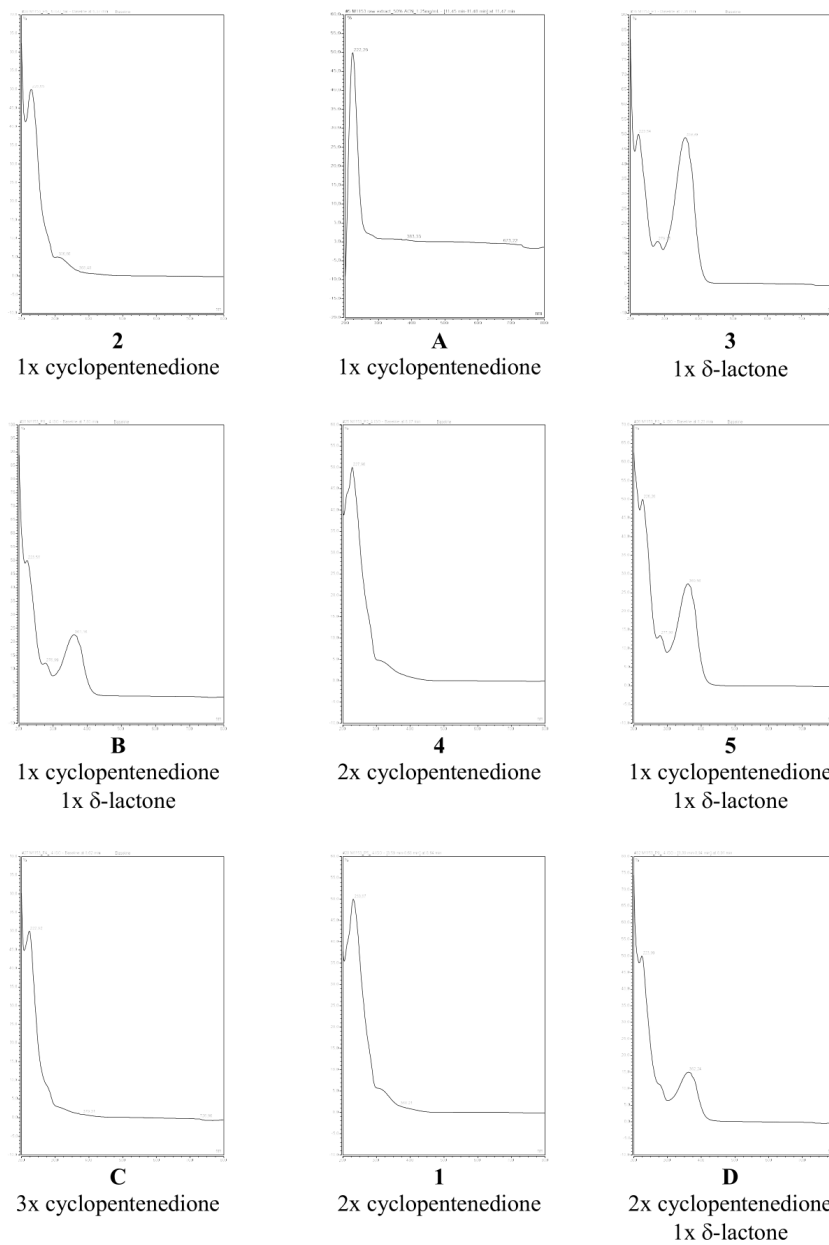


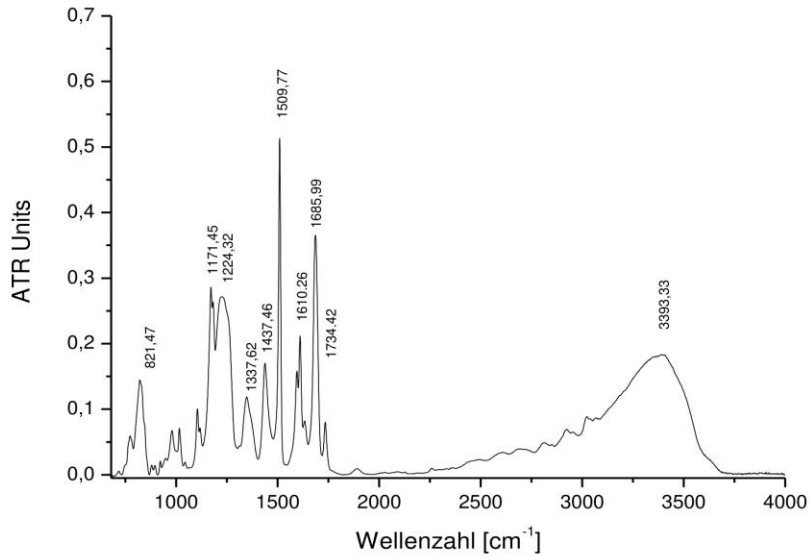
Fig. S2 - UV spectra of the compounds



Spectra shown have been recorded by HPLC-DAD (undefined H₂O / acetonitril mixture + 0.1% formic acid)

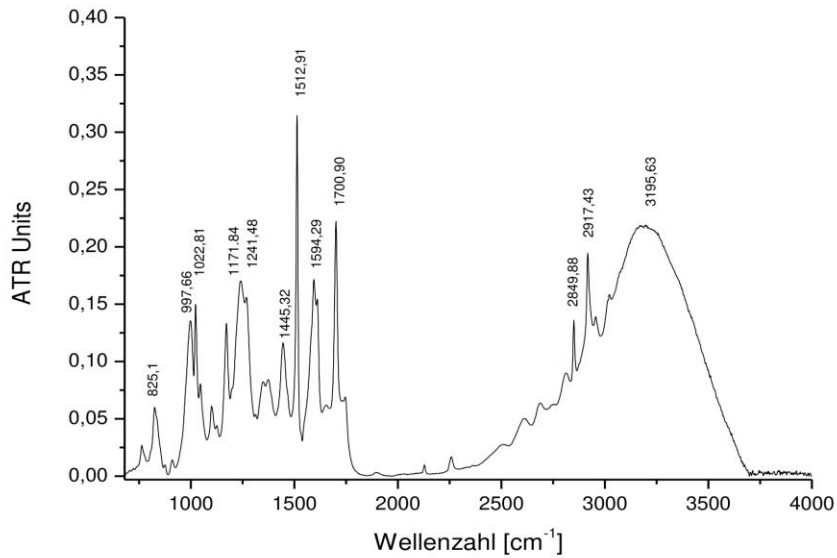
Fig. S3 - IR spectra of the compounds 1 – 5

IR spectrum, of compound 1 (Nostotrebilin 6)



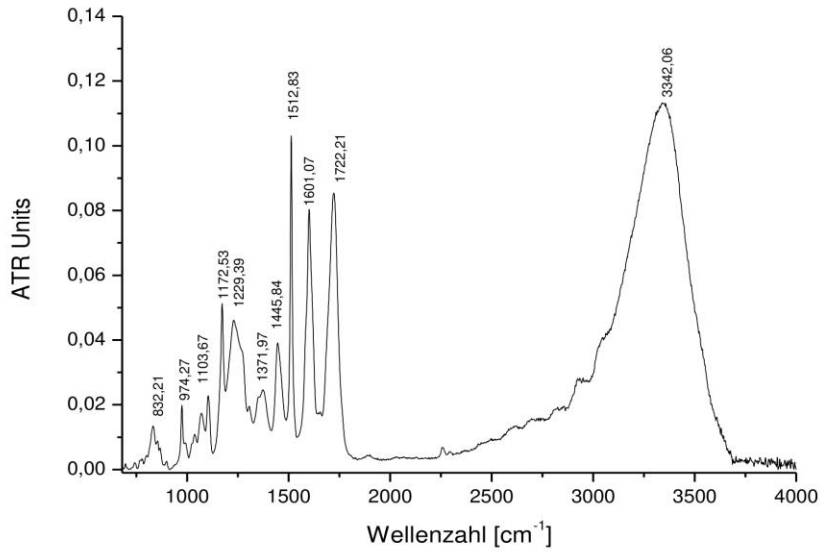
5

IR spectrum, of compound 2 (Nostotrebilin 3)



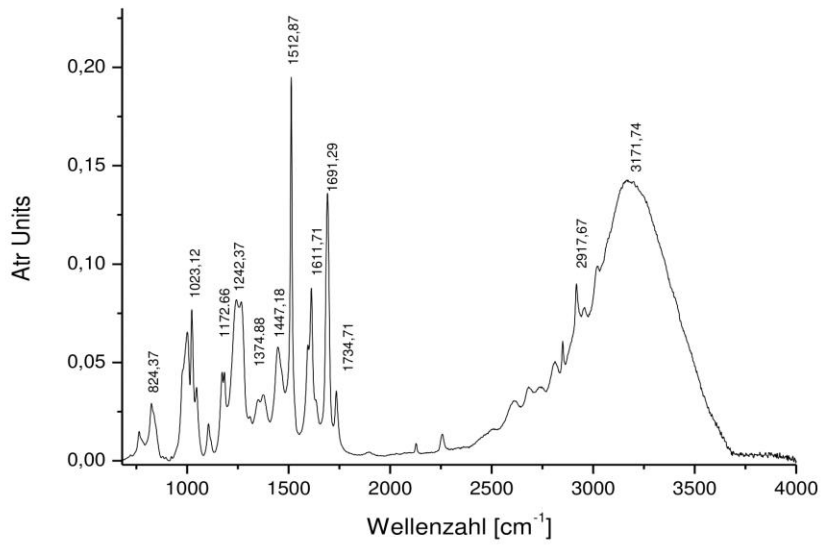
6

IR spectrum, of compound 3 (Nostolactone 4)



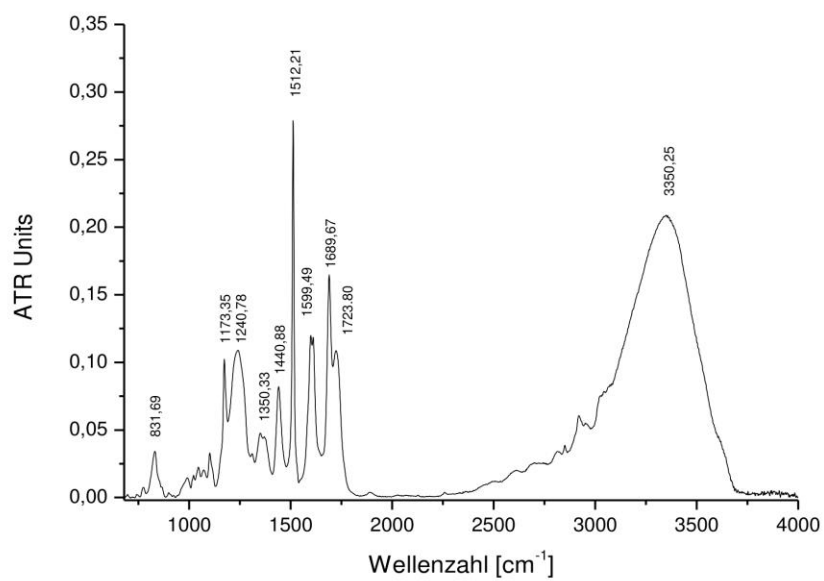
7

IR spectrum, of compound 4 (Nostotrebine 7)



8

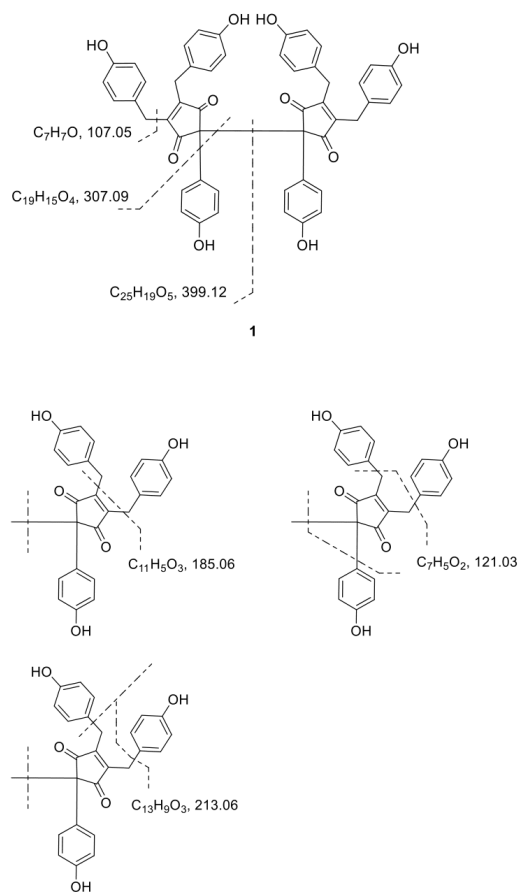
IR spectrum, of compound 5 (Nostotrebinalactone 7)



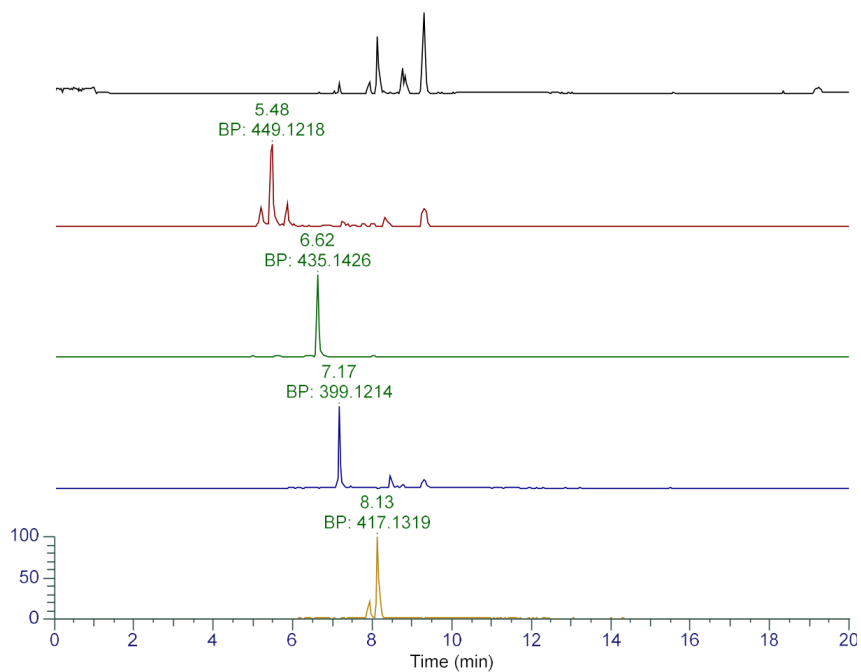
9

Fig. S3 - MS and MS/MS spectra

Characteristic MS/MS fragments of the compounds are especially observed at m/z 107.05 and 307.09. Other fragments observed for many of the compounds are detected at m/z 185.06, 121.03, and 213.06.

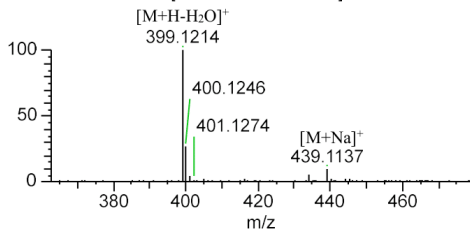
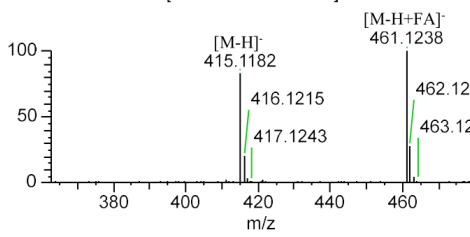
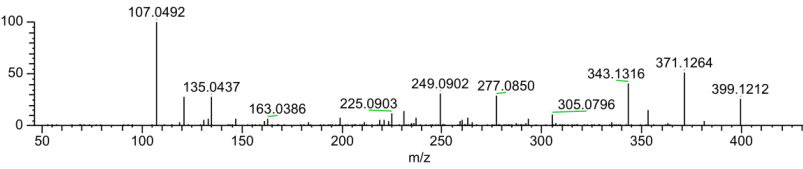
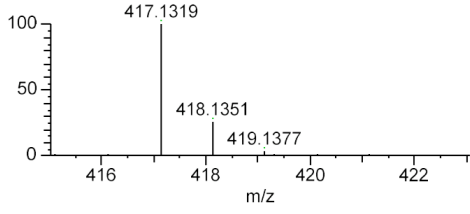
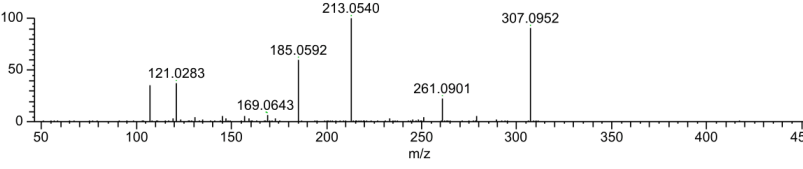


Detectable Monomers

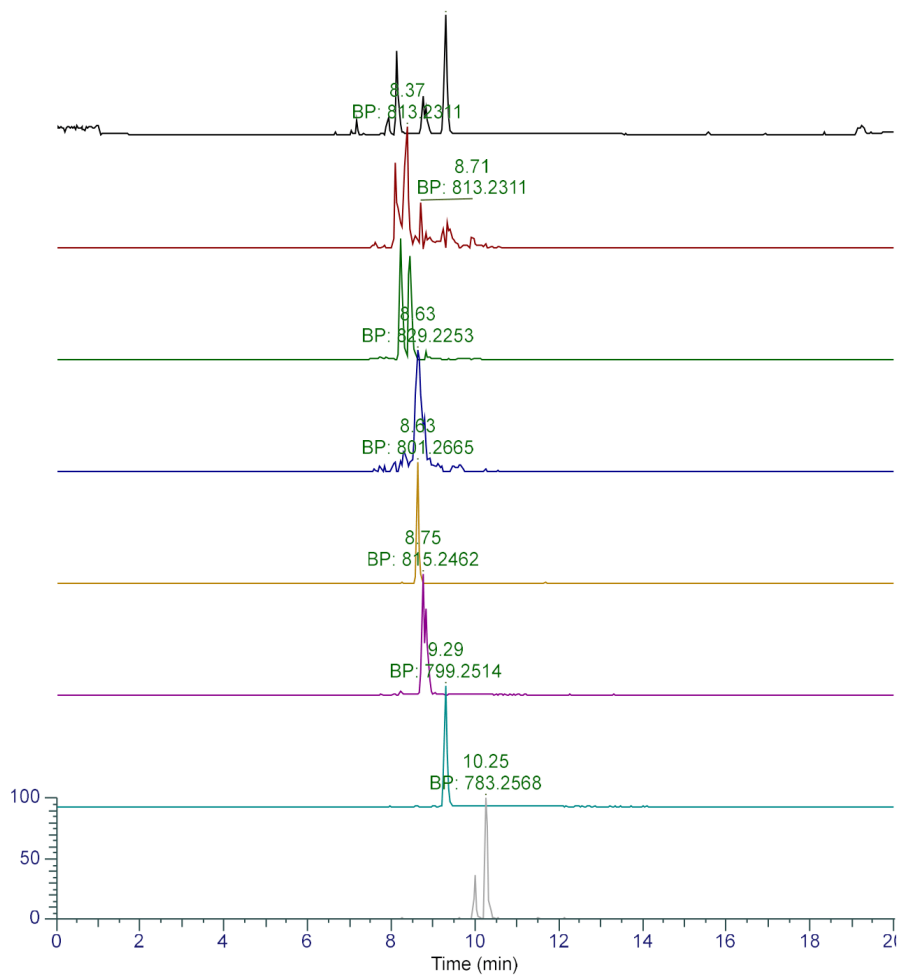


EICs of the detectable monomers summarized in the table below (t_r and m/z of the base peak indicated above the peaks) in comparison with the BPC of the extract chromatogram (top trace, black)

t_r (min)	HRMS [M+H]⁺	sum formula
5.48	M1153_10cm_2 #1483 RT: 5.48 AV: 1 NL: 3.01E+006 T: FTMS + c ESI Full ms [150.0000-2000.0000]	C ₂₅ H ₂₀ O ₈ (Δ 2.8 ppm) dihydroxylated A or 3
	<p>Mass spectrum showing relative intensity (0 to 100) versus m/z (448 to 454). Key peaks are labeled: 449.1218 (base peak), 450.1252, and 451.1278.</p>	
	M1153_10cm_2 #1474 RT: 5.45 AV: 1 NL: 4.40E+005 T: FTMS + c ESI d Full ms 2 449.1217@hcd30.00 [50.0000-475.0000]	
	<p>Reference mass spectrum showing relative intensity (0 to 100) versus m/z (50 to 450). Key peaks are labeled: 107.0492 (base peak), 123.0439, 147.0436, 161.0230, 217.0488, 249.0900, 279.1006, 307.0947, 325.0695, 385.1046, 413.1001, and 449.1213.</p>	
6.62	M1153_10cm_2 #1807 RT: 6.62 AV: 1 NL: 8.91E+006 T: FTMS + c ESI Full ms [150.0000-2000.0000]	C ₂₅ H ₂₂ O ₇ (Δ 2.8 ppm) water adduct of 3 (hydrolysis of the lactone?)
	<p>Mass spectrum showing relative intensity (0 to 100) versus m/z (434 to 440). Key peaks are labeled: 435.1426 (base peak), 436.1460, and 437.1484.</p>	
	M1153_10cm_2 #1810 RT: 6.63 AV: 1 NL: 6.40E+005 T: FTMS + c ESI d Full ms 2 435.1426@hcd30.00 [50.0000-460.0000]	
	<p>Reference mass spectrum showing relative intensity (0 to 100) versus m/z (50 to 450). Key peaks are labeled: 107.0492 (base peak), 123.0439, 157.0643, 175.0385, 215.0695, 261.0901, 311.0902, 323.0900, 371.1269, 399.1219, and 417.1317.</p>	

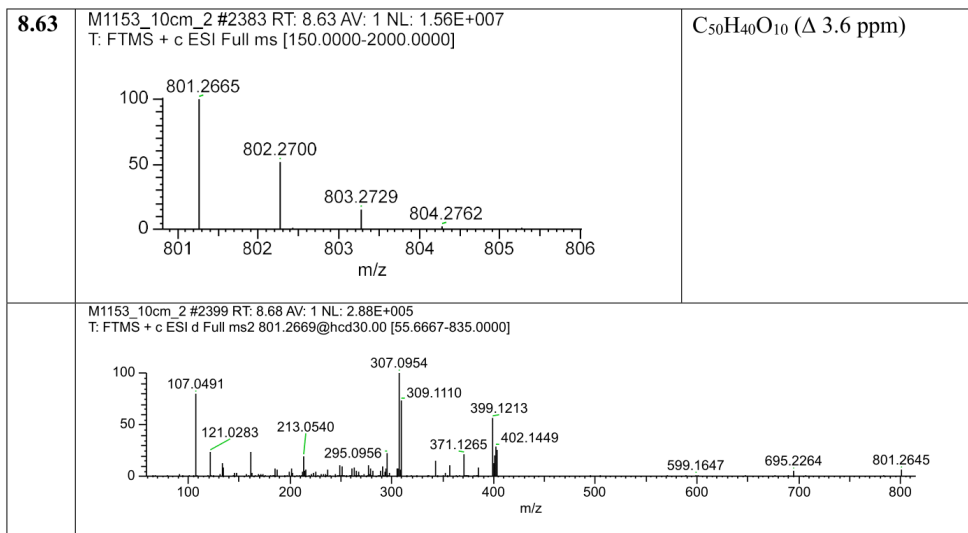
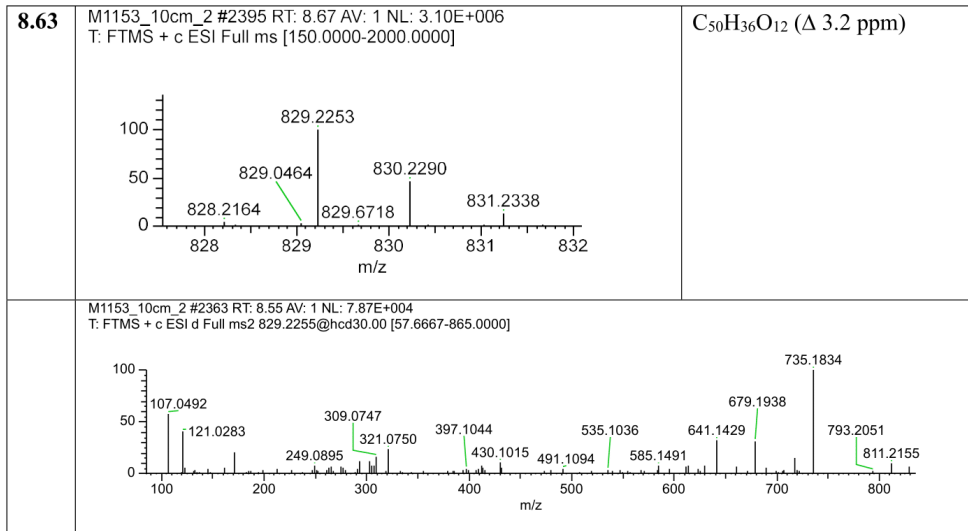
<p>7.17</p>	<p>M1153_10cm_2 #1963 RT: 7.17 AV: 1 NL: 1.22E+008 T: FTMS + c ESI Full ms [150.0000-2000.0000]</p>  <p>M1153_10cm_2 #1969 RT: 7.19 AV: 1 NL: 5.16E+007 T: FTMS - c ESI Full ms [150.0000-2000.0000]</p> 	<p>$C_{25}H_{18}O_5$ (Δ 3.1 ppm) in pos mode (loss of H_2O)</p> <p>$C_{25}H_{20}O_6$ (Δ 1.4 ppm)</p> <p>(2)</p>
	<p>M1153_10cm_2 #1954 RT: 7.14 AV: 1 NL: 3.18E+006 T: FTMS + c ESI d Full ms2 399.1217@hcd30.00 [50.0000-425.0000]</p> 	
<p>7.93</p> <p>8.13</p>	<p>M1153_10cm_2 #2239 RT: 8.13 AV: 1 NL: 6.55E+008 T: FTMS + c ESI Full ms [150.0000-2000.0000]</p> 	<p>$C_{25}H_{20}O_6$ (Δ 3.3 ppm)</p> <p>(A, 3)</p> <p>(compounds with same sum formula and basically identical MS/MS spectrum)</p>
	<p>M1153_10cm_2 #2228 RT: 8.10 AV: 1 NL: 1.74E+007 T: FTMS + c ESI d Full ms2 417.1321@hcd30.00 [50.0000-445.0000]</p> 	

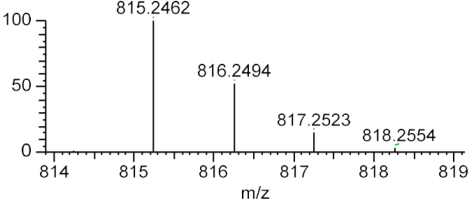
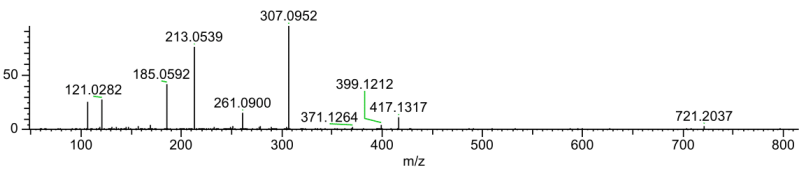
Detectable Dimers

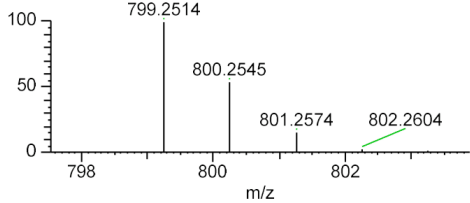
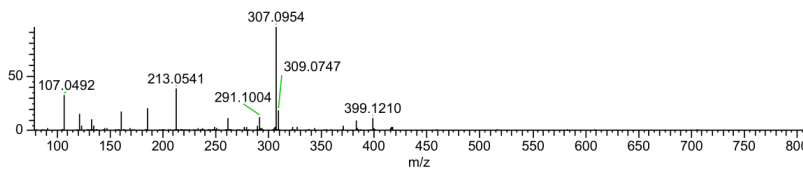


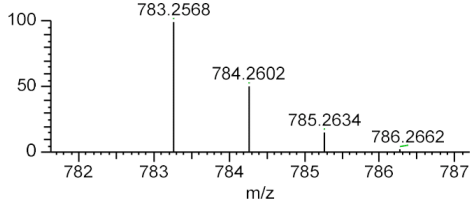
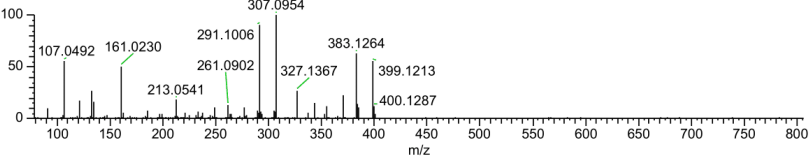
EICs of the detectable dimers summarized in the table below (t_r and m/z of the base peak indicated above the peaks) in comparison with the BPC of the extract chromatogram (top trace, black)

t_r (min)	HRMS [M+H]⁺	sum formula
8.09 8.37	M1153_10cm_2 #2239 RT: 8.13 AV: 1 NL: 1.13E+006 T: FTMS + c ESI Full ms [150.0000-2000.0000]	C ₅₀ H ₃₆ O ₁₁ (Δ 3.2 ppm)
	<p>Mass spectrum showing relative intensity (0 to 100) versus m/z (811 to 817). Key peaks are labeled at m/z 813.2305 and 814.2337.</p>	(compounds with same sum formula and basically identical MS/MS spectrum)
	M1153_10cm_2 #2303 RT: 8.34 AV: 1 NL: 3.58E+005 T: FTMS + c ESI d Full ms2 813.2310@hcd30.00 [56.6667-850.0000]	
	<p>Mass spectrum showing relative intensity (0 to 100) versus m/z (100 to 800). Key peaks are labeled at m/z 107.0491, 185.0593, 213.0540, 261.0901, 305.0797, 307.0954, 321.0747, 415.1164, 603.1636, and 719.1887.</p>	
8.21 8.46	M1153_10cm_2 #2263 RT: 8.21 AV: 1 NL: 1.38E+007 T: FTMS + c ESI Full ms [150.0000-2000.0000]	C ₅₀ H ₃₈ O ₁₂ (Δ 3.1 ppm)
	<p>Mass spectrum showing relative intensity (0 to 60) versus m/z (830 to 836). Key peaks are labeled at m/z 831.2410, 832.2445, 833.2485, and 835.2753.</p>	(B) (compounds with same sum formula and basically identical MS/MS spectrum)
	M1153_10cm_2 #2326 RT: 8.43 AV: 1 NL: 3.16E+006 T: FTMS + c ESI d Full ms2 831.2414@hcd30.00 [57.6667-865.0000]	
	<p>Mass spectrum showing relative intensity (0 to 100) versus m/z (100 to 800). Key peaks are labeled at m/z 121.0283, 185.0592, 213.0540, 261.0900, 307.0952, 309.0744, and 417.1316.</p>	
	M1153_10cm_2 #2326 RT: 8.43 AV: 1 NL: 3.16E+006 T: FTMS + c ESI d Full ms2 831.2414@hcd30.00 [57.6667-865.0000]	
	<p>Mass spectrum showing relative intensity (0 to 100) versus m/z (100 to 320). Key peaks are labeled at m/z 107.0491, 121.0283, 145.0645, 157.0644, 169.0644, 185.0592, 213.0540, 233.0954, 261.0900, 279.1004, 307.0952, and 309.0744.</p>	

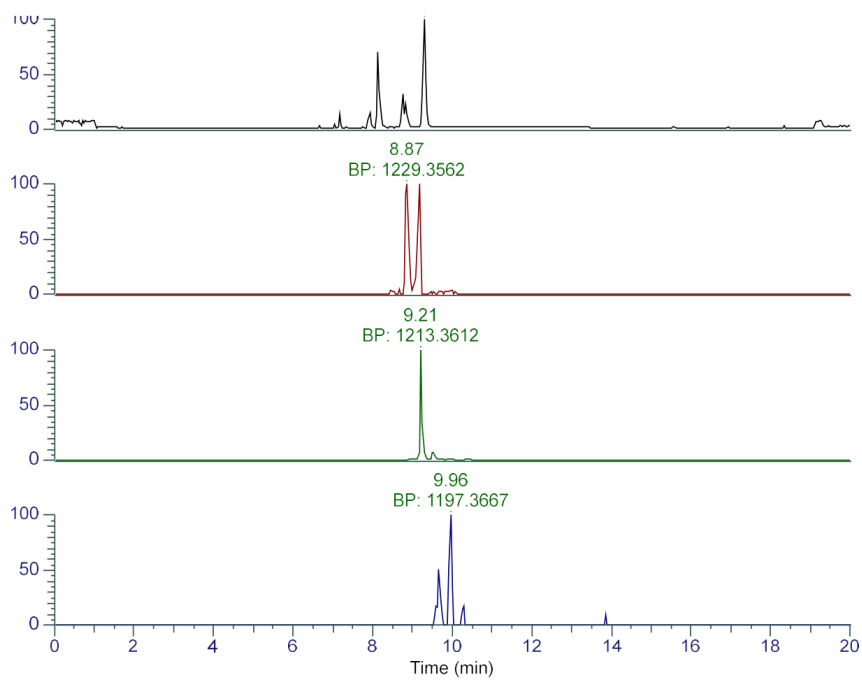


8.75	M1153_10cm_2 #2419 RT: 8.75 AV: 1 NL: 3.01E+008 T: FTMS + c ESI Full ms [150.0000-2000.0000]	$C_{50}H_{38}O_{11}$ (Δ 3.0 ppm)
8.83	 <p>Mass spectrum showing peaks at m/z 815.2462, 816.2494, 817.2523, and 818.2554.</p>	(4, 5) (compounds with same sum formula and basically identical MS/MS spectrum)
<p>M1153_10cm_2 #2398 RT: 8.68 AV: 1 NL: 2.99E+006 T: FTMS + c ESI d Full ms2 815.2462@hcd30.00 [56.6667-850.0000]</p>  <p>Reference mass spectrum showing peaks at m/z 121.0282, 185.0592, 213.0539, 261.0900, 307.0952, 371.1264, 399.1212, 417.1317, and 721.2037.</p>		

9.29	M1153_10cm_2 #2575 RT: 9.29 AV: 1 NL: 9.40E+008 T: FTMS + c ESI Full ms [150.0000-2000.0000]	$C_{50}H_{38}O_{10}$ (Δ 3.0 ppm)
	 <p>Mass spectrum showing peaks at m/z 799.2514, 800.2545, 801.2574, and 802.2604.</p>	(1)
<p>M1153_10cm_2 #2698 RT: 9.71 AV: 1 NL: 4.60E+005 T: FTMS + c ESI d Full ms2 799.2518@hcd30.00 [55.6667-835.0000]</p>  <p>Reference mass spectrum showing peaks at m/z 107.0492, 213.0541, 291.1004, 307.0954, 309.0747, and 399.1210.</p>		

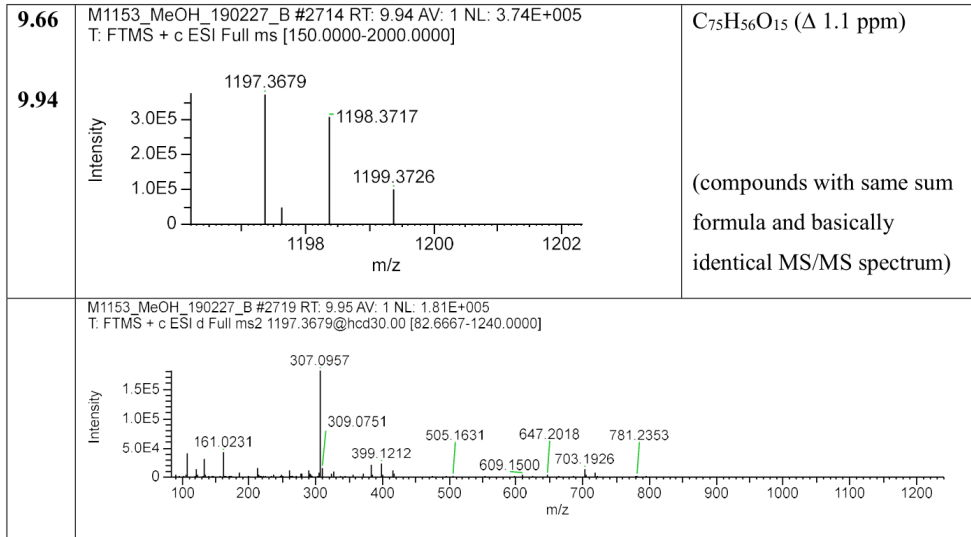
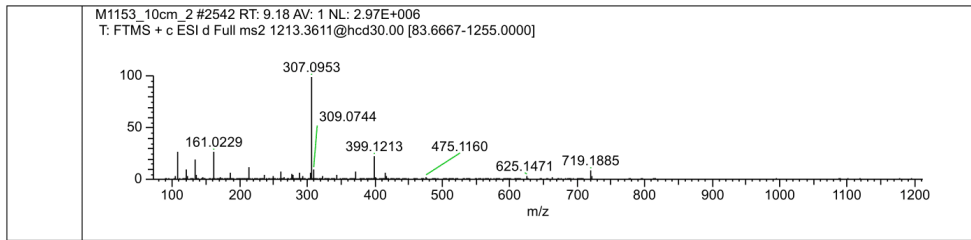
<p>10.00</p> <p>10.25</p>	<p>M1153_10cm_2 #2849 RT: 10.25 AV: 1 NL: 1.59E+007 T: FTMS + c ESI Full ms [150.0000-2000.0000]</p> 	<p>$C_{50}H_{38}O_9$ (Δ 2.6 ppm)</p> <p>(compounds with same sum formula and basically identical MS/MS spectrum)</p>
	<p>M1153_10cm_2 #2852 RT: 10.26 AV: 1 NL: 1.63E+006 T: FTMS + c ESI d Full ms2 783.2568@hcd30.00 [54.3333-815.0000]</p> 	

Detectable Trimers

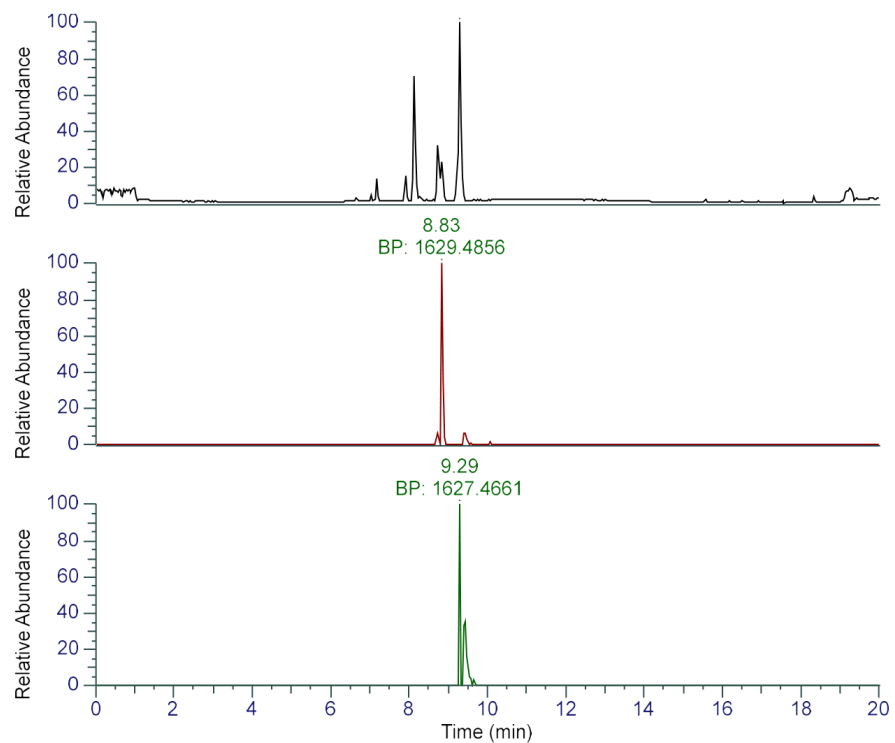


EICs of the detectable trimers summarized in the table below (t_r and m/z of the base peak indicated above the peaks) in comparison with the BPC of the extract chromatogram (top trace, black)

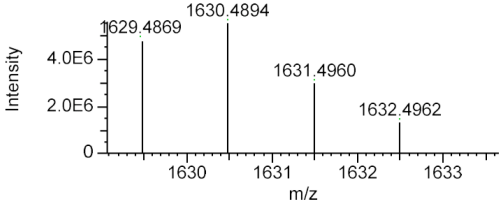
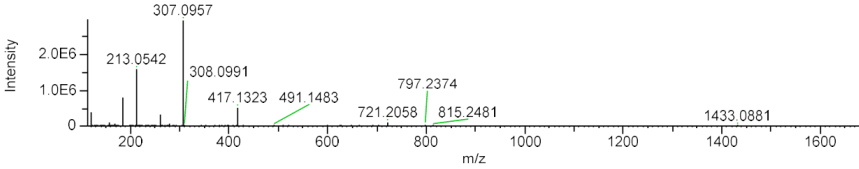
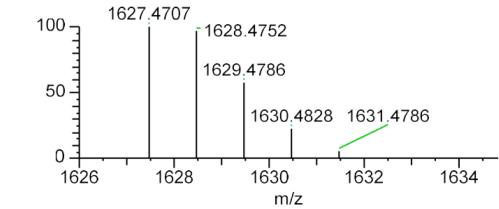
t_r (min)	HRMS [M+H]⁺	sum formula
8.87	M1153_10cm_2 #2539 RT: 9.16 AV: 1 NL: 3.18E+006 T: FTMS + c ESI Full ms [150.0000-2000.0000] T: FTMS + c ESI Full m	C ₇₅ H ₅₆ O ₁₇ (Δ 2.4 ppm)
9.16	<p>Mass spectrum showing relative intensity (0 to 100) versus m/z (1228 to 1234). Key peaks are labeled: 1228.3456, 1229.3561, 1230.3571, 1231.3721, 1232.3757, 1234.3856.</p>	(compounds with same sum formula and basically identical MS/MS spectrum)
	<p>M1153_10cm_2 #2531 RT: 9.14 AV: 1 NL: 1.13E+006 T: FTMS + c ESI d Full ms2 1229.3566@hcd30.00 [84.6667-1270.0000] T: FTMS + c ESI d Full ms2 1229.3566@hcd30.00 [84.6667-1270.00</p> <p>Mass spectrum showing relative intensity (0 to 100) versus m/z (100 to 1200). Key peaks are labeled: 185.0593, 213.0540, 307.0955, 309.0743, 417.1318, 701.1763, 719.1893, 795.2208, 905.2567, 1105.3041, 1211.3490.</p> <p>M1153_10cm_2 #2531 RT: 9.14 AV: 1 NL: 1.13E+006 T: FTMS + c ESI d Full ms2 1229.3566@hcd30.00 [84.6667-1270.0000] T: FTMS + c ESI d Full ms2 1229.3566@hcd30.00 [84.6667-1270.00</p> <p>Mass spectrum showing relative intensity (0 to 100) versus m/z (100 to 320). Key peaks are labeled: 107.0491, 121.0282, 145.0644, 157.0645, 185.0593, 213.0540, 233.0956, 261.0902, 279.1003, 305.0796, 307.0955, 309.0743.</p>	
9.21	M1153_10cm_2 #2551 RT: 9.21 AV: 1 NL: 4.32E+007 T: FTMS + c ESI Full ms [150.0000-2000.0000] T: FTMS + c ESI Full m	C ₇₅ H ₅₆ O ₁₆ (Δ 2.4 ppm)
9.49	<p>Mass spectrum showing relative intensity (0 to 100) versus m/z (1212 to 1218). Key peaks are labeled: 1213.3612, 1214.3643, 1215.3673, 1216.3705, 1217.3733.</p>	(C, D) (compounds with same sum formula and basically identical MS/MS spectrum)



Detectable Tetramers



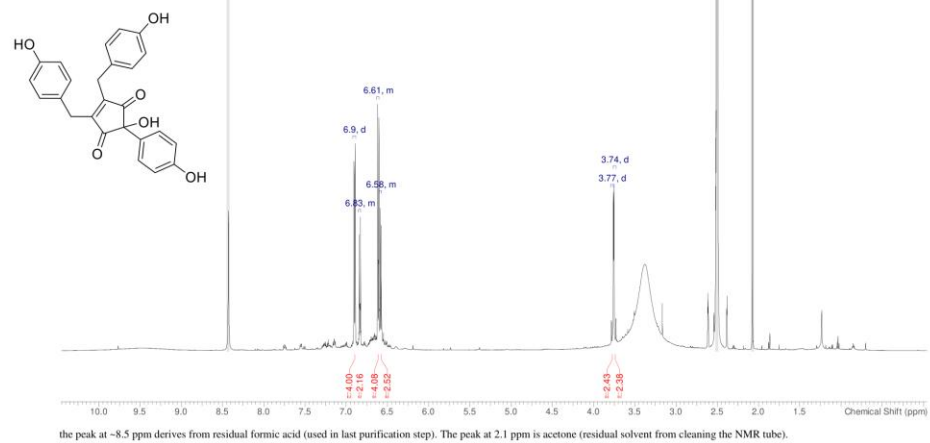
EICs of the detectable tetramers summarized in the table below (t_r and m/z of the base peak indicated above the peaks) in comparison with the BPC of the extract chromatogram (top trace, black)

tr (min)	HRMS [M+2H] ²⁺	sum formula
8.83	M1153_MeOH_190227_B #2397 RT: 8.82 AV: 1 NL: 5.54E+006 T: FTMS + c ESI Full ms [150.0000-2000.0000] 	C ₁₀₀ H ₇₆ O ₂₂ (Δ 2.0 ppm) tetramer
	M1153_MeOH_190227_B #2412 RT: 8.87 AV: 1 NL: 2.96E+006 T: FTMS + c ESI d Full ms2 1629.4879@hcd30.00 [112.0000-1680.0000] 	
9.45	M1153_10cm_2 #2623 RT: 9.45 AV: 1 NL: 4.72E+005 T: FTMS + c ESI Full ms [150.0000-2000.0000] T: FTMS + c ESI Full tr 	C ₁₀₀ H ₇₄ O ₂₂ (Δ 2.3 ppm) tetramer

NMR spectra of compounds 2, 3, 4, 5, and 1

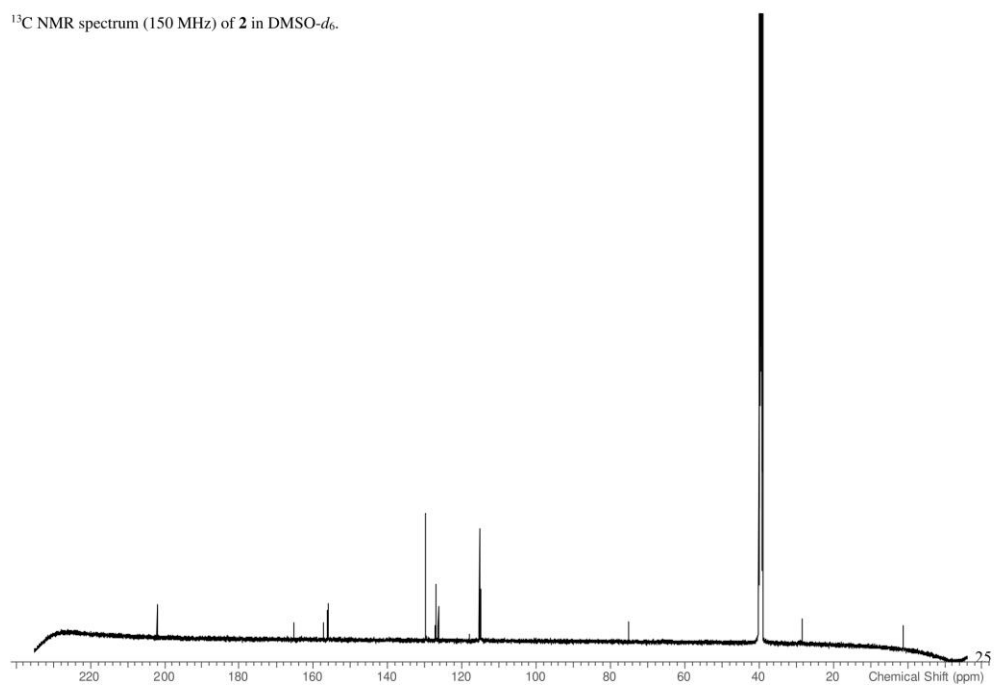
NMR spectra of compound 2 (Nostotrebinol 3)

^1H NMR spectrum (600 MHz) of 2 in $\text{DMSO-}d_6$.

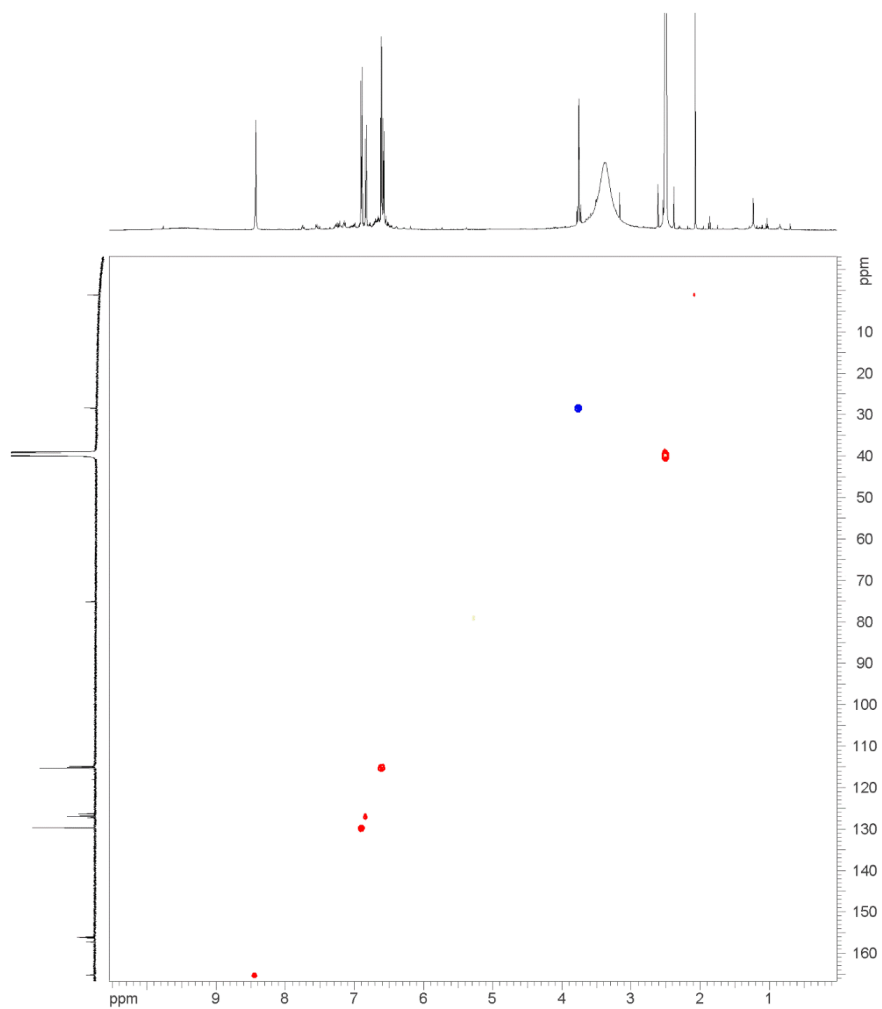


24

^{13}C NMR spectrum (150 MHz) of 2 in $\text{DMSO-}d_6$.

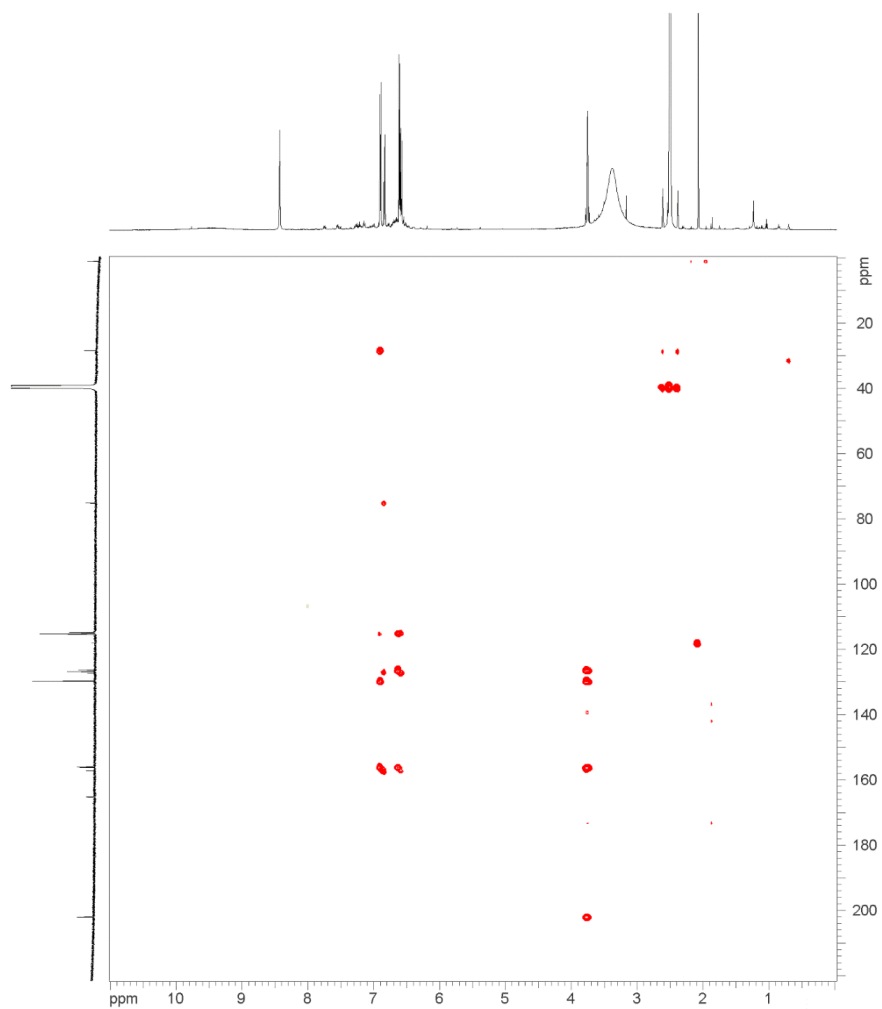


HSQC-DEPT NMR spectrum (600 MHz) of **2** in DMSO-*d*₆.



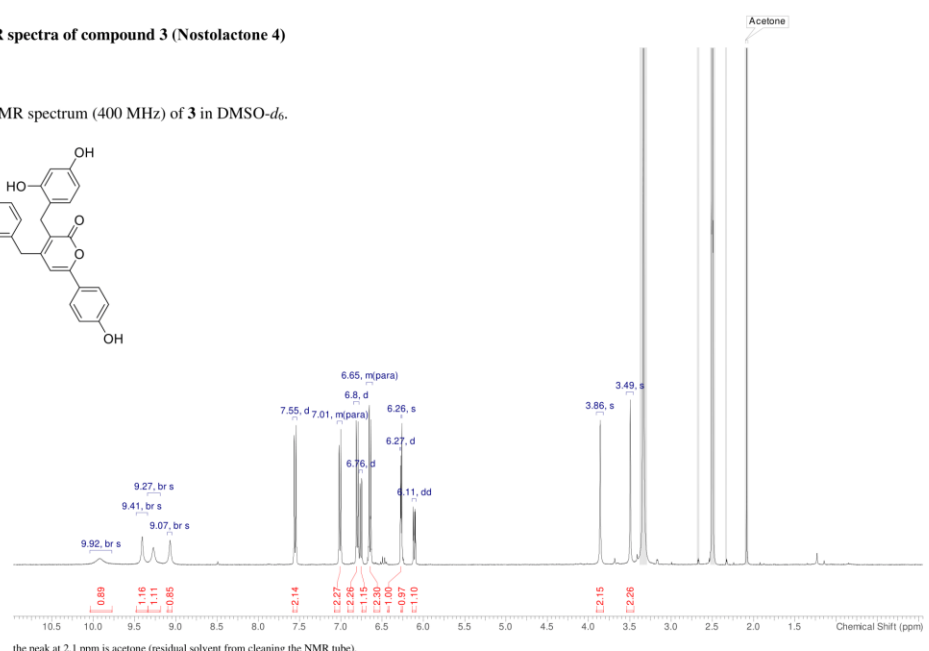
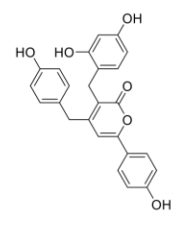
the peak at ~8.5 ppm derives from residual formic acid (used in last purification step).

HMBC spectrum (600 MHz) of **2** in DMSO-*d*₆.



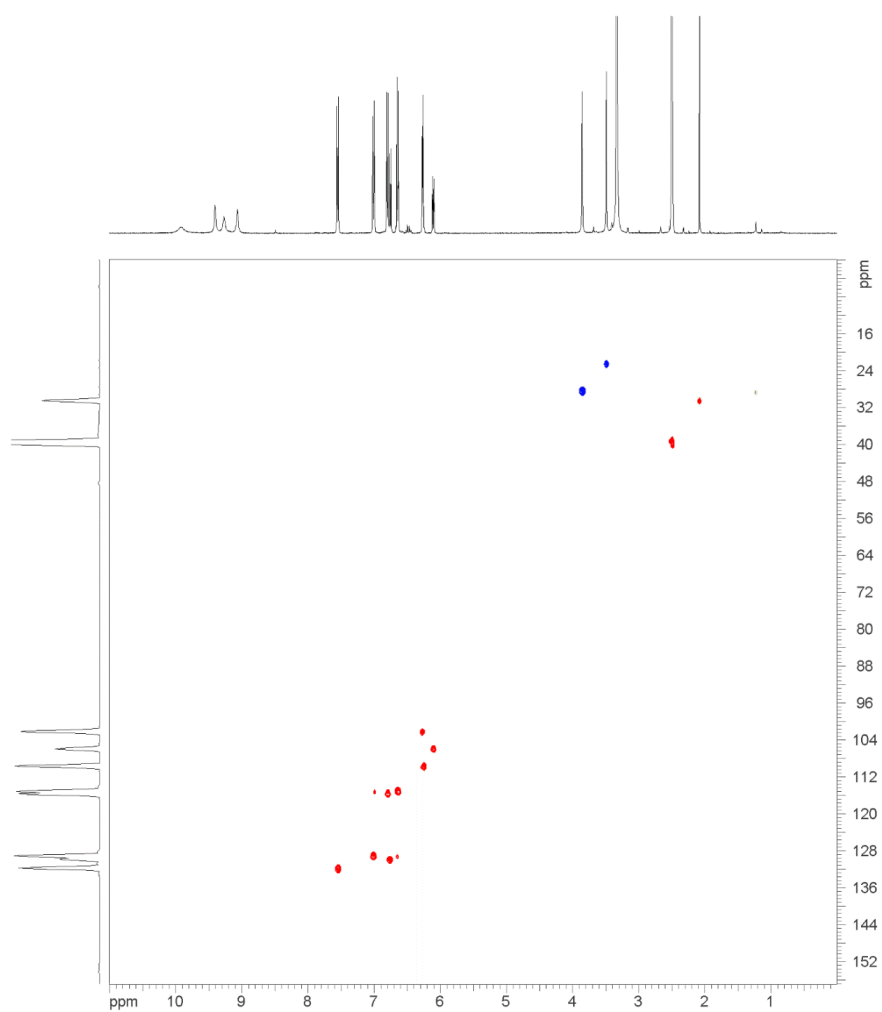
NMR spectra of compound 3 (Nostolactone 4)

¹H NMR spectrum (400 MHz) of 3 in DMSO-*d*₆.

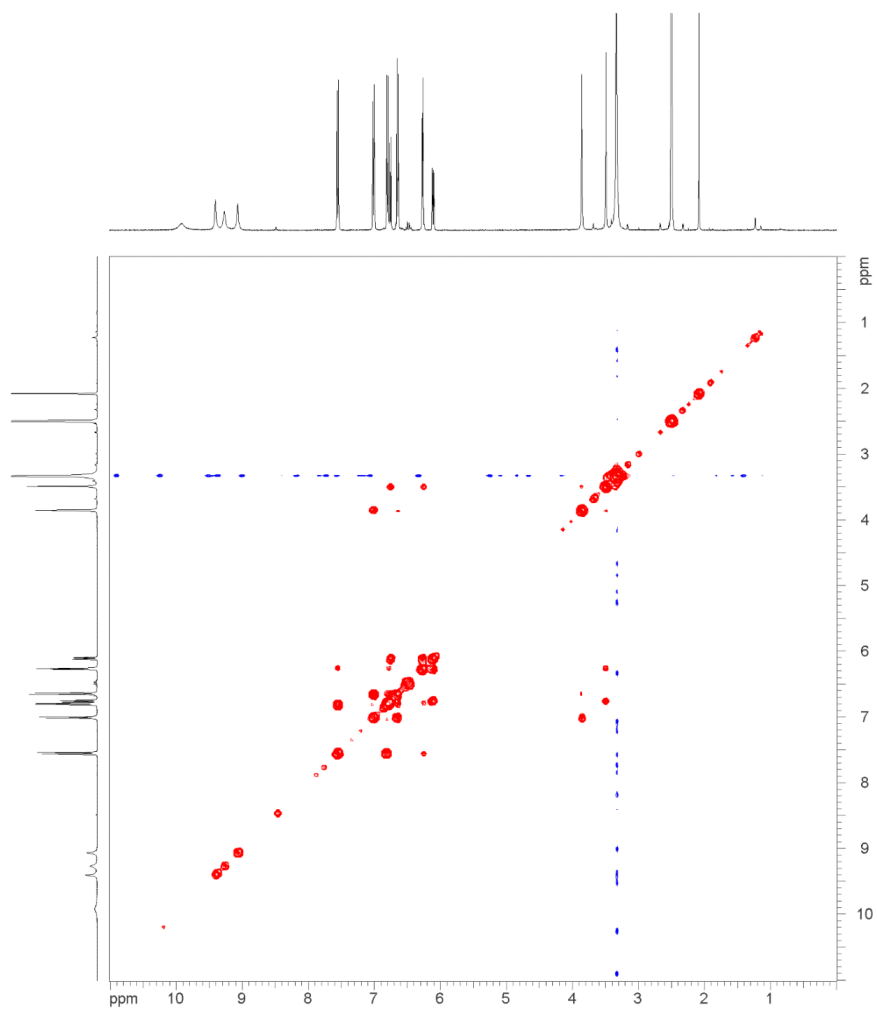


the peak at 2.1 ppm is acetone (residual solvent from cleaning the NMR tube).

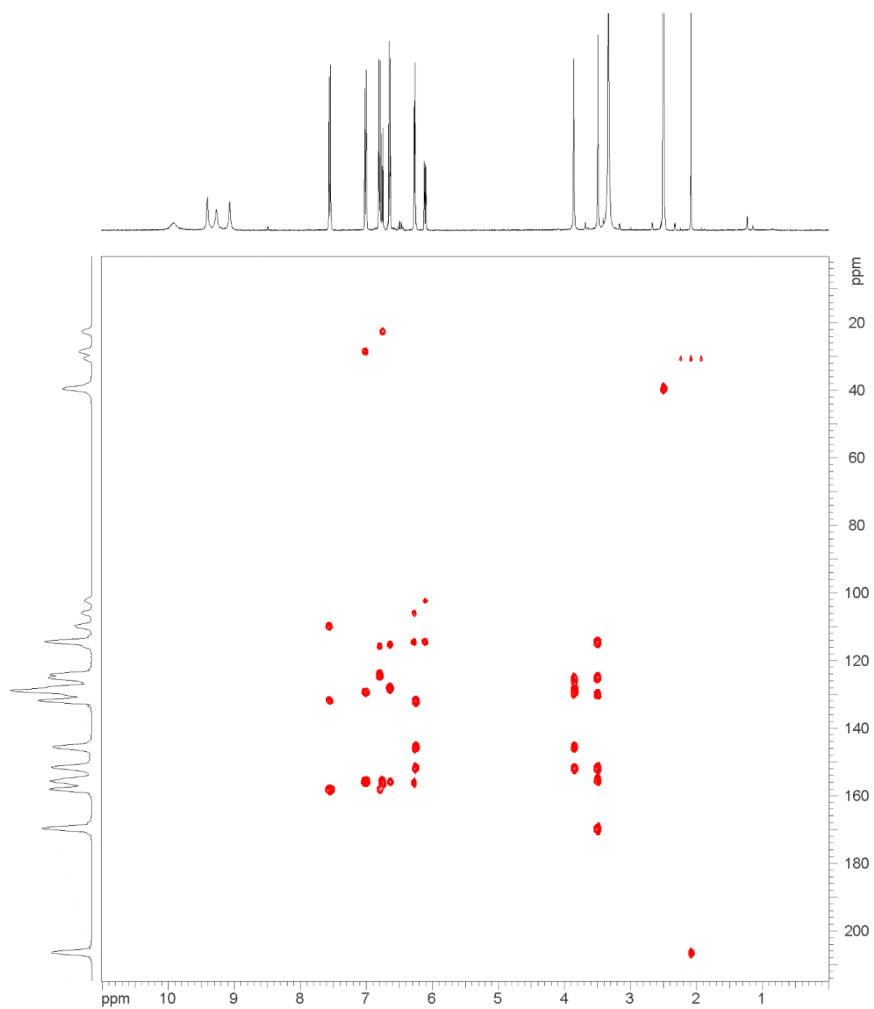
HSQC-DEPT NMR spectrum (400 MHz) of **3** in DMSO-*d*₆.



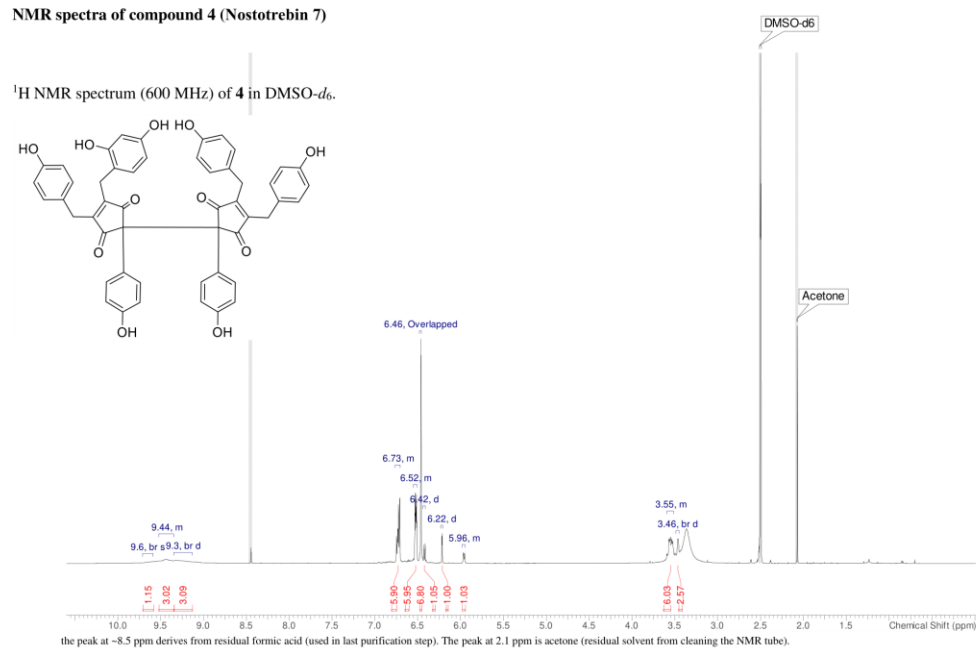
COSY NMR spectrum (400 MHz) of **3** in DMSO-*d*₆.



HMBC NMR spectrum (400 MHz) of **3** in DMSO-*d*₆.

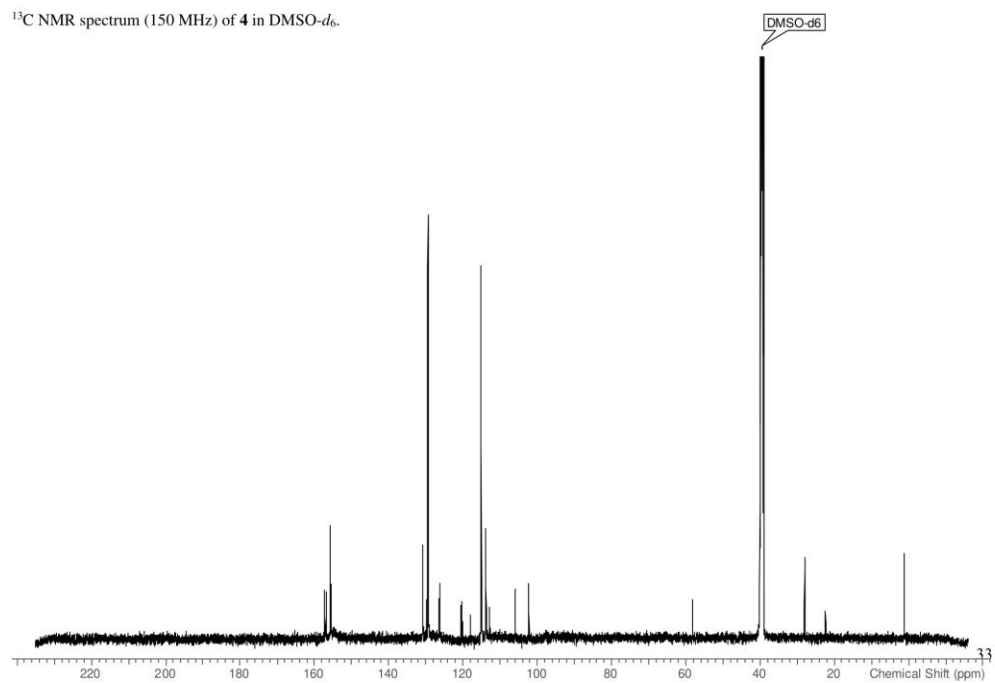


NMR spectra of compound 4 (Nostotrebilin 7)

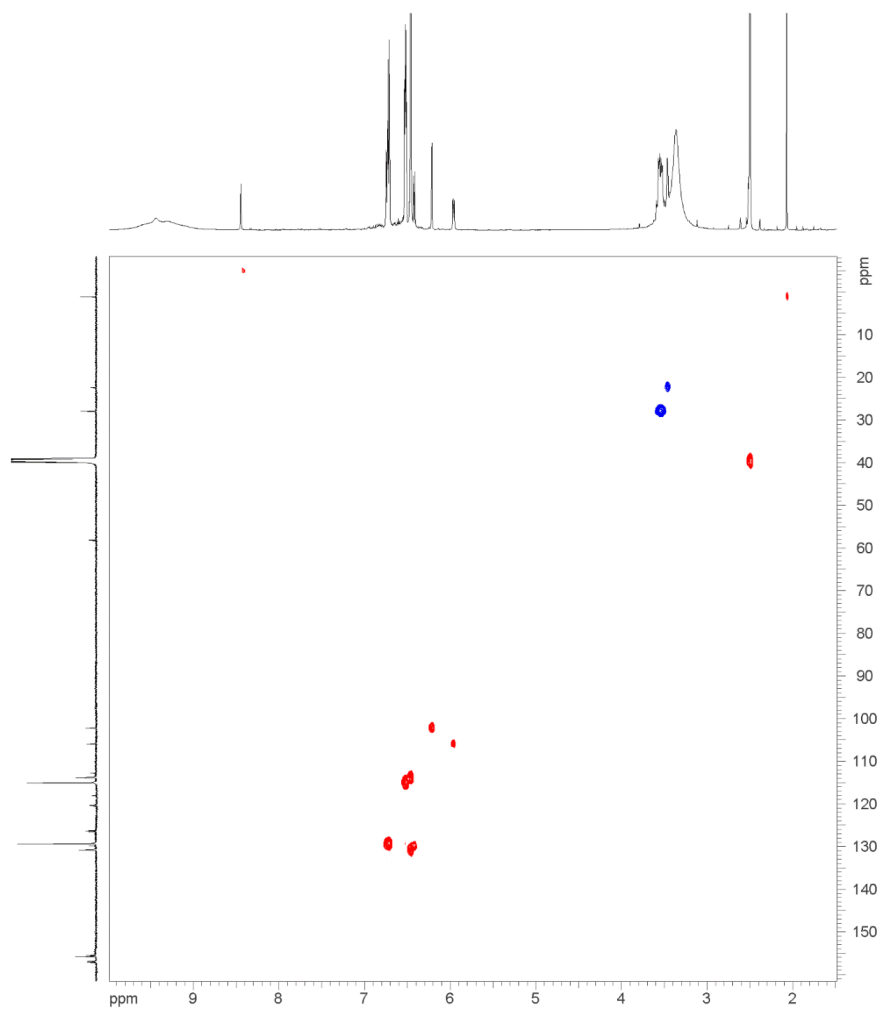


32

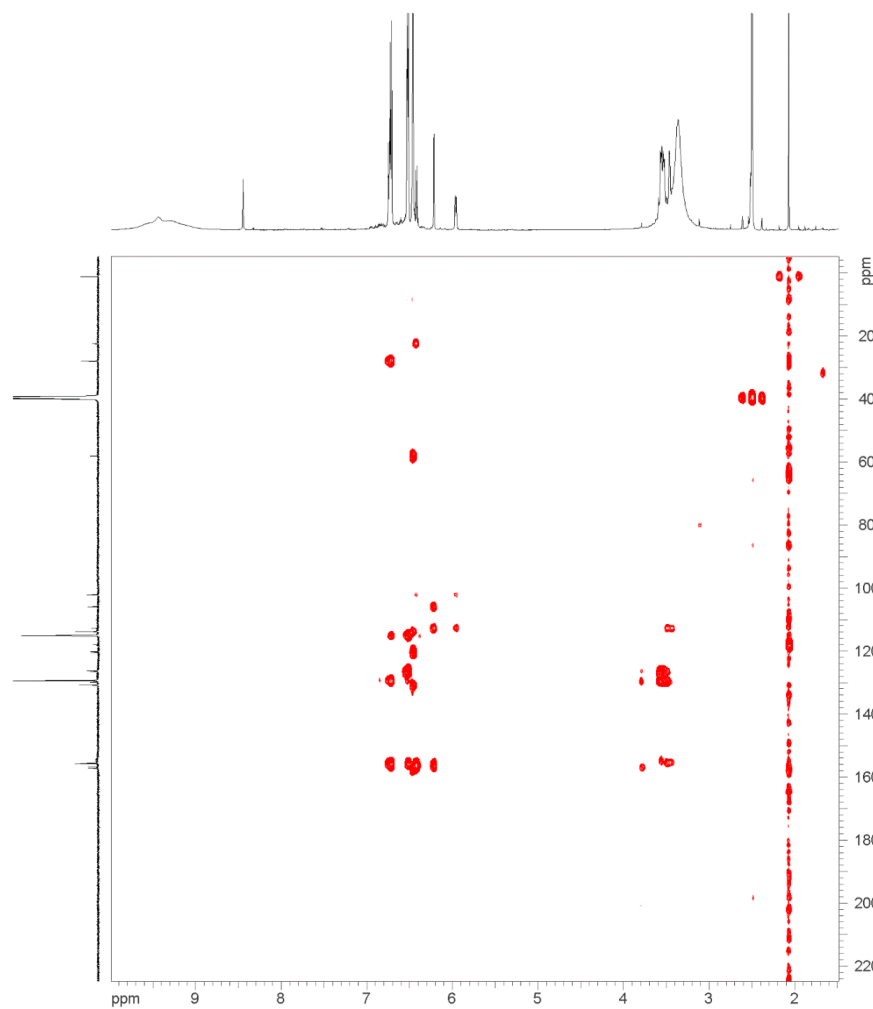
¹³C NMR spectrum (150 MHz) of 4 in DMSO-*d*₆.



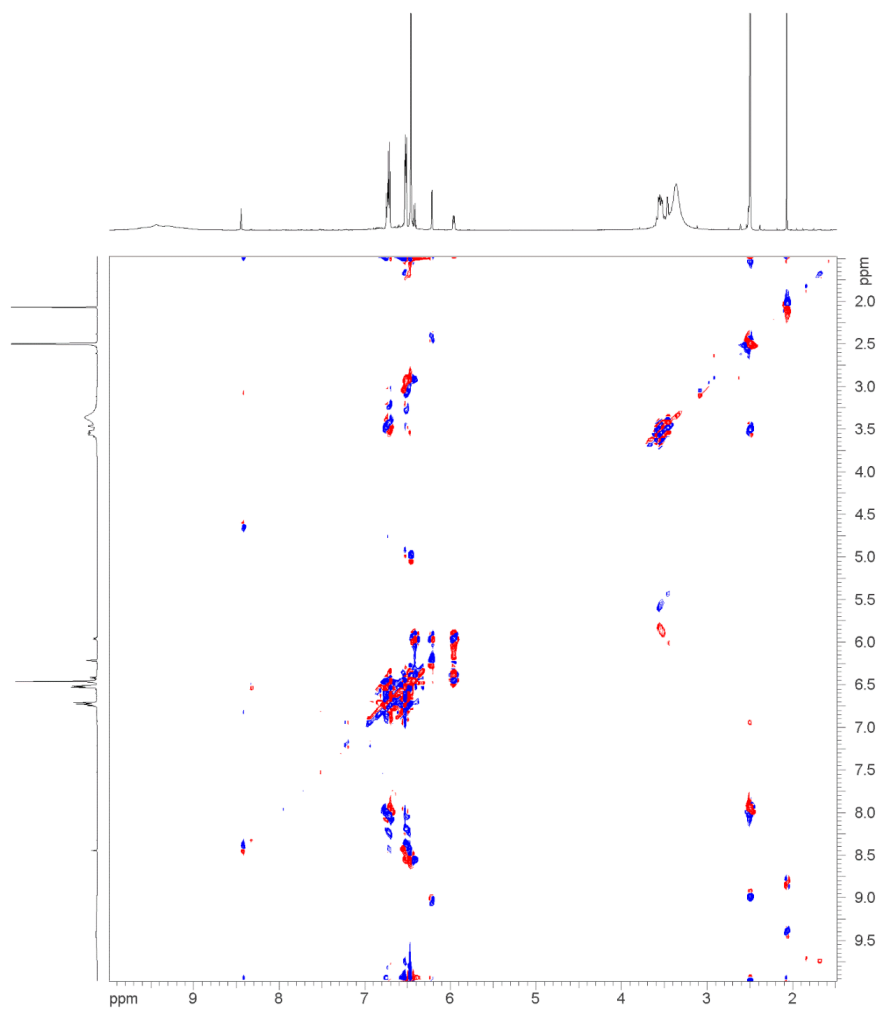
HSQC-DEPT NMR spectrum (600 MHz) of **4** in DMSO-*d*₆.



HMBC NMR spectrum (600 MHz) of **4** in DMSO-*d*₆.

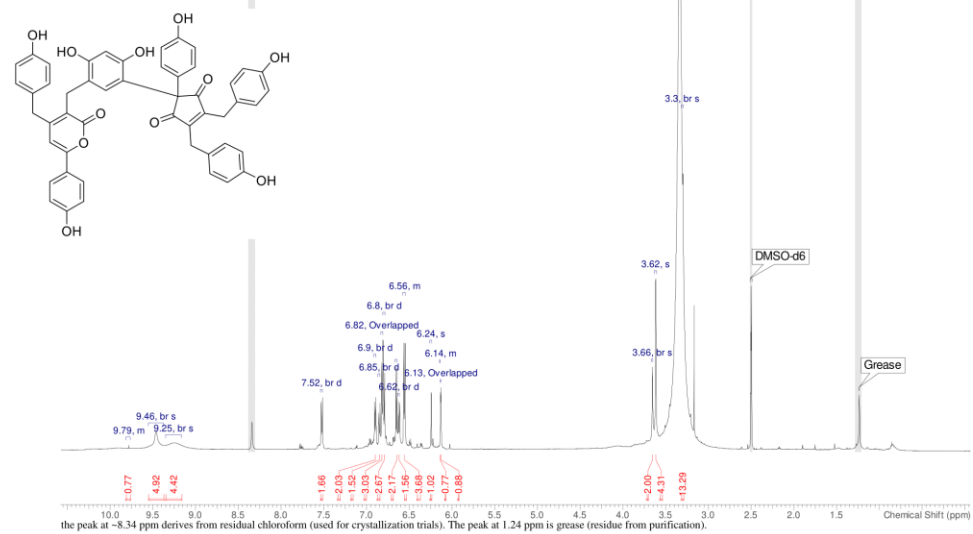


COSY NMR spectrum (600 MHz) of **4** in DMSO-*d*₆.



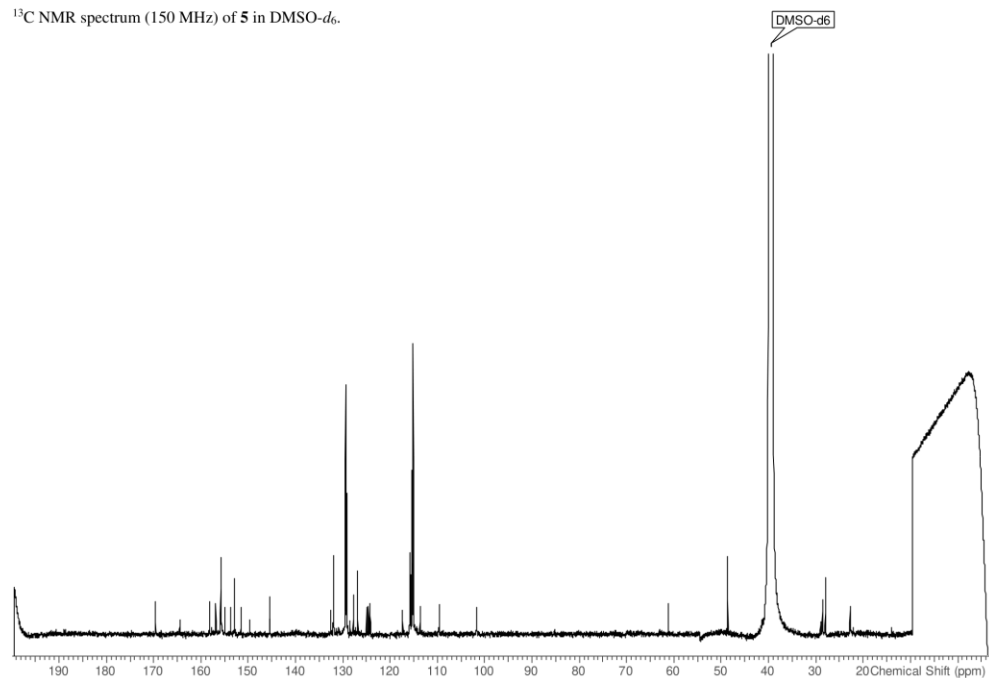
NMR spectra of compound 5 (Nostotrebinalactone 7)

¹H NMR spectrum (600 MHz) of 5 in DMSO-d₆.



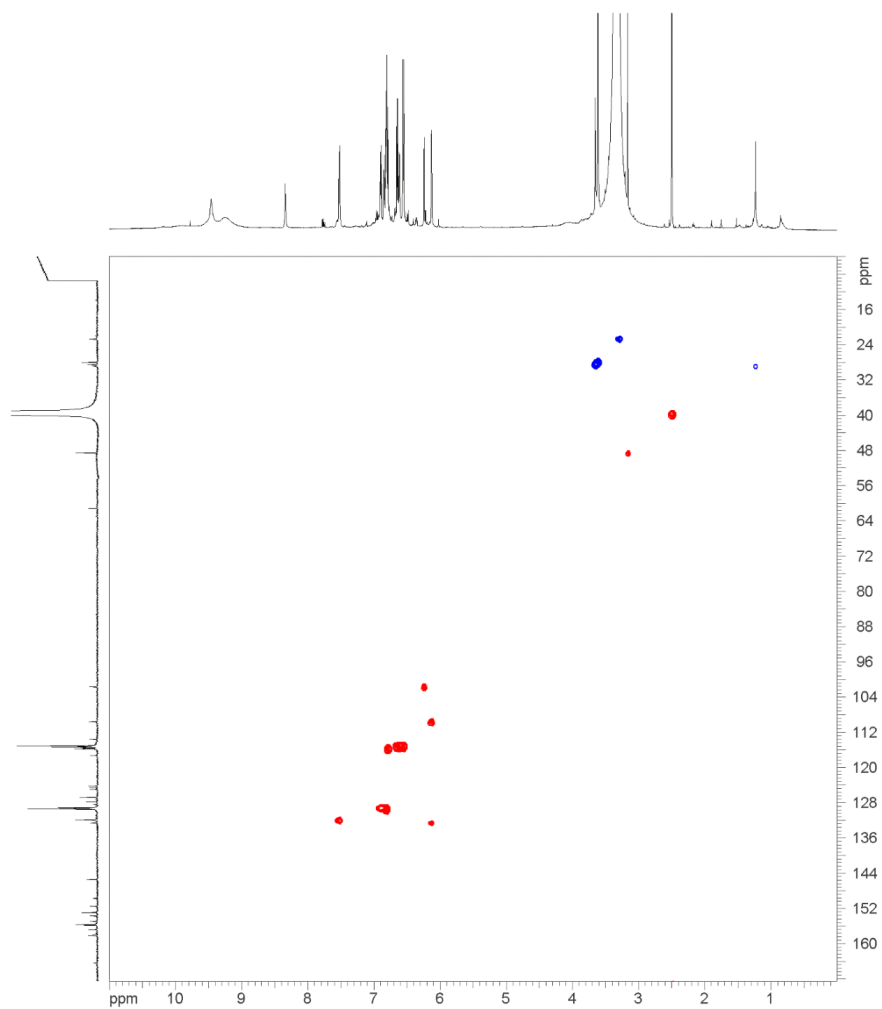
37

¹³C NMR spectrum (150 MHz) of 5 in DMSO-d₆.

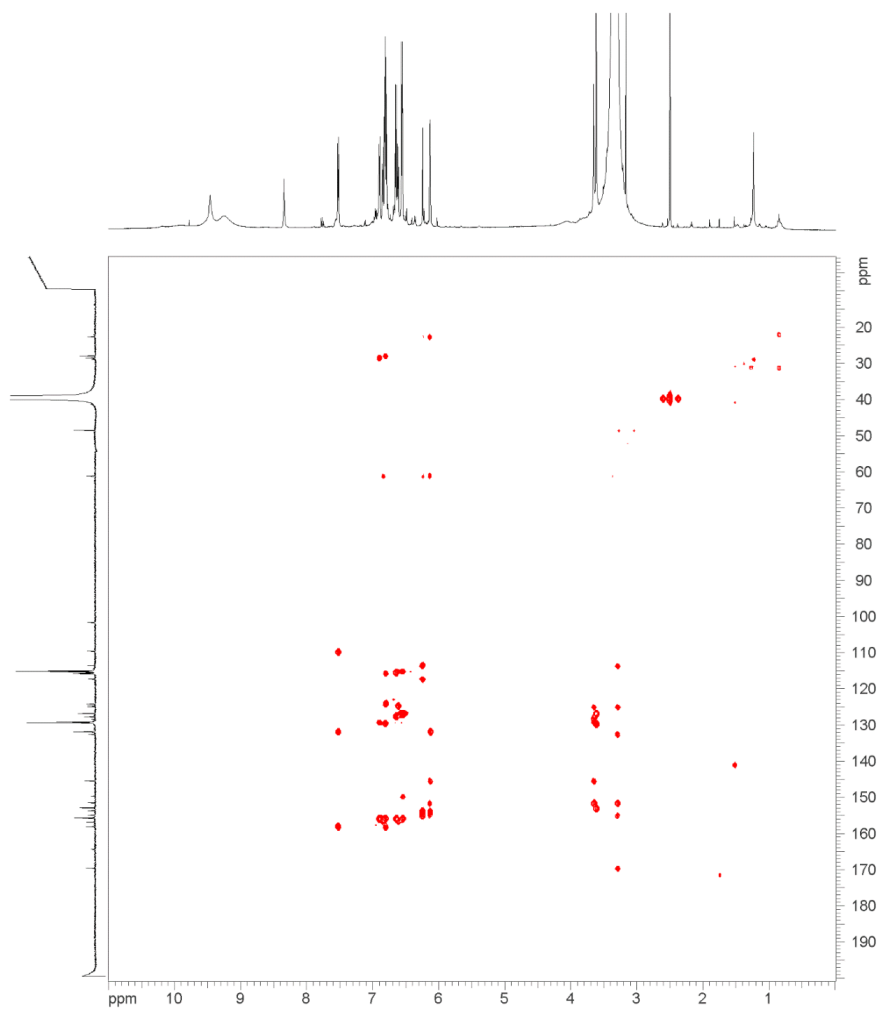


38

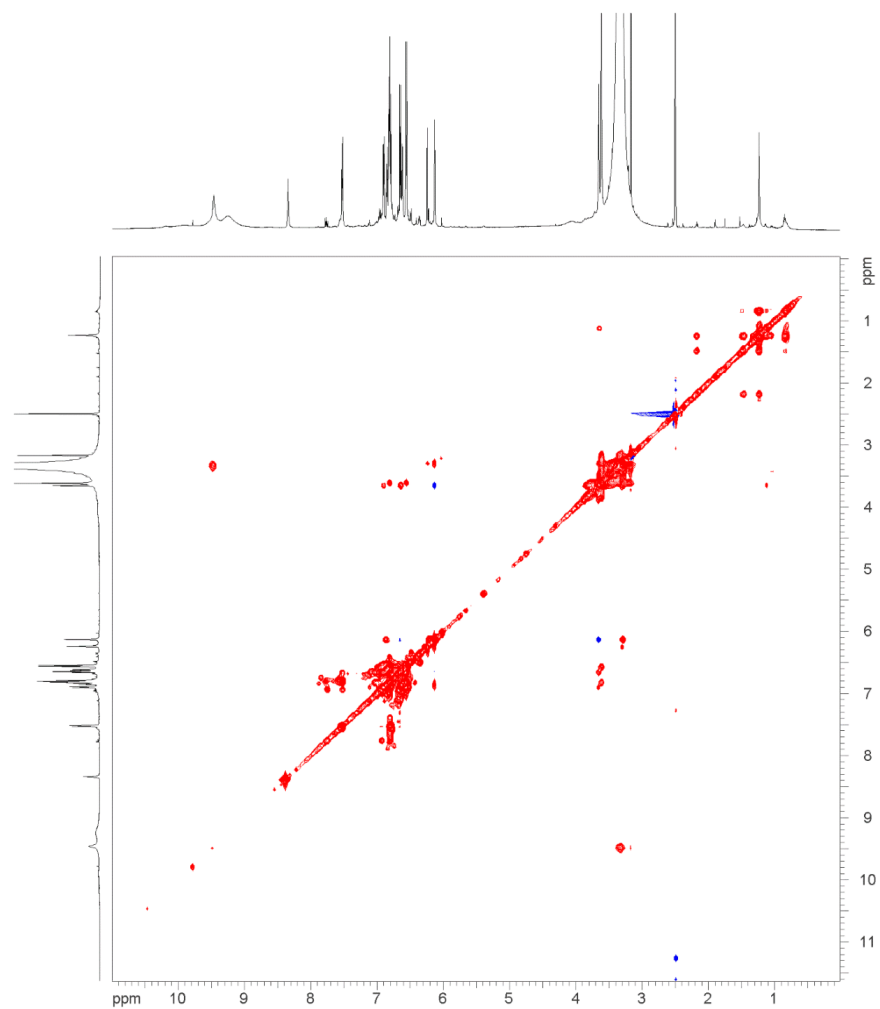
HSQC-DEPT NMR spectrum (600 MHz) of **5** in DMSO-*d*₆.



HMBC NMR spectrum (600 MHz) of **5** in DMSO-*d*₆.

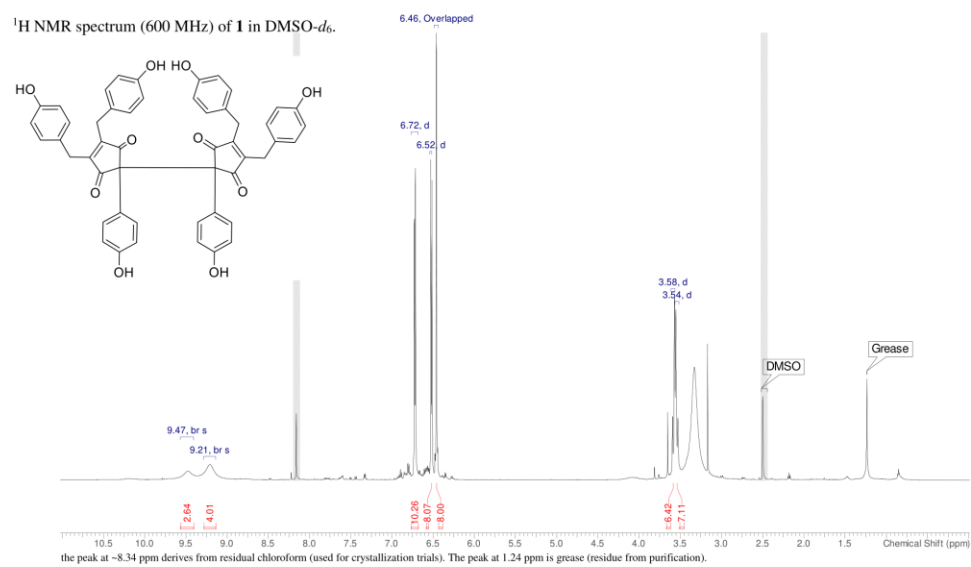


COSY NMR spectrum (600 MHz) of **5** in DMSO-*d*₆.



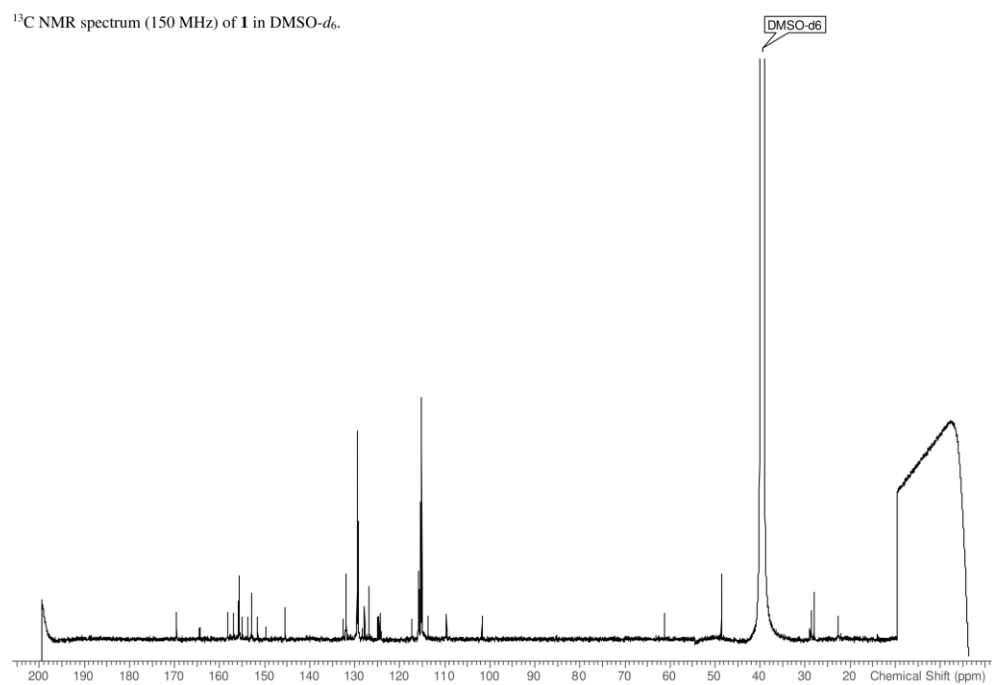
NMR spectra of compound 1 (Nostotrebins 6)

¹H NMR spectrum (600 MHz) of 1 in DMSO-*d*₆.



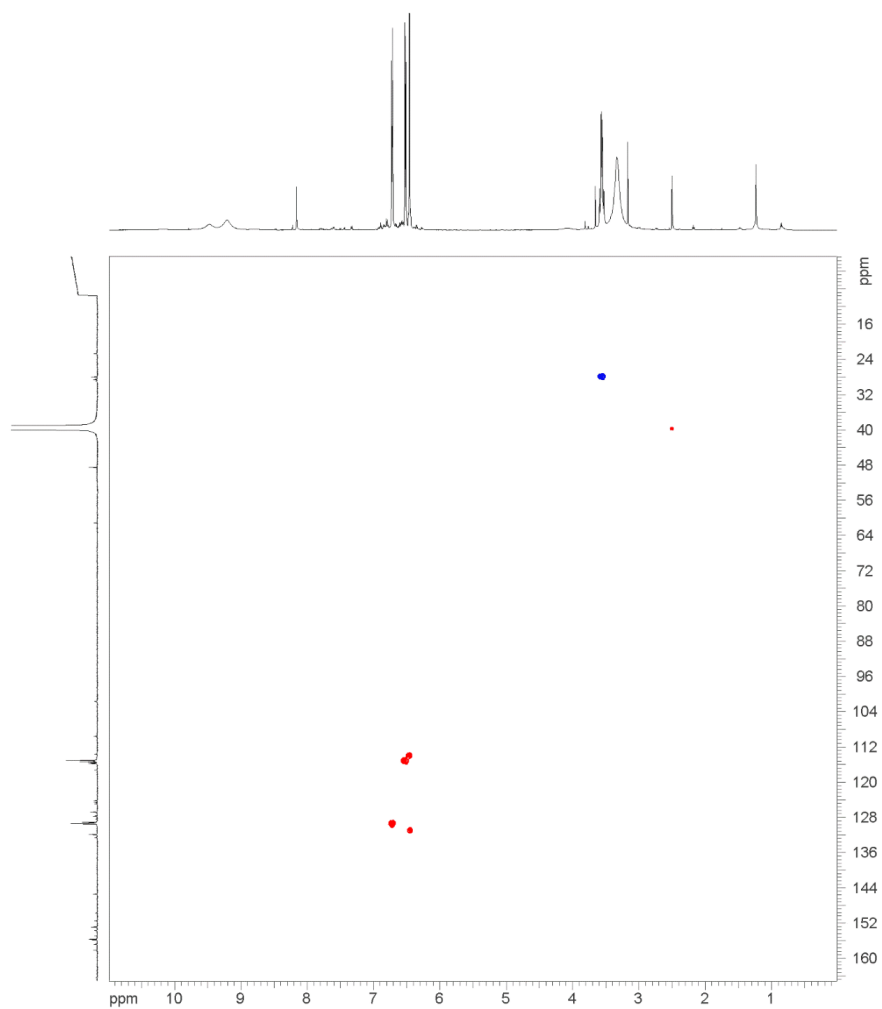
42

¹³C NMR spectrum (150 MHz) of 1 in DMSO-*d*₆.

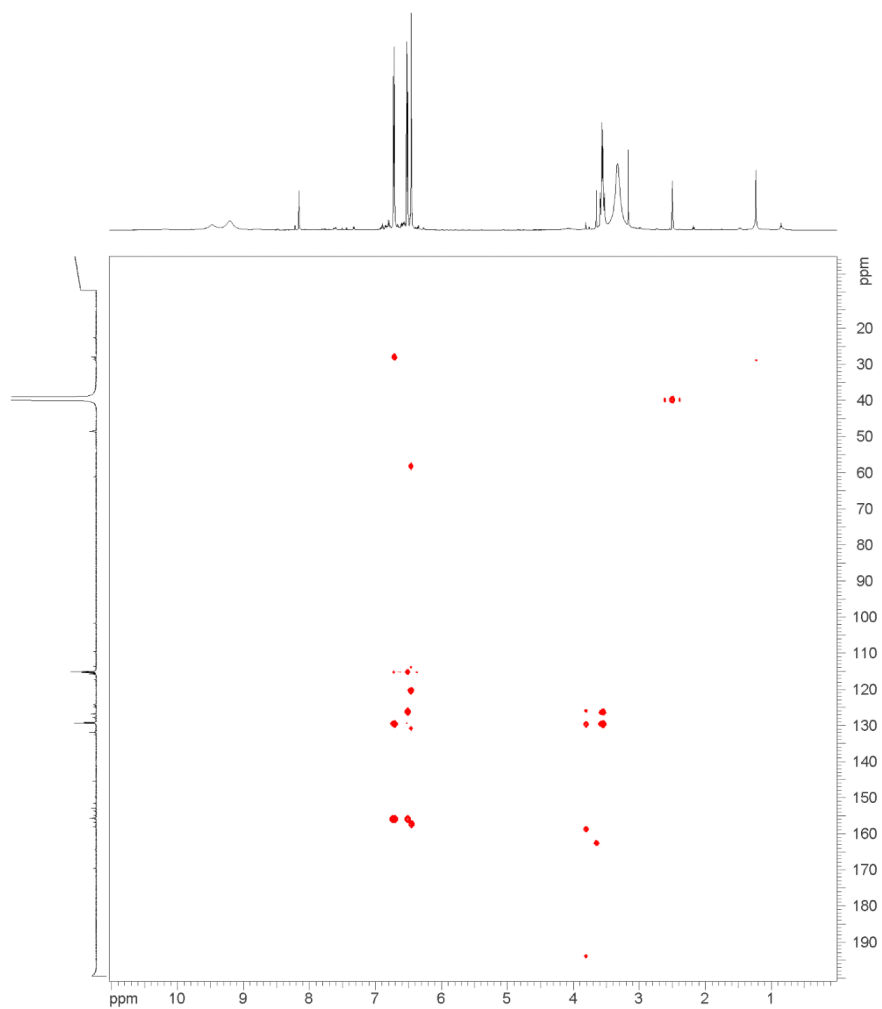


43

HSQC-DEPT NMR spectrum (600 MHz) of **1** in DMSO-*d*₆.



HMBC NMR spectrum (600 MHz) of **1** in DMSO-*d*₆.



Discussion of structural features of **A**, **B**, **C**, and **D**

The UV spectrum of **A** indicated that it is based on core structure **a** (see manuscript, Fig. 1). Its sum formula $C_{25}H_{20}O_6$ (found m/z 417.1319, calcd. 417.1333 for $[M + H]^+$) shows the presence of an additional hydroxy group. Thus, we hypothesize **A** to correspond to the western monomer found in **6**.

The UV spectrum of **B**, which is virtually identical to that of **5**, indicated that it contains one of each monomeric core structures **a** and **b**. The sum formula $C_{50}H_{38}O_{12}$ (found m/z 831.2410, calcd. 831.2436 for $[M + H]^+$) showed the presence of one additional hydroxy group compared to **5**. Thus, we hypothesize **B** to be composed of **A** and **3**. However, it remains unclear how these two monomers are connected.

Both **C** and **D** are trimeric structures, as indicated by their sum formula $C_{75}H_{56}O_{16}$ (found m/z 1213.3612, calcd. 1213.3647 for $[M + H]^+$). The UV spectrum of **C** showed that it solely contains the core structure **a**, while **D** contains one monomer **3** (core structure **b**) (maximum at 360 nm is about one third as intense as the maximum at 230 nm). Again, we could not determine how these two monomers are linked.

Bioactivity characterization

Determination of the inner filter effect

The correction factor of the hydrolysis rate (inner filter effect) was determined for varying concentrations of the test compounds as described in Ludewig et al. (2010).¹ First, the hydrolysis rate for each inhibitor concentration ($v_{raw}(c_{inh})$) was determined, followed by a measurement of buffer, test compound, and 7-Amino-4-methylcoumarin (AMC) without enzyme and substrate, and a measurement of buffer and AMC without test compound, enzyme, and substrate. The final concentration of AMC provided the same fluorescence intensity at $t_0 = 0$ as in the regular assay. The correction factor f_{corr} was calculated by:

$$f_{corr}(c_{inh}) = \frac{F(c_{AMC})}{F(c_{AMC} + c_{inh})}$$

with F as determined fluorescence at a certain AMC concentration c_{AMC} and a certain inhibitor concentration c_{inh} . The resulting correction factor was then applied to correct the regular hydrolysis rate:

$$v_{corr}(c_{inh}) = f_{corr}(c_{inh}) * v_{raw}(c_{inh})$$

with v_{raw} as uncorrected and v_{corr} as corrected, regular hydrolysis rate at a certain concentration of the inhibitor c_{inh} .

Bioactivity of Nostotrebin 6 (1) as previously described in the literature

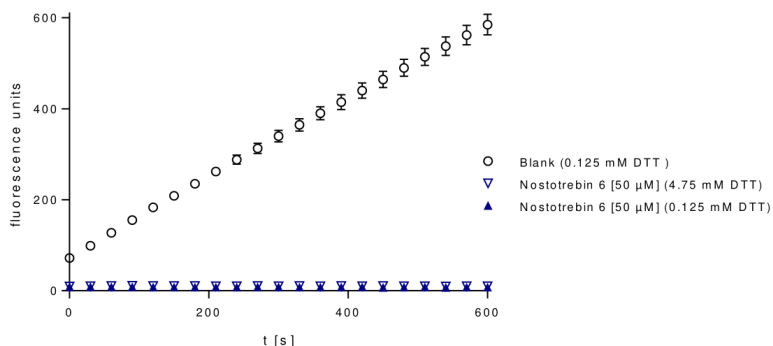
Biological activities of **1** according to literature

	test enzyme or organism	inhibitor concentration (μM)	reference
IC ₅₀	AChE	5.5	2
	BChE	6.1-7.5	2
	Cytotoxicity ^a (NR Assay)	8.5	3
	Cytotoxicity ^a (MTT Assay)	12.2	3
MIC	<i>E. faecium</i> VanA 419/ana*	7.8	4
	<i>E. faecalis</i> CCM4224	7.8	4
	<i>S. aureus</i> CCM4223	7.8	4
	<i>S. aureus</i> CCM3953	7.8	4
	<i>S. aureus</i> MRSA 4591*	19.6	4
	<i>S. haemolyticus</i> A/16568*	15.7	4
	<i>E. coli</i> CCM3954	>1253	4
	<i>P. aeruginosa</i> CCM3955	>1253	4
	<i>C. albicans</i> 978	>1253	4
	<i>C. tropicalis</i> 5	>1253	4
	<i>C. parapsilosis</i> 6	>1253	4

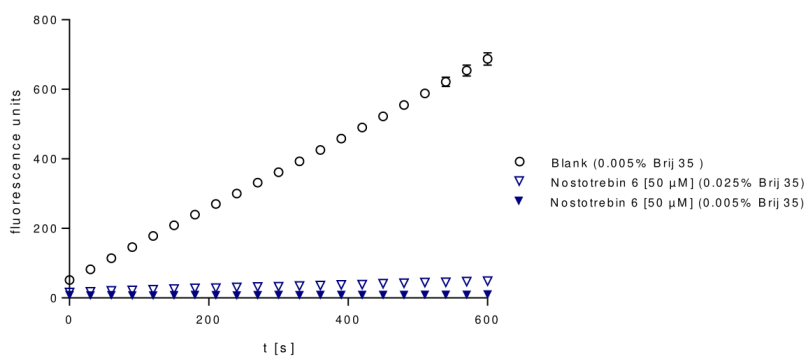
IC₅₀ of **1** against selected enzymes and ^a mouse fibroblasts; Minimal inhibition concentrations (MICs) of **1** against bacteria and fungi, including multidrug-resistant strains (*).

- (1) Ludewig, S.; Kossner, M.; Schiller, M.; Baumann, K.; Schirmeister, T. Enzyme Kinetics and Hit Validation in Fluorimetric Protease Assays. *Current topics in medicinal chemistry* **2010**, *10*, 368–382.
- (2) Zelik, P.; Lukesova, A.; Cejka, J.; Budesinsky, M.; Havlicek, V.; Cegan, A.; Kopecky, J. Nostotrebin 6, a Bis(cyclopentenedione) with Cholinesterase Inhibitory Activity Isolated from Nostoc sp. str. Lukesova 27/97. *The Journal of Enzyme Inhibition and Medicinal Chemistry* **2010**, *25*, 414–420.
- (3) Vacek, J.; Hrbáč, J.; Kopecký, J.; Vostálová, J. Cytotoxicity and Pro-Apoptotic Activity of 2,2'-Bis[4,5-bis(4-hydroxybenzyl)-2-(4-hydroxyphenyl)cyclopent-4-en-1,3-dione], a Phenolic Cyclopentenedione Isolated from the Cyanobacterium Strain Nostoc sp. str. Lukešová 27/97. *Molecules* **2011**, *16*, 4254–4263.
- (4) Cheel, J.; Bogdanová, K.; Ignatova, S.; Garrard, I.; Hewitson, P.; Kolář, M.; Kopecký, J.; Hrouzek, P.; Vacek, J. Dimeric Cyanobacterial Cyclopent-4-ene-1,3-dione as Selective Inhibitor of Gram-positive Bacteria Growth: Bio-Production Approach and Preparative Isolation by HPCCC. *Algal Research* **2016**, *18*, 244–249.

Rhodesain Assay



Determination of the residual activity of rhodesain in the presence of nostotrebine 6 (1): Residual activity of rhodesain with low (0.125 mM) and high (4.75 mM) concentration of DTT in the assay buffer. All values are mean values of at least two independent assays. As the reaction rate does not increase in the presence of DTT, unselective binding to the thiol groups of DTT can be excluded.



Determination of the residual activity of rhodesain in the presence of nostotrebine 6 (1): Residual activity of rhodesain with low (0.005%) and high (0.025%) concentration of Brij35 in the assay buffer. All values are mean values of at least two independent assays. The reaction rate does not increase significantly in the presence of Brij35, thus, unspecific inhibition by the formation of aggregates can be precluded.

6.4. Acknowledgements

Die vorliegende Dissertation entstand während meiner Tätigkeit als wissenschaftliche Mitarbeiterin am Interfakultären Institut für Mikrobiologie und Infektionsmedizin der Eberhard Karls Universität Tübingen und am Institut für Pharmazie der Martin-Luther-Universität Halle-Wittenberg. Die Arbeit wurde im Rahmen des Projekts „Accessing Novel Bacterial Producers from Biodiversity-rich Habitats in Indonesia“ (ANoBIn) angefertigt, welches durch das Bundesministerium für Bildung und Forschung (BMBF) gefördert wurde.

Mein besonderer Dank gilt Prof. Dr. Timo Niedermeyer für die Betreuung meiner Arbeit und die lehrreiche und spannende Zeit in seiner Arbeitsgruppe. Seine Unterstützung, Ideen und die wissenschaftlichen Diskussionen waren sehr wertvoll und haben zum Gelingen dieser Arbeit beigetragen. Herzlich danken möchte ich auch Prof. Dr. Karl Forchhammer für den fachlichen Austausch über Cyanobakterien, das Bereitstellen seiner Kultivierungsräume und für das Erstellen des Zweitgutachtens. Prof. Dr. Wolfgang Wohlleben möchte ich dafür danken, dass er unsere Arbeitsgruppe während des Wechsels zwischen der Eberhard Karls Universität Tübingen und der Martin-Luther-Universität Halle-Wittenberg unterstützt hat. Allen Projektpartner:innen innerhalb des ANoBIn-Projektes danke ich für die gute Zusammenarbeit, insbesondere Dr. Dwi Susilaningih Setyawan und Dr. Delicia Yunita Rahman für ihre Hilfe bei der Probennahme in Indonesien. Elke Klenk möchte ich für ihre tatkräftige Unterstützung im Labor, ihre Hilfsbereitschaft und ihre Freundschaft danken. Andreas Kulik danke ich für die unzähligen HPLC-MS-Messungen und die Unterstützung bei der Aufreinigung der Naturstoffe. Ein großer Dank geht an Trang Nguyen für die Unterstützung innerhalb ihrer Masterarbeit.

Der Umzug unserer Arbeitsgruppe hat viel Kraft und Nerven gekostet und ich danke meinen Kolleg:innen aus tiefstem Herzen für den Zusammenhalt und für viele einzigartige Erinnerungen. Steffen und Tomasz möchte ich für die grandiose Hilfe in Computer- und Analytik-Fragen danken. Nico danke ich für seine Gastfreundschaft und Hilfsbereitschaft insbesondere zu Beginn meiner Zeit in Tübingen. Mein ganz besonderer Dank gilt Julia, für ihre Freundschaft und ihren (fachlichen) Rat in allen Labor- und Lebenslagen. Meiner Familie möchte ich dafür danken, dass sie immer an mich glaubt und mich aufbaut. Meinen Freund:innen Elena, Anne, Catherine und Mandy danke ich fürs Zuhören und Bestärken. Ganz besonders danke ich Carsten für seinen Zuspruch und sein Vertrauen.

6.5. Rights of Use for Third Party Property



Nostotrebins 6 Related Cyclopentenediones and δ -Lactones with Broad Activity Spectrum Isolated from the Cultivation Medium of the Cyanobacterium *Nostoc* sp. CBT1153

Author: Ronja Kossack, Steffen Breinlinger, Trang Nguyen, et al

Publication: Journal of Natural Products

Publisher: American Chemical Society

Date: Feb 1, 2020

Copyright © 2020, American Chemical Society

PERMISSION/LICENSE IS GRANTED FOR YOUR ORDER AT NO CHARGE

This type of permission/license, instead of the standard Terms & Conditions, is sent to you because no fee is being charged for your order. Please note the following:

- Permission is granted for your request in both print and electronic formats, and translations.
- If figures and/or tables were requested, they may be adapted or used in part.
- Please print this page for your records and send a copy of it to your publisher/graduate school.
- Appropriate credit for the requested material should be given as follows: "Reprinted (adapted) with permission from (COMPLETE REFERENCE CITATION). Copyright (YEAR) American Chemical Society." Insert appropriate information in place of the capitalized words.
- One-time permission is granted only for the use specified in your request. No additional uses are granted (such as derivative works or other editions). For any other uses, please submit a new request.

BACK

CLOSE WINDOW